

THE DEVELOPMENT OF A MEDIUM ENERGY  
ION REFLECTION SPECTROMETER AND SOME  
PROBLEMS ASSOCIATED WITH ITS  
APPLICATION TO MATERIALS ANALYSIS



by

WILLIAM FREDERICK SKIPPER POEHLMAN, B.S., B.Sc., M.Sc.

A Thesis

Submitted to the School of Graduate Studies  
in Partial Fulfillment of the Requirements  
for the Degree  
Doctor of Philosophy

McMaster University

March 1980

A Medium Energy Ion Reflection Spectrometer

Doctor of Philosophy (1980)  
(Electrical Engineering)

McMaster University  
Hamilton, Ontario

TITLE: The Development of a Medium Energy Ion Reflection  
Spectrometer and Some Problems Associated with its  
Application to Materials Analysis

AUTHOR: William Frederick Skipper Poehlman,

B.S. (Niagara University)

B.Sc. (Brock University)

M.Sc. (McMaster University)

SUPERVISOR: Dr. D.A. Thompson

NUMBER OF PAGES: xxiv, 303

## ABSTRACT

This thesis reports on the development and characteristics of an ion reflection spectrometer designed to operate in the 20 - 150 keV range with specific application to near surface analysis of solids. The work is divided into two parts.

Part I details the design, operation and calibration of the systems within the spectrometer. They include a high resolution electrostatic analyzer and a premium solid state detector cooled to provide an excellent resolution figure. Control of the spectrometer is via a small minicomputer programmed with machine language in a real-time operating environment. Both energy and geometrical calibration procedures as well as results are provided. Examples are given which illustrate the performance characteristics of the spectrometer. Various corrections to both ESA (eg. neutral component) and solid state detector (eg. pulse height defect) results are determined and applied where necessary.

Part II shows the capabilities of the spectrometer as exhibited during the study of three areas of medium energy ion-solid interactions. The first is an examination of the large angle scattering cross section behaviour for various incident ions ( $1 \leq Z_1 \leq 10$ ) in gold layers. The results are compared to current theoretical predictions and experimental values. The second is an investigation of the neutralization of charged particles ( $1 \leq Z_1 \leq 10$ ) as they exit from clean gold surfaces. Other experimental values, as well as various theories are discussed in

relation to the observed results. The last study includes the determination of the stopping of light mass particles (H,He) in Au films. These values are obtained after the application of several corrections based on methods and results of the previous sections. The stopping powers are related to other experimental results.

From the foregoing investigations, it is concluded that the state of medium energy ion-solid interactions is by no means as quantitative as in the higher energy regime. The energy loss processes and charge neutralization behaviour are not well understood so that there is a great need for reliable and accurate experimental measurements that can provide a solid foundation on which to base a better theoretical model of the processes involved.

## Acknowledgements

I wish to thank my supervisor, Dr. D.A. Thompson, for his support and guidance during the course of this work.

The many valuable discussions afforded me by Dr. H.D. Barber and Dr. J.A. Davies are gratefully acknowledged.

I would like to thank Dr. A.B. Campbell, Dr. R.S. Walker and Dr. R. Bhattacharya for their helpful discussions and generous assistance so freely given.

It is a pleasure to thank the staff of the McMaster Tandem Accelerator Laboratory: in particular R. McNaught, H. Blanchard and E. DeVries of the electronics section; J. Parkinson and J. Rosenthal of the fabrication section; as well as J. McKay and J. Stark of operations.

I would like to express my gratitude to S. den Bleker who transformed written scribbles into a typed thesis and M. Krystalski who generated intelligible drawings from various sketches.

Also, I would like to thank B. Ley, professionally for her many helpful suggestions, and personally for providing constant encouragement.

Finally, I want to express my appreciation to my parents for their patience and understanding during the course of my studies.

Leaf viii omitted in page numbering

## Table of Contents

	<u>Page No.</u>
1. INTRODUCTION	1
PART I	
2. INTRODUCTION	5
3. SYSTEM DESIGN AND CONTROL	7
3.1 Introduction	7
3.2 Beam Transport	8
3.2.1 Beam Production and Shaping	9
3.2.2 Differential Pumping Region	13
3.2.3 The UHV Scattering Chamber	14
3.3 Sample Handling Systems	15
3.3.1 The Sample Rotator and Target Carousel	15
3.3.2 The Sample Quick Load Device	21
3.4 The Electrostatic Analysis System	26
3.4.1 Analyzer Design	26
3.4.2 The ESA Particle Detector	34
3.4.3 Target Alignment Procedure	35
3.5 Solid State Detector Systems	35
3.6 Computer Control	38
3.6.1 Electrostatic Analyzer Operation	39
3.6.2 Surface Barrier Detector Operation	43
3.6.3 Data Handling Operations	51



	<u>Page No.</u>
4. SYSTEM CALIBRATION AND PERFORMANCE	55
4.1 Introduction	55
4.2 Accelerator Energy Calibrations	55
4.3 The Electrostatic Analysis System	57
4.3.1 ESA Energy Calibrations	57
4.3.2 ESA Spectrum Corrections	61
4.4 The Surface Barrier Detector System	63
4.4.1 Detector Geometry Calibrations	68
4.4.2 Detector Energy Calibrations	73
4.4.3 Detector Charge-to-Neutral Ratio Determinations	75
4.5 The Medium Energy Detector Pulse Height Defect Determination	78
4.5.1 Experimental Measurement of the Detector Pulse Height Defect	79
4.5.2 Dead Layer Theoretical Predictions	86
4.5.3 Monte Carlo Simulation of the Detector Pulse Height Defect	95
4.5.4 Discussion of the Results	99
PART II	
5. INTRODUCTION	111
6. NUCLEAR SCATTERING CROSS SECTION	119
6.1 Introduction	119
6.2 Collision Theory I	119
6.2.1 Basic Assumptions	120

	<u>Page No.</u>
6.2.2 The Two-Body Collision	121
6.2.3 The Interatomic Potential	124
6.2.4 The Nuclear Scattering Cross Section	128
6.3 Principles and Technique	132
6.3.1 Features of Backscattered Spectra	132
6.3.2 Experimental and Analysis Procedure	137
6.4 Results and Discussion	140
7. CHARGE NEUTRALIZATION MEASUREMENTS	147
7.1 Introduction	147
7.2 Theoretical Framework for Ion Neutralization Behaviour	149
7.2.1 Low Energy Processes	150
7.2.2 High Energy Processes	151
7.2.3 Medium Energy Processes	155
7.3 Experimental and Analysis Procedure	159
7.4 Results and Discussion	165
8. STOPPING CROSS SECTIONS AND STRAGGLING DETERMINATIONS	183
8.1 Introduction	183
8.2 Collision Theory II	184
8.2.1 The Stopping Powers	185
8.2.2 Nuclear Stopping Cross Section	186
8.2.3 Electronic Stopping Cross Section	187
8.2.4 Energy Straggling	191
8.3 Experimental and Analysis Procedure	195
8.3.1 Stopping Cross Section Determination	195

	<u>Page No.</u>
8.3.2 The Stragglng Determinations	201
8.4 Results and Discussion	203
8.4.1 Stopping Cross Sections in Gold	204
8.4.2 Stragglng in Gold	210
9. SUMMARY	213
A. APPENDIX	217
A.1 MES11 -- Medium Energy Scattering Control Code	219
A.2 MES11 INS -- Operating Instructions for MES11	255
A.3 Link Control Codes	
A.3.1 PIP15.MAC -- for PDP11/05	265
A.3.2 PIP11 SRC -- for PDP15/20	270
REFERENCES	291

## List of Figures

	<u>Page No.</u>
3.1 The Medium Energy Ion Reflection Spectrometer	11
3.2 Side view of the UHV scattering chamber	17
3.3 The design of the beam chopper Faraday cup	19
3.4 The sample manipulation and carousel rotator	23
3.5 (a) The vacuum quick load device	25
(b) The target carousel and claw	25
3.6 The electrostatic analyzer and associated apparatus	29
3.7 (a) Illustration of the ESA refocussing property	33
(b) Energy resolution as determined by the ESA exit aperture	33
(c) Departure from perfect refocussing of the ESA	33
3.8 The Medium Energy Ion Reflection Spectrometer System	41
3.9 Computer interface for ESA control	45
3.10 Computer interface for display and pulse height analysis system	49
4.1 Non-linear least squares edge fitting of an ESA spectrum	59
4.2 Energy calibration for the ESA, relating detected particle energy and plate voltage	63
4.3 The application of two major corrections to an ESA spectrum	67
4.4 An example of a RBS spectrum of heavy impurities embedded in a lighter mass host using the cooled surface barrier detector	71

	<u>Page No.</u>
4.5 (a) Spectra which show the measured charged + neutral and neutral backscattered component	77
(b) The calculated charged fractions as determined from (a)	77
4.6 (a) A measure of the surface barrier detector pulse height defect	81
(b) The solid state detector and ESA responses to <sup>0</sup> 10 A of Au on Si.	81
4.7 Experimental results giving pulse height defect data for the solid state detector	85
4.8 A typical surface barrier detector configuration	89
4.9 (a) The fraction of elastic energy deposition in silicon	91
(b) The fraction of elastic energy deposition in gold	91
4.10 Theoretical predictions of the pulse height defect of the solid state detector	93
4.11 Monte Carlo simulation results for the solid state detector pulse height defect	97
4.12 A comparison of a Monte Carlo simulation and the experimental determination	103
5.1 Some ion beam analysis techniques in relation to stopping cross sections and incident beam energy	113
6.1 (a) A binary encounter in the laboratory frame	123
(b) The same collision in the center of mass frame	123

	<u>Page No.</u>
6.2 (a) A qualitative description of the interatomic potential	127
(b) A comparison of various proposed potentials between two copper atoms	127
6.3 The universal differential scattering function and various approximations	131
6.4 The principles of impurity atom detection via back-scattering	135
6.5 Measured screening functions for reduced scattering cross sections	143
6.6 The results of figure 6.5 normalized to the Thomas-Fermi cross section	145
7.1 (a) Electron diagram for resonance tunnelling neutralization processes	153
(b) Electron energy diagram for the Auger neutralization process	153
7.2 The energy spectra for 120 keV protons backscattered from a clean gold surface	161
7.3 The charged fractions for figure 7.2 as a function of backscattered energy	163
7.4 The charged fractions of $H^+$ and $D^+$ backscattered from clean gold surfaces	167
7.5 The charged fractions for $H^+$ and $He^+$ plotted against exit velocity	171

	<u>Page No.</u>
7.6 Charged fractions of $\text{Li}^+$ , $\text{B}^+$ , $\text{C}^+$ , $\text{N}^+$ , $\text{F}^+$ and $\text{Ne}^+$ plotted against exit velocity	173
7.7 The present work charged fractions plotted as a function of the reduced velocity	177
7.8 The present work charged fractions versus the reciprocal velocity component normal to target surface	179
8.1 The nuclear and electronic stopping power in reduced units	189
8.2 Electronic stopping power for incident ions with $v = 0.63 v_0$ on carbon from Fastrup et al <sup>141</sup>	193
8.3 A typical ESA spectrum from 90 keV $\text{H}^+$ on 100 Å of Au <sup>0</sup> showing (a) fit, (b) differentiated curve and (c) scattering geometry	197
8.4 (a) Measured stopping cross sections for $\text{H}^+$ in Au	207
(b) Measured stopping cross sections for $\text{He}^+$ in Au	207
8.5 The normalized straggling measurements for (a) $\text{H}^+$ in Au and (b) $\text{He}^+$ in Au	209

## List of Tables

	<u>Page No.</u>
3.1 UHV Chamber Partial Pressures	20
4.1 Surface Barrier Detector Solid Angle Determinations	72
4.2 Monte Carlo Predictions for the Number of Collisions and Defects Produced Per Incident Particle at 100 keV	98
4.3 Comparison of Theory and Simulation to Experiment at 100 keV	100
4.4 Predicted Silicon Dead Layer Thickness ( $\overset{0}{A}$ ) from Simulation	105
5.1 Typical Features of Some Basic Ion Beam Analysis Techniques	115
6.1 Measured Values of the Scattering Cross Section and the Corresponding Screening Function	139
7.1 The Transition Parameters of Tunnelling Processes for Heavy Ions as Determined from the Present Work	181
8.1 Comparison of Coefficients for fitting H Stopping Powers in Au	205



Leaf xviii omitted in page numbering

## List of Symbols

	<u>Page No.</u>
a - the Thomas Fermi screening length	124
- a critical distance associated with Auger neutrali- zation	151
$a_0$ - radius of the first Bohr orbit for the H atom	125
A - the transition rate for Auger neutralization at the surface	151
b - the collision diameter	125
C - channel number	60
d - the interatomic spacing	124
e - the electronic charge in Coulombs	27
e-h - electron-hole pairs generated by electronic collisions with an energetic particle	88
$E_0$ - incident projectile energy in the laboratory frame of reference	124
$E_1$ - the energy of the scattered ion in the laboratory frame of reference	123
$E_2$ - the energy of the recoiling atom in the laboratory frame of reference	123
$E_p$ - emerging proton beam kinetic energy in keV	155
$E_D$ - amount of energy sensed (output) by the detector	94
$E_I$ - amount of energy deposited within the detector	94
- effective electronic ionization energy of a single atom near a solid surface	152

	<u>Page No.</u>
$E_T$ - total energy lost in collision processes	87
$E_x$ - effective electronic excitation energy of an atom undergoing charge transfer	152
$E(C)$ - energy corresponding to channel number C	64
$f^C(C)$ - the charged fraction backscattered from a target at an energy corresponding to channel number C	75
G - energy calibration (gain measured in keV/channel)	64
k - elastic scattering kinematic factor	132
$L_d$ - a measure of electrostatic analyzer departure from perfect refocussing	31
$L_e$ - the distance at the electrostatic analyzer exit aperture between the position of two particles differing in velocity	30
LSS - a theoretical approach developed by Lindhard Scharff and Schiott <sup>2-5</sup>	1
m - a parameter used in the definition of the power cross-section approximation	129
$m_e$ - mass of the electron	125
$M_1$ - atomic mass of the projectile	121
$M_2$ - atomic mass of the target atom	121
$n_0$ - the metal conduction electron density in keV	155
N - target atom density	154
p - impact parameter for the collision	121
Q - sample fluence or dose from the incident beam	137
r - the separation variable between two colliding masses	121



	<u>Page No.</u>
$r_0$ - the central circular orbit traced by a charged particle in the electrostatic analyzer	27
$S_1$ - the electrostatic analyzer entrance aperture diameter	32
$S_2$ - the electrostatic analyzer exit aperture diameter	32
$S(E)$ - total stopping cross section	136
$S_e(E)$ - electronic stopping cross section	204
$S_n(E)$ - nuclear stopping cross section	204
$t$ - the depth increment in the target corresponding to one energy channel width	136
$T$ - the total energy transfer in a binary encounter	128
$T_e$ - inelastic energy transfer	212
$T_M$ - maximum energy transfer in a binary collision	128
$v$ - projectile velocity	121
$v_0$ - the velocity of an ion such that it traces the central circular path in a radial field	30
	the velocity of the first Bohr orbital electron 149
$v_{\perp}$ - the backscattered particle exit velocity component which is normal to the target surfaces	151
$V(r)$ - the interatomic potential	124
$Y(C)$ - the yield (number of counts) at channel number C	60
YLD - the integrated area (usually from under a spectral peak)	137

	<u>Page No.</u>
$z$ - the longitudinal direction (parallel to the target incident beam)	137
$Z$ - the units of charge of a particle	27
$Z_1$ - the atomic number of the projectile	120
$Z_2$ - the atomic number of the target atom	120

#### Greek Symbols

(including partial symbols)

$\alpha$ - incident beam half angle at the electrostatic analyzer entrance aperture	31
$\beta$ - a parameter used to define the electrostatic analyzer resolving power	30
$\gamma$ - the fractional maximum energy transfer	128
$\Delta E$ - the energy width of a channel in backscattered energy spectra	136
$\Delta E_1$ - the energy loss experienced by a particle in its inbound path through the target	218
$\Delta E_2$ - the energy loss experienced by a particle on its outbound path through the target	218
$\Delta E_{\text{obs}}$ - the energy difference measured between the zero target depth and depth $\Delta x$	216
$\Delta E/E$ - the fractional resolution of the analysis device	64
$\Delta t$ - the target thickness	137
$N\Delta t$ - the sample density	137

	<u>Page No.</u>
$\Delta\Omega$ - the solid angle subtended by a detector	137
$\epsilon$ - the LSS reduced energy parameter	125
$S_e(\epsilon)$ - electronic stopping cross section in LSS reduced units	205
$S_n(\epsilon)$ - nuclear stopping cross section in LSS reduced units	205
$\eta(E)$ energy deposition due to inelastic collisions	87
$\theta_c$ - the angle of deflection in the center of gravity coordinate system	87
$\theta_L$ - the angle between the incident beam direction and the detector in the laboratory frame of reference	123
$\kappa$ - the LSS value for the electronic stopping coefficient	208
$\lambda$ - the fitting parameter in the numerical approximation to the Thomas-Fermi scattering cross section	129
$\lambda_m$ - the fitting parameter for the power law scattering cross section approximation	129
$\nu(E)$ - the amount of energy deposited into elastic collisions	87
$\mathcal{E}$ - the radial electric field as associated with the electrostatic analyzer	27
$\rho$ - the reduced range parameter associated with LSS	208

	<u>Page No.</u>
$\sigma_c$ - the cross section for an electron capture of a particle in or near a solid	154
$\sigma_\ell$ - the cross section for an electron loss of a particle in or near a solid	154
$d\sigma/d\Omega$ - the differential nuclear scattering cross section	133
$\tau$ - the LSS reduced independent parameter for the nuclear scattering cross section and screening function	128
$f(\tau^{\frac{1}{2}})$ - the screening function for the LSS derived reduced scattering cross sections	128
$\phi$ - the work function associated with a solid	152
$\phi(r/a)$ - the Thomas-Fermi screening function	125
$\Omega^2$ - the energy straggling parameter	209

## CHAPTER 1

### Introduction

It is only since the middle of this century that the particle-solid interaction has become a major field of study. Much of the initial impetus stemmed from a need to understand effects occurring in high power vacuum tubes and the requirement for better devices for the measurement of vacuum. In the late 1940's the use of nuclear fission reactors provided a ready means of examining the atom-solid interaction as well as providing a new motivation for studying such effects and the resulting radiation damage. During this time Bohr<sup>1</sup> published an initial theory of particle penetration through matter. More than a decade later, his basic principles were developed into a comprehensive unified theory of atomic stopping by the work of J. Lindhard and his collaborators<sup>2-5</sup>, now commonly referred to as LSS theory. Since then, the experimental use of low energy ( $\sim 0.5 - 10$  keV) ion beams to sputter etch and analyze surfaces, of medium energy ( $\sim 50 - 500$  keV) ion beams to dope semiconductors for device application, and of high energy ( $\sim 1 - 3$  MeV) ion beams to probe bulk and surface layer phenomena in solids have become standard techniques.

Currently there exists high activity in the particle-solid interaction field resulting from a major research effort to develop nuclear fusion as a future energy source. A fusion plasma with sufficiently high temperature to achieve ignition will contain



primarily ions from the low energy regime but with energies extending into the medium energy region. The energy balance in a fusion reactor and hence the temperature profile will be strongly influenced by particles which have escaped the plasma and subsequently are reflected back into the interaction volume from the containment vessel first wall. Thus, the reflection coefficient<sup>6</sup>, charge states<sup>7</sup>, and impurity production<sup>8</sup>, from the recycled particles will be crucial<sup>9</sup> in determining the feasibility of nuclear fusion as a practical large scale energy source.

It is in this milieu, then, that the development of a medium energy ion reflection spectrometer has taken place, in order to determine some of the basic fundamentals of the atomic collision process; also to assess the technique of surface analysis via the light ions in this energy regime thus allowing the extension of ion implantation accelerators (involving typically 50 - 200 keV energies) for on-line surface studies.

This thesis is logically divided into two parts: part I includes in Chapter 3 the design and development of the spectrometer while Chapter 4 provides most of the performance properties of the system. Part II reports on the measurement of some basic parameters which aid in the characterization of ion-solid interactions and also which indicate some of the capabilities of the spectrometer. Each of these two sections are prefaced by a more detailed introduction.

PART I

THE SPECTROMETER

1

Leaf 4 omitted in page numbering

## CHAPTER 2

### Introduction

In this section, the design, operation and performance of the medium energy ion reflection spectrometer (M.E.I.R.S.) is given. Chapter 3 provides a general overview of the ion-beam production and transport system as well as the target chamber with emphasis on the spectrometer components and modes of operation. Chapter 4 gives a detailed explanation of calibration techniques and measurement characteristics of the spectrometer. The basic theory appropriate to this chapter is briefly outlined. A more detailed theoretical description is deferred to Part II, where a natural progression of fundamentals is introduced and developed, as required, to discuss the experimental results

Leaf 6 omitted in page numbering

## CHAPTER 3

### System Design and Control

#### 3.1 Introduction

Ion reflection in the medium energy range has analysis capabilities similar to those of MeV backscattering but with smaller accessible depths<sup>10</sup>. Scattering cross sections are larger in this regime allowing shorter analysis times. Such advantages are lost when solid state detectors are employed, however, due to the associated pulse pile-up problems. The use of an electrostatic analyzer (ESA) resolves this problem, although at the expense of longer analysis times which are needed since this is a single channel counting device. However, one advantage of the ESA system is the depth resolution figure which can be as low as 5-10 angstroms ( $\text{\AA}$ )<sup>0</sup> for protons and He on gold. In fact, recently, an ESA has been designed for up to 1 MeV backscattering work alone with  $\sim 0.4\%$  resolution<sup>11</sup>. The ESA also has one major disadvantage in that it collects only charged ions. This means that for quantitative information the backscattered yields must be corrected for the ignored neutral fractions of the backscattered particles. The neutral fractions are only important in light ion (H or He) scattering at energies  $\leq 200$  keV where they begin to become significant. This is the region of interest in this study. Here, charged fractions can be obtained by combining a solid state detector

with electrostatic charged particle deflection plates interposed between the target and the detector. For this application the rather poor energy resolution of the solid state detector is not a significant problem. Thus the basic spectrometer includes a solid state detector to generate in-situ determinations of the charged and neutral particle fractions to correct the ESA spectra, the ESA itself, and devices to measure beam currents on the target as well as to provide sample manipulations.

In this chapter a detailed discussion is given of the components which comprise the spectrometer. Also described are various design considerations as well as modes of operation. Section 3.1 outlines the ion accelerators and the beam transportation leading to the ultra-high vacuum (UHV) scattering chamber. Details of the sample handling devices are given in section 3.2. The middle two sections, 3.3 and 3.4, describe the two main analysis systems: the former for the ESA detector and the latter section for the solid state detector. The last section, 3.5, details the computer control aspect of the two detection systems through both hardware and software considerations.

### 3.2 Beam Transport

Although most of the emphasis in this chapter is on the design, operation and characteristics of the systems in the UHV chamber, this section is concerned with the production of ion beams of both medium (20 - 150 keV) and high (> 500 keV) energy and their subsequent transport to the UHV scattering chamber.

Figure 3.2 shows the entire M.E.I.,R.S. system. Section 3.2.1 examines in detail the coupled accelerator system while the transition from low vacuum areas of the accelerators to the UHV environment is discussed in section 3.2.2. The last subsection concerns the description of UHV chamber components that are not directly associated with the particle analysis devices, such as the faraday cup and results of residual gas analysis of the vacuum environment.

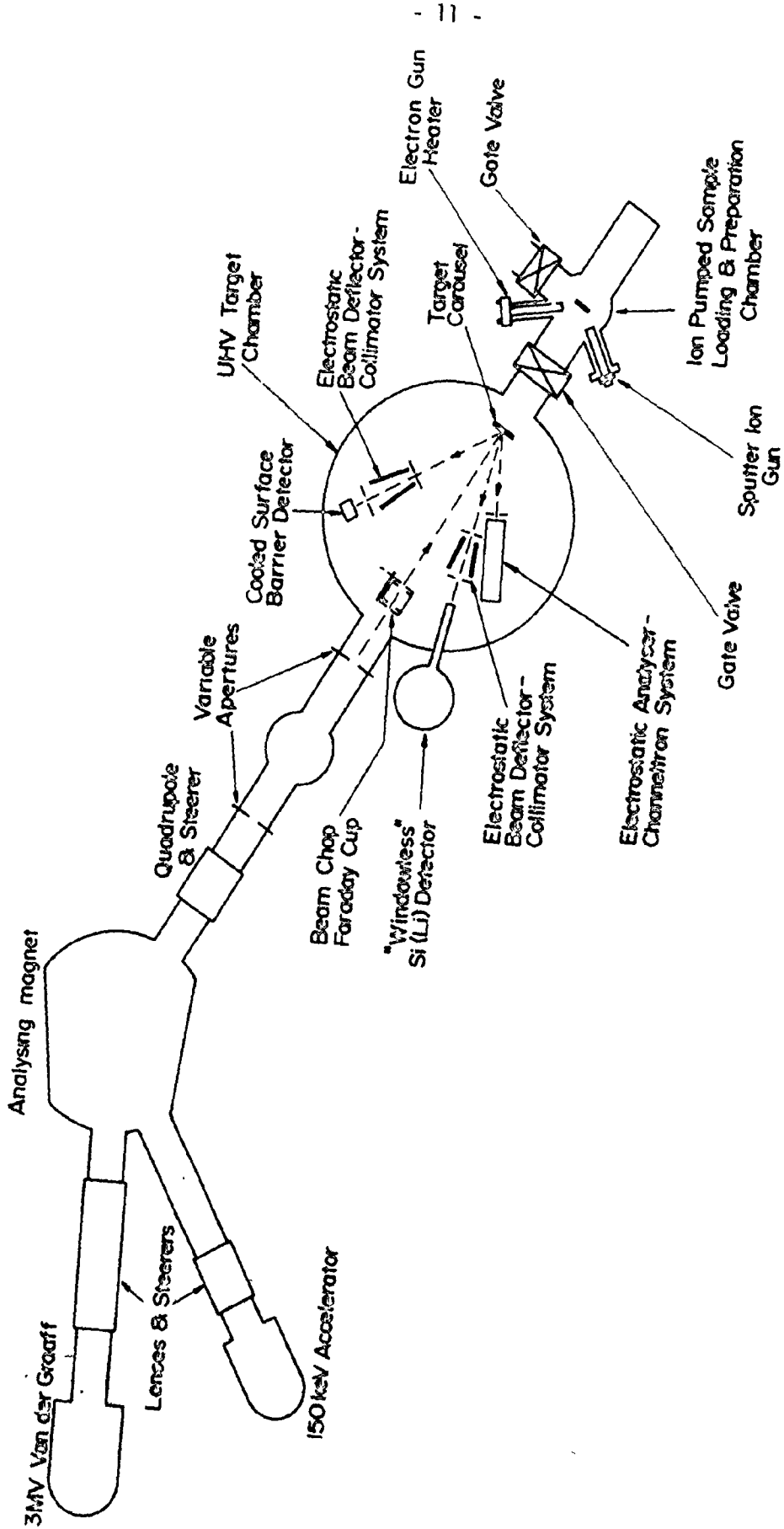
### 3.2.1 Beam Production and Shaping

As shown in figure 3.1, the beam from either accelerator may be brought into the UHV target chamber via the common analyzing magnet and a differential pumping region. Energy stabilization of  $< 0.5\%$  is attained for both accelerators by monitoring the beam current striking slits placed after the analyzing magnet. A feedback circuit adjusts the energy of the beam so that the currents are equalized.

The ion implantation accelerator is a Texas Nuclear Corporation Model 9509 Cockcroft Walton neutron generator modified to accommodate a Danfysik 911A universal ion source. This is a hot cathode source having an auxiliary heating filament so that solid, as well as gaseous sources may be employed<sup>12,13</sup>. The solid, depending on its vapour pressure curve, can be placed inside one of these holders which adjust the source temperature by changing the distance from the heating filament. To achieve the discharge, a carrier gas (usually Ar) is used; however, when the source material is gaseous, the ovens and carrier gas can be eliminated. Using an



Figure 3.1 The Medium Energy Ion Reflection Spectrometer including the scattering chamber beam transport system and the coupled accelerator facility.



extraction potential of  $\sim 10$  keV, the beam is extracted from the ion source with a diverging exit envelope. It is then focussed to a slightly converging envelope via an Einzel lens assembly located between the extraction electrode and the acceleration column with a continuously variable potential up to 30 kV. The ion source can provide beam intensities of up to several  $\mu\text{A}/\text{cm}^2$  on the target. The vacuum in the 150 kV accelerator is maintained by an oil diffusion pump equipped with a liquid nitrogen cooled vapour trap while the ion source is differentially pumped with a small Edwards Diffstak system. Base pressure is  $1 \times 10^{-7}$  torr. The beam lines are evacuated to typically  $1 \times 10^{-6}$  torr.

The higher energy beams ( $> 500$  keV) are supplied by a High Voltage Engineering model KN single-ended Van de Graaff electrostatic accelerator. The ion source is a radio-frequency type providing H or He beams of close to  $250 \mu\text{A}/\text{cm}^2$  currents on target. The base pressure in the machine is  $5 \times 10^{-7}$  torr maintained by a 450  $\ell/\text{s}$  turbomolecular pump.

Beam manipulation is accomplished with various magnetic steerers and quadrupole lenses. The lenses are positioned so as to optimize their effect on maintaining a reasonably small beam spot ( $< 2$  mm diameter in cross section) from anywhere along the distance between the colimating apertures and the target area. This was accomplished through the use of first order linear beam optics calculations<sup>13,14</sup>.

### 3.2.2 Differential Pumping Region

The final section of beam shaping along the transport system occurs in the differential pumping region. It is composed of a set of variable size apertures and an Edwards 160 mm diameter Diffstak system with a pumping speed of 1300  $\ell/s$  for H and 700  $\ell/s$  for air.

This region serves the dual purposes of 1) an intermediate vacuum region at  $10^{-8}$  torr to interface between the accelerator pressure ( $\sim 5 \times 10^{-7}$  torr) and the target chamber which operates in the  $10^{-9}$  torr range and 2) beam shape definition with variable sized apertures that collimate the beam to at best a  $0.05^\circ$  half angle divergence. These collimators, located 1 m apart, are movable vertically (resettable to  $\leq 0.02$  mm) to allow either a 0.5 mm 1.0 mm or 2.0 mm diameter beam. When samples in the target chamber are to be sputter-cleaned, the 2 mm apertures are used. During analysis, however, they are returned to 0.5 mm diameter for solid state detector work or to 1.0 mm diameter for the electrostatic analyzer. The effect of these changes on vacuum is such that the region is maintained to better than  $1 \times 10^{-7}$  torr and typically  $1 \times 10^{-8}$  torr which for the latter is in good agreement with design calculations taken from the work of Jones<sup>15</sup> and Shapiro<sup>16</sup>. Also located within the differentially pumped region is a liquid nitrogen cold shield which reduces beam hydrocarbon deposition on target samples inside the UHV scattering chamber.

### 3.2.3 The UHV Scattering Chamber

The ultrahigh vacuum scattering chamber is the heart of the spectrometer. As shown in figure 3.2. it houses the particle detection systems, beam current measuring Faraday cup, as well as various vacuum pumps and gauges. It also has attached to it a vacuum quick load device and a sample manipulator arm. The latter two units form the main topic of discussion for the next section while the particle detection systems are described in sections 3.3 and 3.4.

The chamber is maintained at  $\lesssim 5 \times 10^{-9}$  torr under static conditions (as measured by a nude ionization gauge) via a 220  $\mu$ /sec noble vacion pump. Occasional use of a titanium getter pump lowers the pressure to  $< 2 \times 10^{-9}$  torr. By means of a mass quadrupole spectrometer (Vacuum Generators model Q4) residual gas analyzer, the chamber partial pressures have been measured and are given in table 3.1. After several days of bakeout, with a  $150^{\circ}$  C skin temperature, the H, OH, and  $H_2O$  contents are reduced by a factor of two; however, a week later with no auxillary pumping or heat application, they return to levels shown in table 3.1. During target bombardment, the pressure can increase up to  $10 \times 10^{-9}$  torr mainly due to increased hydrocarbon contamination whose partial pressures rise  $\sim 10\%$ . Pressure rises inside the chamber are directly proportional to input beam intensity.

The beam current is measured by means of a beam chop Faraday cup. This device is configured so as to be able to fit in front of the ESA support and solid state detector beam collimation

and deflection system. The cup itself is composed of copper, electropolated with 250  $\mu\text{m}$  of Ni, while the backplate rotator is made from tantalum. The entrance aperture is a grounded front plate behind which is placed an electrically isolated aperture maintained at -100 V dc to suppress electrons from escaping through the entrance<sup>17</sup>.

### 3.3 Sample Handling Systems

Early in the design of the spectrometer, it became apparent that the facility of a multiple sample holder and a quick load transfer device<sup>18</sup> would greatly reduce the required accesses into the chamber. This was deemed necessary when the chamber, after opening to atmospheric pressures for sample input, took several days to return to a  $10^{-8}$  torr vacuum environment. Currently, a sample can be mounted in the quick load device, pumped down to  $\sim 5 \times 10^{-7}$  torr in about one hour, and then injected into the chamber resulting in a pressure rise to only  $1 \times 10^{-8}$  torr. In several minutes, the target carousel can be mounted on the sample rotator and the quick load device, QLD, withdrawn leaving the chamber at  $5 \times 10^{-9}$  torr within minutes<sup>39</sup>.

#### 3.3.1 The Sample Rotator and Target Carousel

The UHV sample rotator is a modified Physical Electronics manipulator. It allows both X, Y and Z translation, vertical tilt and vertical axis of rotation that is converted via gears to a horizontal axis of rotation (perpendicular to the beam direction) which is used to turn the target carousel. Both manipulator and

Figure 3.2. Side view of the UHV scattering chamber showing the orientation of the quick load transfer device and the sample manipulation arm. The cut away section reveals the internal configuration of the two particle analysis and detection systems: the electrostatic analyzer and the solid state detector with its charged particle deflection plates.

THE MEDIUM ENERGY ION REFLECTION SPECTROMETER

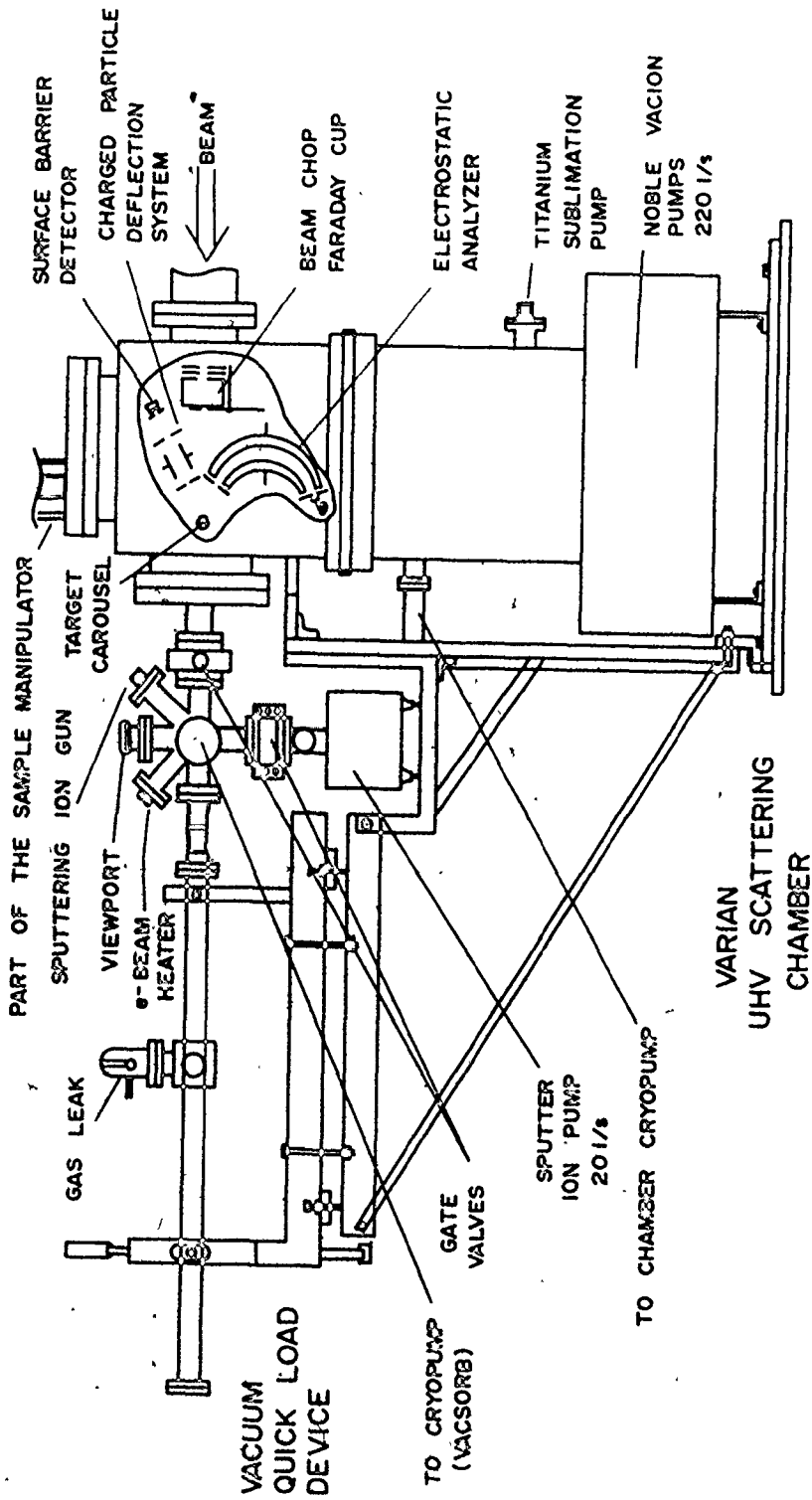




Figure 3.3. The design of the beam chopper type Faraday cup. The orientation is such as to place the cup in front of the electrostatic analyzer and target where the beam enters the chamber. The chopper vane is given a 10 rpm movement by an external HURST type motor. The motion is transmitted to the vane via a UHV rotary feedthrough (Varian #954 5151) and several gear sets. Electron suppression voltage is -110 V dc.

BEAM CHOP FARADAY CUP

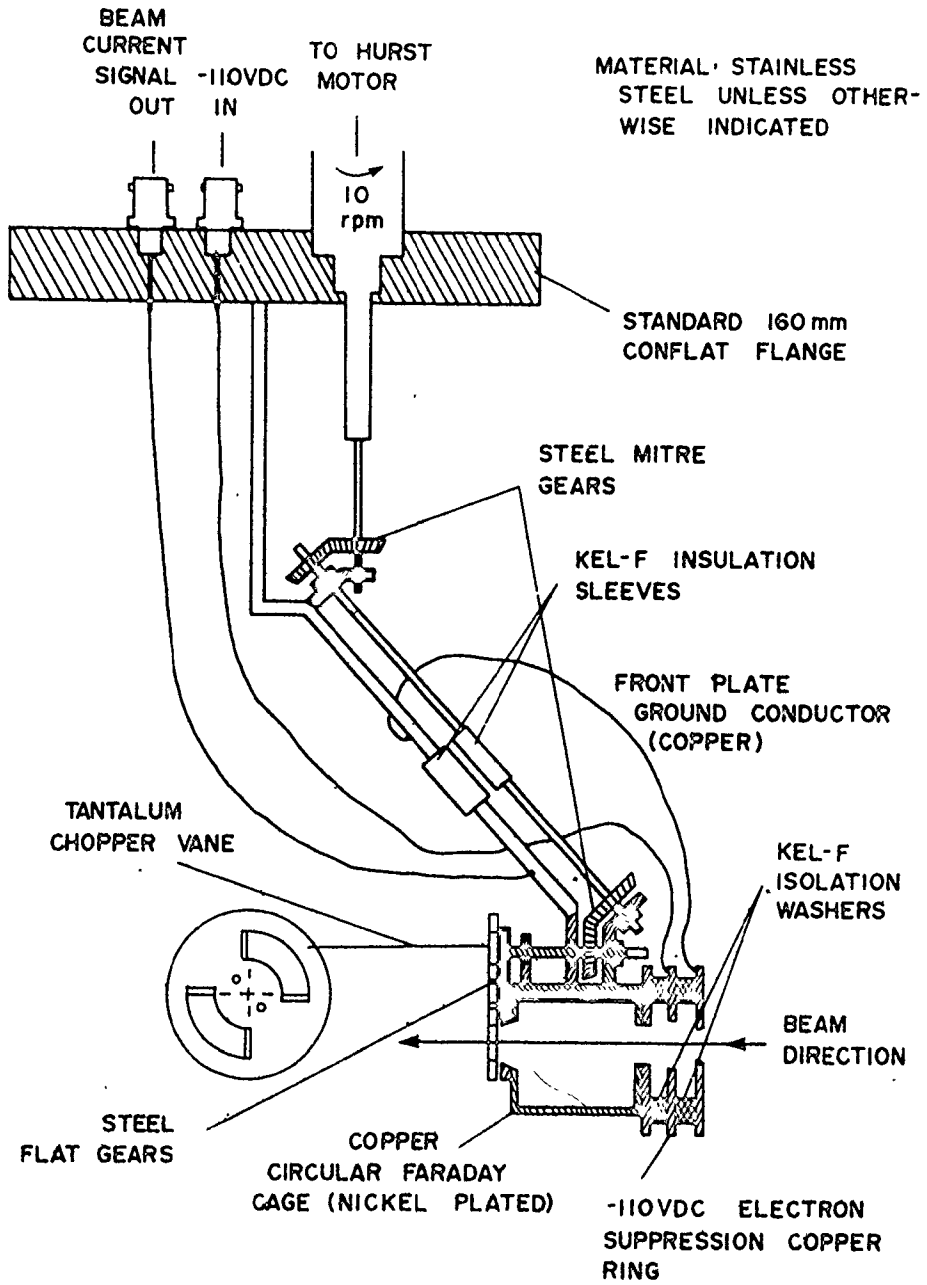


TABLE 3.1

UHV CHAMBER PARTIAL PRESSURES

Total pressure  $\sim 5 \times 10^{-9}$  torr

Element	Pressure $\times 10^{-10}$ torr ( $\pm 10\%$ )	Molecule	Pressure $\times 10^{-10}$ torr ( $\pm 10\%$ )
H	9	CH <sub>3</sub>	2
		CH <sub>4</sub> + O	2
He	0.1	OH	2
		H <sub>2</sub> O	6
C	0.5	C <sub>2</sub> H <sub>2</sub>	1
		C <sub>2</sub> H <sub>3</sub>	3
N	1	N <sub>2</sub> + CO	4
		C <sub>2</sub> H <sub>5</sub>	2.5
Ne	0.5	O <sub>2</sub>	0.25
		C <sub>3</sub> H <sub>3</sub>	2
Cl	0.5	C <sub>3</sub> H <sub>5</sub>	2.5
		C <sub>3</sub> H <sub>7</sub>	2
Ar	1	CO <sub>2</sub>	1.5
		C <sub>4</sub> H <sub>3</sub>	0.5
		C <sub>4</sub> H <sub>5</sub>	0.5
		C <sub>4</sub> H <sub>7</sub>	1.5
		C <sub>4</sub> H <sub>9</sub>	1

carousel are illustrated in figure 3.4. The former contains a "kink" in the rotary transmission axis since the target position is not centrally located within the chamber but is 100 mm to the rear of the chamber center to allow space for the ESA. The rotation is resettable to only  $\sim 4^\circ$ .

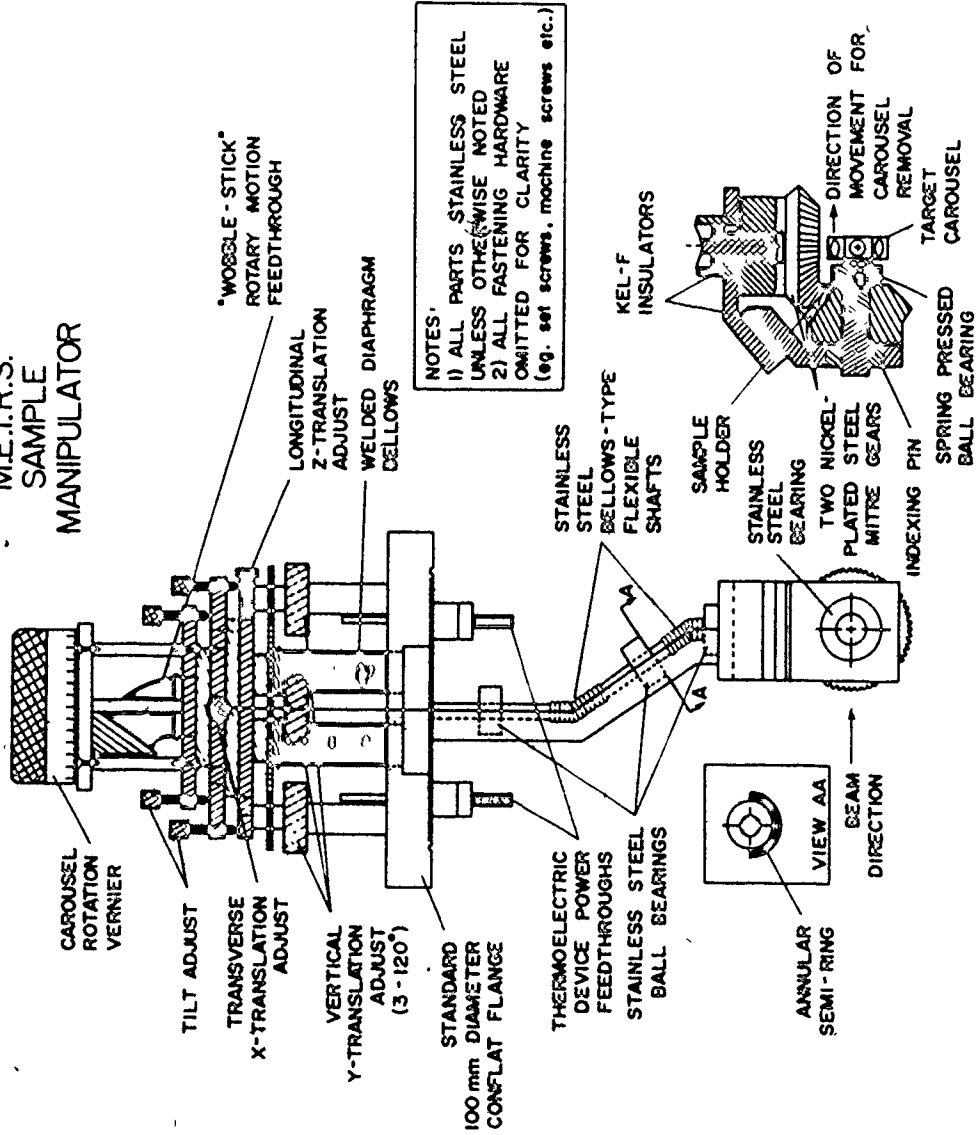
The sample carousel usually contains 5 samples of up to 7 mm square x 1 mm thick size while the 6 th position is reserved for a sample of  $Al_2O_3$  which fluoresces when exposed to light mass ions of at least 60 keV energies and 10 nA currents. The beam can thus be optically centered on the target via sample manipulator translational motion. The carousel, carried on a claw from the QLD can be "snapped" into the sample holder via a pressure motion along the axis of rotation. This action seats a spring exposed ball bearing into the carousel circular shaft groove. Note that the carousel must be aligned in an orientation which accommodates the shaft index pin. In order to reduce UHV "weld" effect for similar metals, the holder is fabricated from type 304 stainless steel while the carousel shafts are made from molybdenum. The claw and carousel are shown in detail in figure 3.5 (b).

### 3.3.2 The Sample Quick Load Device

The quick load device, QLD, is shown in Figure 3.5(a) and is primarily composed of a rack and pinion set. The stainless steel type 316 rack slides on bearings of type 304 stainless steel with the aid of molybdenum disulphide dry lubricant. They are housed inside a stainless steel tube supported on one end with a

✓  
Figure 3.4. The sample manipulator and carousel rotator. The former is a modified Physical Electronics goniometer while the latter is a stainless steel arm that converts the vertical axis of rotation into the horizontal. This allows any one of six target positions to be set into analysis position. Other sample movements are possible (see text). The target carousel is held with light pressure by means of seating a ball bearing exposed in the holder into a groove on the carousel shaft. Rotational freedom is denied the carousel relative to the holder by the use of a longitudinal channel in the carousel shaft which accommodates an index pin welded in the target holder. These must be aligned before acceptance of the carousel by the holder.

# M.E.I.R.S. SAMPLE MANIPULATOR

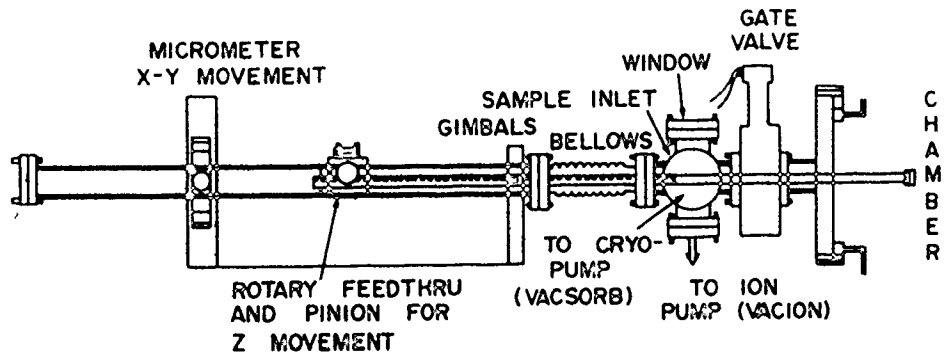


NOTES:  
 1) ALL PARTS STAINLESS STEEL UNLESS OTHERWISE NOTED  
 2) ALL FASTENING HARDWARE OMITTED FOR CLARITY (eg. set screws, machine screws etc.)

Figure 3.5 (a) The quick load device used to provide target access to the scattering chamber without the necessity of exposing the chamber to atmospheric pressures. Local vacuum pumps attached to the device allow changes in pressure independent of that in the scattering chamber.

(b). The target carousel is carried by the claw which is attached to the end of the quick load device rack. This carousel can be either extracted from the holder on the manipulator arm within the chamber and withdrawn or it can insert a new carousel into the chamber and deposit it on the manipulator arm. In either case the rack is then withdrawn and the gate valve closed.

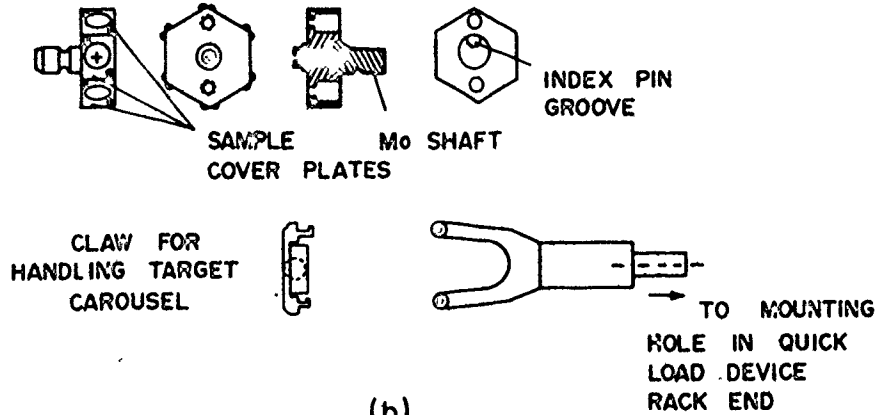
### SAMPLE QUICK-LOAD DEVICE



(a)

### TARGET CAROUSEL

NOTE: ALL MATERIAL IS STAINLESS STEEL UNLESS NOTED OTHERWISE



(b)



micrometer X-Y translator and at the other end with a set of X-Y gimbals. This structure allows the claw and carousel to be manipulated and pressed into its pocket mounted on the sample goniometer. The tube is connected to an eight-fold cross (two are not shown for clarity) via a bellows set. The cross allows independent pump down from atmospheric pressures using the attached liquid nitrogen cryopump (a Varian vacsorb) and a 20 l/s vacion pump both isolatable from the device. The cross also provides a view port and access port for sample entry. Sequential use of these two pumps gives the QLD a recycling time of 30 - 40 minutes with a "before-UHV-entry" pressure of  $\sim 1 \times 10^{-7}$  torr.

#### 3.4 The Electrostatic Analysis System

The ESA is composed of the energy analyzer for the scattered ions and two particle detectors. The former is Hughes-Rojanski<sup>19-21</sup> type 127<sup>0</sup> 17' cylindrical analyzer while the latter involves two channel electron multipliers which serve to detect the ions that transit the analyzer. For target alignment purposes, a solid state detector is mounted on the ESA support. The configuration of the system is shown in figure 3.6. These elements are each detailed in the subsections which follow.

##### 3.4.1 Analyzer Design

In 1929 Hughes and Rojanski pointed out that a two dimensional inverse first power radial field has a refocussing property for charged particle orbits. Consider figure 3.7(a). If a charged particle with energy  $E_0$  is moving at point, P, perpendicular to the radius vector

at that point, then under the influence of the radial electric field, it will describe a circular path concentric with the axis of the field. Charged particles with the same energy but moving in different directions at the same point, P, will trace paths which refocus at point F which is  $127^{\circ} 17'$  from point P. This angle then becomes the basis of the electrostatic analyzer design as does  $90^{\circ}$  for magnetic analyzers.

The inverse first power field is obtained using two concentric cylindrical surfaces with radius  $r_1$  and  $r_2$  and a potential difference of V. The resulting electric field,  $\xi$  is

$$\xi = \frac{V}{r_0 \ln \left[ \frac{r_1}{r_2} \right]} \quad (3.1)$$

where  $r_0$  is the central circular orbit traced by the charged particle,

$$r_0 = \frac{1}{2} (r_1 + r_2) \quad (3.2)$$

Hence the energy,  $E_0$  of the ion having Z units of charge is

$$E_0 = \frac{V Ze}{2 \ln(r_1/r_2)} \quad (3.3)$$

where e is the electronic charge.

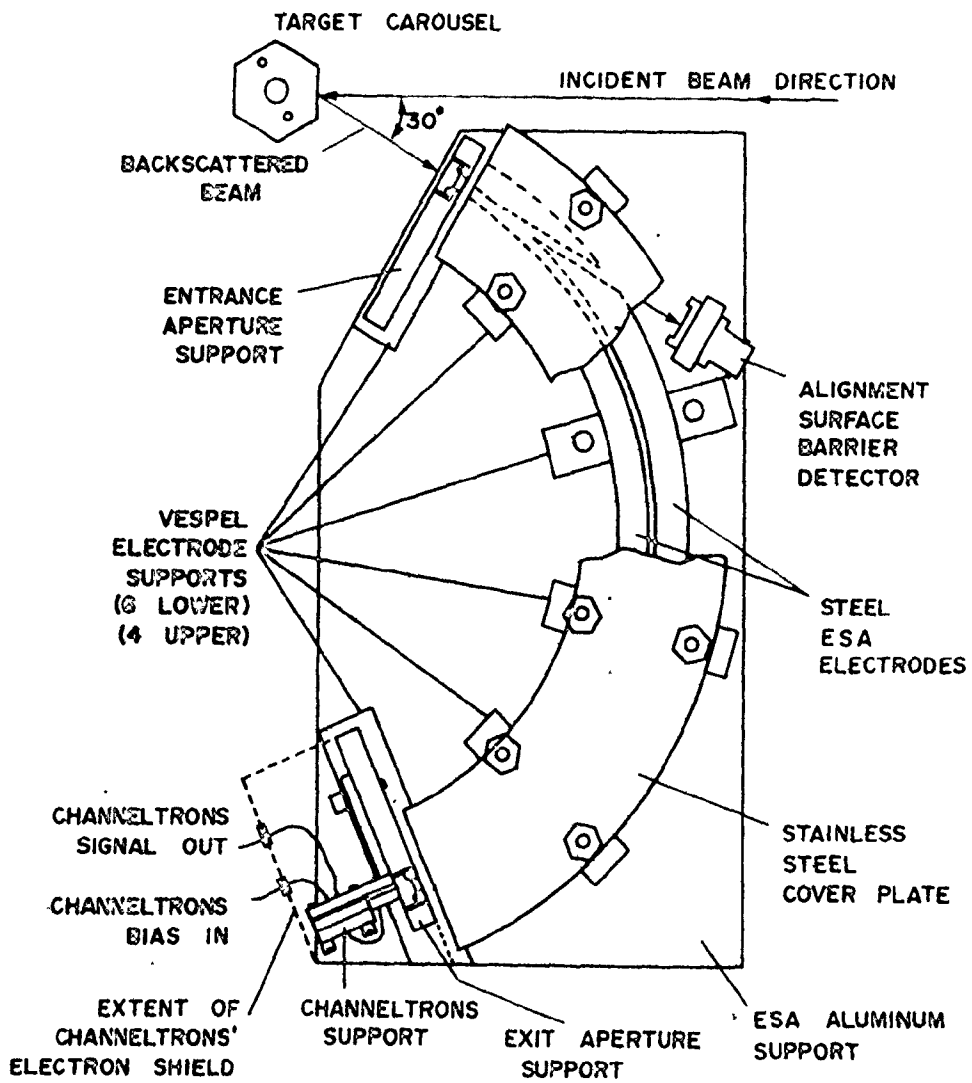
Thus the analysis of 150 keV single charged ions with a gap of 2 mm and central radius of 10 cm requires a plate potential difference of 6 kV. The 10 cm radius is the maximum allowable size for the ESA to remain within the confines of the upper half of the UHV scattering chamber. The use of two 3 KV supplies allows

Figure 3.6. The electrostatic analyzer and associated apparatus. The cutaway reveals a portion of the steel electrodes which are supported by blocks of VESPEL, a Dupont polyimide resin. These, in turn, are compressed by a stainless steel cover on the top and the aluminum ESA support on the back. Shown are the entrance and exit apertures which slide into slots in the aperture supports. Also included are the channel electron multiplier radiation detectors as well as an auxillary solid state detector used for target alignment.

### ELECTROSTATIC ANALYZER CONFIGURATION

ANGULAR DEFLECTION •  $127^{\circ} 17'$   
CENTRAL RADIUS • 101.6 mm  
ELECTRODE GAP •  $2.03 \pm 0.01$  mm

SIDE VIEW



rather easy computer control, in this case remote resistance voltage programming, allowing the plates to operate from zero to + 3 Kv and - 3 KV with a zero voltage condition along the central circular orbit of  $r_0$ . The analyzer electrodes were cut from cold rolled steel cylinders and finished with a thin coating of Ni. They are separated by a gap of  $2.03 \pm 0.01$  mm maintained through upper and lower insulating supports fabricated from VESPEL, a Dupont polyimide resin. VESPEL possesses good electrical insulation properties and yet a low enough vapour pressure to be able to be used within the UHV chamber. Being slightly hydroscopic in nature, the VESPEL was subjected to a vacuum bakeout of  $200^\circ$  C before installation inside the chamber.

Having decided on the ESA external dimensions, the selection of entrance and exit aperture sizes solely remains. These critical widths determine the analyzers' performance, i.e. resolution figures. Hughes and Rojanski<sup>19</sup> have calculated the ESA resolving power to be

$$L_e = (2\beta - 4\beta^2)r_0 \quad (3.4)$$

and 
$$\beta = \frac{v_0 - v}{v_0}$$

where  $L_e$  is the distance between the radius of the circular path  $r_0$  which a charged particle of velocity  $v_0$  will describe and the radius vector,  $r$ , of the path of another particle of velocity  $v$ , measured at the exit aperture. These parameters are depicted in figure 3.8(b). For 1% resolution,  $E = 0.99 E_0$  giving  $\beta = 5 \times 10^{-3}$  and  $L_e = 0.503$  mm. Thus the exit aperture, for  $\frac{E}{\Delta E} = 100$ , must be at

least of 1 mm diameter.

Because the ESA is rather close to the sample active area (exposed to the incident beam), this region cannot be considered as a point source. Consider figure 3.7(c) where, for large entrance angles ( $> 1^\circ$ ) the departure from perfect refocussing of the analyzer cannot be ignored. Again, Hughes and Rojanski<sup>19</sup> have calculated the second order effect and give a measure of this distance,  $L_d$

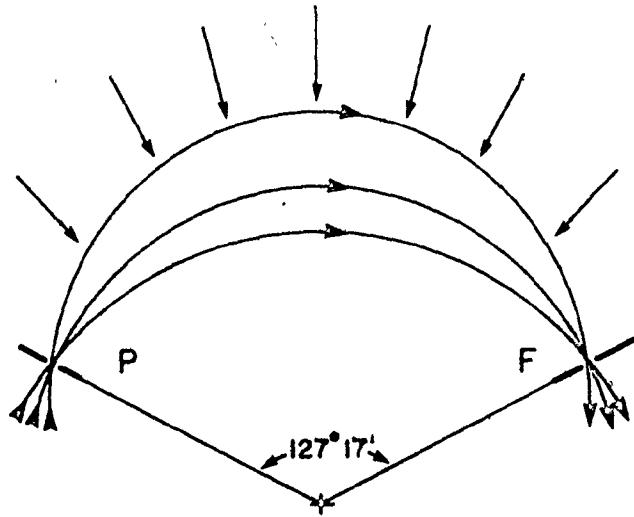
$$L_d = \frac{4\alpha^2 r_0}{3} \quad (3.5)$$

where  $L_d$  is the distance between the central radius,  $r_0$ , and the actual focussing point at the exit aperture for an entrance half angle,  $\alpha$ , subtended by the beam area striking the target using the 1 mm collimating apertures of the MEIRS differential pumping region. For these geometrical conditions,  $\alpha = 0.5^\circ$ , and  $L_d = 0.579$  mm so that in order to maximize the capture rate of the backscattered particles from the target, an exit aperture of 0.6 mm is needed.

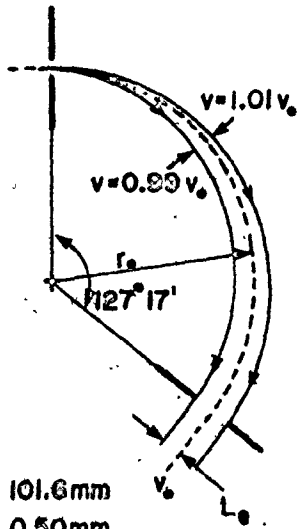
Thus the exit aperture chosen was 1 mm in width. The entrance aperture width was fixed at 0.5 mm width. This is the best compromise between achieving a suitable solid angle for particle acceptance and reducing collimated beam scattering between the analyzer electrodes (which contribute to a constant output background). The length of the exit aperture is 22.2 mm which accommodates two channel electron multipliers with rectangular entrance cones (12 mm x 3 mm) while the ESA entrance aperture length is 4.8 mm, so that the "shadow" of this aperture produced by particles

- Figure 3.7 (a) Illustration of the refocussing property of charged particles at  $127^{\circ} 17'$  in the presence of a radial electric field,  $\xi$ .
- (b) The diagram shows the role played by the analyzer exit aperture size,  $L_e$ , in determining the energy resolution, set here to 1%.
- (c) Using the variable entrance angle,  $\alpha$ , to calculate the departure from perfect refocussing,  $L_d$ , for an extended source of charged particles.  $S_1$  and  $S_2$  are the entrance and exit apertures of the ESA.

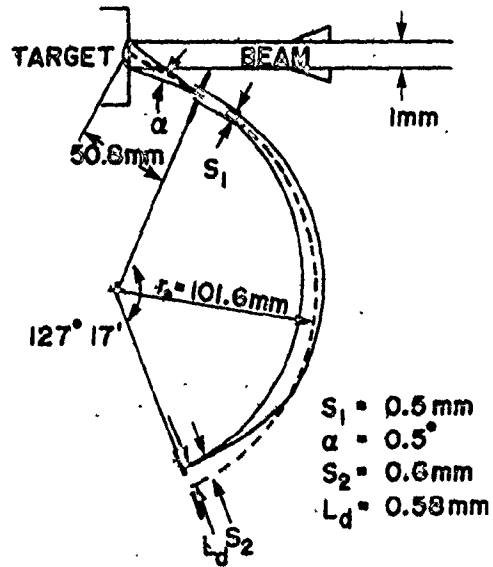
RADIAL FIELD,  $\epsilon$



(a)



(b)



(c)



from a point source located 50.8 mm from the analyzer coincides with the exit aperture length. As shown in figure 3.6, these apertures are mounted on supports which are insulated from the body (electrical ground) of the support structure. This allows biasing of either or both apertures to provide pre-detection acceleration or de-acceleration of the particles. In the present work, however, both apertures are maintained at ground potential.

#### 3.4.2 The ESA Particle Detector

The particle detection circuit of the ESA, unlike the solid state detector system, need only provide signals to determine the presence or absence of analyzed ions, that is, no energy information is required from pulse heights since the energy is determined by the ESA electric field. The devices used are two channel electron multipliers (CEM) obtained from Mullard, Model number B213L, and connected in parallel to yield an output charge pulse when either detector collects a charged particle. Among the advantages of the windowless radiation detectors, are simplicity, bakeable to  $1000^{\circ}$  C, 100% efficiency at energies above 5 keV<sup>22</sup> and at count rates below  $10^2/\text{sec}$ <sup>23</sup>, as well as being small and compact. The disadvantages include fragility and susceptibility to electrons. The latter property meant that the devices must be enclosed in electron shields (electrons mainly from the ionization gauges, ion beam induced secondary electrons and vacuum pump residuals). These detectors are biased at -1500 V dc such that their entrance cones impart a slight post-analysis acceleration to the incoming positively charged ions.

### 3.4.3 Target Alignment Procedure

During the initial stages of operation, it became evident that the positioning of the target with respect to the ESA analysis apertures was extremely critical. The method employed for alignment is to backscatter a high intensity beam ( $\sim 3 \mu\text{A}/\text{cm}^2$ ) of particles from a heavy mass target to provide a large backscattered current. Usually a gold sample is placed in one of six carousel positions of the target holder. The sample position is adjusted so as to maximize the signal obtained from an auxiliary solid state detector. This detector is mounted at the back of the ESA such that through a 2 mm diameter hole bored in the upper (+) electrode, and through the ESA entrance aperture, the detector has a line of sight to the target. The integral of all backscattered particles detected by this device can be routed to a linear rate meter whose count rate is monitored as function of the target position. In this way, the target can be manipulated to an optimum position. The time taken for an alignment is typically 5 minutes.

### 3.5 Solid State Detector Systems

The solid state detector system fulfills two separate applications: 1) it serves as a MeV beam Rutherford backscattering system as described in Part II of this thesis and, 2) together with a set of electrostatic beam deflection plates and collimators, it is used to determine the spectra of both neutral and total (charged + neutral) particles backscattered at medium energies from solid surfaces in order to calculate the ratios of ions to atoms.

These charged-to-neutral ratios, C/N, can then be used to correct the corresponding spectra derived from ESA work.

The solid state detector was obtained commercially from Oak Ridge Technical Enterprises Corporation in Tennessee, U.S.A. It is a specially selected low noise partially depleted surface barrier detector model number ORTEC CA-14-50-300-S with an active area of  $50 \text{ mm}^2$ , a depletion (sensitive) region of  $300 \text{ }\mu\text{m}$ , and a nominal resistivity of  $4.5 \text{ K}\Omega \text{ cm}$ . Normally, a  $40 \text{ }\mu\text{g/cm}^2$  gold entrance window is supplied, however, by request, the thickness was reduced to  $20 \text{ }\mu\text{g/cm}^2$ . The thinner entrance window results in less energy loss of the incident particle before it reaches the sensitive semiconductor region which is particularly important in the medium energy region. The back electrode is a  $40.1 \text{ }\mu\text{g/cm}^2$  deposit of Al. A reverse bias leakage current of  $190 \text{ nA}$  is observed when the device is operated at the suggested  $+ 80 \text{ V}$  dc potential.

In order to further improve the resolution of the device, it is mounted within an Al cylinder of  $8 \text{ cm}$  diameter and  $5 \text{ cm}$  height which is cooled via a Cambion model 3959 thermoelectric device (TED). The TED is sandwiched between the Al detector block and a stainless steel sink composed of a hollow plate ( $5 \times 5 \times 2 \text{ cm}$ ) through which chilled water at  $10^0 \text{ C}$  is circulated. The TED maintains the detector at  $0^0 \text{ C}$  when operating at  $3.5 \text{ volts}$  and  $8 \text{ amperes}$ . From a room temperature start, the process requires  $1 \text{ hour}$  to reach the base temperature with no observed increase in the chamber pressure of  $\sim 5 \times 10^{-9} \text{ torr}$ . The detector exhibits a

14% improvement in the resolution figure over room temperature when cooled in this manner. For all the experimental work which follows, the detector is maintained at 0° C when used. The configuration is shown in figure 3.8 in the next section.

This entire detector ensemble is mounted so as to detect particles backscattered through 150° and is located in the vertical plane; that is, in the same configuration as the electrostatic analyzer. In front of the detector is mounted a tantalum aperture of slightly smaller area (7.5 mm in diameter) than the active area of the detector to eliminate detector edge effects. It also serves to define the acceptance solid angle of the detector which is required for absolute measurements in the Rutherford scattering regime. Also included is an externally operated shutter which shields the detector when not in use. This is particularly important when using the ESA which requires such large backscattered beam intensities ( $\sim 1 \mu\text{A}/\text{cm}^2$ ) that, for the detector if left unshielded, would result in a large increase in the radiation damage accumulated.

Because the ESA is insensitive to neutral particles, a determination of the charged fraction of the backscattered particles is necessary in order to correct the ESA results and obtain quantitative analysis. This is carried out by electrostatically deflecting charged particles out of the detector bound backscattered beam leaving only the neutral component. The total backscattered beam (charged + neutrals) is also measured in the absence of any deflecting potential. As shown later, the charged yield can be calculated from these

measurements which relies on the fact that the solid state detector is energy sensitive and not charge sensitive.

It was calculated<sup>24,25</sup> that two stainless steel plates, 55 mm in length, separated by 6.35 mm, maintained at a 4 KV dc potential difference and located 75 mm from the detector, would be able to deflect a 150 keV ion 8 mm at the detector front, that is off the sensitive region. In order to reduce low angle scattering of the lower energy particles into the detector a set of grounded carbon collimators (6 mm thick) were placed immediately before and after the deflection plates at ground potential. All sharp corners were rounded in order to eliminate electron field emission which increases the solid state detector background in the very low energy region.

### 3.6 Computer Control

The control of the entire spectrometer is accomplished through a PDP11/05 minicomputer containing 28 kW of core memory and operating from a floppy disk based software system, RT-11 from Digital Equipment Corporation (DEC). The computer is assembly language programmed to control the ESA in a single channel mode of operation involving a dose driven multichannel scaling process as described in section 3.5.1, and to perform multichannel pulse height analysis on the solid state detector pulses as explained in section 3.5.2. It provides various data manipulation operations involving simple arithmetic operations between groups

(usually of 256 channel spectra) stored single precision in a 4 kW channel buffer. The data may be also displayed on a Tektronix model 602 display unit, stored in a DEC RX01 floppy disk or printed on a LA36 decwriter. All these operations may be done concurrently with data acquisition as detailed in section 3.6.3.

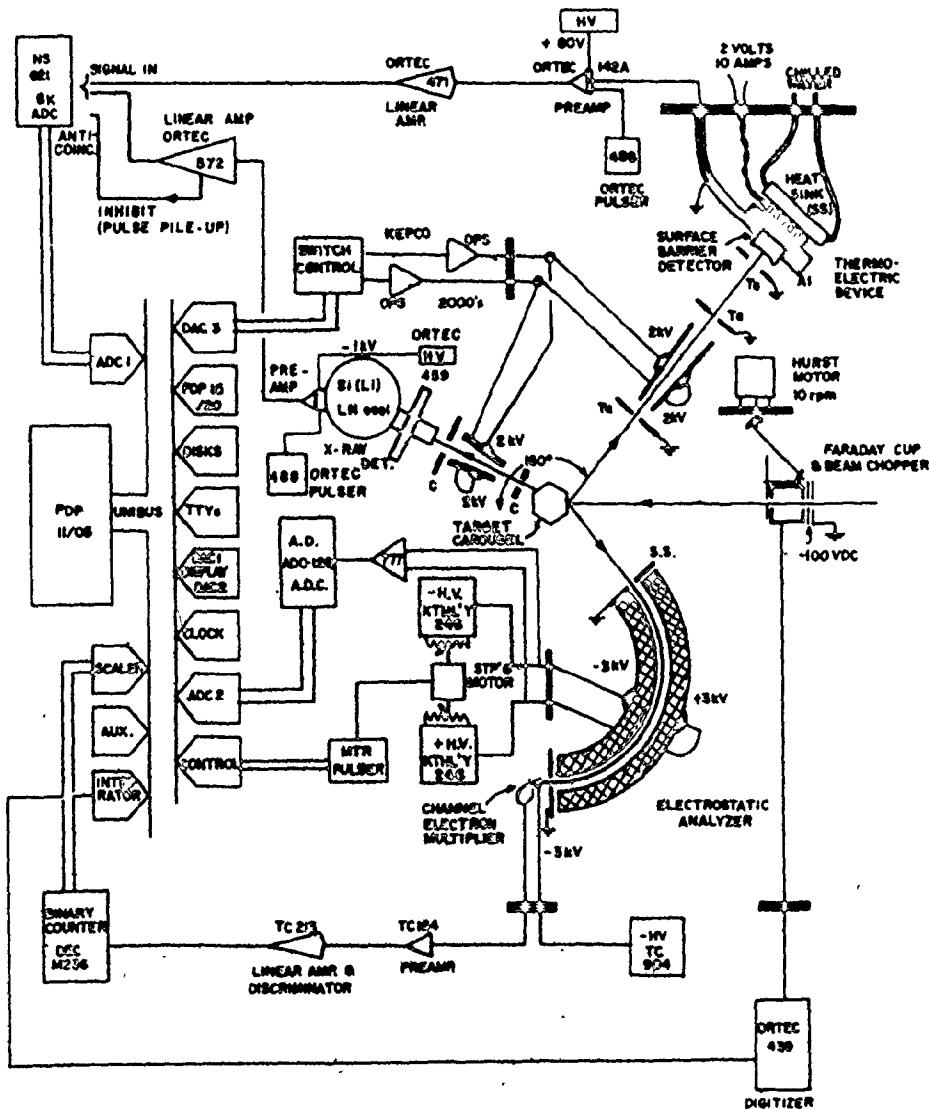
Also in this last section are described the data handling procedures used which are common to both MEIRS detection systems as well, some characteristics of the software system are given at this time. The MEIRS operating program is MES11 (Medium Energy Scattering on the PDP11) and is reproduced in the appendix, section AI, along with a command explanation section in AII. A block diagram of the MEIRS control system is shown in figure 3.8. For completeness, figure 3.8 also contains a schematic of a commercially obtained "windowless" Si(Li) X-ray detector from ORTEC Inc. This device has not been used during the course of the thesis work and hence will not be considered in any detail here. Figure 3.9 and 3.10 illustrate the computer interfaces constructed to operate the MEIRS. Explanation of the various facets of the design and operation of the computer systems are made where appropriate throughout the remainder of this chapter.

### 3.6.1 Electrostatic Analyzer Operation

The hardware system interfaced to the computer occupies the lower half of figure 3.8. The computer, through software control, can pulse a stepping motor (Superior Electric HS50 with 400 steps per 360<sup>0</sup> revolution and pulser STM1800CV) which turn in either

Figure 3.8. The Medium Energy Ion Reflection Spectrometer System including scattering chamber components, associated electronics and computer control configuration.

MEDIUM ENERGY ION REFLECTING SPECTROMETER - 1979





direction through anti-backlash gears two sets of doubly ganged Beckman 20 turn 1.5 M $\Omega$  potentiometers (doubly ganged due to a maximum breakdown voltage of 1.5 kV for each). These potentiometers control two Keithley Model 246 3 KV remote resistance programmed power supplies which charge the two ESA plates and a precision (0.5%) resistor chain. The chain allows 30 volts to be tapped from the 6 KV developed across the plates for a feedback circuit from which the computer sets the ESA potential. This feedback signal is summed by a gain adjustable operational amplifier whose 0 - 10 volt output is digitized on software command by a 12 bit Analog Devices Model ADC-12Q, A/D converter.

The operation of the ESA system is analogous to a multi-channel scaling technique where, until a preset value is reached, the computer counts all events into a single channel (or energy). In this case, the analyzed particle count is tabulated in a binary up/down counter whose contents are transferred to memory at the address of the active channel when counting is complete. Upon reaching this preset, which may be determined by time or dose, etc. the computer stops accepting events, moves the plate potentials either up or down (depending on the current scanning direction) one step until the feedback signal change equals the step width change and then resumes counting in the new channel. This new counting channel may be adjacent to the previous one, or may be a variable number of channels beyond; that is, the computer allows up to 7 regions of interest to be selected from the display, each to be sequentially scanned. This reduces acquisition time for

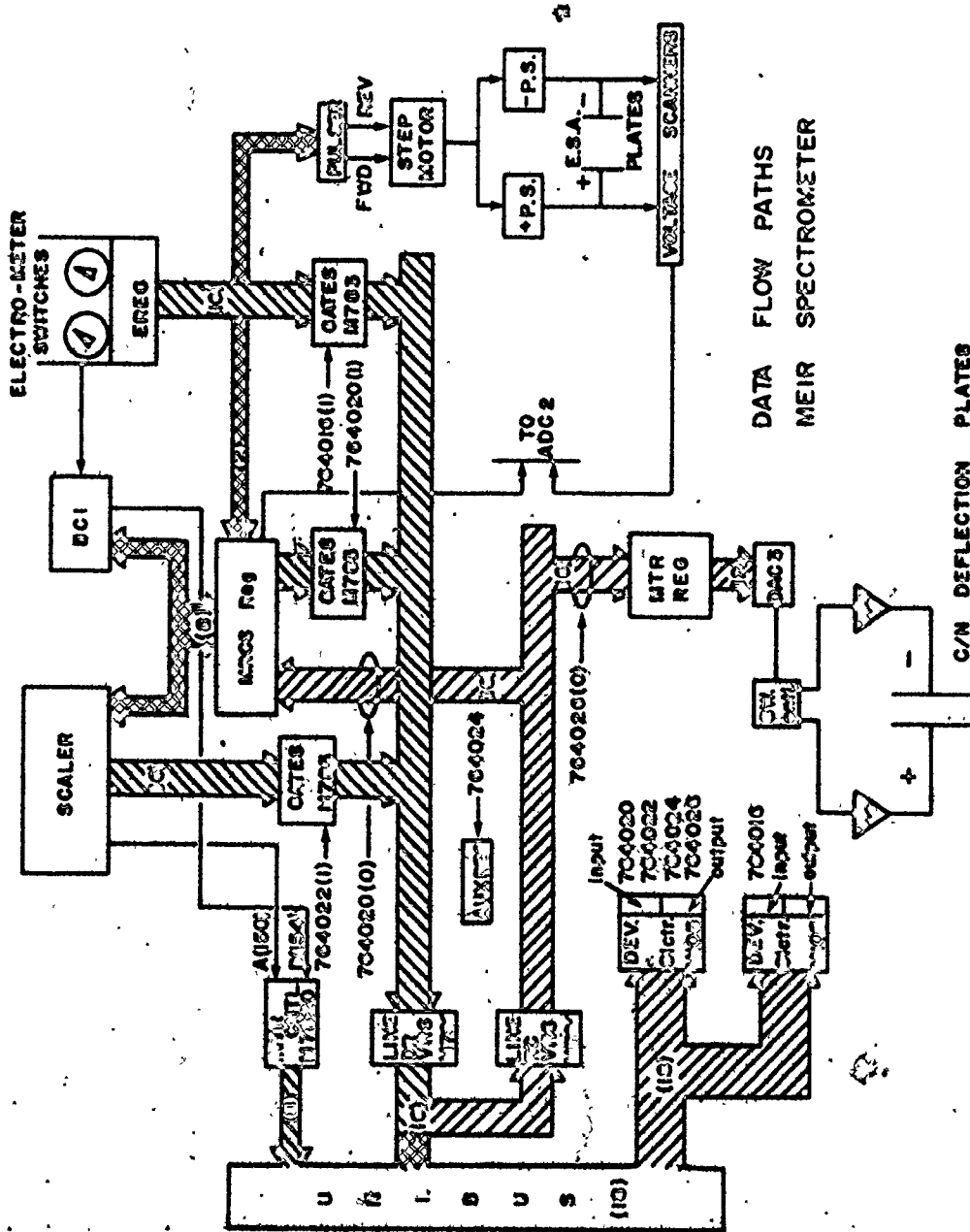
spectral generation from the ESA and also minimizes target exposure to the ion beam.

In detail, the feedback loop provides a digital result from a second A/D converter (ADC2) whose conversion gain is set, in software, to coincide with the selected display channel width. This allows a direct correlation between the active channel on the display and the output of ADC2 which is proportional to the potential developed across the ESA plates. This simplifies software operation since, during scanning, the current counting channel number is the value to which the digitized feedback output is set by adjusting the ESA plate potential through appropriate pulses sent to the stepping motor. The counting procedure is to scan each channel of the regions in ascending order until finished all the regions or spectrum and then reverse the procedure by scanning in descending order. The number of complete scans (once up, once down) is user specified. The preset value to which each channel is left active is a dose measurement number that is calculated knowing the number of channels involved in the regions of interest, the number of scans requested and the total dose required to generate the spectrum. For the work carried out in this thesis, the first channel stores the incoming pulses from an ORTEC Model 439 beam current integrator/digitizer and it is this running total that signals a channel advance when the preset is reached.

### 3.6.2 Surface Barrier Detector Operation

As mentioned in section 3.4, the surface barrier detector can be operated in two modes. The normal mode involves the use

Figure 3.9. Computer interface to the spectrometer providing voltage control and multichannel scaling capability for the electrostatic analyzer.



of the detector in Rutherford backscattering operation, (MeV region), where a spectrum is obtained either as a function of dose as determined from the Faraday cup or as a function of time as derived from a nuclear instrumentation module, NIM, standard timer/scaler. The second mode is the specialized charged fraction operation where the electrostatic deflection plates are energized or de-energized and appropriate spectral routing occurs.

In the normal mode of operation, the detected events are pulse height analyzed by a commercially obtained A/D converter from Northern Scientific, NS621, which is a 50.MHz, 13 bit ADC. Usually, the completion of spectral accumulation is signalled by reaching a preset dose. The running dose total originates from the commercial current digitizer whose output pulse produces an interrupt signal whenever the set particle charge amount is reached. This digitizer signal is set by software to enter the top priority interrupt level 7 so that no time delay is involved while waiting for higher level interrupt requests to be serviced. It is in the digitizer interrupt service routine, once the preset is reached, that the ADC1 and digitizer systems are disabled. The service routine for ADC1 operates on level 6 and together with the NS621 yield a dead time of 70 microseconds. More details on these aspects are given in section 3.6.3.

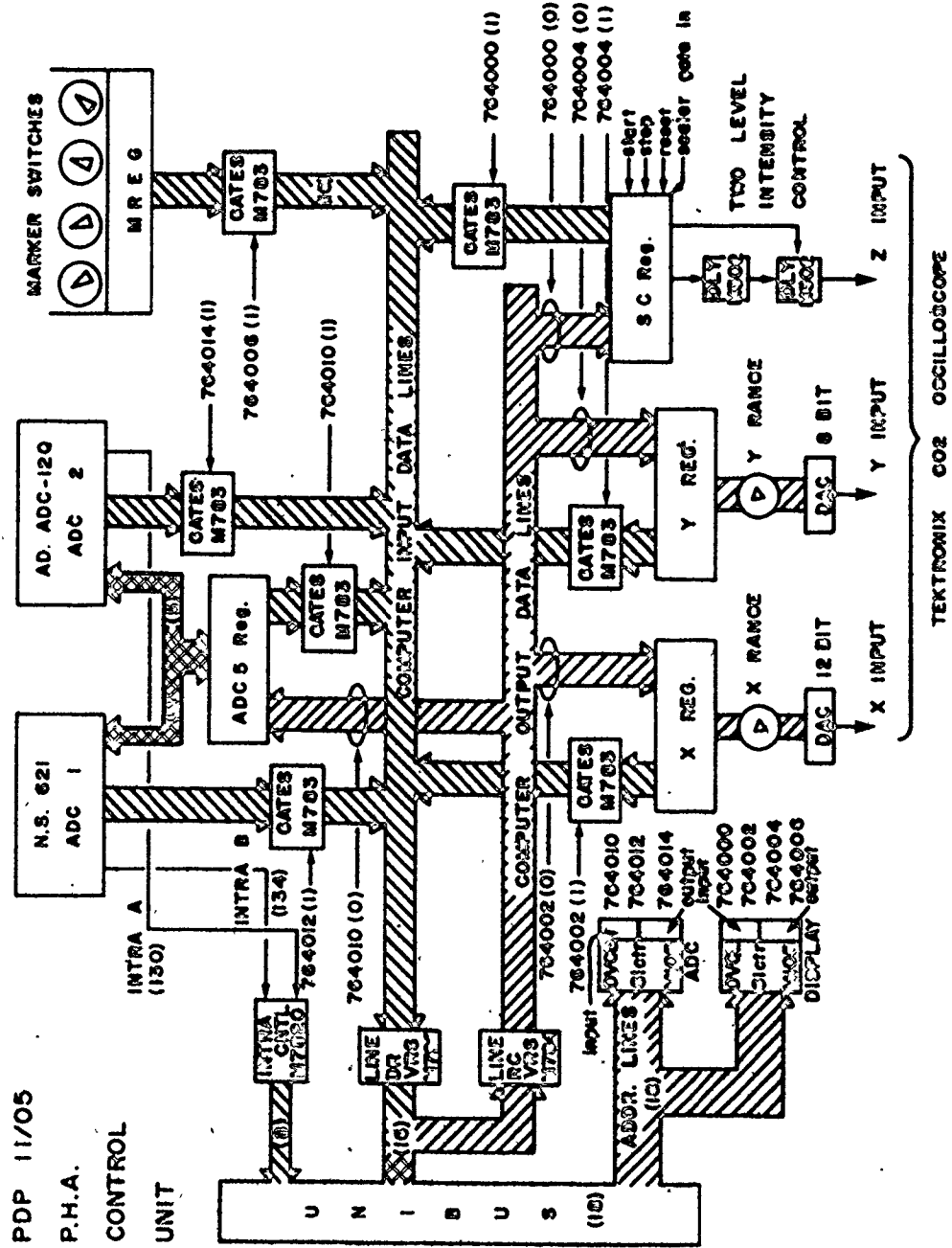
The special mode of operation of the surface barrier detector involves the collecting of two spectra one, when voltage is applied to the electrostatic deflection plates, and one when not. The basic components involved in this operation are shown

in figure 3.8. Here, a computer controlled digital-to-analogue converter (DAC3) signals either a 0 or 8 volt dc level to two optoisolators and operational amplifiers which present two small dc control levels, one negative and one positive to two high speed KEPCO OPS-2000 power supplies with a slew rate of 1 volt/  $\mu$ s in order to switch the plate potentials to either 0 or 2000 V. The computer interfaces are shown in block diagram form in figures 3.9 and 3.10.

Software operation during this special mode initially utilizes the system time clock and an external pulse generator. The computer follows the prescription given below:

- 1) an approximate dwell time for each spectral collection period is keyboard entered (typically 2 seconds)
- 2) using intensified points (markers) on the display which are movement controlled by setting rotary switches, a display window is designated about a pulser generated peak in the pulse height analyzed spectrum. (This artificially generated peak is kept upstream in the display from any particle detected regions of interest by adjusting the linear amplifier gain so as to allow for this.)
- 3) these set of pulses are counted by allowing ADC1 active for the time specified in step 1. Upon time completion, the events contained between the markers are integrated and it is this value which becomes the preset, which, when reached, signals a switch of the plate potential and rerouting of spectral events

Figure 3.10. Computer interface to the spectrometer providing spectral display and multichannel pulse height analysis capability.





- 4) begin actual data collection run by proceeding as follows:
  - a) turn on the OPS supplies and wait 1.5 seconds (It was determined that the switching from 0 to 4 keV affected the surface barrier detector severely by inducing a long pulse,  $\sim 1$  second, within the device. This baseline shift as measured by ADC1 degraded the detector resolution unless the ADC enable is delayed.)
  - b) enable ADC1 and route events to group 1 in memory until the pulser peak window events integrate to the preset value of step 3.
  - c) disable ADC1, zero the OPS supplies, erase the pulser peak window contents and wait 1.5 seconds.
  - d) enable ADC1 and route all acquired events to group 2 (another portion of memory) until preset is again reached.
  - e) repeat step c).
  - f) go to step b).
- 5) loop through steps b) to f) until by software command the run is terminated.

In this manner the two spectra, one representing neutral back-scattered particles (H.V. on) and the other charged + neutral backscattered particles (H.V. off), are generated. Because the pulse generator events are collected along with detected events and these counts are used as switching criterion, the spectra are collected in "live time" so that they are already "dead time corrected". Hence they can be subtracted and divided "as is" in

order to obtain the charged fraction as outlined in section 4.4.5.

### 3.6.3 Data Handling Operations

This section outlines various facets of the computer hardware and software systems that are common to both ESA and solid state detector operations.

Figure 3.8 shows the various devices attached to the PDP-11/05 unibus. The clock, teletype (TTY) and transceiver to the PDP 15/20 are commercial units obtained from DEC. The remaining devices were developed for use on the spectrometer system.

Figure 3.10 depicts the pulse height analysis units as interfaced to the unibus. The design, with very few modifications is taken from the work of R.A. McNaught<sup>26</sup> and uses DEC series M logic boards to interface directly into the unibus structure. It provides two command and status registers, one for the two A/D converters (ADCSR), and one for the display scope (SCR). Various bit assignments for these registers are given in the appendix. An external timer/scaler operating with NIM logic can also provide timing confirmation through the scope command register inputs of START, STOP, RESET and T/S GATEIN. Three other registers are used for display purposes, two for controlling the X and Y coordinates of the analogue display unit DAC's and one for the marker which contains the channel address of an intensified display point as set by four independent rotary marker switches. Both ADC's can interrupt the computer when a digitized result is available. In the PDP11 system all interrupts are vectored so that a time

consuming polling procedure is avoided when servicing the requests.

Figure 3.9 illustrates the interfacing required to provide for the operation of MEIRS devices not directly involved in the pulse height analysis system. The ON/OFF control of the C/N deflection plate potentials is accomplished by writing ONES or ZEROES into the meter register (MTR) which drives a D/A converter (DAC3) whose output signals the control lines of the OPS supplies. Beam current integration is accomplished by allowing the pulse output from the commercial unit (carrying the charge or dose information) to interrupt the computer. The ESA single channel scanning procedure, as outlined in the preceding section, involves stepping a motor either up or down to vary the voltage developed across the ESA electrodes until ADC2 in the feedback loop indicates the desired potential. Both ADC2 and the stepping motor pulser are controlled by the MEIRS command and status register, MRCSR. It also controls the scaler used to count events from the ESA. This 16 bit scaler can be read from or written into the computer and also generates an interrupt signal when an overflow condition is reached. In both figures 3.9 and 3.10, the addresses of all registers and various devices are unique and selected by changing the jumper configurations on the device selector boards (DECM105). These are given in the appendix, section AII.

The last topic of this chapter involves software considerations. The real time requirements of the MEIRS has necessitated an assembly language approach to control software (the code MES11 is listed in section AI of the appendix). The DEC RT-11 operating

system provides an environment aptly suited to these stringent time requirements. The software system operation allows a single user monitor or a foreground/background option (F/B) where two programs are shared during execution. The single job (SJ) system was selected since the interrupt-request-to-interrupt-service time is minimal, that is, 5 - 20  $\mu$ sec for SJ versus 50 - 200  $\mu$ sec for F/B<sup>27</sup>. The purchased software also allows the use of various pre-programmed MACROS (assembly language subroutines) for teletype output and floppy disk I/O with directory update for all spectrum files.

These spectra so stored are then transferred, off-line, to a 56 KW PDP-15/20 computer via a high speed asynchronous bidirectional link. This computer, running under ADSS/XVM then stores the spectra on DECTAPE for later use in a fortran analysis program which applies various corrections, fitting procedures, energy calibrations, etc. as outlined in the next chapter. The software implementation of the link involved running two programs on each of the linked processors, PIP11 on the PDP-15 and PIP15 on the PDP-11 (cf. appendix section AIII). The programs transfer 7-bit ASCII data with a parity bit at 4800 baud. Since the information is stored as signed integer ASCII digits, the 16 bit/18 bit word difference between the two CPU's is not a problem. The receiver opens a file and waits for data from the sender. The sender reads a block of data (256 characters) from the disk and sends it a character at a time to the receiver who stores it in a buffer. When the buffer of the receiver is full, it is then written onto disk and another block is read from the disk by the sender. On end-of-file at the receiver,

the unit times out and closes the data set. Delay routines are provided for the different disk access times on the two computers since one uses a flexible disk (PDP-11) and the other (PDP-15) a fixed head platter disk (DEC: RF01). The mode of transfer works successfully for files of varying size. A 256 channel spectrum is stored in a 4 block data file and requires about 1 second to transfer one block of data.

## CHAPTER 4

### System Calibration and Performance

#### 4.1 Introduction

This chapter outlines the energy and geometry calibrations and necessary spectral corrections applied to the two basic MEIRS detection systems: the ESA and the solid state surface barrier detector. Results are presented which indicate the MEIRS performance characteristics. Before any particle detection system can be calibrated for either energy or geometry, the incident beam energy must be known. Hence the chapter begins with the procedure followed to determine the output particle energies in both MeV and keV ranges for the two accelerators used by the MEIRS. In section 4.3, the ESA energy calibration is given and the spectral manipulations associated with the constant resolution factor and the charge-to-neutral ratio (C/N) corrections are described. The surface barrier detector system calibrations are given with respect to scattering geometry in section 4.4 and its losses when applied to the medium energy regime in section 4.5.

#### 4.2 Accelerator Energy Calibrations

The determination of beam energies for the two accelerators cannot be accomplished in the same manner. The 150 KV machine accelerating potentials can be measured directly by electronic means; for the 3 MV machine, one must resort to a nuclear reaction

technique where a rather narrow band of energies striking a sample excite a measurable gamma ray response.

For the 150 KV accelerator, a portion of the accelerating potential is tapped from a precision resistor bleeder chain attached between the high voltage terminal and ground. This signal is measured via a gain adjustable digital voltmeter with a reading sensitivity of  $10^{-4}$ . Using a well calibrated high voltage probe and a precision digital multimeter, the voltmeter can be set for direct voltage reading to within 2%. This figure is less than or comparable to (depending on the voltage) the variation in beam energy maintained by the beam energy stabilization system.

For the 3 MV accelerator, the  $Al(p,\gamma)Si$  nuclear reaction can be used to provide known proton energies in the MeV range from the 1.78 MeV gamma ray resonance of the Si nucleus. Using a 500 Å film of aluminum on a tantalum substrate target and an auxiliary 3 x 3 inch NaI(Tl) detector system, the gamma ray yield is maximized as a function of the accelerator terminal voltage. This corresponds to a proton beam resonance energy of 992 keV. The higher proton resonance of 1120 keV is used to verify the system linearity which shows no deviation outside the uncertainty in beam energy stability (< 1%). A generating voltmeter is used to monitor terminal voltage and includes, for readout, a precision digital voltmeter with a reading sensitivity of  $10^{-4}$ . This device is then calibrated<sup>23</sup> to better than 2%. The long term reproducibility of the digital voltmeter readout, after performing a duplicate calibration, is about 0.5%. The target thickness of 500 Å of Al provides

a signal that is reasonably intense and yet not thick enough to extend the response peak width significantly; that is, no asymmetry of the gaussian shape for the gamma ray peak is observed as a function of the terminal voltage.

#### 4.3 The Electrostatic Analysis System

Before the ESA can be employed in any quantitative manner, the system must be calibrated with respect to ion energy versus the applied electric field, its energy resolution, scattering geometry, etc. while the resultant spectra must be corrected for the ignored neutral component of the backscattered beam and constant resolution. The techniques used to perform these calibrations and the results of such analyses are presented in sections 4.3.1 and 4.3.2 respectively.

##### 4.3.1 ESA Energy Calibrations

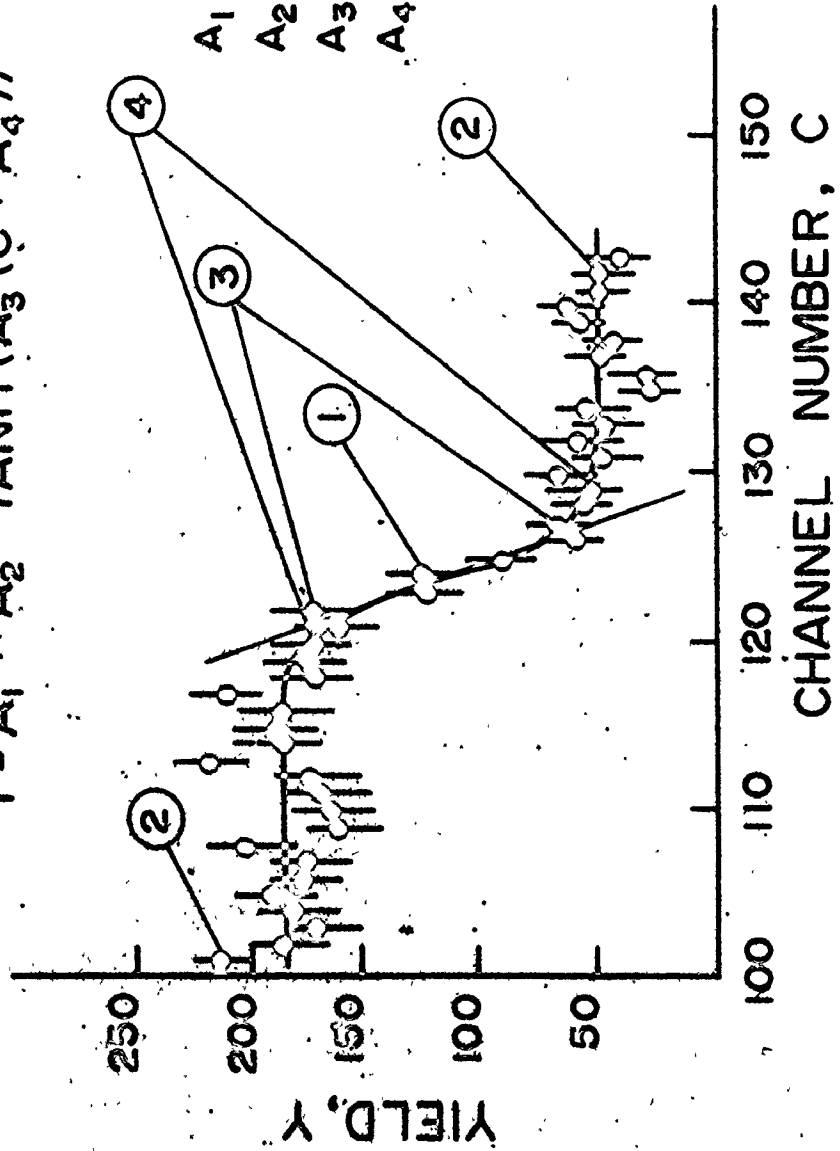
The assignment of an energy value to the applied plate potential of the ESA and hence to the channel number of the current counting interval can be made by means of a backscattering experiment. The target is a thick ( $\sim 2800 \text{ \AA}$ ) e-beam evaporated gold layer onto a polished Si substrate. It is placed normal (to within  $1-2^\circ$ ) to the incident beam of  $\text{He}^+$  ions. The resulting backscattered spectrum yields an edge whose energy at the inflection point can be calculated by use of the scattering kinematic factor to within 1%. (General backscattering concepts are detailed in section 6.3.1 -- especially equation 6.27). Note that at a  $150^\circ$  backscattered angle a change of greater than  $5^\circ$  will affect the



Figure 4.1. Non-linear least squares edge fitting of the ESA response to 100 keV He<sup>+</sup> backscattered from a solid Al target. The form of the fitting function is shown along with the final parameter values which minimize  $\chi^2$ . The first guess at the parameters is accomplished by specifying seven channel numbers (see text).

100 keV He<sup>+</sup> ON Al  
 $Y = A_1 + A_2 \cdot \text{TANH}(A_3(C + A_4))$

$A_1 = 135$   
 $A_2 = -49$   
 $A_3 = .37$   
 $A_4 = -124$



kinematic factor by less than 0.5%. The inflection point of the edge can be determined accurately ( $\sim 0.1$  of a channel) by a non-linear least squares fitting procedure<sup>29</sup> which minimizes  $\chi^2$  via variation of the fitting parameters<sup>30</sup>. The form of the fitting function is

$$Y(C) = A_1 + A_2 \text{TANH}(A_3(C + A_4)) \quad (4.1)$$

where  $Y(C)$  is the yield in channel  $C$  and the  $A$ 's are the fitting parameters.

Because the fit involves an iterative procedure, a first guess at the shape of the edge must be made. As shown in figure 4.1, this is accomplished by specifying seven points or channel numbers on the spectrum. They are: 1) the inflection point channel number; 2) a pair delineating the region of fit; 3) another pair located so as to define the slope of the curve at the inflection point; and 4) the final pair used in conjunction with pair #2 to define the ordinate levels of the spectrum before and after the occurrence of the edge. The computer program then proceeds to minimize  $\chi^2$  to better than a 1% convergence limit, usually within three to four parameter variations. A typical final fit showing both left and right hand edges is given in figure 8.3(a). The inflection point occurs at  $(C, Y) = (-A_4, A_1)$ . It is this channel number that can be assigned an energy value. The results of the ESA energy calibration are shown in figure 4:2. The calculated relationship determined by linear regression is

$$E(\text{keV}) = (0.559 \pm 0.009) C + (1.56 \pm 0.03) \quad (4.2)$$

Using the geometry design equation of the previous chapter, approximate confirmation of this result can be made. By software command, the computer can hold the potential across the ESA plates at a requested channel number so that the exact ESA plate voltage differential can be measured. By means of this technique and equation 3.1, the calibration is found to be

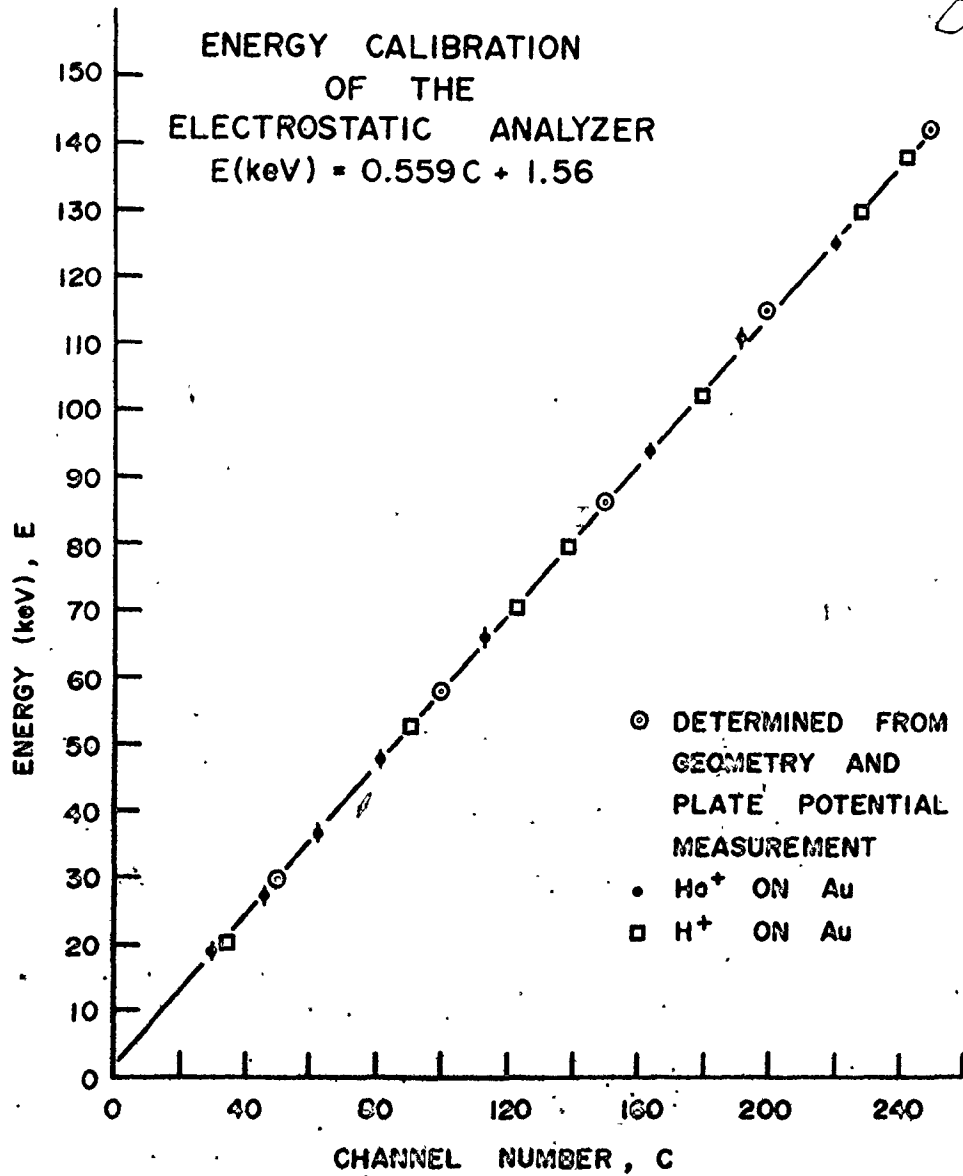
$$E(\text{keV}) = 0.566 C + 1.20 \quad (4.3)$$

which is in excellent agreement with equation 4.2. The energy calibration as expressed by equation 4.2, is used throughout this work and has remained within 1% of this relationship when periodic checks on the calibration have been made.

#### 4.3.2 ESA Spectrum Corrections

As shown in Chapter 3, the ESA possesses a resolution characteristic which depends on the geometrical configuration of the device since the effective energy window is proportional to the energy of the ions accepted. Hence the resolution figure ( $\sim 1.4\%$ ) is a constant fraction of the energy being analyzed rather than fixed at 3 - 10 keV as in a solid state detector. Also the ESA, being an energy upon charge (E/q) filter, only collects the charged ions, ignoring the neutral fraction of the backscattered yield which may be substantial. How both corrections are applied is outlined next. Figure 4.3 illustrates the two corrections as applied to an ESA generated spectrum.

Figure 4.2. Energy calibration for the ESA relating detected particle energy and plate voltage (channel number). Two methods are used: 1) a direct plate potential measurement using the geometry design equations of Chapter 3 and, 2) the energy of the backscattered particles as derived from the accelerator energy calibration and the scattering kinematic factor.



To account for the variation in the analyzer energy resolution, each channel yield is corrected<sup>31</sup> by the following factor,

$$Y_{\text{corr}} = Y \left[ \frac{\text{counts}}{\text{channel}} \right] \times \frac{G(\text{keV/channel})}{\left[ \frac{\Delta E}{E} \right] E(\text{keV})} \quad (4.4)$$

where  $Y$  is the measured counts/channel,

$G$  is the energy calibration slope in keV/channel

and  $\frac{\Delta E}{E}$  is the fractional resolution (typically from 1.3 to 1.5%)

and  $E$  is the energy corresponding to the channel number of the yield function.

The resolution can be simply obtained by differentiation of equation 4.1 using the best fit parameters. The result is a gaussian-like curve based on the  $\text{sech}^2$  function. The resolution is given by the FWHM of this curve. This procedure and the subsequent system resolution calculation is given in greater detail in chapter 8, section 8.3.2.

The second correction involves knowing the charged fraction, which for the MEIRS system described is obtained using the solid state detector system. If  $f^C(C_i)$  represents the charged fraction backscattered from the sample at channel  $C_i$  and provided the energy calibration for the spectrum is known, say  $E(C_i)$ , then the yield of the ESA spectrum at  $C_j$ ,  $Y(C_j)$  becomes

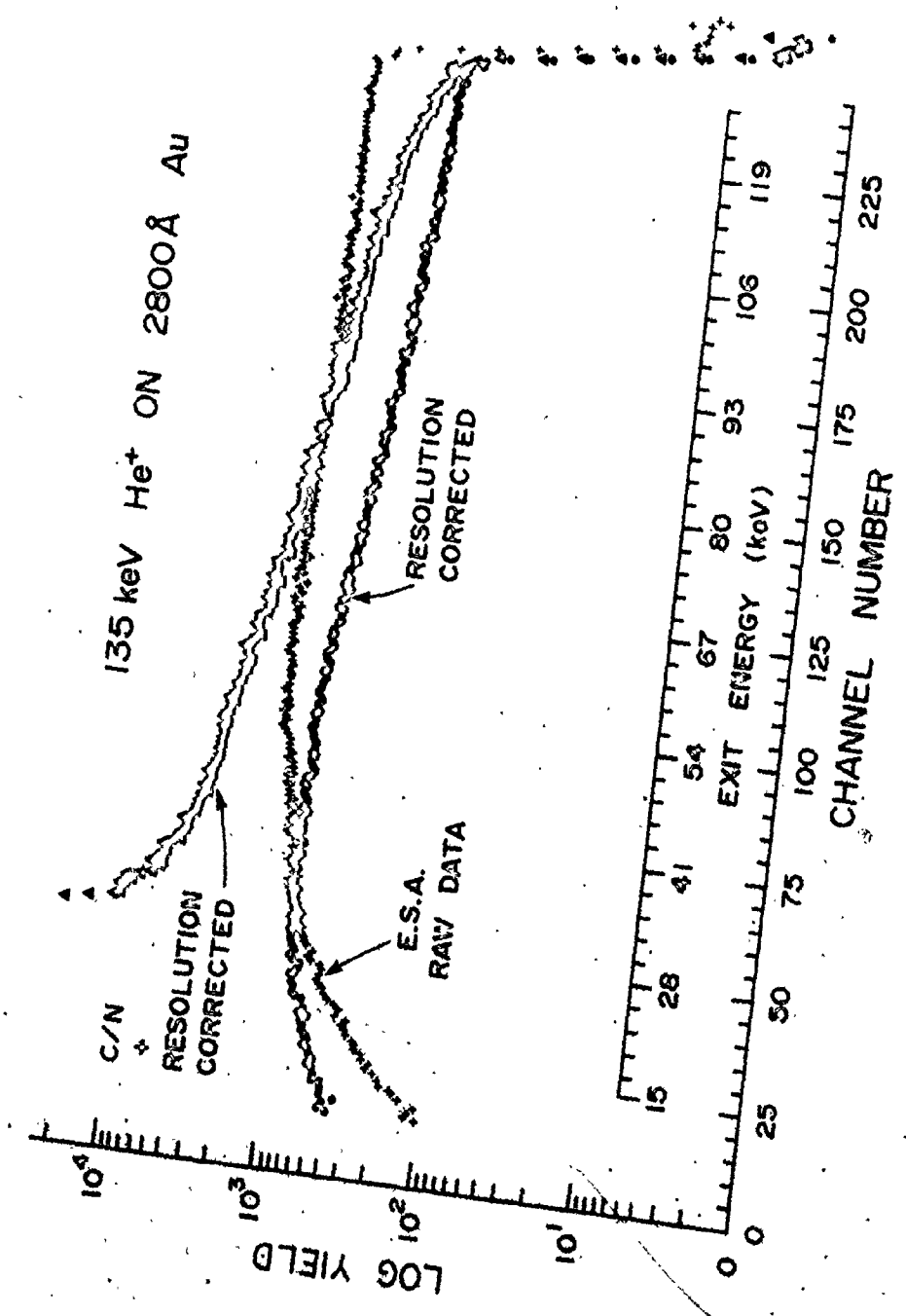
$$Y(C_j)_{\text{corr}} = \frac{Y(C_j)}{f^C(C_i)} \quad (4.5)$$

where  $E(C_j) = E(C_i)$ , (4.6)

Equation 4.6 expresses the condition that the correction must be applied at the same particle exit energy, that is, the channel  $C_i$  energy  $E(C_i)$  for the charge-to-neutral ratio spectrum must correspond to the energy  $E(C_j)$  at channel  $C_j$  of the ESA spectrum. If  $C_i$  is found to be non-integer (eg.  $C_i = C_i + 0.5$ ) then a linear interpolation between  $Y(C_i)$  and  $Y(C_i + 1)$  for both the charged and charged + neutral spectra is used to determine  $f^C(C_i + 0.5)$ . Thus it is required that the solid state detector absolute energy calibration be determined and this necessitates corrections due to the dead layer losses within the detector itself. This topic forms the main discussion of section 4.5. The C/N ratio correction is shown in figure 4.3 as applied to the ESA spectrum which is already resolution corrected. The final ESA spectrum is now comparable in shape to that obtained via the solid state detector as illustrated in figure 7.4. Note that the final ESA corrected curve does not proceed below 25 keV. This is due to the high thermal noise level which rapidly increases below the 25 keV value in solid state detector derived spectra so that spectral subtractions in this area become meaningless. The 25 keV energy represents a practical lower limit in all solid state charged particle detectors although the use of sophisticated electronics can compensate for the low signal-to-noise ratio extending this lower limit down to 10 keV<sup>32</sup>. It is for this reason that these detectors are rarely employed in the low energy regime and are replaced by either ESA's, sometimes with charge exchange cells, or time-of-flight (TOF) systems<sup>33,34</sup>. Note also in figure 4.3,



Figure 4.3. The backscattered spectrum from 135 keV  $H^+$  on  $^{2800}Au^0$  Au as obtained by the ESA is subjected to the two major spectral corrections to account for the constant resolution factor and the neutral fraction (C/N correction).



that the gold edge response of 135 keV  $H^+$  backscattered particles is much sharper than that of figure 7.2 indicating the great improvement (from 4.8 keV or 4% to 1.4 keV or 1.1%) in resolution when the ESA is employed. More comparisons of this nature are provided in the next section.

#### 4.4 The Surface Barrier Detector System

The solid state detector is employed, not only in the medium energy range but also in the higher energy regime where MeV light ion particle backscattering is called Rutherford backscattering, RBS. The latter can be used for quantitative determinations of target film thickness (cf. chapter 8) or impurity concentrations (cf. chapter 7) when the system geometry is known (i.e. calibrated). This determination is outlined next. Because RBS is a very reliable technique, as detailed in chapter 6 (see section 6.3.1) the primary energy calibration is also carried out in this region. By means of a precision pulse generator (PPG) it is then extended electronically into the medium energy regime<sup>35</sup> with suitable corrections as considered in section 4.4.2.

##### 4.4.1 Detector Geometry Calibrations

The determination of the solid angle subtended by the detector can be accomplished by RBS analysis of a known thickness of a heavy atom film evaporated on a lighter mass substrate or a known concentration of a heavy atom implanted into a low Z host substrate. Both targets of this kind have been used and yield a successful cross-check. A film of  $\sim 10 \text{ \AA}$  of gold e-beam evaporated onto a  $\langle 111 \rangle$

silicon substrate was RBS analyzed in the adjacent calibrated system<sup>36</sup> using a 1 MeV He<sup>+</sup> beam to determine the thickness,  $N\Delta t(\text{cm}^{-2})$  to within 2% accuracy that is,<sup>37</sup>

$$N\Delta t = 1.602 \times 10^{-13} \text{ YLD} / \left( \frac{d\sigma}{d\Omega} \cdot \Delta\Omega \cdot Q \right) \quad (4.7)$$

where YLD is the background corrected area under the gold peak

Q is the total charge in  $\mu\text{C}$  received by the target during the measurement

$\Delta\Omega$  is the solid angle in steradians

and  $\frac{d\sigma}{d\Omega}$  is the Rutherford cross section for He/Au in  $\text{cm}^2$  per steradian and is corrected for screening effects (cf. section 6.3.1).

The procedure is reversed when the gold standard sample is RBS analyzed in the MEIRS chamber. Hence  $\Delta\Omega$  is measured, knowing  $N\Delta t$ . The detection efficiency of the detector is assumed to be 100% for the He particles (The 4 mm diameter aperture positioned immediately in front of the device ensures the absence of edge effects and so 100% efficiency for all charged particles.). Table 4.1 shows the results of the solid angle determinations for the three possible beam aperture diameters. Careful cross-checking of the solid angles using a Bi implanted Si standard also calibrated at the Chalk River Nuclear Laboratories (CRNL)<sup>38</sup> shows agreement to better than 2%.

As a slight digression from the medium energy region, figure 4.4 illustrates the use of RBS to determine impurity concentrations. Here an aluminum sample, previously contaminated with trace amounts of Ar, Fe, Mo and Ta, has been RBS analyzed in the MEIRS system using a 1 MeV He<sup>+</sup> beam<sup>8</sup>. The impurity concentrations given in the

Figure 4.4. An RBS spectrum (using 1 MeV  $\text{He}^+$ ) from a contaminated Al disc showing the cooled surface barrier detector response to heavy impurities embedded in the lighter mass host<sup>8</sup>. The high energy resolution is 2% or 11 keV at 600 keV.

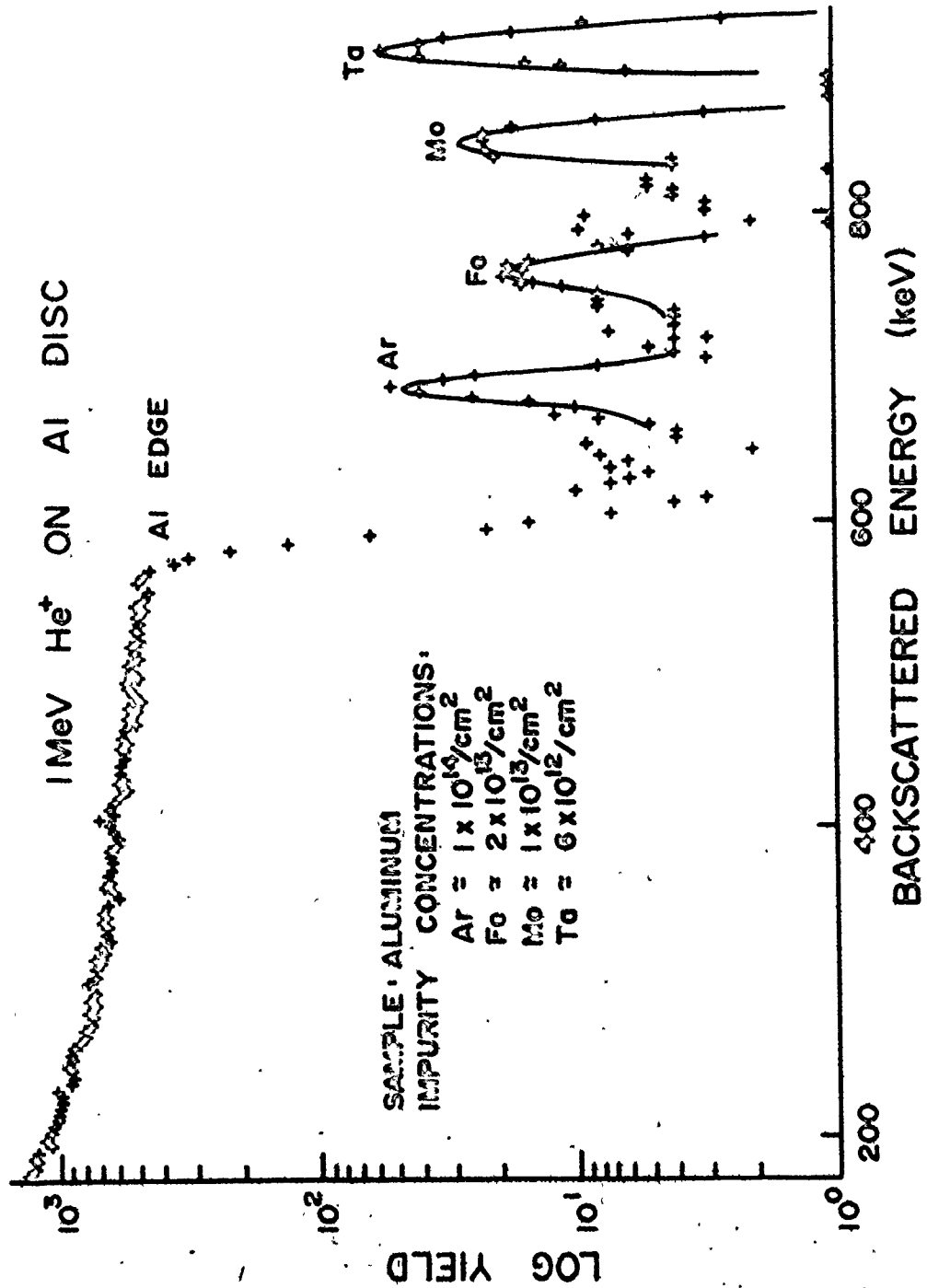


TABLE 4.1

Surface Barrier Detector Solid Angle Determinations

Size of the Beam Collimeters [first, second] (diameter in mm)	Solid Angle $\Delta\Omega \pm 2\%$ ( $\times 10^{-4}$ sr)
[0.5, 0.5]	2.16
[1,1]	4.53
[2,2]	6.80
geometrical measurement	5.2 $\pm$ 0.5

figure are based on the known solid angle, beam energy and cross sections. The detector resolution values in the MeV range are for He at 600 keV, 11 keV or 2% and at 1 MeV (not shown), 13 keV or 1.3%. All previous resolution determinations are taken with the surface barrier detector cooled to 0°C via the thermoelectric device.

#### 4.4.2 Detector Energy Calibrations

A beam of 1.0 MeV He<sup>+</sup> particles is backscattered from a previously Bi implanted Si sample. The scattered events are collected in the cooled surface barrier detector. From the RBS spectrum so generated the centroid from a gaussian fitted Bi peak (such as shown in figure 4.6) and a TANH fitted Si edge (see section 4.3.1) serve as calibration and check points for setting the normalization potentiometer on the precision pulse generator (PPG). Thus the pulse height control (a ten turn potentiometer with vernier scales) on the PPG becomes direct reading in MeV to better than 0.5 keV.

The value to which the pulse generator is set is calculated below. The Bi peak energy occurs at the incident beam energy (as determined from the accelerator energy calibration) reduced by the scattering kinematic factor,  $k_{\text{He/Bi}}$ . There are however, some corrections which must be made to the energy assigned to the backscattered peak. The Bi dopant is implanted at an energy of 30 keV so that the projected range (onto the z-axis) in Si is  $\sim 200 \text{ \AA}$  using LSS theory from reference 158. Thus the energy loss of the He<sup>+</sup> beam in traversing this distance in Si twice is



$$\begin{aligned}
 k_{\text{He/Bi}} \left\{ (E_0 - \Delta E_{\text{in}}(E_0)) \right\} - \Delta E_{\text{out}}(k_{\text{He/Bi}} E_0) & \quad (4.8) \\
 = k_{\text{He/Bi}} E_0 - (k_{\text{He/Bi}} \Delta E_{\text{in}}(E_0) + \Delta E_{\text{out}}(k_{\text{He/Bi}} E_0)) \\
 = k_{\text{He/Bi}} E_0 - \Delta E(\text{Bi depth})
 \end{aligned}$$

which, as determined from Ziegler<sup>131</sup> is  $\sim 7$  keV (a 1% correction). The backscattered beam must also penetrate the front gold contact region of the detector. This entrance window is an insensitive area for the detector and hence is called the dead layer. In the MEIRS detector, the manufacturers have quoted its thickness to be  $20 \mu\text{g}/\text{cm}^2$  or  $\sim 100 \text{ \AA}$ . The energy loss for 931 keV  $\text{He}^+$  particles in transit of the layer is  $\sim 16 \text{ keV}^{131}$  ( $\sim 2\%$  correction). Thus the value to which the PPG normalization is set (for  $E_0 = 1 \text{ MeV}$   $\text{He}^+$  beam backscattering from the Bi/Si target when pulsing the same channel (at the same pulse height) in which the Bi response peak centroid occurs) is

$$\begin{aligned}
 E(\text{PPG}) &= k_{\text{He/Bi}} E_0 - \Delta E(\text{Bi depth}) - \Delta E(\text{dead layer}) \quad (4.9) \\
 &= 0.931 \times 1000 - 7 - 16 \\
 &= 908 \text{ keV}
 \end{aligned}$$

As a cross-check, a  $10 \text{ \AA}$  gold layer (e-beam evaporated onto a Si  $\langle 111 \rangle$  sample) was also exposed to the same beam. Here only the dead layer loss need to be applied so that

$$\begin{aligned}
 E(\text{PPG}) &= k_{\text{He/Au}} E_0 - \Delta E(\text{dead layer}) \quad (4.10) \\
 &= 0.927 \times 1000 - 16 \\
 &= 911 \text{ keV}
 \end{aligned}$$

The energy of the gold peak is predicted by the pulser to within 1% of the calculated value of equation 4.10. Thus the energy deposited inside the particle detector can be determined from the PPG for He in the 1 MeV range. Note, however, that the energy of the scattered ions, incident on the detector, if different from the 1 MeV region is still unknown due to the aforementioned dead layer and pulse height losses within the device. Hence the absolute energy calibration in the medium energy region must involve these corrections for the detector, measured not only as a function of particle energy but also species.

#### 4.4.3 Detector Charge-to-Neutral Ratio Determinations

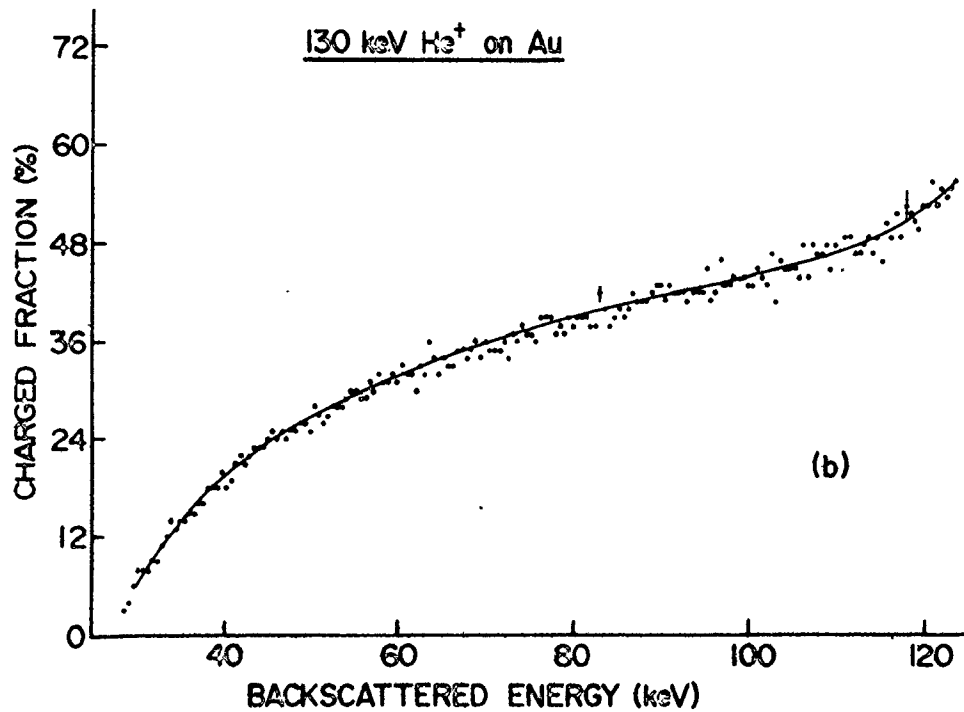
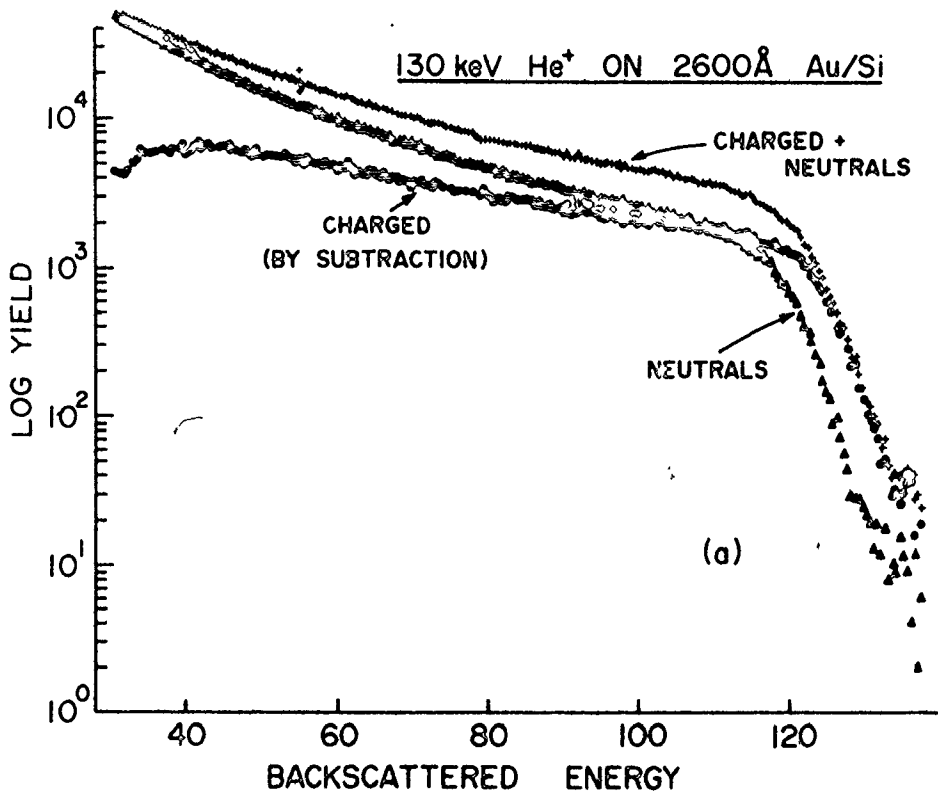
The importance and use of charge-to-neutral ratios, C/N, has been mentioned throughout this thesis, and so will not be reproduced here. The charged fractions can be obtained by using the solid state detector and an electrostatic beam deflection technique. Two separate but dose identical spectra are obtained, as shown in figure 4.5(a), one with field zero ( $Y_{C+N}$  = neutrals + ions) and the other with voltage applied ( $Y_N$  = neutrals only). The charge yield can be found by subtraction and division by the total number of events to give the charged fraction  $f^C(C)$  at channel C as

$$f^C(C) = (Y_{C+N}(C) - Y_N(C))/Y_{C+N}(C) \quad (4.11)$$

Another actual result is illustrated in figure 7.3.

In contrast to most  $f^C$  determinations which collect one spectrum,  $Y_{C+N}$ , and then the other,  $Y_N$ , to dose equivalence, the MEIRS system uses a rapid alternating collection of these two spectra.

- Figure 4.5 (a) The charged fraction measurements for 130 keV  $\text{He}^+$  backscattered from 2600 Å  $\text{Au}$  on a Si substrate. The charged + neutral and neutral spectra are directly determined while the third spectrum (charged) is generated by a point by point subtraction of the first two.
- (b) The calculated charged fraction as derived from the data in figure (a). The occasional vertical lines represent the statistical uncertainty of the point after the performed calculations outlined in the text.



For all measurements made during the course of this thesis, the dwell time in each mode is  $\sim 2$  seconds. Since the beam fluctuations are random and small during this short counting time in each spectrum, the two spectra over the long total exposure time are dose equivalent. As detailed in Chapter 3, the use of the pulser provides the preset mechanism for switching while at the same time correcting for any dead time losses incurred in the pulse height analyzer. This latter effect is very pronounced for large charged fractions, such as found with H and Li projectiles (compare Fig. 4.5(a) with Fig. 7.2) where the low neutrals count rate is contrasted with the high charged+ neutral yield for the same beam currents. This "simultaneous" C/N collection method is used in order to maintain the same sample conditions between the two spectra to be manipulated. This reduces the possibility of surface condition changes occurring only in one spectrum and not in the other during the course of the experiment which would yield misleading results.

#### 4.5 The Medium Energy Detector Pulse Height Defect Determination

Both the gold surface electrode thickness of the solid state detector, the elastic stopping in silicon, and the depth below the gold-silicon interface of the active depletion region represent insensitive areas for any deposited energy from incoming particles. That is, any electron-hole pairs created by the particle-detector interaction in these regions do not contribute to the output pulse from the detector, resulting in a pulse height defect (PHD).

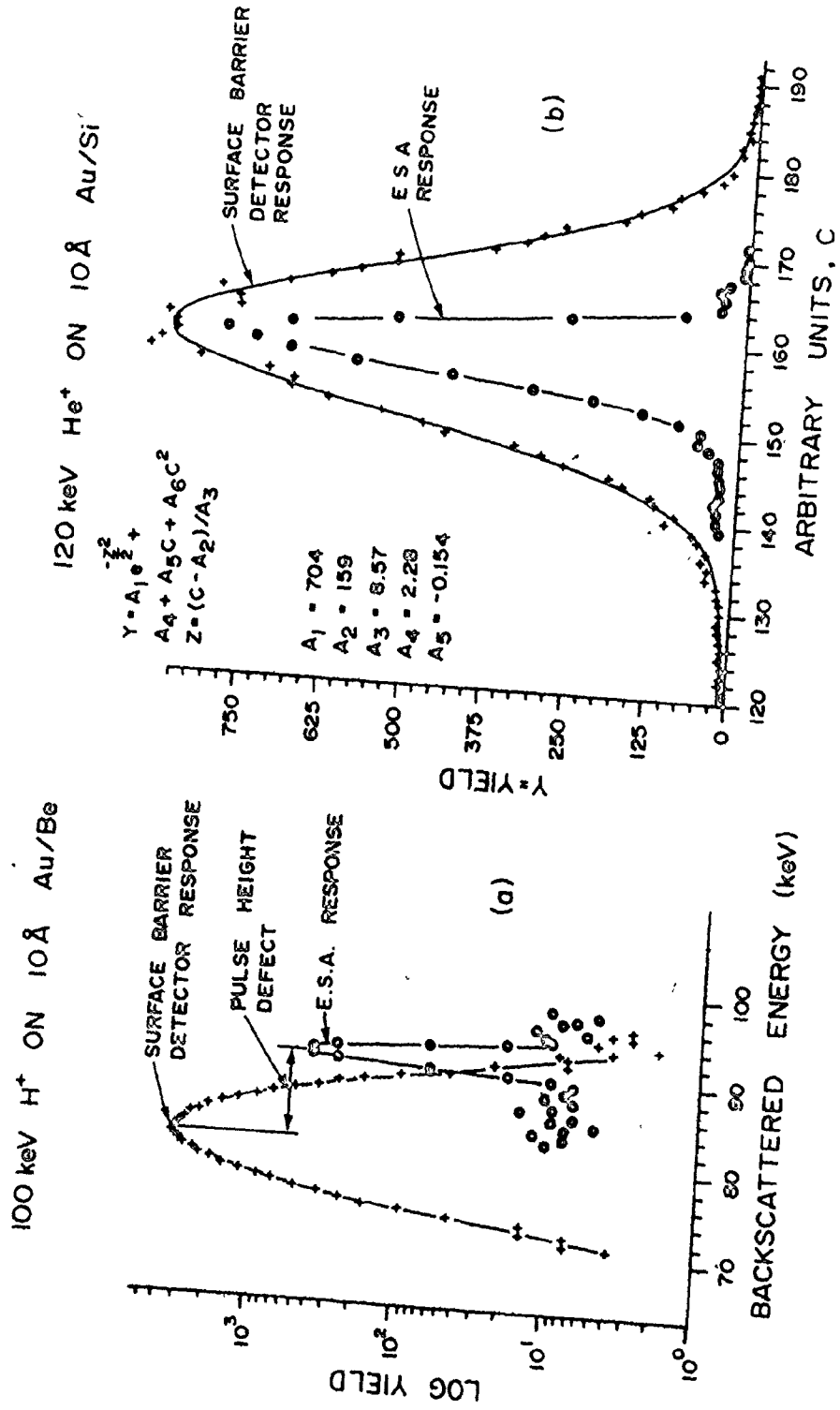
As shown in section 4.4.3, these detector losses can lead to a small correction in the MeV energy calibration. However, in the MEIRS range, these energy absorbing dead layers may subtract a large percentage of the total detector incident energy. In the case of neon this amounts to more than 70% at 100 keV. In order to energy calibrate the solid state detector in this region then, these losses must be determined.

The approach adopted is by direct measurement of the pulse height defect using both detection systems (the electrostatic analyzer and the surface barrier detector). These values are compared to calculated values obtained through theoretical considerations and also by using a Monte Carlo calculation based upon the detector structure. These alternate methods of pulse height defect determination are shown to be inadequate, even if certain parameters within the Monte Carlo simulation are altered. However a detailed discussion of the comparison of these results is omitted since it is the purpose of this work only to provide the best possible means to produce detector corrections needed for the generation of the solid state detector energy calibration.

#### 4.5.1 Experimental Measurement of the Detector Pulse Height Defect

There are several methods which can be employed to determine the energy losses due to the detector dead layers. One method is to use a detector tilting technique whereby the thickness of the layer can be measured<sup>40</sup>. This is accomplished by varying the angle of incidence of the charged particle beam and measuring the changes

- Figure 4.6 (a) A measure of the surface barrier detector pulse height defect can be obtained by use of both MEIRS particle detection systems and their corresponding energy calibrations. The two detector responses to a  $10 \text{ \AA}$  Au film on Be substrate for an incident beam of  $100 \text{ keV H}^+$  is shown where the gain of the solid state detector spectrum is selected to match that of the ESA.
- (b) The detector responses to another sample of  $10 \text{ \AA}$  of Au on Si after use in the pulse height defect determination experiment. The surface barrier detector response can still be fitted with a gaussian curve; however, the ESA, with much improved resolution over the solid state detector, shows the Au/Si interface deterioration after heavy ion bombardment.





in the signal amplitude output. This indirect method is possible only where the detector is accurately movable with respect to the monoenergetic ion beam. A more direct method is possible with the current MEIRS system. Since the energy calibrated ESA possesses none of the window related disadvantages of the solid state detector, a series of experiments can be performed to directly map the detector dead layer energy losses and pulse height defect as a function of projectile incident energy and species.

Several samples composed of  $10 - 15 \text{ \AA}$  of e-beam evaporated ( $< 1 \times 10^{-6}$  torr) gold (99.999% pure) on  $\langle 111 \rangle$  silicon were prepared. Beams of varying energy and species at normal incidence were backscattered at  $150^\circ$  from the gold sample producing results such as shown in figure 4.6(a). Using  $[0.5, 0.5]$  mm diameter apertures, a solid state detector spectrum was obtained. Since the thin gold layer is smaller than the detector depth resolution, ( $\sim 100 \text{ \AA}$ ) the resulting data can be fitted with a gaussian function as shown by the larger curve of figure 4.6(b). Also generated at this time is a pulser calibration spectrum containing as many as five peaks of known energy (from the pulse height vernier reading). These centroids are used to calculate via the method of linear least squares a channel number - energy relation. Thus, the above gaussian centroids in energy units represent the detected energy of the backscattered beam after pulse height losses. Next, without changing any beam energy parameters, the backscattered beam is detected via the ESA system using the  $[1, 1]$  mm diameter apertures (employed simply in order to reduce the acquisition time).

With the previously obtained energy calibration, the gold peak centroid can be converted into an energy unit which represents the backscattered energy incident on the solid state detector. In this way, the data of figure 4.7 have been obtained. The estimated uncertainties, where larger than the representing data point symbol are indicated by horizontal lines.

In figure 4.6(a) not only is the response of the surface barrier detector to the 10 Å<sup>0</sup> gold film given but also the response of the ESA taken at approximately the same gain (keV/channel). The separation of the two centroids is due to the pulse height defect within the solid state detector. The ESA, however provides a direct measurement of the energy of the backscattered ions once the energy calibration is determined. In figure 4.6 note the asymmetry of this ESA spectrum. This is due to the destruction of the Au/Si interface by recoil effects, that is, for the heavier particles the many collisions (eg. see table 4.2) give rise to secondary and recoil gold atoms which, near the interface, are driven into the silicon producing an intermixing of species. Thus an ESA peak as shown in figure 4.6(b) cannot be used to accurately determine the centroid by gaussian curve fitting. It is for this reason that over a dozen samples were eventually created and used first for many light ion runs and then several heavy ion runs. Between these latter exposures the light ion backscattered ESA spectrum was monitored to determine the usefulness of the sample. For the heavy ions, the solid state detector response covered more than 100 channels so that the centroid could

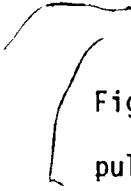
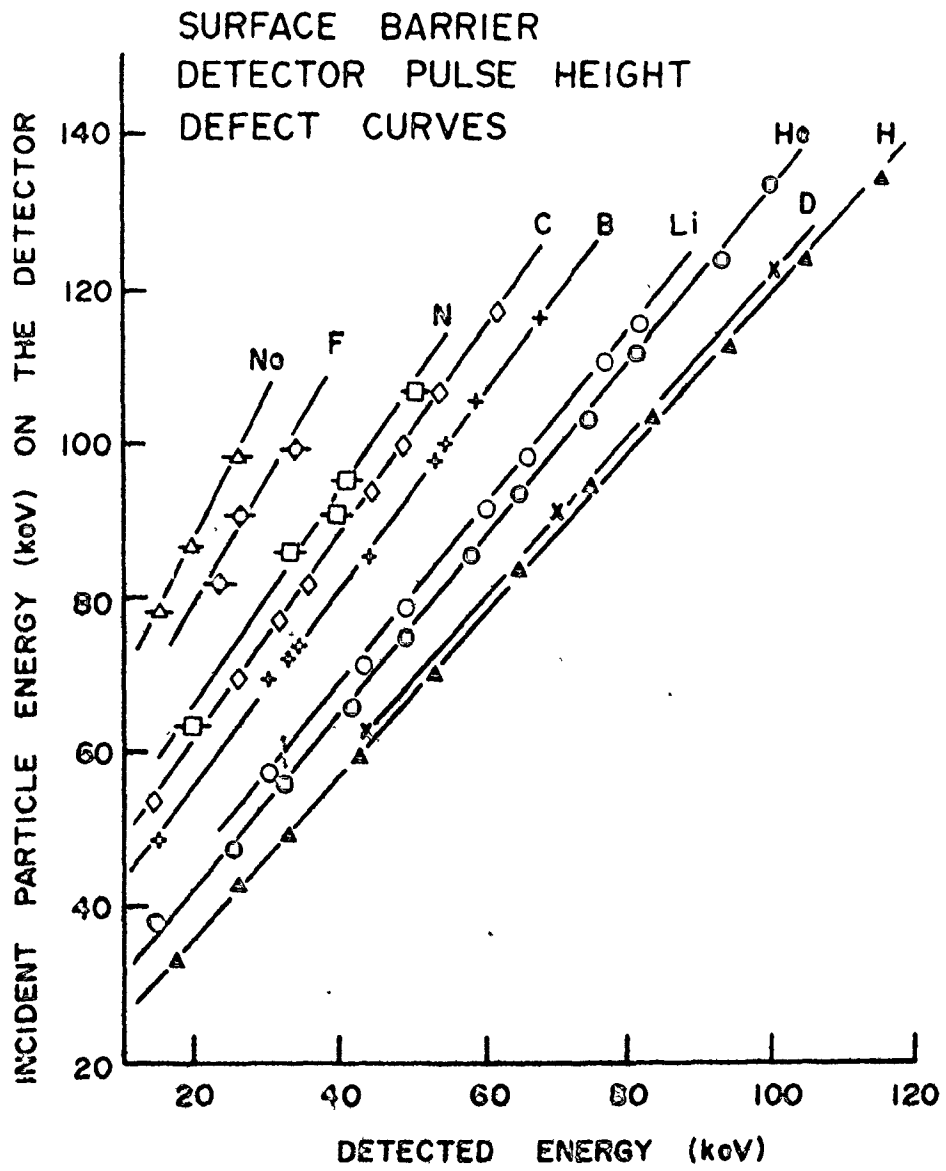


Figure 4.7. The results of the experimental determination of the pulse height defect for the MEIRS surface barrier detector. Where the experimental uncertainties exceed the size of the symbol they are shown by the short horizontal line through that symbol.



not be localized to better than several channels. Hence, this straggling effect is mainly responsible for the error bars given in Figure 4.7 involving the Ne and F particles. ✓

At this juncture, it is pertinent to mention that the same effects observed in the target are occurring about the solid state detector gold entrance electrode and silicon substrate interface from the heavy ion exposures, producing both Au recoil doping in Si and radiation damage in the Si depletion layer itself<sup>41,42</sup> which degrades resolution. However, the damaging beam is doing so at a much lesser rate due to the reduced backscattering energies and intensities (currents). Thus, the spectra produced from the heavy ion work do not contain 1% statistics as do the spectra from the light ion work due to this dose accumulative radiation damage effect. No noticeable degradation in the resolution figure has become apparent by periodic checks based on the backscattering of thin gold films.

#### 4.5.2 Dead Layer Theoretical Predictions

In order to calculate the energy losses within the solid state detector, a brief outline of the particle detection mechanism is necessary. Unfortunately, in the medium energy regime, the state of theoretical predictions of the characteristics for the particle-solid interaction do not approach the accuracy that is available in the MeV ranges. The experimental determination of these characteristics is the basic premise underlying the direction of research carried out in part two of this thesis. The best estimate for theory-experiment correlation is currently believed to be within

20% and thus any theoretical loss corrections so generated are not expected to be accurate to better than this figure. A detailed examination of the particle-solid energy loss processes is delayed to part II.

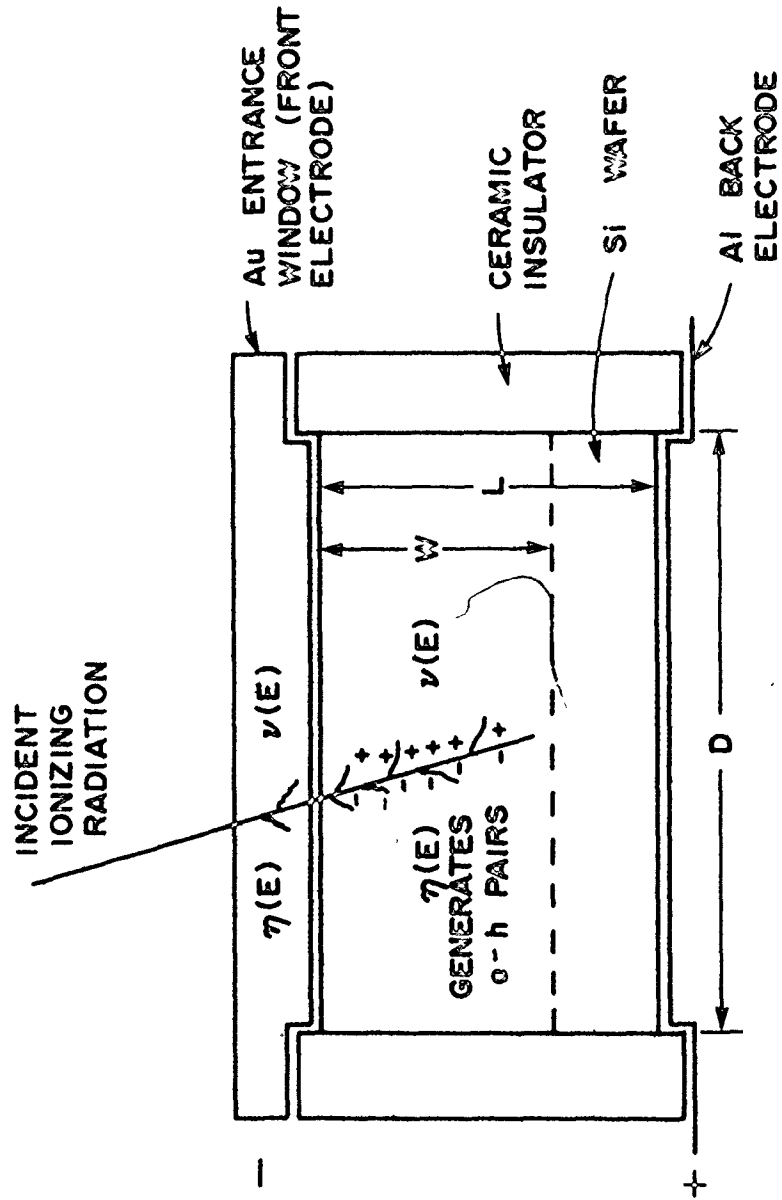
Consider figure 4.8. When a particle enters a surface barrier Si detector, it first encounters a surface gold electrode. The MEIRS detector contains  $20 \mu\text{g}/\text{cm}^2$  or  $\sim 100 \text{ \AA}$  layer of gold as quoted by the manufacturer which is usually within 10% of the independently measured thickness<sup>28</sup>. High energy light mass particles are only slightly affected while heavier masses are greatly reduced in energy due to many atomic collisions. The energy loss suffered by these particles in traversing the gold layer can be predicted by LSS theory<sup>2-5</sup>. (Much more detail is given about their work in part II of this thesis.)

Once through the gold electrode, the projectiles then interact with the bulk silicon of the detector. Some of these collisions involve the atoms (screened) while others involve the lighter mass electrons. If the energy lost to the former process is called the elastic deposited energy,  $v(E)$ , and the latter is termed inelastic ionization energy,  $\eta(E)$ , then the total energy lost can be expressed as

$$E_T = v(E) + \eta(E) \quad (4.12)$$

Figure 4.9(a) shows the fractional elastic deposited energy,  $v(E)/E_T$ , in silicon as a function of energy for the eight of the nine projectiles used for the experimental dead layer determination. These results are based on an approach by

Figure 4.8. A typical detector configuration with  $D$  the effective diameter corresponding to the active area of the device;  $W$  is the depth of the depletion (sensitive) region;  $L$  is the total thickness of the Si wafer. The incident particle loses energy to both electron collisions,  $\eta(E)$ , (producing electron-hole pairs, e-h), and nuclear collision,  $\nu(E)$ , in both the Au and Si but only the  $\eta(E)$  component in  $W$  produces e-h pairs which contribute to the detector output pulse height.



SCHEMATIC OF A TYPICAL  
SURFACE BARRIER DETECTOR  
(NOT TO SCALE)



Figure 4.9. The fraction of energy being deposited in (a) silicon and (b) gold due to elastic collisions with various particle species as a function of their incident energy. These results are calculated from reference 43.

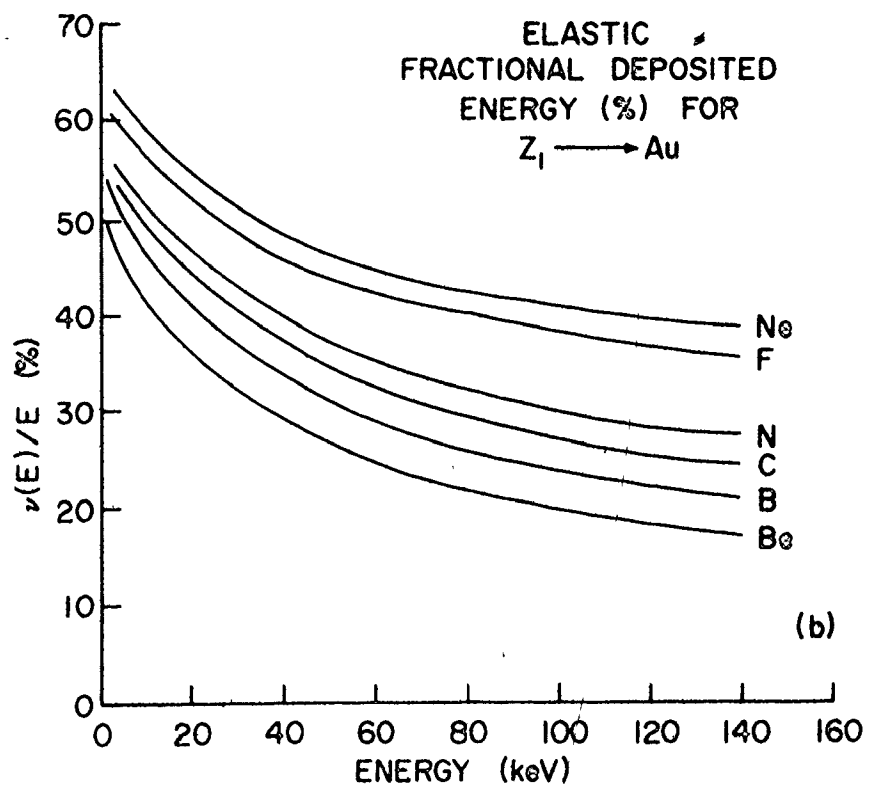
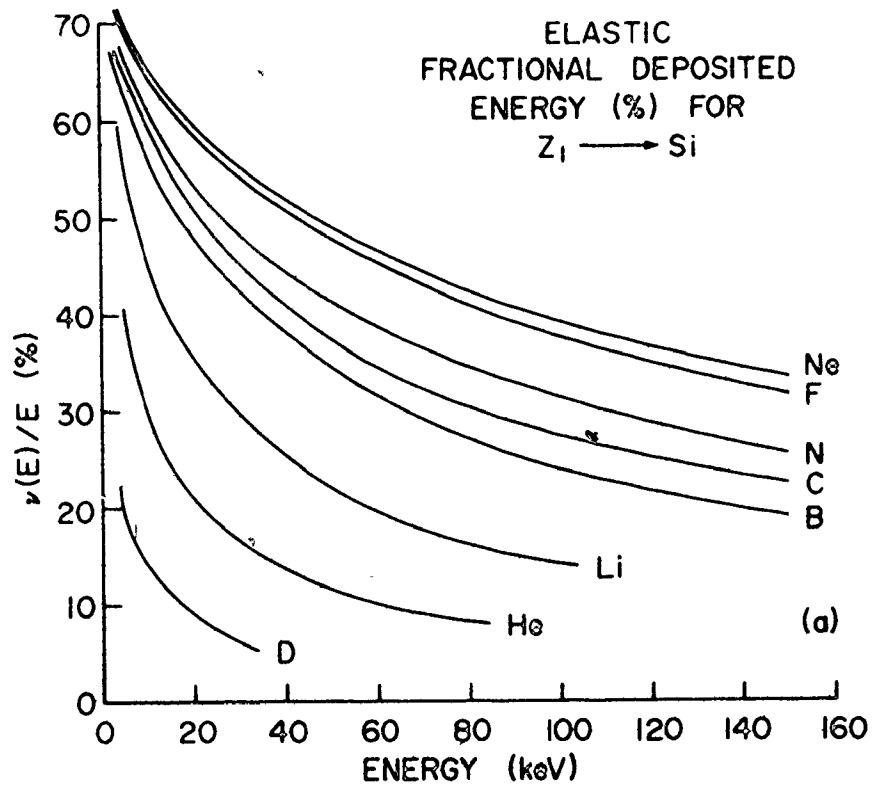
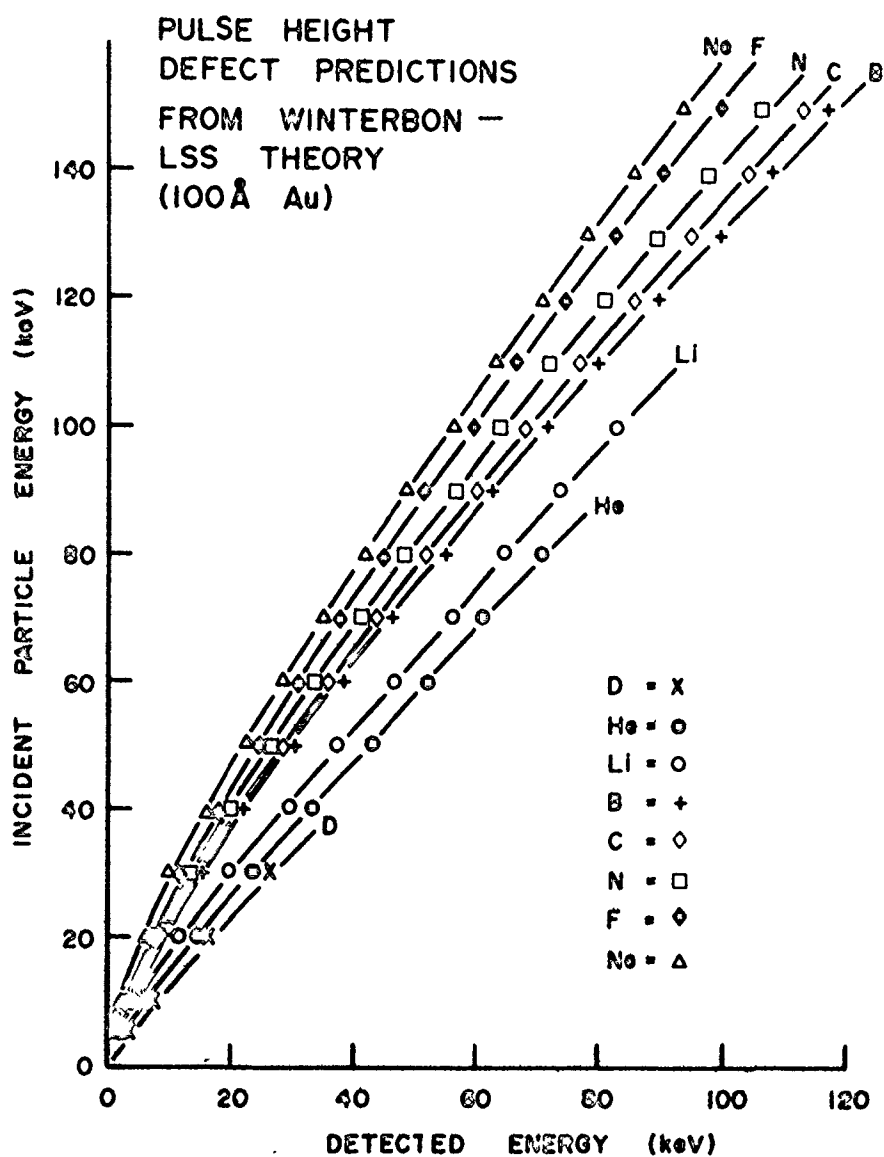


Figure 4.10. The theoretical predictions of the pulse height defect due to entrance window dead layer effect and the elastic energy within the silicon wafer. The former effect is calculated from LSS theory<sup>2-5</sup> using a 100 Å<sup>0</sup> thick Au layer, while the latter is interpolated from a tabulation of fractional deposited energies due to Winterbon<sup>43</sup>.



Winterbon, Sigmund and Sanders<sup>82</sup> usually referred to as WSS. Winterbon<sup>43</sup> has tabulated range and energy deposition distributions for several ion-target combinations. These results are based upon numerical integrations of LSS theory involving uniform and infinite targets with uncorrelated atom positions. The high energy cut off for Li, He, D and the complete absence of a curve for H indicate the limits of applicability of the theory which is primarily dedicated to the ion implantation area. Figure 4.9(b) shows for comparison the behaviour of the nuclear deposited energy for various projectiles in gold. The fraction of the particle energy used in ionizing electrons in the silicon is the important quantity to be studied since it is those created electron-hole pairs (e-h) which are swept out of the depletion region to the end electrodes and contribute to a charge pulse. All other losses, those in gold, and non-ionizing ones in the silicon depletion region, do not contribute to the output height of the pulse. Thus the detected energy,  $E_D$ , can be related to the energy incident on the detector,  $E_I$ , by

$$E_D = E_I - \Delta E_{LSS} - v_{WSS}(E_I - \Delta E_{LSS}) \quad (4.13)$$

where  $\Delta E_{LSS}$  is the energy lost in transit of the gold electrode as calculated from LSS theory and the last term is the non-ionizing (elastic) deposited energy as determined from WSS theory. The results of these calculations (interpolated from reference 43) are illustrated in figure 4.10. This predicted data is expected to be within 20% of the actual situation for a gold layer thickness of 100 Å and zero

thickness for the silicon dead layer which may be present if the depletion or sensitive layer starts some distance below the gold-silicon interface. The silicon dead layer condition is elaborated on in later sections.

#### 4.5.3 A Monte Carlo Simulation of the Detector Pulse Height Defect

Because of the approximate nature of the theoretical modelling of the previous section, the use of Monte Carlo simulation can prove to be a better measure of the detector dead layer response. For instance, the Monte Carlo technique approaches the actual experimental conditions whereby a statistical ensemble is involved in the production of the pulse height detector response (eg. a distribution of particle energies exists after traversing the insensitive areas into the detector sensitive regions) and not just the theoretical average.

An existing Monte Carlo code<sup>44,45</sup>, MONTY, was modified for two layer operation<sup>46</sup> and to provide both non-ionizing and electron ionization energy depth distributions. In this way the total detector dead layer configuration as well as the pulse height defect phenomenon can be studied and the effect of various parameter changes, such as gold layer thickness, can be investigated. The overlay structured code is run on a 56K PDP-15/20 computer operating under the advanced monitor system, ADSSXVM.

Figure 4.11 reproduces the results in a graph comparable to the preceding figure 4.10. Although MONTY uses LSS and WSS theory to calculate energy loss values, it is known that for

Figure 4.11. The pulse height defect for the MEIRS surface barrier detector as simulated by the Monte Carlo technique. The parameters used are given in the text. The statistical uncertainty if larger than the representative symbol is given by a horizontal line through that symbol.

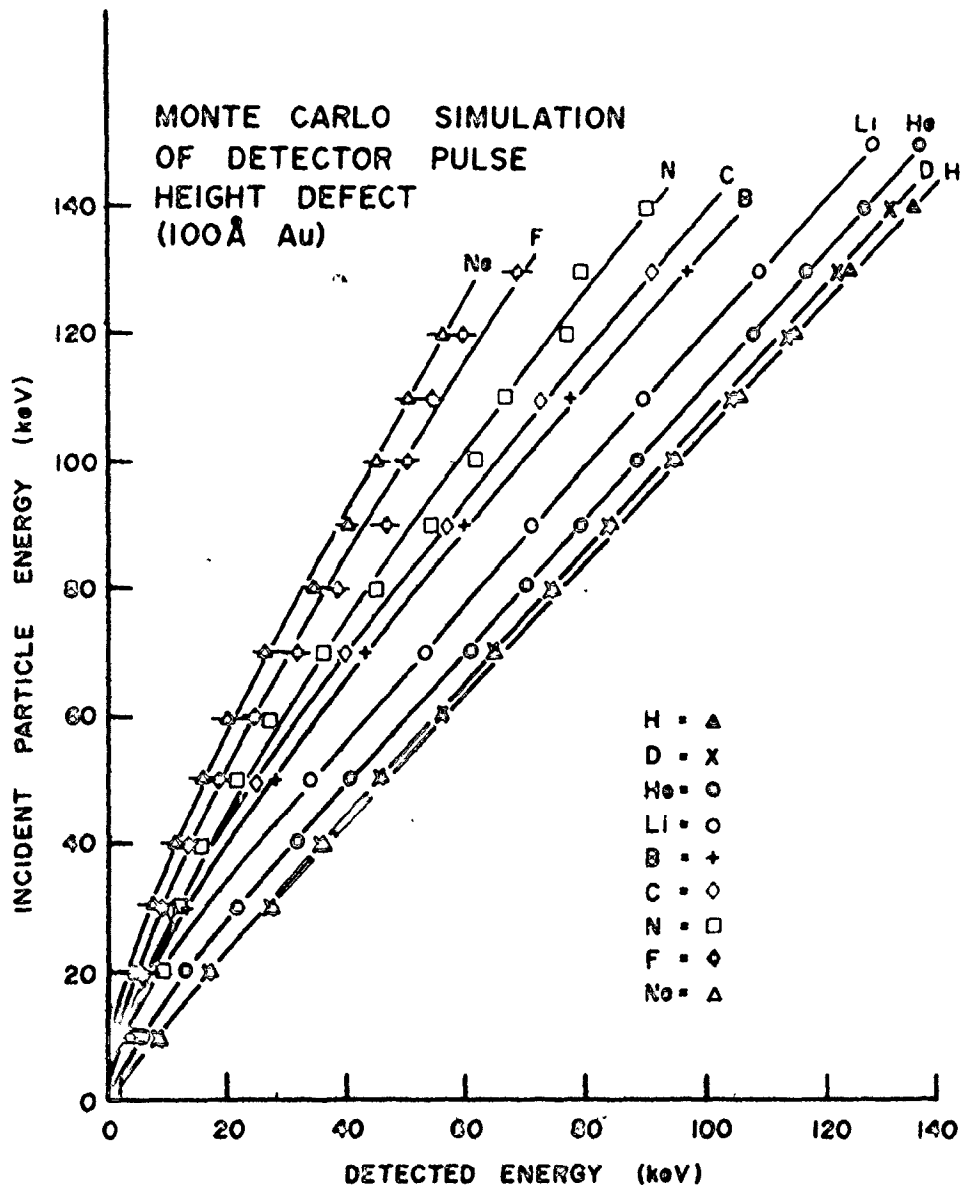




TABLE 4.2

Monte Carlo Predictions for the Number of Collisions and  
Defects Produced Per Incident Particle at 100 keV

Ion	Number of Particles Run	Collisions per Particle	Defects Produced per Particle
Neon	20	1600	1100
Fluorine	30	1480	1000
Nitrogen	40	1050	700
Carbon	50	900	620
Boron	60	880	580
Lithium	70	420	300
Helium	80	200	150
Deuterium	90	35	25
Hydrogen	100	10	5

different ions the LSS stopping does underestimate<sup>47</sup> the experimentally observed values. In order to better simulate actual observed conditions, the LSS inelastic (ionizing) stopping constant is scaled as follows for each incident ion species: H(1.45), D(1.45), He(1.45), Li(1.30), B(1.50), C(1.40), N(1.30), F(1.0), and Ne(1.0). These scaling factors are perhaps the weakest parameters input as they are based on a silicon rather than gold substrate simply because no reliable experimental values on inelastic stopping are available (as is shown in Chapter 8) on which to compare LSS theory. The displacement energies used for the simulation are for gold 25 eV and in silicon 14 eV. Table 4.2 gives the number of collisions and the number of defects produced for each of the nine species incident on the detector at 100 keV. It also indicates the number of incident particles used for the simulation on which those results are based. The average time for the simulation to run one species to completion is 8 - 10 hours, ranging from several minutes per particle for H to 30 minutes per particle for Ne.

#### 4.5.4 Discussion of the Results

Table 4.3 shows that neither the theoretical approach of section 4.5.2 nor the Monte Carlo simulation of section 4.5.3 can predict the measured pulse height defect detector response. These results have been taken from figures 4.8, 4.10 and 4.11 for 100 keV incident energy on the detector and are representative of the total range of energies covered. The percentages presented give the pulse height defect (theory prediction/experimental) value

TABLE 4.3

Comparison of Theory and Simulation to  
Experiment at 100 keV

Discrepancy of Dead Layer Energy Loss (%)

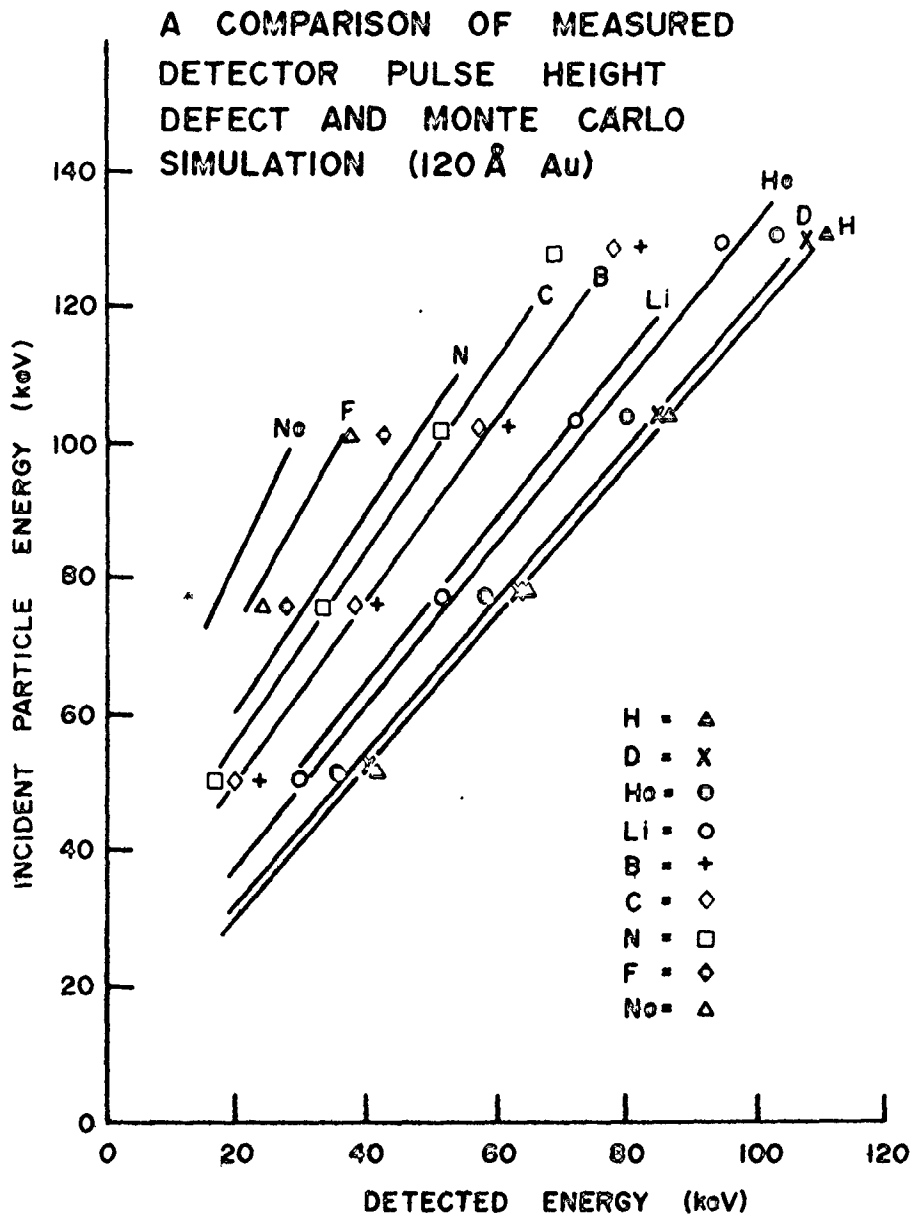
Ion	LSS/WSS	Monte
	Theory	Carlo
Neon	100	61
Fluorine	67	39
Nitrogen	36	28
Carbon	33	29
Boron	26	23
Lithium	17	14
Helium	--	22
Deuterium	--	16
Hydrogen	--	14

discrepancy ratio at 100 keV. That is, for Neon with 100%, the prediction/experiment ratio is 2.

The trend of the two calculational techniques is to deviate from the observed experimental pulse height defect values in two different aspects. First a general shift is noticed (similar to a zero shift) where a constant energy loss must be subtracted from the light ions to bring about correlation except in the case of helium. Secondly, there is also a general trend away from the heavy ions which varies as mass (a gain shift) in the sense that the heavier the ion the larger the discrepancy. Thus there must be other effects which contribute to the dead layer energy losses than just gold. In fact, increasing the gold thickness in MONTY<sup>0</sup> to 120 Å allows a direct correlation at 100 keV for H ions and within statistics for both D and Li but as shown in figure 4.12, when the ions increase in mass so does the discrepancy up to Ne at 36%. The situation for He remains an unexplained feature of the analysis.

Even assuming that both the theoretical approach and the Monte Carlo simulation are valid to within 20%, they are still not acceptable descriptions of the experimentally observed results. In fact, other discrepancies derived from experimental work alone involving solid state detectors have been noticed, although no experiments up to the present time have examined the response of these detectors to heavy ions in the medium energy regime. It is in the MeV range that many anomalies (see reference 48 for example) have been noted for these solid state

Figure 4.12. A comparison of a Monte Carlo simulation, represented by the symbols and the experimental results of section 4.5.1, reproduced in the form of solid lines. Using an entrance window thickness of  $120 \text{ \AA}$  of Au, the light ion simulations correlate with experiment. The heavy ions do not.



detectors since their invention during the late 1950's and early 1960's. The fact that heavy mass ions invoke a reduced energy response in these detectors when compared to the lighter mass species is simply the recognition that there is a loss of electron-hole pairs which contribute to the output charge pulse. The pulse height defect for these ions is compared to the light mass species, usually the alpha particle or the proton sometimes after having accounted for mass and entrance window effects (usually through the use of LSS parameters). Initially it was studied using incident fission fragments of MeV energies<sup>49</sup>; but with the advent of heavier mass accelerators, the major contributing factor to PHD have been identified as the loss of free electrons by recombination<sup>50</sup> and through trapping sites such as lattice defects or impurities<sup>51</sup>.

It was recognized early on that the depletion region in the silicon for surface barrier detectors did not always extend up to the Au/Si interface. Even some present day detectors still retain this property where as much as 700 Å<sup>0</sup> of silicon is undepleted<sup>51</sup>. Returning once again to the 100 Å<sup>0</sup> Au MONTY results, table 4.4 gives the depth below the Au/Si interface that the depletion region must begin in order to produce an exact correlation between simulation and experiment. As is the case for increasing the gold layer thickness, this effect cannot account wholly for the heavier mass behaviour either. Note that the same effect as the extended silicon dead layer can be produced by impurities at the Au/Si interface such as oxygen which is

TABLE 4.4

Predicted Silicon Dead Layer Thickness ( $\text{\AA}$ ) from Simulation

Ion	Energy					
	40 keV	60 keV	80 keV	100 keV	120 keV	140 keV
Neon	1000	350	400	400	350	500
Fluorine	400	225	250	250	200	350
Nitrogen	450	200	250	250	250	250
Carbon	300	200	200	250	300	300
Boron	300	200	200	200	300	300
Lithium	250	300	300	300	300	300
Helium	350	400	350	350	400	400
Deuterium	550	500	400	450	400	450
Hydrogen	500	350	300	350	400	400



known to act as an electron acceptor<sup>51</sup>. But again no preferential treatment can be attributed to the type of effect for the heavier mass species.

The only other area that has not been examined is the production and collection of e-h pairs within the depletion region itself. There are perhaps two processes which may be put forth where these electron numbers contributing to the pulse height defect may not be proportional to the deposited energy as the mass is varied. There are the aforementioned recombination effects and the fact that the ionization energy for production of electrons may vary with projectile species. The latter anomaly has been observed experimentally for silicon solid state detectors but only with the lighter mass projectiles<sup>52-54</sup>. The results for surface barrier detectors in the 0.5 to 2.5 MeV energy range show a discrepancy of 1.1% for He<sup>+</sup> and 3.3% for Li<sup>+</sup> when compared to the e-h ionization energy with protons<sup>28</sup>. There is simply no data available at these energies for the heavier mass projectiles so that the general trend to larger differences with greater masses cannot be verified. Hence it remains unknown whether this effect in the medium energy range contributes substantially to the observed PHD.

The last consideration of this section is the possible enhancement of electron recombinations due to the plasma effect<sup>55,56</sup>. This effect increases as the mass of the projectile increases simply because the defect production increases to the point where all along the particle track a large number of atoms are in motion. This is best shown in table 4.2 where the number of defects predicted by

MONTY increases by a factor of 200 from hydrogen to neon projectiles at 100 keV. Certainly this last model can provide the means to explain such a large discrepancy which increases with mass as the plasma effect does. However, the theory is just not advanced enough to provide quantitative results so that it has been only qualitatively successful in predicting the PHD experimentally observed for fission fragment masses in the 50 MeV region<sup>57</sup>. More data is needed especially in the lower energy regimes.

Therefore, of all the mentioned theories to account for the observed PHD in the MEIRS region, the plasma-recombination defect seems to be the most probable. It is apparent, in any case, that the prediction of energy losses in solid state detectors is by no means a simple problem. A detailed analysis of these effects is beyond the scope of this thesis. However the foregoing work has shown that in order to produce reliable pulse height defect corrections in the medium energy regime, a simple theoretical approach is not suitable. Even the more sophisticated Monte Carlo simulation technique cannot account for the observed anomalies in the heavier mass regions. Thus, for any given solid state detector to be accurately energy calibrated in this energy regime an empirical determination of the pulse height defect is mandatory.

Leaf 108 omitted in page numbering

PART II

APPLICATIONS

Leaf 110 omitted in page numbering

## CHAPTER 5

### Introduction

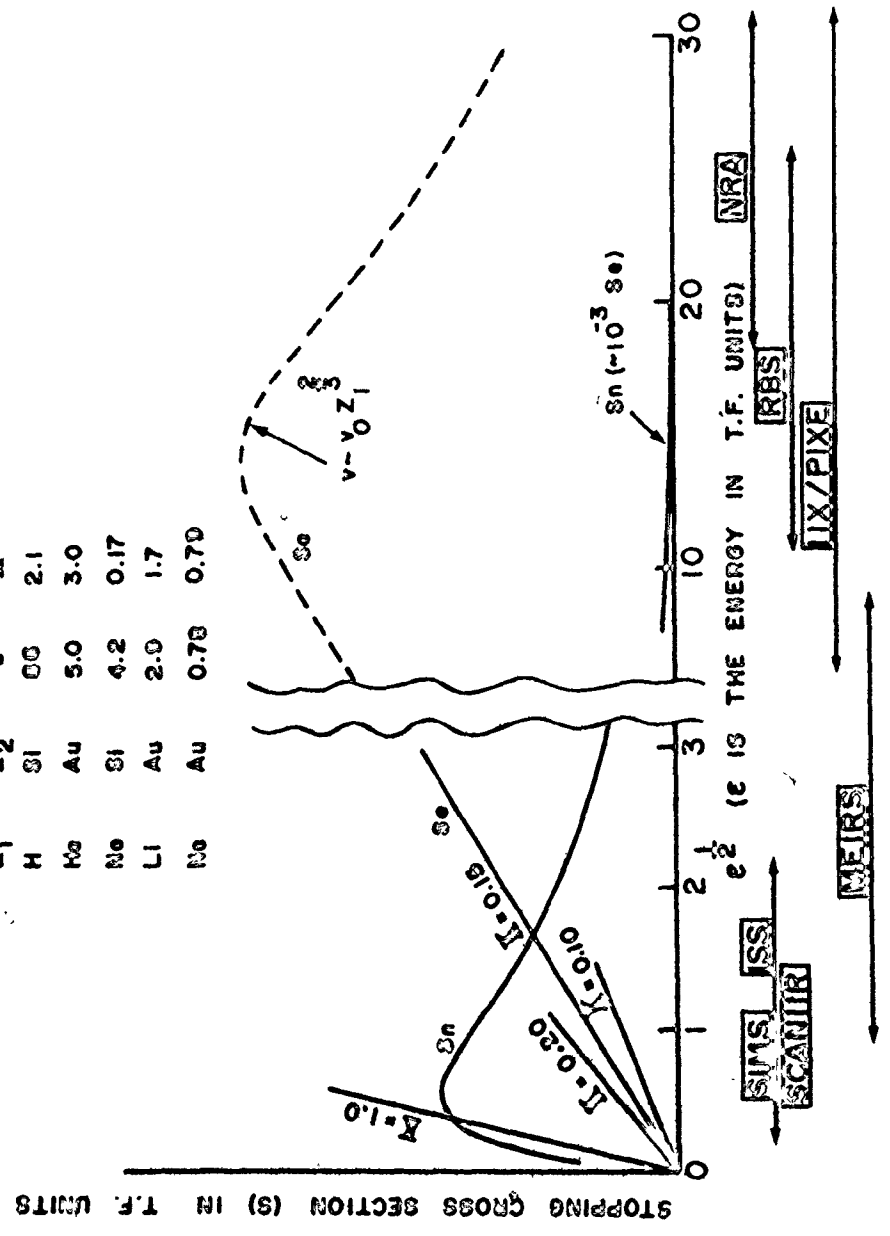
Part II of this thesis reports on applications of the MEIRS to study some of the fundamental parameters encountered when an ion interacts with a solid. Specifically, 1) the scattering cross section at large angles and its comparison with theory, 2) the charge state of backscattered particles, and 3) the energy dependence of the rate of energy loss as the particle penetrates the matter, are discussed. To this end, Chapter 6 provides details on the measurement of scattering cross sections; Chapter 7 includes a study of the charge exchange process for ion-gold interactions; and an investigation of light ion stopping powers is reported on in Chapter 8.

A knowledge of these basic processes of the ion-solid interaction are required to determine whether medium energy ion reflection spectroscopy can be employed as a reliable and quantitative technique for surface analysis. Since this energy region, as indicated in Chapter 1, is accessible with many ion implantation systems, it could allow both ion implantation and in-situ evaluation of the implanted layer with the same accelerator. The situation at higher energies (1 - 2 MeV) has already demonstrated that ion scattering, termed Rutherford Backscattering Analysis, RBS, is capable of non-destructively analyzing surfaces, of determining surface contaminations, and of probing quantitatively

Figure 5.1 Some ion beam analysis techniques (boxed) mentioned in the text in relation to the basic ion ( $Z_1$ )-solid ( $Z_2$ ) interaction parameter of stopping cross section(s) and incident beam energy parameter ( $\sqrt{\epsilon}$ ). Both units are from the LSS theory and are in terms of Thomas-Fermi (T.F.) reduced values: predictions are for a universal stopping curve ( $s_n$ ) due to nuclear derived events while for electronic derived events a family of curves results whose proportionality constant ( $\kappa$ ) with different ion-solid species is given in the accompanying table. The arrows below the technique boxes represent the region of applicability for each technique with respect to the epsilon of the interaction pair.

SOME TYPICAL 100keV CASES

Z1	Z2	$\epsilon$	K
H	Si	00	2.1
Na	Au	5.0	3.0
Ne	Si	4.2	0.17
Li	Au	2.0	1.7
Ne	Au	0.78	0.70





a region extending 1 - 2 microns into a solid<sup>58, 59</sup>. This is essentially because in this energy region the physics of the scattering and energy loss mechanisms is well developed. Medium energy scattering, therefore should provide similar information with less set-up cost and potentially better depth resolution than RBS, although depth information with MEIRS could only be obtained over a much shallower region<sup>60</sup>.

Figure 5.1 indicates several ion beam analysis techniques and shows the region of application in terms of the probing projectile energy and the stopping cross section, i.e. the energy loss per unit length inside the target solid as well as the predominant energy loss mechanism. A more detailed consideration of stopping powers is provided in Chapter 8. These techniques accomplish their analysis via measuring properties of the ejected species. Where conditions permit, these methods may analyze the scattered incident particle, an induced X-ray, a nuclear reaction product, a sputtered particle or an emitted optical photon depending on the best aspect of the technique to be exploited<sup>61</sup>. For instance, the object of analysis may include one or several of the following requirements: elemental identification, impurity detection, quantitative doping concentration measurements, depth profile information, lattice location, as well as destructive versus non-destructive analysis, surface versus bulk properties, etc. Table 5.1 summarizes the main features of the techniques discussed. Where specific quantities are provided (such as for depth resolution and sensitivity) there

TABLE 5 1  
TYPICAL FEATURES OF SOME BASIC ION BEAM ANALYSIS TECHNIQUES

REQUIREMENTS AND FEATURES	TECHNIQUE						
	SCANIR	SIMS	ISS	PIX PIXIE	RBS	NRA	MEIS
ION BEAM SPECIES ENERGY	O, Ar ~ 1 KEV	O, Ar ~ 1 KEV	H, He ~ 1 KEV	H ~ 1 MeV	He, N 1 MeV	REACTION ~ 10 MeV	H, He ~ 100 KEV
PARTICLE ANALYSED	OPTICAL PHOTON	SPUTTERED TARGET SPECIES	BACKSCATTERED INCIDENT PARTICLE	X-RAY PHOTON	BACKSCATTERED INCIDENT ION	REACTION PRODUCT	BACKSCATTERED INCIDENT ION
UHV	No	Yes	Yes	No	No	No	PREFERRED
DESTRUCTIVE(?)	Yes	Yes	No	No	No	No	No
QUANTITATIVE(?)	No	No	No	Yes	Yes	Yes	Yes
AREA OF APPLICATION S = SURFACE B = BULK	S, B*	S, B*	S	B	B	B	S & B
DEPTH RESOLUTION	VARIES WITH DEPTH	~ 100 Å <sup>0</sup>	~ 20 Å <sup>0</sup>	NA	~ 50 Å <sup>0</sup>	RESONANCE WIDTH	~ 30 Å <sup>0</sup>
SENSITIVITY (ATOMIC FRACTION)	10 <sup>-4</sup> - 10 <sup>-1</sup>	~ 10 <sup>-5</sup>	~ 10 <sup>-2</sup>	~ 10 <sup>-6</sup>	~ 10 <sup>-4</sup>	~ 10 <sup>-4</sup>	~ 10 <sup>-3</sup>
LATTICE LOCATION DETERMINATION(?)	No	No	Yes	Yes	Yes	Yes	Yes
ELEMENTS ANALYZABLE	H-U	H-U	LI-U LOW Z POOR HIGH Z PAIR	C-U	HEAVIER THAN SUBSTRATE LOW Z POOR HIGH Z GOOD	LOW Z	LI-U LOW Z POOR HIGH Z GOOD

\* VIA THE SLOW PROCESS OF SURFACE EROSION

is usually a range of values which may be quoted. These typical values may account for different configurations (eg. RGS - glancing incidence) or perhaps target element (eg. SCANIIR - various fluorescence yields) and so on.

A brief discussion ensues which proceeds from the lower incident energy ion beam techniques to the higher. Generally, the higher the probing energy of the projectile, the greater the shift away from surface feature analysis in favour of bulk analysis properties. However, for Secondary Ion Mass Spectrometry (SIMS), and SCANIIR or Surface Composition by Analysis of Neutral and Ion Impact Radiation, the employment of destructive surface erosion beams allows bulk analysis, which is a slow process. The former method involves the detection and analysis via mass spectroscopy of the ejected species of the target subjected to low energy heavy ion (typically O or Ar) bombardment. By continuous monitoring of these secondary ions as the surface is eroded by sputtering, depth profile information is obtained. The latter method uses essentially the same incident ion beam but analysis occurs through the use of optical spectrometry on photons emitted from the excited sputtered atoms. In a similar manner as above, the depth profiles can be obtained at the expense of sample destruction. If surface destruction is a problem then consideration should be made of low energy (0.5 - 10 keV) ion reflection or Ion Surface Scattering (ISS). It is usually employed to obtain information on the atomic composition and structure of the surface due to its extreme sensitivity to the outermost atomic layer<sup>62</sup>. On the other hand, if

high energy ions are used; the characteristic x-rays from elements in the bulk of the target can be excited and detected with high resolution x-ray spectrometers<sup>63</sup>. Thus, Ion Induced x-rays (IIX) or Proton Induced X-ray Excitation (PIXE) techniques can be utilized to nondestructively determine the species and approximate concentrations<sup>64,65</sup>. With the advent of "windowless" high resolution Si(Li) x-ray solid state detectors, it is possible to include studies of low Z ( $Z \geq 6$ ) x-rays<sup>66</sup>. In the area of semiconductor device production, fast determination of light mass surface contamination such as oxygen can be of great importance. It is this precise condition of light element impurities on heavy mass substrates that RBS fails to provide reliable quantitative results due to a loss in sensitivity as later shown in Chapter 6. Rutherford backscattering is, however, one of the more widely used non-destructive techniques due to its reliability and excellent quantitative accuracy ( $\sim 1\%$ ), although for  $M_2 \geq 30$  mass resolution becomes rather poor because of a more slowly varying kinematic scattering factor. In circumstances where RBS fails to provide reasonable quantitative results, the use of Nuclear Reaction Analysis (NRA) may be more advantageous. Although this technique usually requires high energies with large ion fluences and produces high background of scattered particles, it allows, where a suitable nuclear reaction exists, the measurement of light mass impurity concentrations, (such as O, via an  $^{16}\text{O}(d,p)^{17}\text{O}$  reaction) on a heavy Z target<sup>67</sup>. To determine H concentrations, heavy ion

projectiles have been employed, eg.  $H(^{11}B, \alpha)2\alpha^{110}$ .

Although not mentioned in figure 5.1, similar techniques exist which use the analysis of secondary electron energy spectra resulting from the bombardment of the surface under analysis via non-ion beams. The excitation may be provided by beams of x-rays (ESCA - Electron Spectroscopy for Chemical Analysis), electrons (AES - Auger Electron Spectroscopy), etc.<sup>69, 70</sup>. Again depth profiles can be obtained by using the surface erosion (sputtering) resulting from heavy ion bombardment (here typically 5 keV Ar).

From the above considerations, it may be concluded that all these analysis techniques should be considered complementary rather than competitive, each with its special area of optimum performance. Thus the MEIRS system bridges the gap between the low energy surface spectrometers with their excellent depth resolution involving essentially the first monolayer, as well as good mass resolution, and the higher energy materials analysis systems with good quantitative accuracy but somewhat poorer depth resolution ( $\sim 50 - 250 \text{ \AA}$  -- depending on the scattering geometry) and poor mass resolution for heavier elements.

## CHAPTER 6

### Nuclear Scattering Cross Section

#### 6.1 Introduction

When considering the interaction of energetic ions with matter, the basic quantity governing the interaction is the ion-atom differential scattering cross section. This determines the projectile energy loss in the elastic binary collision event and the subsequent particle direction. For the medium energy region (typically  $< 500$  keV) when the interaction is strongly influenced by the electron cloud surrounding the target atoms, a study of the elastic scattering of ions on atoms yields information on the screening of the Coulomb interaction by these atomic electrons and is thus of interest in determining information about the inter-atomic potential.

The purpose of this chapter is to report upon measured values of the differential scattering cross section using the MEIRS and compare these results with current theoretical predictions, as well as other recent cross section investigations in this region.

#### 6.2 Collision theory I

As mentioned previously, due to the wide field of applications (ion implantation, sputtering, surface analysis, radiation damage, etc.) many combinations of projectiles, energies and target

materials are of interest. A major simplification in the description of the ion-atom interaction is due to Lindhard and co-workers<sup>2-5</sup> who developed a unified theory of the interaction based upon the Thomas-Fermi statistical model of the atom.

### 6.2.1 Basic assumptions

The theory is based upon the following assumptions:

- (i) the collision is binary.
- (ii) the initial charge of the projectile is known.
- (iii) the possibility of correlated collision sequences is ignored.
- (iv) the collision description is treated classically.
- (v) the target atoms are considered stationary during the collision.

Condition (ii) simplifies the theory considerably although when an ion enters a material it will lose and capture electrons during collisions with the target atoms. Recent calculations<sup>71</sup> reveal that an effective screened charge can be ascribed to these ions to better predict experimental results. However, in the medium energy regime, the ion carries most of its electrons since its velocity is lower than the orbital electron velocities of the target atoms. (These important parameters are examined in more detail in Chapter 8 as they play a crucial role in the energy loss process.) Hence, the theory operates in a region where essentially all the  $Z_1 + Z_2$  atomic electrons are able to screen the nuclear charge. The third assumption is valid as long as a random struc-

ture is assumed for the target, although even for crystalline material the theoretical predictions have been reasonably accurate. The classical treatment<sup>72, 73</sup> of condition (iv) is found to be adequate in the medium energy regime as shown by a full relativistic quantal treatment of the subject<sup>74</sup>. Assumption (v) remains valid as long as the particle energy is much greater than the thermal energy of the atom. Only near the end of its trajectory does the projectile produce significant collective effects giving rise to non-linearities. These occurrences have been discussed in Chapter 4 and also considered experimentally by many in recent literature<sup>75, 76</sup>.

### 6.2.2 The two-body collision

Consider two particles with masses  $M_1$  and  $M_2$ . In the laboratory frame of reference, LABCS,  $M_1$  moves with the velocity  $v$ , before the collision whereas  $M_2$  is assumed initially at rest as illustrated in figure 6.1 (a). Since many features are simpler in the centre-of-mass frame, CMCS, consider figure 6.1 (b). It can be shown<sup>77</sup> that the CMCS scattering angle,  $\theta_c$  is given by

$$\theta_c = \pi - 2p \int_0^{u_0} \frac{du}{(1 - v(u)/E' - p^2 u^2)^{1/2}} \quad 6.1$$

where  $p$  = impact parameter

$$E' = M_2 E_0 / (M_1 + M_2)$$

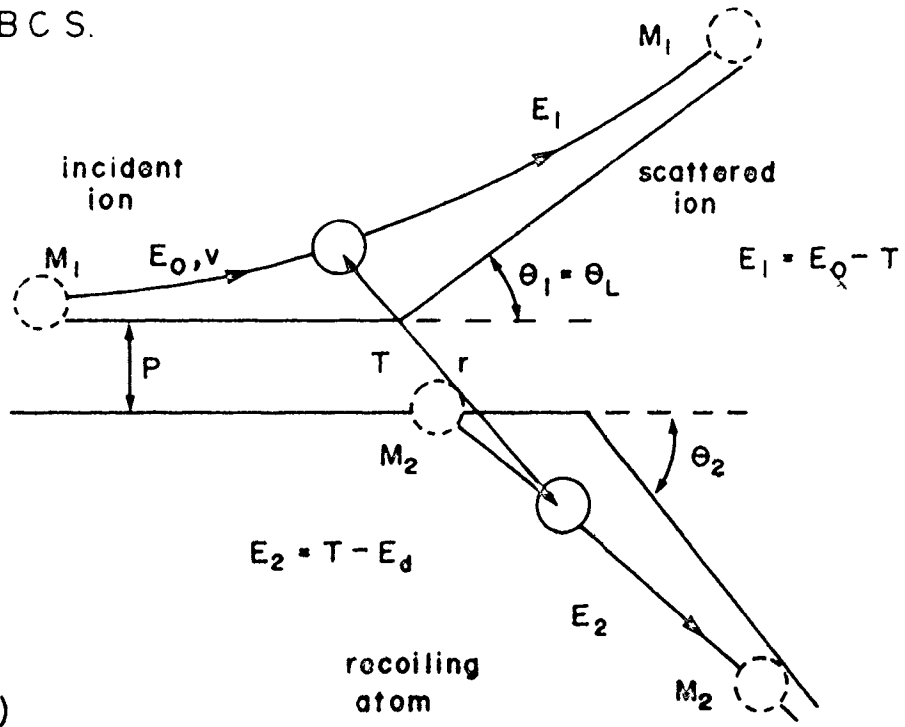
$$u = 1/r$$

$$u_0 = 1/r_0$$



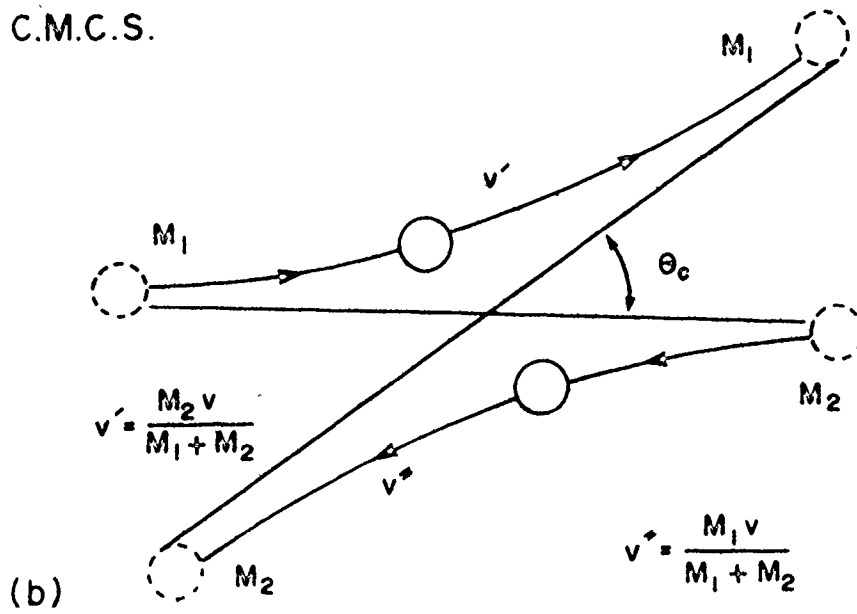
- Figure 6.1 (a) A binary encounter in the laboratory coordinate system (LAB.C.S.).
- (b) The same collision in the centre of mass coordinate system (C.M.C.S.).

LABC S.



(a)

C.M.C.S.



(b)

$r_0$  = distance of closest approach

$V(u)$  = interatomic potential

and  $E_0$  = incident particle energy

Thus before the scattering angle, which characterizes the collision, can be determined, more detailed information about the two-body potential governing the interaction is required.

### 6.2.3 The interatomic potential

Figure 6.2 (a) shows the form of the interatomic potential as a function of the interatomic separation. It can be seen that the force between two atoms is attractive for large separation, reaches a maximum near the equilibrium lattice spacing,  $d$ , and becomes rapidly repulsive at smaller separation distances when the electron clouds strongly overlap and the nuclear forces begin to play a role. Several models have been proposed to describe the interatomic potential which are based on an internuclear Coulomb force while accommodating the screening effect of the electrons as a function of the separation  $r$ . These are shown in figure 6.2 (b). For  $r \lesssim d$ , the Born-Mayer potential<sup>78</sup> has been developed while for  $r \ll d$ , the Bohr<sup>1</sup> and Thomas-Fermi<sup>79, 80</sup> potentials have been proposed. The Bohr model<sup>1</sup> takes a potential of the form

$$V(r) = \frac{Z_1 Z_2 e^2}{r} \exp(-r/a) \quad 6.2$$

where  $a$  is called the electron screening radius and is found to be

$$a = \frac{1}{2} \left( \frac{3\pi}{4} \right)^{2/3} \frac{a_0}{Z_2^{1/3}} \quad 6.3$$

with  $a_0 = \frac{\hbar^2}{m_e e^2}$  representing the electronic first Bohr radius of hydrogen. The Thomas-Fermi potential is given as

$$V(r) = \frac{Z_1 Z_2 e^2}{r} \cdot \phi\left(\frac{Z_1}{Z_2}, \frac{r}{a}\right) \quad 6.4$$

where  $\phi$  is a tabulated <sup>81</sup> screening function which tends to unity as  $r \rightarrow 0$  (approaching simple Coulombic scattering) and towards zero as  $r \rightarrow \infty$ .

Lindhard extended this treatment to give the screening radius between dissimilar atoms, occurring in ion-solid interactions, as

$$a = \frac{0.8853 a_0}{(Z_1^{2/3} + Z_2^{2/3})^{1/2}} \quad 6.5$$

Using equations 6.4 and 6.5 it is found that

$$\theta = \theta\left(\frac{Z_1}{Z_2}, \frac{b}{a}, \frac{p}{a}\right) \quad 6.6$$

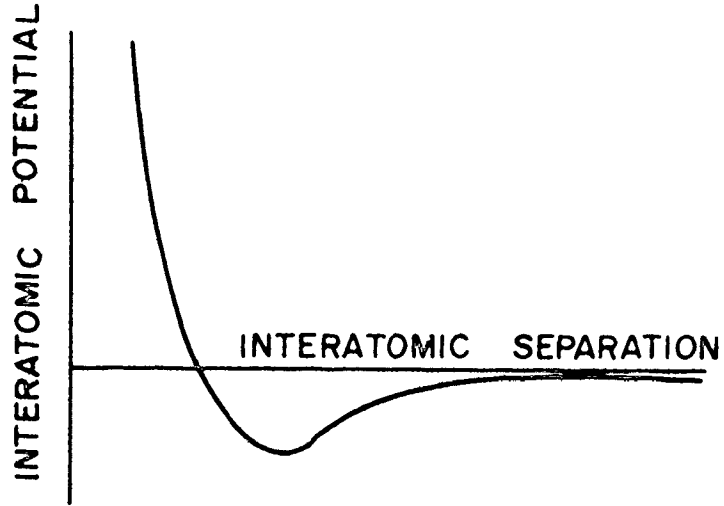
where the collision diameter,  $b$ , has been defined as

$$b = \frac{2 Z_1 Z_2 e^2}{E'} \quad 6.7$$

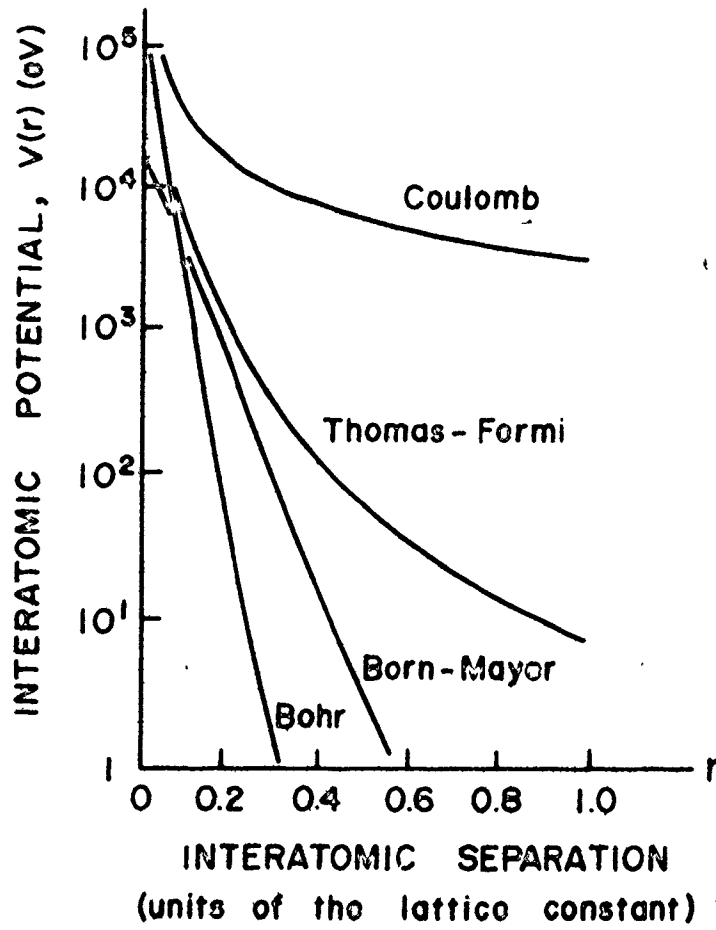
The LSS quantity,  $\frac{b}{a}$ , appears often in this theory and is referred to as the reduced energy

$$\begin{aligned} \epsilon &\equiv \frac{a}{b} \\ &= \frac{E'}{Z_1 Z_2 e^2 / a} \end{aligned} \quad 6.8$$

- Figure 6.2 (a) A qualitative description of the interatomic potential.
- (b) A comparison of various proposed potentials between two copper atoms.



(a)



(b)

which represents the kinematic energy of the relative motion in units of the Thomas-Fermi (T.F.) energy,  $Z_1 Z_2 e^2/a$ .

Using equation 6.5 and the above parameters, the scattering angle can now be expressed as a function of  $\epsilon$  and  $\frac{p}{a}$  alone

$$\theta = \theta(\epsilon, \frac{p}{a}) \quad 6.9$$

#### 6.2.4 The nuclear scattering cross section

Using the T.F. potential, Lindhard et al<sup>79</sup> solved equation 6.1 via perturbation theory, which is valid for small  $\theta$ , and extrapolated the results to large  $\theta$ . By means of this approach it is possible to reduce the dependence of the scattering cross section,  $d\sigma$ , to a single parameter,  $\tau$ :

$$\tau = \epsilon^2 \frac{T}{T_M} = \epsilon^2 \sin^2\left(\frac{\theta_C}{2}\right) \quad 6.10$$

$$\text{where } T = T_M \sin^2\left(\frac{\theta_C}{2}\right) \quad 6.11$$

$$\text{with } T_M = YE \quad 6.12$$

$$\text{and } \gamma = \frac{4 M_1 M_2}{(M_1 + M_2)^2} \quad 6.13$$

$$\text{so that } d\sigma = 2\pi p dp \quad 6.14$$

$$\text{becomes } d\sigma = \frac{\pi a^2 f(\tau^{1/2})}{2\tau^{3/2}} d\tau \quad 6.15$$

where  $f(\tau^{1/2})$  is a universal screening function derived from the

potential screening function,  $\phi$ .

Because the same  $\phi$  can be used for all  $Z_1$  and  $Z_2$  combinations with reasonable accuracy, the same function  $f(\tau^{1/2})$  can describe all collisions independent of  $Z_1$  and  $Z_2$  values. Thus, due to this similarity property, all events derived from the elastic collision process can, in general, be represented by one universal curve.

The universal screening function, sometimes called the reduced scattering cross section, can be calculated numerically using the Thomas-Fermi treatment; however an analytical approximation has been developed by Winterbon, Sigmund and Sanders<sup>82</sup>, hereafter referred to as WSS. This approximation is of the form

$$f(\tau^{1/2}) = \frac{\lambda \tau^{1/2}}{(1+(2\lambda\tau^{2/3})^{2/3})^{3/2}} \quad 6.16$$

where  $\lambda = 1.309$ , the fitting parameter.

Another convenient approximation is the power law derived from a power structure imposed on the interatomic potential. It leads to the following cross section approximation<sup>83</sup>:

$$f(\tau^{1/2}) = \lambda_m / (\tau)^{m-1/2} \quad 6.17$$

where  $0 \leq m \leq 1$  and is chosen to best approach  $f(\tau^{1/2})_{TF}$  in the region of interest.

They include:

Coulombic scattering -  $m = 1$ ,  $\lambda_1 = 1/2$  for  $\epsilon \gtrsim 2$

inverse square potential -  $m = 1/2$ ,  $\lambda_2 = 0.327$  for

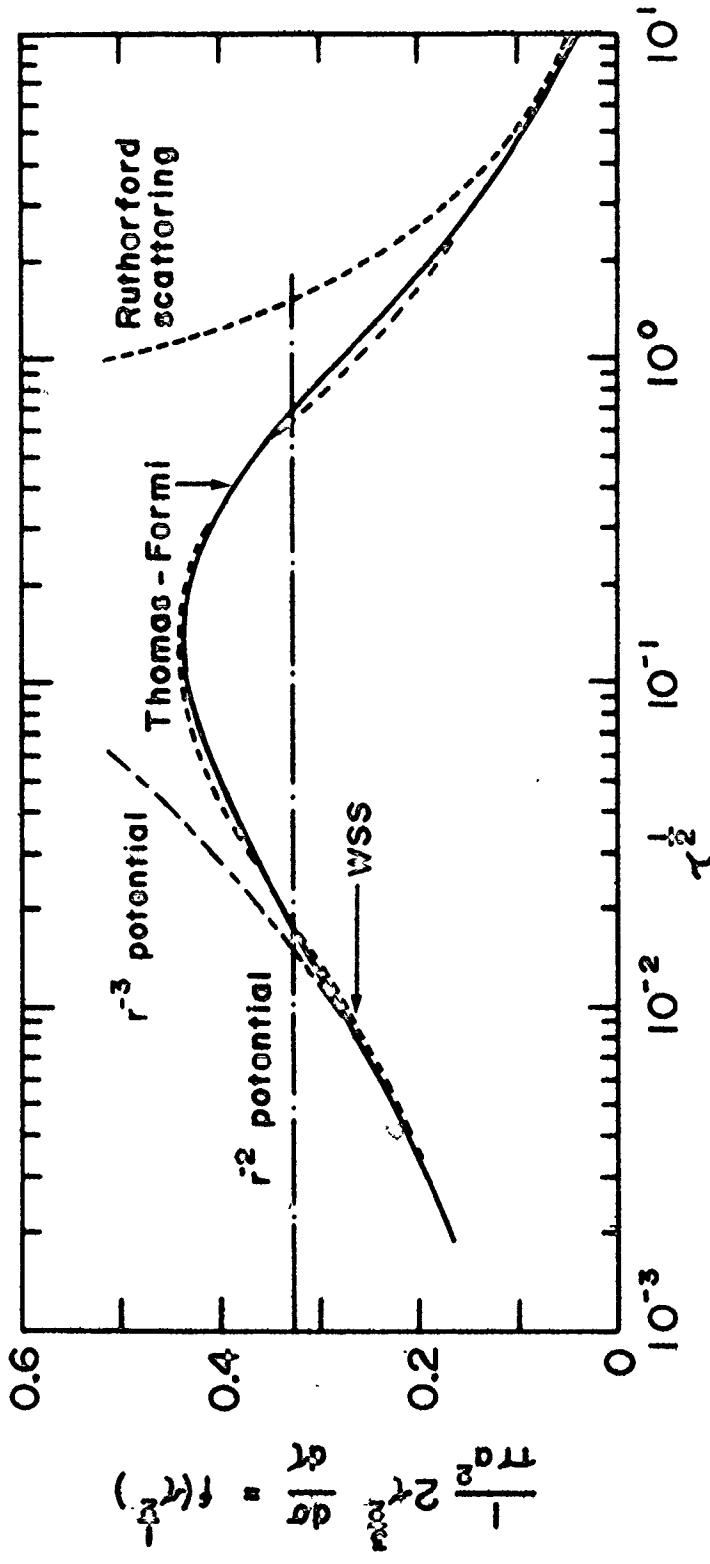
$0.08 \lesssim \epsilon \lesssim 2$

inverse cube potential -  $m = 1/3$ ,  $\lambda_3 = 1.309$  for  $\epsilon \lesssim 0.2$



Figure 6.3 The universal differential scattering function for elastic nuclear collisions and its approximations: — Thomas Fermi

numerical calculation; --- Winterbon et al (WSS) analytical description; --- the reciprocal cube potential approximation; --- the reciprocal square potential approximation; --- the pure Coulomb potential (Rutherford scattering)



UNIVERSAL DIFFERENTIAL SCATTERING FUNCTION FOR ELASTIC  
NUCLEAR COLLISIONS

The above approximations are shown in figure 6.3.

### 6.3 Principles and Technique

The experimental procedure involves measurements using Rutherford backscattering, RBS, with 1 MeV He<sup>+</sup> to determine the density of scattering centres, and medium energy ion reflection, MEIR, to determine the yield of backscattered ( $\theta_L = 150^\circ$ ) particles in the 20 - 150 keV range.

#### 6.3.1 Features of Backscattered Spectra

The general shape of spectra obtained by either method of RBS or MEIRS is shown in figure 6.4. The inelastic energy loss processes indicated are detailed in Chapter 8 while the elastic loss can be calculated from energy and momentum considerations as outlined in the preceding sections. If  $k$  is the kinematic factor or the elastic energy loss fraction, then

$$E_1 = kE_0 \quad 6.18$$

where

$$k = \frac{M_1 \cos \theta_L}{(M_1 + M_2)} + \left\{ \left[ \frac{M_1 \cos \theta_L}{(M_1 + M_2)} \right]^2 + \frac{(M_2 - M_1)}{(M_1 + M_2)} \right\}^{1/2} \quad 6.19$$

For He incident on gold at  $\theta_L = 150^\circ$ ;  $k = 0.9274$ .

When an ion-target system can be characterized by  $\tau \geq 100$ , where  $\tau = \epsilon^2 T / T_M$  then the appropriate cross section, being pure Coulombic, i.e. Rutherford scattering, is given by

$$\frac{d\sigma}{d\Omega} = \left[ \frac{Z_1 Z_2 e^2}{4 E_0} \right]^2 \frac{(1 + \gamma^2)}{(\gamma \cos \theta_c + 1)} \left[ \frac{\sin \theta_L}{\sin \theta_c} \right]^3 \csc^4 \left[ \frac{\theta_L}{2} \right] \quad 6.20$$

or in Lindhard's reduced system

$$\frac{d\sigma}{d\Omega} = \frac{\pi a^2}{2\tau^{2/3}} f_{RUTH}(\tau^{1/2}) \quad 6.21$$

$$\text{where } f_{RUTH}(\tau^{1/2}) = \frac{1}{2\tau^{1/2}} \quad 6.22$$

From these considerations it can be shown that for large angle scattering, Rutherford backscattering is characterized by small impact parameters ( $p \lesssim 10^{-3} \text{ \AA}$ ) and large cross sections making it an ideal tool for quantitative studies of heavy impurities in lighter host substrates.

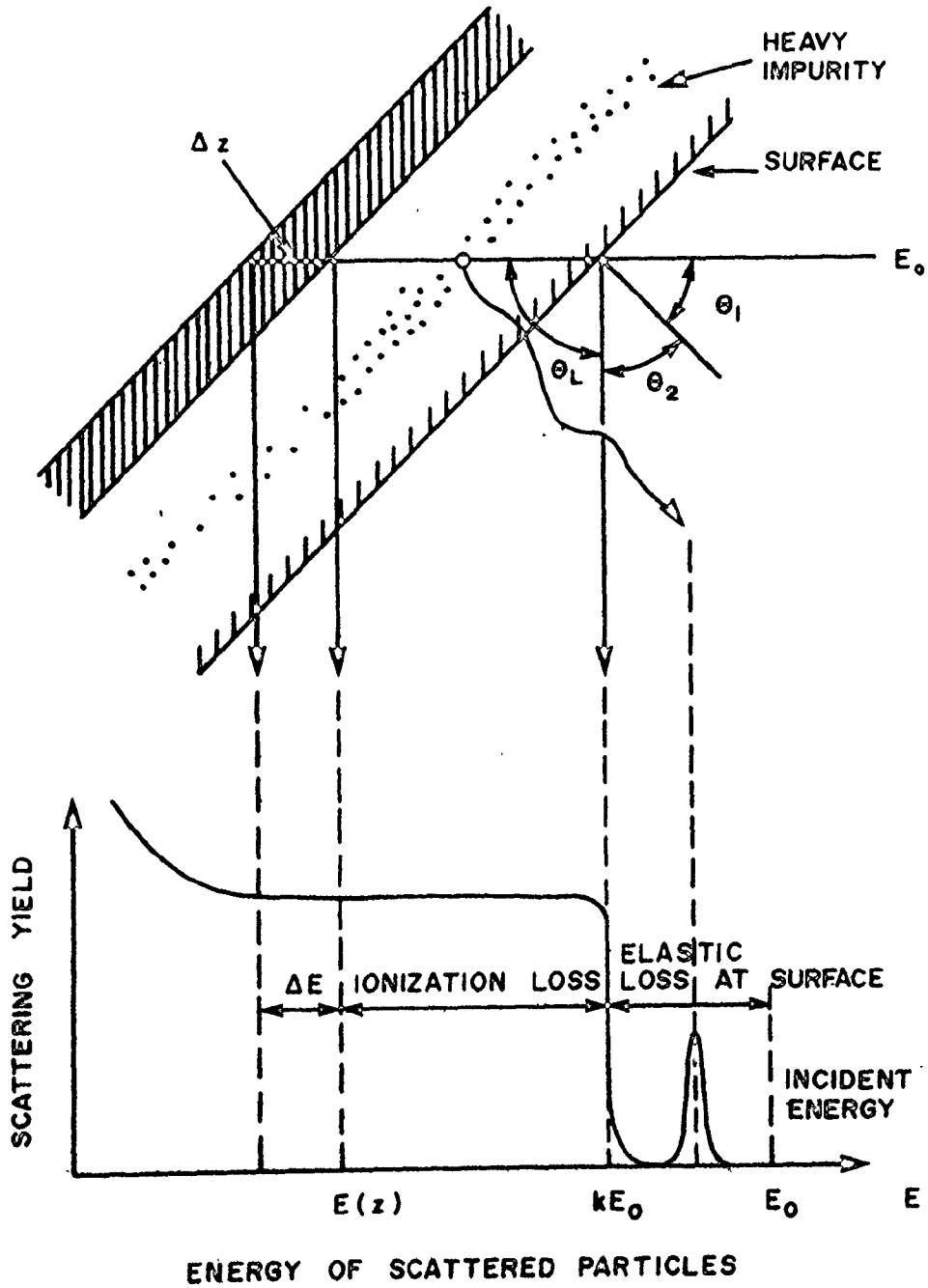
In recent studies<sup>84, 85</sup> it has been discovered experimentally, for 1 MeV He scattering by high Z atoms, that the use of the Rutherford cross section introduces a small error since a slight screening effect is still present which reduces the cross section by 1 - 2%. L'Ecuyer et al<sup>84</sup> apply a correction to the Rutherford cross section,  $\sigma_{RUTH}$ , of the form

$$\frac{d\sigma(\theta)_{corr}}{d\Omega} = \frac{d\sigma_{RUTH}(\theta)}{d\Omega} \left[ 1 - \frac{0.049 Z_1 Z_2^{4/3}}{E} \right] \quad 6.23$$

where E is the centre of mass energy in keV. Using these formulations, all the experimental calculations in this thesis have been corrected for this Rutherford screening effect.

Figure 6.4: The principles of impurity atom detection via back-scattering: a light substrate containing a small fraction of heavier atoms in a near surface region is bombarded with a beam of light ions of energy,  $E_0$ . The lower portion of the figure shows the resulting energy spectrum of scattered particles.

ORIGIN OF BACKSCATTERED SPECTRA



For a particle which penetrates the target surface and backscatters at a depth,  $t$ , the energy loss suffered by the particle in the target both before and after the backscattering event is due to ionization and excitation of the target atoms. If  $S(E)$  is the stopping cross section, then a continuous spectrum of backscattered particles will result for  $E$  since

$$E(z) = k \left[ E_0 - \int_0^t N S(E) dz \right] - \int_{\frac{t}{\cos \theta_L}}^0 N S(E) dz \quad 6.24$$

which for our shallow depths reduces to

$$E(z) = k E_0 - t \left[ k N S(E_0) + \frac{N S(E_1)}{\cos \theta_L} \right] \quad 6.25$$

since  $S(E)$  can be assumed relatively constant. Hence if  $S(E)$  is known, the energy scale of figure 6.4 can be readily converted into a depth scale such that one channel in energy units,  $\Delta E$ , becomes in depth units,

$$t = \frac{\Delta E}{\left[ k S(E_0) + \frac{S(E)}{\cos \theta_L} \right]} \quad 6.26$$

For a very thin layer of heavy impurities on the surface of a lighter mass substrate, the backscattered energy spectrum corresponding to the heavy impurity has a Gaussian shape. This occurs provided the layer is thin compared to the system depth

resolution which is determined from the detector energy resolution and application of equation 6.26. The area under the peak, YLD, then can be related to the density of this layer,  $N\Delta t$ , provided that the incident beam fluence,  $Q$ , and the solid angle subtended by the detector,  $\Delta\Omega$ , is known. If the layer thickness is sufficiently thin that the energy loss of the analyzing beam in penetrating and exiting the target is negligible, then

$$YLD = \int_0^{\Delta t} \Delta\Omega \frac{d\sigma(E_0)}{d\Omega} Q N dz \quad 6.27$$

where  $\frac{d\sigma}{d\Omega}$  is the differential elastic scattering cross section.

### 6.3.2 Experimental and Analysis Procedure

The samples used were polished Si single crystals with  $\sim 10^0$  Å of Au e-beam evaporated onto the surface. The base pressure in the evaporator was  $1 \times 10^{-6}$  torr. This Au thickness provides a backscattered signal sufficiently less than the detector equivalent depth resolution of the system so that a Gaussian response is obtained. Measurements using MEIRS with the electrostatic analyser on similar samples show a sharp Au edge at the substrate interface indicating the absence of large thickness nonuniformities. The possible presence of island formations has not been verified although this should not affect the backscattering results significantly. The gold targets are mounted on the hexagonal carousel mentioned in part I of this thesis and are inserted into the scattering chamber, maintained at  $< 1 \times 10^{-8}$  torr. Use of the coupled accelerator system of the MEIRS allows a very accurate RBS



analysis of the thin gold layer thickness both before and after bombardment by medium energy ions since exact geometrical conditions can be maintained rather easily. It is these medium energy ions ( $20 \geq M_1 \geq 1$  amu) that are used to determine scattering cross sections.

Consider the RBS experiments using 1 MeV  $\text{He}^+$  incident on the Au/Si samples. The governing expression, using equation 6.27, is

$$\text{YLD}(\text{He}) = N\Delta t \Delta\Omega Q(\text{He}) \frac{d\sigma(\text{He})_{\text{corr}}}{d\Omega} \quad 6.28$$

For the medium energy backscattering, ME

$$\text{YLD}(\text{ME}) = N\Delta t \Delta\Omega Q(\text{ME}) \frac{d\sigma}{d\Omega} (\text{ME}) \quad 6.29$$

Combining equations 6.28 and 6.29

$$\frac{d\sigma(\text{ME})}{d\Omega} = \frac{Q(\text{He})}{Q(\text{ME})} \frac{d\sigma(\text{He})_{\text{corr}}}{d\Omega} \frac{\text{YLD}(\text{ME})}{\text{YLD}(\text{He})} \quad 6.30$$

Using equation 6.15 and 6.30

$$f(\tau^{1/2}) = \frac{Q(\text{He})}{Q(\text{ME})} \frac{d\sigma(\text{He})_{\text{corr}}}{d\Omega} \frac{\text{YLD}(\text{ME})}{\text{YLD}(\text{He})} \frac{8\tau^{3/2} \sin \theta_L}{a^2 \epsilon^2 \sin \theta_c} \quad 6.31$$

$$\left\{ 1 + \frac{\frac{M_1}{M_2} \cos \theta_L}{\left[ 1 - \left[ \frac{M_1}{M_2} \sin \theta_L \right]^2 \right]^{1/2}} \right\}$$

Table 6.1

Measured Values of the Scattering Cross Section and the Corresponding Screening Function.

Ion Energy (keV)	Species	$\tau^{1/2}$	$\frac{d\sigma}{d\Omega} (\frac{\text{cm}^2}{\text{sr}} \times 10^{-20})$	$f(\tau^{1/2})$
126	Neon	0.95	4.28 ± 0.27	0.32 ± 0.02
114		0.86	5.38 ± 0.44	0.37 ± 0.03
132	Nitrogen	1.50	1.63 ± 0.16	0.21 ± 0.02
112		1.27	2.20 ± 0.18	0.24 ± 0.02
133	Carbon	1.80	1.48 ± 0.15	0.20 ± 0.02
87		1.17	3.1 ± 0.30	0.27 ± 0.03
130	Boron	2.14	1.1 ± 0.14	0.16 ± 0.02
85		1.40	2.3 ± 0.20	0.24 ± 0.02
132	Lithium	3.74	0.44 ± 0.04	0.12 ± 0.01
132	Helium	5.75	0.20 ± 0.02	0.081 ± 0.009
89		3.87	0.40 ± 0.04	0.106 ± 0.010
134	Deuterium	11.95	0.054 ± 0.003	0.040 ± 0.003
99		8.82	0.086 ± 0.009	0.050 ± 0.006
66		5.93	0.21 ± 0.02	0.082 ± 0.008

$$\text{where } \frac{d\tau}{d\Omega} = \frac{\epsilon^2}{4\pi} \frac{\sin \theta_c}{\sin \theta_L} \left\{ 1 + \frac{\frac{M_1}{M_2} \cos \theta_L}{\left[ 1 - \left[ \frac{M_1}{M_2} \sin \theta_L \right]^2 \right]^{1/2}} \right\} \quad 6.32$$

from  $d\Omega = 2\pi \sin \theta_L d\theta$

$$\text{and } \theta_c = \theta_L + \tan^{-1} \left\{ \left[ \frac{M_1}{M_2} \sin \theta_L \right] / \left[ 1 - \left[ \frac{M_1}{M_2} \sin \theta_L \right]^2 \right]^{1/2} \right\}$$

Thus by measuring the dose  $Q$  and the number of scattering events corresponding to the Au peak by both RBS and MEIRS, it is possible to determine the screening parameter,  $f(\tau^{1/2})$ . The Au scattering centre density is measured before and after medium energy ion exposure to compensate for any Au loss due to sputtering. Care is also taken to maintain identical geometries among the three runs required for each  $f(\tau^{1/2})$  determination.

#### 6.4 Results and Discussion

Table 6.1 summarizes the experimental results while figure 6.5 shows the reduced cross sections compared to LSS theory based on the Thomas-Fermi screening function and expected Rutherford (pure Coulombic) behaviour. Figure 6.6 compares the present data with similar experiments performed elsewhere.

The agreement between the LSS prediction and experiment is extremely good offering strong support for the  $Z_1 Z_2$  scaling. The fixed ion-target combinations when taken as a group and differing only in energy justify the validity of the wide angle extra-

polation at least out to  $\theta_L = 150^\circ$ . However the actual magnitude of the cross section is somewhat larger than predicted when  $\tau^{1/2} < 1.5$ . This slight divergence has also been noted by several other investigators<sup>85-88</sup> using small angle scattering ( $\theta_L = \text{small}$ ) and transmission studies, all of which required multiple scattering corrections thereby increasing possible inaccuracies. The use of the backscattering technique, for wide angle scattering with thin films ( $t < 15 \text{ \AA}$ ) requires no such correction (eg.  $< 1\%$  correction)<sup>88</sup>. Although, by the very use of large  $\theta_L$ , a direct comparison of these results to theirs is somewhat tenuous. So far as is known, the only other investigation involving backscattering is that due to van Wijngaarden et al<sup>88</sup>. They backscattered ( $\theta_L = 134.6^\circ$ ) 50 - 110 keV  $\text{H}^+$ ,  $\text{He}^+$ ,  $\text{Li}^+$  and  $\text{B}^+$  ions from 75 - 340  $\text{\AA}$  Au films, vacuum evaporated onto Be substrates, into a solid state detector. Their results, together with those from Andersen et al<sup>87</sup> which is representative of the  $\theta_L = \text{small}$  transmission studies, agree with the present measurements as shown in figure 6.6. However the van Wijngaarden et al<sup>88</sup> data exhibit a larger scatter possibly from the applied multiple scattering corrections ( $\sim 25\%$  for the largest correction involving 100 keV  $^{11}\text{B}$  on 120  $\text{\AA}$  Au). Because they did not analyze their data in terms of  $f(\tau^{1/2})$ , it is difficult to compare their results for different ions. There are many reports in the literature of scattering cross section measurements where use is made of ion beams interacting with gaseous targets (cf. reference 85) and general agreement is found with the LSS calculations even at lower  $\tau^{1/2}$  values although the uncertainty in the results is rather large.

Figure 6.5 Measured screening functions for reduced scattering cross sections of gold for a large number of combinations of projectiles and incident energies. These data are compared to the theoretical predictions due to Lindhard et al<sup>79</sup> and that of a pure Coulombic (Rutherford) interaction.

SCREENING FUNCTION  
FOR  
REDUCED SCATTERING  
CROSS SECTIONS

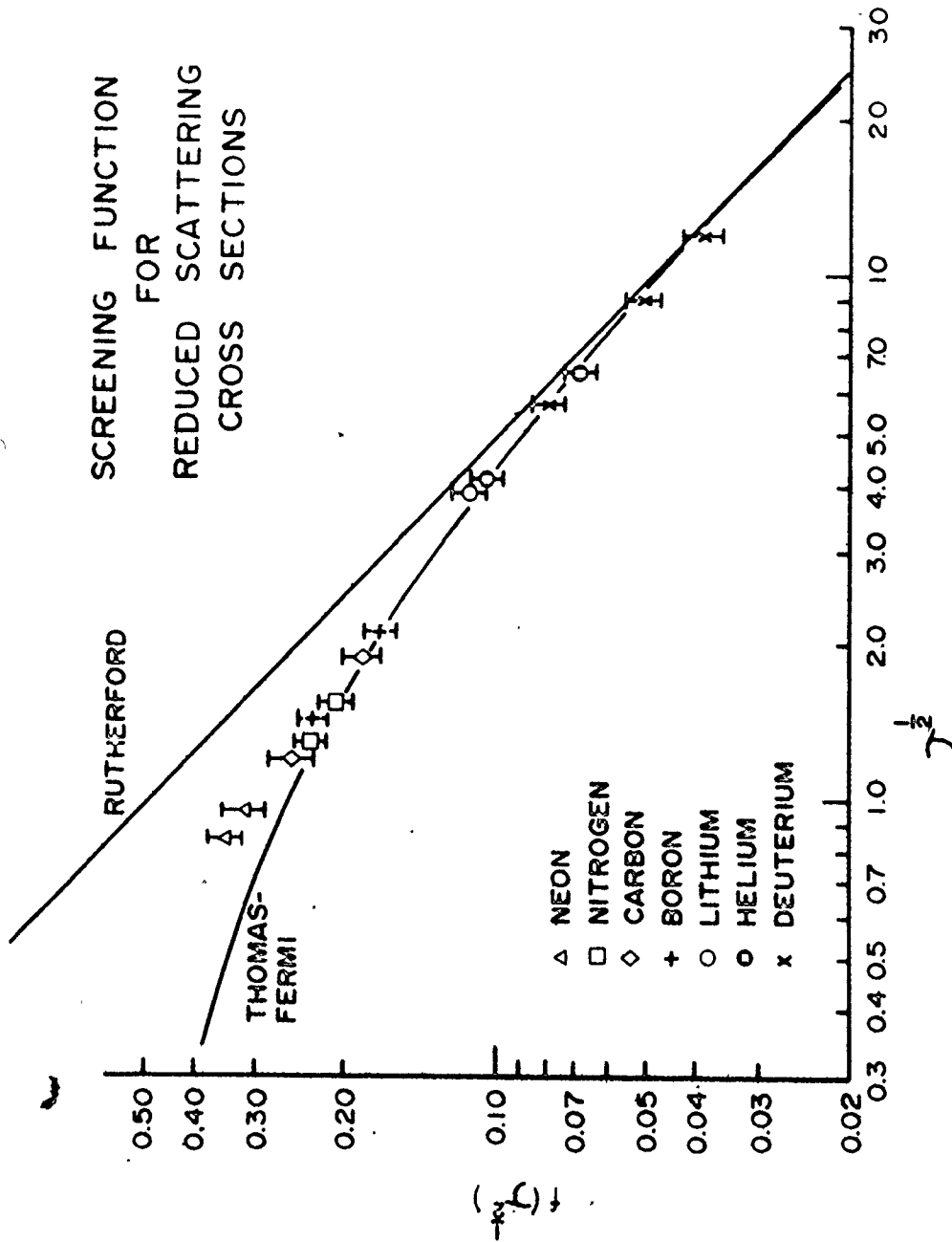
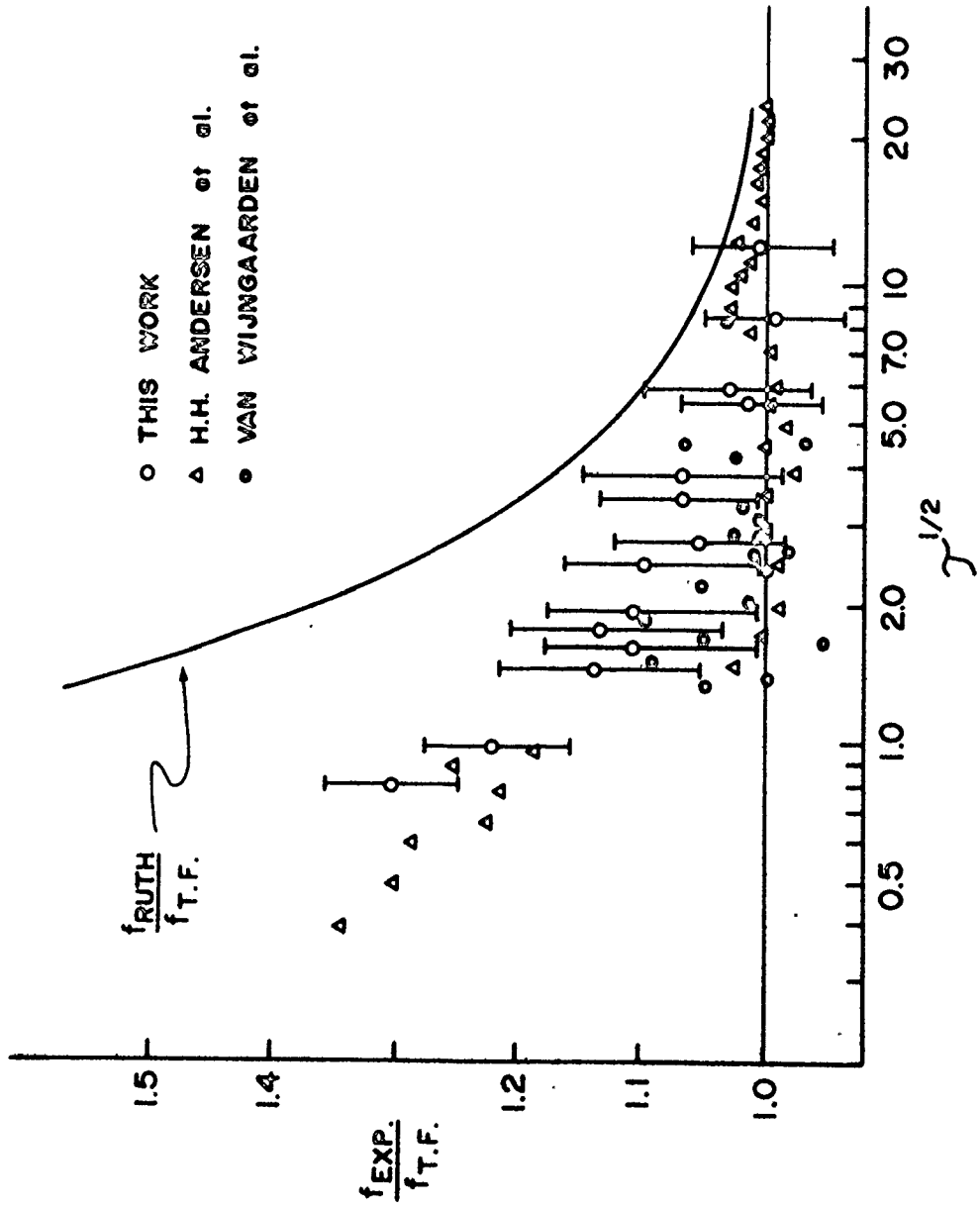


Figure 6.6 The results of Figure 6.5 normalized to the Thomas-Fermi cross section. Other results due to Andersen et al<sup>87</sup> and Wijngaarden et al<sup>88</sup> are also presented.





Thus, the prediction of the LSS theory provides a rather good approximation to the experimental observations. The scaling properties are reasonably fulfilled in the interval  $0.8 \leq \tau \leq 10$ ; and the magnitude of the differential cross section closely agrees with the Thomas-Fermi cross section except for the lower  $\tau^{1/2}$  values where the theory seems to overestimate the screening effect.

## CHAPTER 7

### Charge Neutralization Measurements

#### 7.1 Introduction

Inelastic outershell processes have received a significant amount of recent attention for several reasons. These processes form the basis of a number of surface analytical techniques such as ISS, SCANIIR, and SIMS. The importance of charge-to-neutral ratios (cf Chapter 5) has already been discussed as a correction needed in quantitative ESA work and this is put to use in Chapter 8 with respect to the determinations of stopping powers and straggling. The current need to understand the charge exchange interaction of a confined plasma with the first wall surface has become one of the most significant problems in the effort to achieve controlled thermonuclear fusion. In addition, this area itself has proven to be a fruitful region of basic research with substantial overlapping interests in atomic physics, solid state physics, nuclear physics, chemical physics, surface physics as well as space physics.

In the case of light mass projectiles, several experimental studies related to the charge states of H, D and He beams emerging from solid surfaces have been performed over the last few years<sup>89-93</sup>. Interest in the studies of charge states of H and D has been primarily generated by tokamak fusion research where information on the neutralization probability of the particle backscattered from the wall is required since the charged particles are not able to

re-enter the plasma.  $\text{He}^+$  received attention because of its use in characterizing solids and surfaces by backscattering. Theoretical efforts<sup>94 - 99</sup> in this area are also limited to explaining the charge fraction of H and He only. These theories do not adequately explain the phenomena of neutralization of ions emerging from a solid surface.

The charge neutralization behaviour of heavy ions in the 10 - 100 keV range in solids remains completely unexplored both with respect to theory and experiment although there are some results available for ion fractions of backscattered Ne and Ar in the lower energy region<sup>100,101</sup>. Thus there is a requirement for experimental determinations of charged fractions for various ions in order to provide a better basis for a theoretical understanding of this type of phenomena. Also, for this energy regime, the use of heavy ions backscattered from solids may provide advantages to the surface characterization technique including continuous sputter cleaning of the target, and improved impurity sensitivity. The analogue method already in use, in the MeV region, for Rutherford backscattering analysis, employs heavy ions such as carbon<sup>102</sup> and nitrogen<sup>103</sup>. Not only is there improved sensitivity, but the use of those heavier projectiles avoids the detrimental effect of pulse pile up since the technique is insensitive to backscattered events originating from any incident ion collisions with a target atom which is lighter in mass than the projectile.

This chapter begins with the theoretical framework of section 7.2 which presents the various highlights of the prominent

theories, some of which are at odds with others. Following this, the next section outlines the analysis procedure used and briefly reviews the experimental technique which has already been presented in detail in Chapter 4. Section 7.4 reports on the measurements of charged fractions for H, D, He, Li, B, C, N, F and Ne back-scattered from Au in the energy region of 25 to 150 keV. In the latter six ions, the experiments are the first, so far as is known, performed on solid surfaces in this energy regime.

## 7.2 Theoretical Framework for Ion Neutralization Behaviour

As in the case of stopping powers, the neutralization behaviour of ions differs when their velocities are such that  $v \gg v_0$  and  $v \ll v_0$  where  $v_0$  is the Bohr velocity. For most low energy ( $v \ll v_0$ ) ion-target combinations, the processes of Auger neutralization and resonance tunnelling from the valence band into atomic states seems adequate to predict experiment<sup>104</sup>. On the other hand for  $v \gg v_0$ , at high energies, the use of electron capture and loss coefficients in suitable rate of change equations<sup>1,31,105</sup> has provided rather successful comparisons to experiments<sup>106,107</sup>. In the medium energy regime for the lighter particles with  $v \sim v_0$  both of the above theoretical approaches may be expected to be valid to some extent. They are examined in the next two sections while in the last section, several special schemes which have been proposed explicitly for the medium energy region are examined.

### 7.2.1 Low Energy Processes

When an atom or ion is near a solid surface for a sufficiently long period of time, (the lifetime of the initial states of the (de) excitation process under consideration here is  $\sim 10^{-14}$  seconds<sup>108</sup>) there are several processes which may occur to (de) neutralize the species. Consider figure 7.1 (a), where the one-electron operation of resonance neutralization is depicted. Here the filled portion of the conduction band in the metal is shown from which an electronic transition labelled 1 occurs involving the atomic potential well of an outgoing particle near the surface. Since the electron moves from a filled level in the solid below the Fermi level into the atomic excited level of the same energy, a resonance condition is fulfilled. A complementary ionization of a neutral atom can also occur, where from a filled excited state, an electron, labelled 2, can transit into an unfilled level in the metal above the Fermi level. Figure 7.1 also serves to define several energy quantities such as work function of the solid,  $\phi$ , the effective ionization and excitation energies,  $E_I$  and  $E_X$  respectively of the atom outside the solid, as well as its distance of separation from the solid,  $S$ . In figure 7.1 (b) the two-electron process of Auger neutralization is shown. Here, one electron tunnels into the ion ground state from a level in the solid while a second electron is simultaneously excited from another level with exactly the same energy.

These processes all have an exponential dependence on separation distance,  $s$  for the transition rate at which they

become involved in a specific operation. It is the transition probability per unit time,  $R(s)$ , and is defined as<sup>109</sup>

$$R(s) = Ae^{-as} \quad 7.1$$

where  $A$  is the transition rate at the surface and  $a$  is a critical distance. Reasonable values for  $a \sim 2 \text{ \AA}^{-1}$  and for  $A \sim 10^{14} - 10^{16} \text{ sec.}^{-1}$ <sup>110</sup>. These numbers show that the transition rate for this process is very large for short distances,  $s \sim 1 - 2 \text{ \AA}$ . It can be shown<sup>111</sup> that the probability,  $P(s, v_{\perp})$ , that a particle whose velocity component normal to the solid surface,  $v_{\perp}$ , will reach a distance  $s$ , with its original charge and excitation state is

$$P(s, v_{\perp}) = \exp \left[ \frac{A}{a} v_{\perp} (e^{-as} - 1) \right] \quad 7.2$$

Thus the probability that the particle has escaped without having undergone a transition is

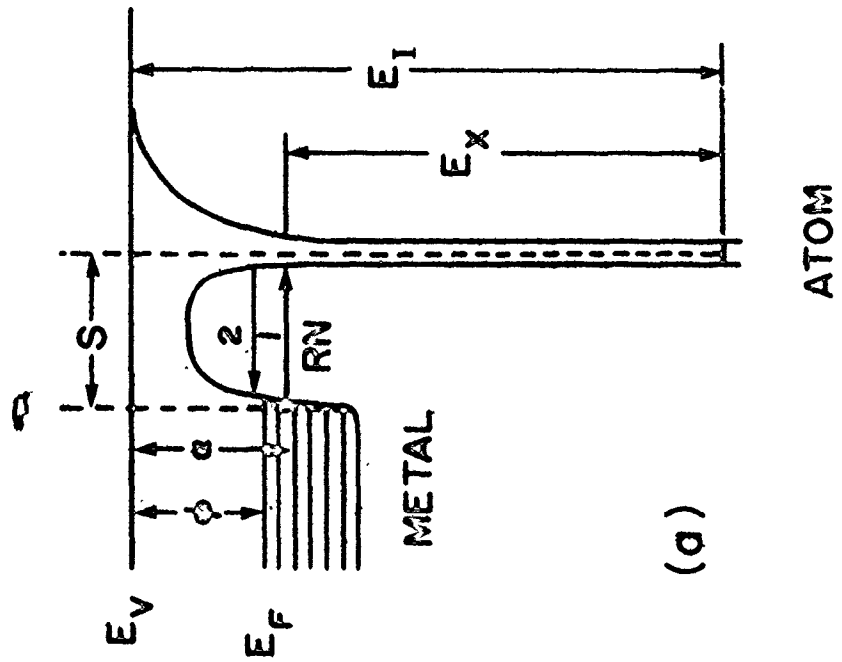
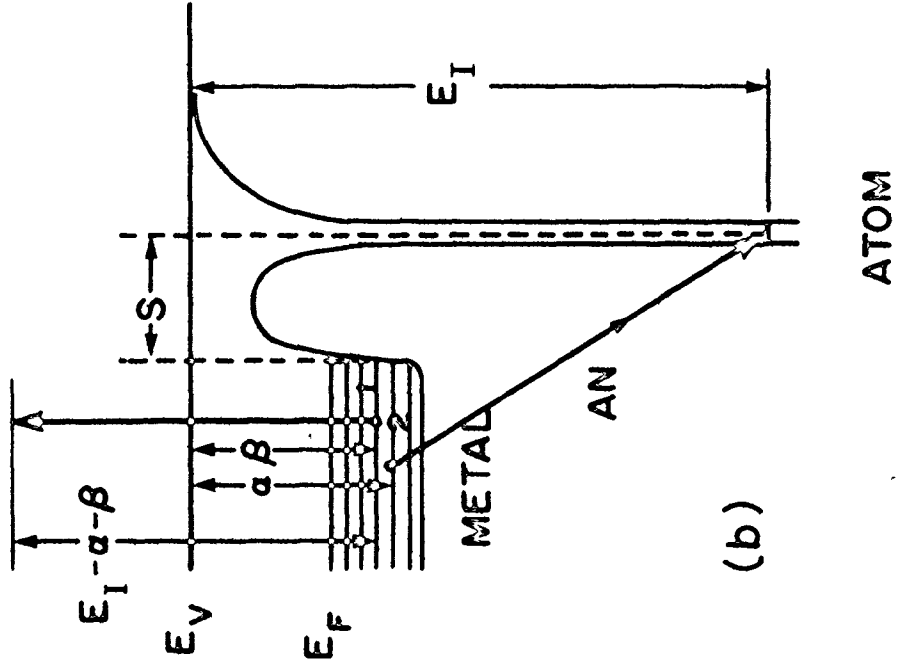
$$P(\infty, v_{\perp}) = e^{-\frac{A}{a} v_{\perp}} \quad 7.3$$

where  $\frac{A}{a}$  is usually called the survival parameter and is of the order of  $10^7 \text{ cm/sec}$ .

### 7.2.2 High Energy Processes

The first neutralization mechanism to be proposed<sup>1,31,105</sup> was that involving the bound states of electrons around the projectile while traversing the solid. After passage through some minimum thickness of material, an average equilibrium charge state is established at a particular velocity. If  $f^c = Y_c / (Y_N + Y_c)$  represents the charged fraction then its rate of change along the

- Figure 7.1 (a) Electron energy diagram of an atom and metal surface at a separation distance  $s$ , illustrating several, (1) and (2), resonance tunneling processes. The solid work function is  $\phi$ , while  $E_x$  and  $E_I$  are the effective excitation and ionization energies respectively of the single atom.
- (b) Electron energy diagram for the two-electron Auger neutralization process where one electron tunnels into the ground state from the metal level "2" while a second electron is simultaneously excited from another level labelled "1". These electrons respectively lose and gain the same amount of energy in this radiationless process.





beam direction,  $z$  is

$$\frac{df^C}{dz} = N \left[ (1 - f^C)\sigma_\ell - f^C\sigma_c \right] \quad 7.4$$

where  $N$  is the target atom density and  $\sigma_c$  and  $\sigma_\ell$  are the electron capture and loss cross sections for the particle respectively.

The equilibrium ion fraction can now be obtained by setting  $df^C/dz = 0$  so that

$$f_{eq}^C = \left( 1 + \frac{\sigma_c}{\sigma_\ell} \right)^{-1} \quad 7.5$$

The general expressions for the cross sections of atoms with atomic number  $Z_2$  have been quoted<sup>112</sup> as

$$\sigma_c = \pi a_0^2 \frac{2^{18}}{5} \frac{Z_2^5}{\left[ \left( \frac{v}{v_0} \right)^6 \left( \left( \frac{v}{v_0} \right)^2 + \frac{2^6}{3\sqrt{40}} Z_2^{14/9} \right) \right]^3}$$

and

$$\sigma_\ell = \frac{\pi a_0^2 Z_2^{2/3}}{\left[ Z_2^{2/3} + \left( \frac{v}{v_0} \right) \right]^6} \frac{4 Z_2^{1/3} (Z_2 + 1)}{4 Z_2^{1/3} (Z_2 + 1) + \frac{v}{v_0}}$$

where  $a_0$  is the Bohr radius and  $v_0$  is the Bohr velocity.

These results have adequately accounted for the observed variation of charged fractions in solid foils for proton energies above 1 MeV<sup>112</sup>.

### 7.2.3 Medium Energy Processes

In the medium energy regime, the low energy processes of neutralization are no longer in operation, at least for the light mass ions since the time or close proximity of ion and surface region is so short. On the other hand, the higher energy processes are no longer valid since the electron screening felt by the lower energy projectile prevents any bound state from existing in the solid <sup>95</sup>.

Thus several theories for light ions were proposed to account for the charge neutralization process occurring outside the solid in the tail of the electron distribution. In 1966, Yavlinskii et al <sup>97</sup>, proposed the recombination of ions with electrons in the surface distribution for various energy regions. Specifically for protons, where  $v_p < v_0$ ,

$$f^c = \exp \left[ - \left[ \frac{136}{E_p} \right]^{1/2} \left[ \frac{n_0}{10^{22}} \right]^{1/6} \right] \quad 7.7 (a)$$

and for  $v_p > v_0$

$$f^c = \exp \left[ - \left[ \frac{6.5}{E_p} \right] \left[ \frac{n_0}{10^{22}} \right]^{1/2} \right] \quad 7.7 (b)$$

where in both cases  $E_p$  is the emerging proton beam kinetic energy in keV and  $n_0$  is the metal conduction electron density in  $\text{cm}^{-3}$ .

Later Trubnikov and Yavlinskii <sup>96</sup> calculated the probability of resonant tunneling of electrons from the metal out to the ion.

They show that the neutral yield should decrease approximately as

$E_p^{-4}$  for energies above 150 keV. They also suggest that both their mechanisms as well as Auger neutralization may contribute to the total neutralization probability.

Another proton-solid charge neutralization theory is that provided by Kitagawa and Ohtsuki<sup>98</sup>. Again assuming only surface ion neutralization, they use the quantum mechanical theory as formulated by Bates<sup>113</sup>. The theory predicts a strong dependence of ion fractions on the angle of emergence and is the only calculation that considers an angular effect. In fact, capture and loss cross section theory does not predict any angular dependence whatsoever.

One medium energy neutralization expression is that due to Brandt and Sizmann<sup>95</sup>. It applies to 10 - 100 keV protons or 40 - 400 keV  $\text{He}^+$  and derivation details have not yet been published. They state however that a building up of a correlation in speed and direction between proton and electron inside the solid leads to capture at the surface if this correlation persists to the surface. The ion fraction is given as:

$$f^+ = \left[ 1 + \frac{1}{40E} \right]^{-1} \quad 7.8$$

where  $10^{-2} < E < 10^{-1}$  and represents the kinetic energy of the emerging particle in MeV per atomic mass unit. They argue against neutralization inside the solid not only due to electron screening but also due to collision broadening at high energies. The latter effect is the uncertainty in the energy of the bound

state because of its shorter lifetime at higher velocities. These concepts have been recently challenged by Cross<sup>99,114</sup>, who has reinvestigated the question of neutralization inside the solid through electron capture and loss from bound states on the proton. He makes the following points: 1) for protons above several  $v_0$ , the collective screening charge is left behind a distance of many Bohr radii so that bound states are not prevented; 2) it can be shown that, although an electronic state around a fast proton in a solid has a short lifetime, collision broadening is unimportant as it is for the electrons involved in heavy ion charge exchange which is well predicted by the capture-loss bound state model; and 3) the use of ion-gas measured (from hydrocarbon vapors) electron capture and loss cross sections can be used successfully to predict neutral fractions of high energy hydrogen scattered from carbon foils as well as those at medium energies scattered from practical gold surfaces. (Practical in this case denoting possibly contaminated with carbon -- these considerations are dealt with in the results and discussion section of this chapter.)

The final two predictions of the neutralization behaviour of ions are calculations based on empirical data and as such can perhaps lend themselves to application in the medium energy heavy ion regime. The first does have a basis in theory in that the outermost electrons only can contribute to the capture and loss process. Since these processes depend on the relative velocities of the moving ion and the electron within the ion (atom) which is being captured (lost), it may be possible to find a semi-empirical

relationship of  $f^+$  with  $Z$  and  $v$  by plotting  $f^+$  as a function of a reduced velocity. Using the electron velocities determined via Thomas-Fermi theory<sup>115</sup>

$$f^+ = \frac{v}{v_0 Z_2^{2/3}} \quad 7.9$$

where  $v_0$  is the Bohr velocity.

This approach has proven that a unified representation of experimental data is possible for the equilibrium charge,  $\bar{q}$ , of energetic (MeV) heavy ions passing through gaseous as well as solid targets. In some cases, by changing the power of  $Z_2$  from  $2/3$  to  $0.55$  or  $0.45$  a better unification is found<sup>115</sup>.

The final outline concerns a calculation due to Zaidins<sup>116</sup> and is based on a set of statistical probabilities and assumptions developed by Dmitriev<sup>117</sup>. The latter assumes that the probability for the loss of an electron in a given atom is independent of the loss of other electrons and depends only on the ion velocity; as well, the velocity of the electron in a given atom does not depend on the degree of ionization of the atom and can be obtained from the ionization potential for that electron. From these assumptions of Dmitriev, Zaidins has obtained the ion fractions for various projectiles heavier than He by choosing the functional form of the probability that the  $j$ th electron is not lost as

$$N_j(v) = \exp \left[ -A_j \left( \frac{v}{v_j} \right)^{B_j} \right] \quad 7.10$$

where  $v$  is the velocity of the ion and  $v_j$  is the velocity corre-

sponding to the kinetic energy necessary for the  $j$ th electron to overcome its ionization potential  $I_j$ . The  $I_j$  are given by

$$v_j = \left[ \frac{I_j}{2m_e} \right]^{1/2} \quad 7.11$$

The parameters  $A_j$  and  $B_j$  are obtained by fitting the experimental charge state data then currently available. These were taken from predominantly higher (MeV) regions. Using the laws of probability, Zaidins extrapolated the charged fractions of ions into velocity regions where no experimental results exist, namely in the low charge states of 1 or 2 which are predominant in the heavy ion medium energy range.

Thus, the medium energy regime is very difficult to treat theoretically. As the velocity is reduced, at the higher energy end, the collective screening by valence electrons is becoming increasingly important while at the lower end, the single resonance processes are expected to be of reduced value as the width of the resonance is many electron volts for  $v \sim v_0$ . Hence the theoretical approach has been historically from the extreme between  $v \ll v_0$  and  $v \gg v_0$ , into an area where therefore some of these are of doubtful validity.

### 7.3 Experimental and Analysis Procedure

A general experimental and analysis technique has been detailed in Chapter 4; however, the specifics to these set of ion fraction and charge state determinations are outlined below. The analyzing beam from the 150 kV accelerator is passed through the

Figure 7.2 The energy spectra for 120 keV protons backscattered from a clean gold surface where 0 -- gives the collected spectrum for charged + neutral particles, ● -- gives the collected spectrum for neutrals only, and + -- gives the difference between these two spectra, that is, corresponding to the charged particles only.

120 keVH<sup>+</sup> ON 2800 Å AU

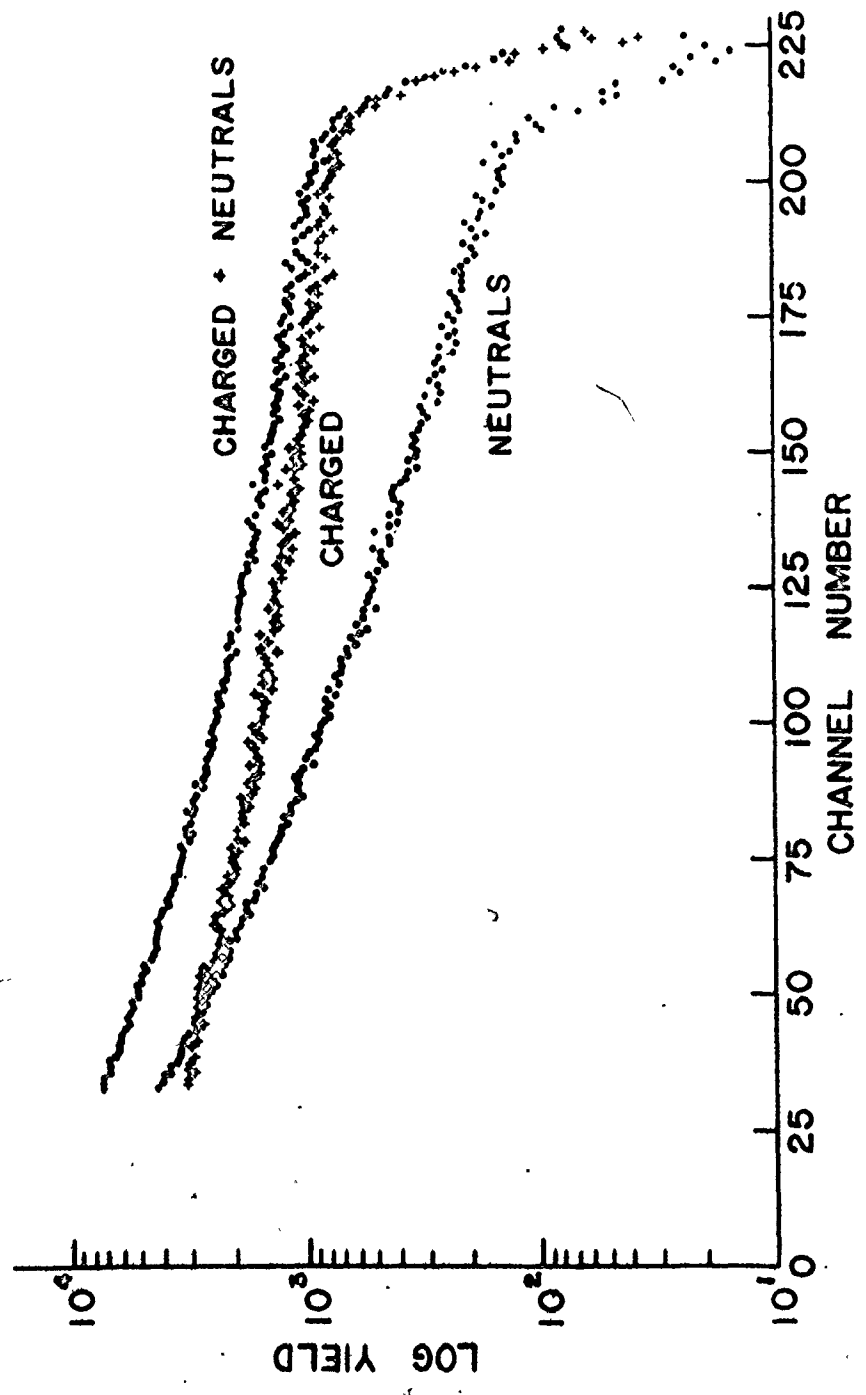
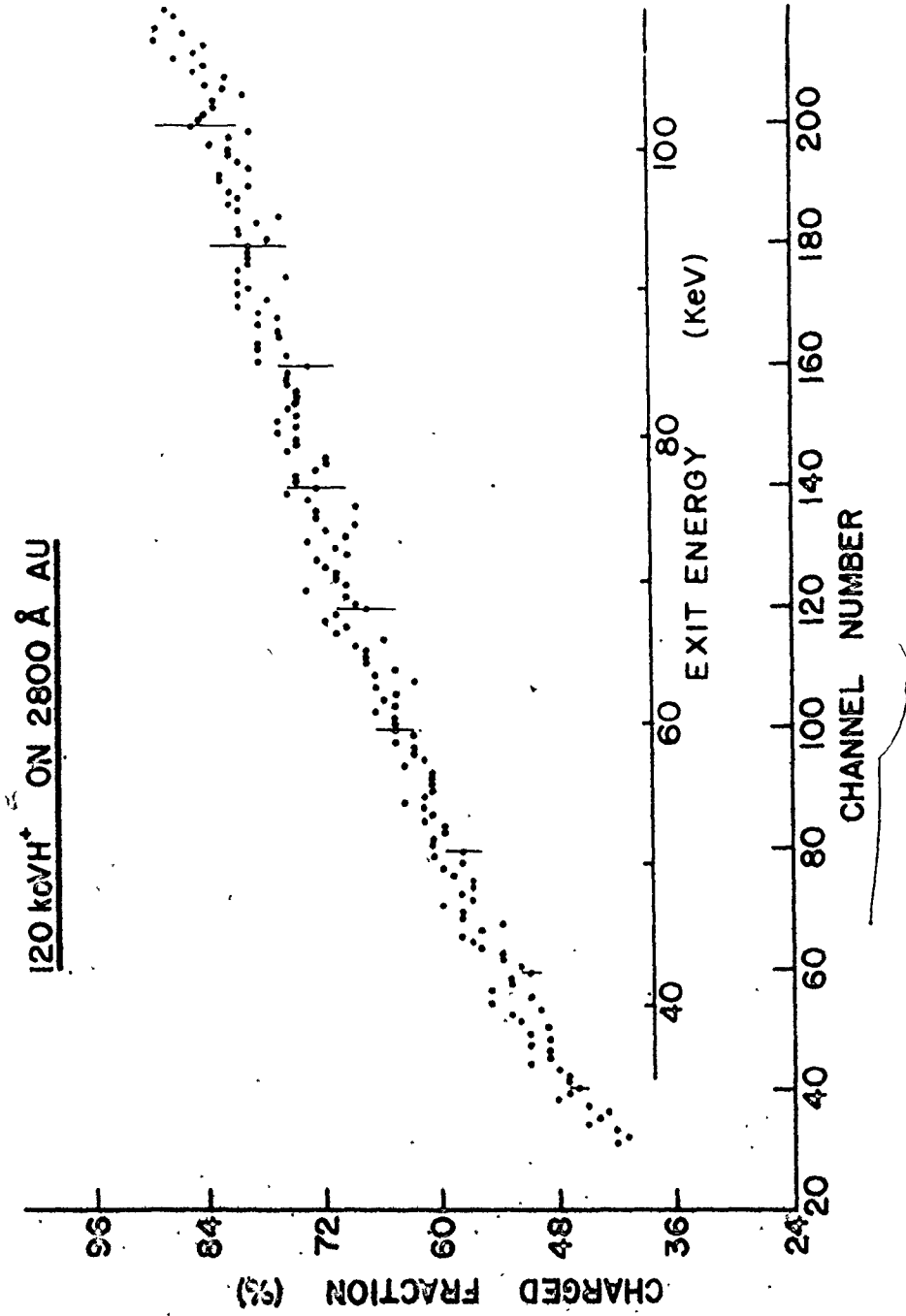




Figure 7.3 The charged fractions of 120 keV  $H^+$  scattered from a clean gold surface vs. the backscattered energy. Note the slight upward turn at high energies which is only found to be present when the target surface is clean. These results have been derived from the data of figure 7.2.



1/2 mm diameter apertures for solid state detector analysis while for ESA operations, the 1 mm diameter apertures are used. The latter system is employed for backscattered ion charge state measurements while the former detection system is used to determine the charge-to-neutral ratios in the usual manner. This includes measuring alternatively, for  $\sim 2$  second durations, (1) the total number (neutral + charged) of backscattered particles and (2) the neutral component via electrostatic deflection. The energy calibrations have been determined using the procedure outlined in Chapter 4 which for the solid state detector includes a dead layer loss correction. During these operations, the UHV target chamber is maintained between  $(6 - 10) \times 10^{-9}$  torr. The pressure however doubled to  $\sim 2 \times 10^{-8}$  torr when the sample was sputter cleaned using the 2 mm diameter apertures. The sputtering beam was either 60 keV N or 60 keV Ar employed to fluences of approximately  $1 \times 10^{15}$  ion/cm<sup>2</sup>.

The samples used in the charged fraction determinations were obtained by the e-beam evaporation of <sup>0</sup>2800 Å of gold onto a chemically etched surface of Be. The samples were then loaded into the scattering chamber and before each run were sputter cleaned. Through the use of 1 MeV He<sup>+</sup> particle Rutherford back-scattering, the samples were found to have initially carbon contamination in the form of several monolayers. After sputter cleaning, this impurity could not be detected to within the sensitivity of the technique which is estimated here to be about  $2 \times 10^{15}$  atoms/cm<sup>2</sup>. For the target configuration of

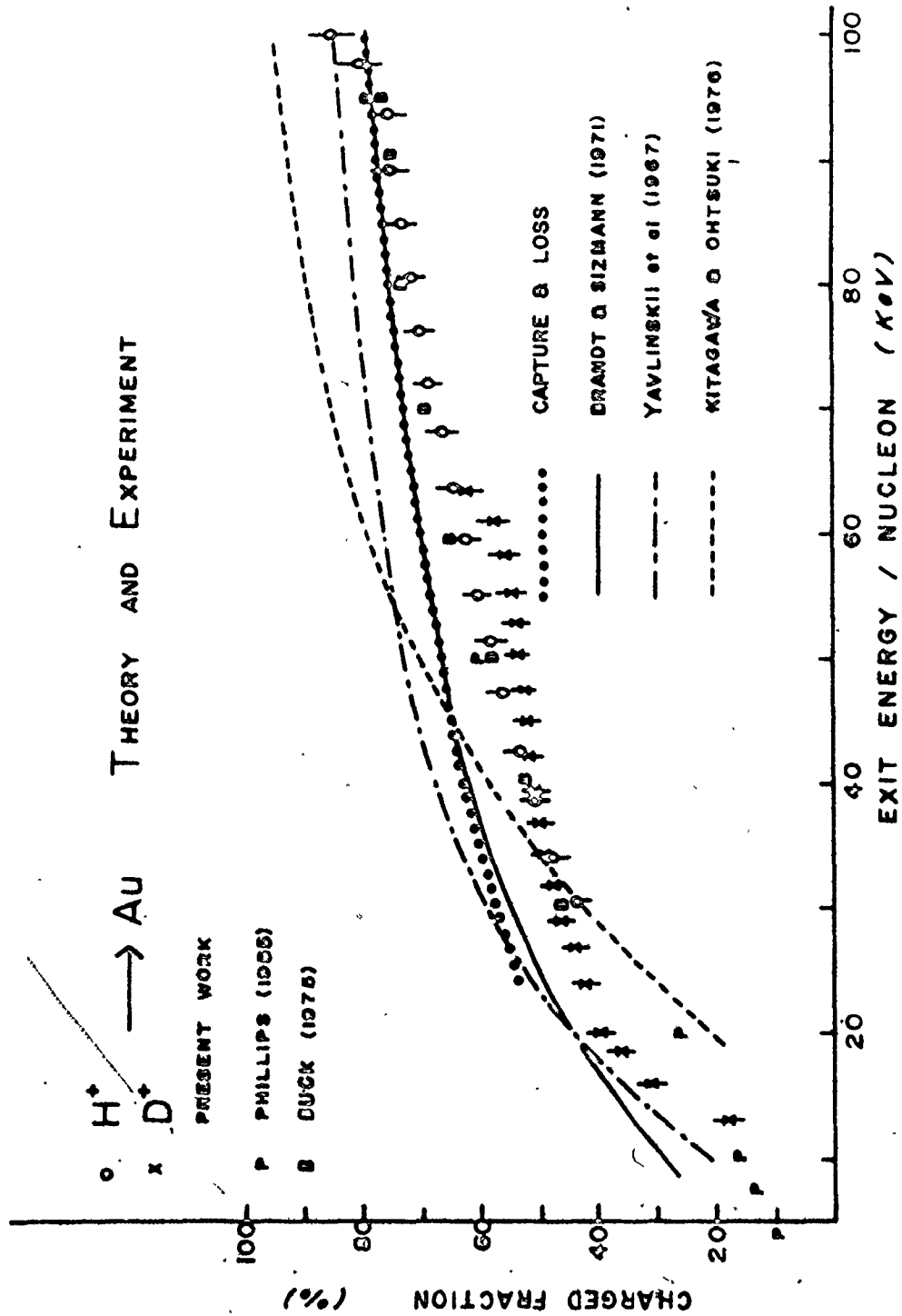
surface carbon on  $\sim 10 \text{ \AA}^0$  Au evaporated onto the Be substrate, there is a small background contribution ( $\sim 3\%$ ) under the carbon peak mainly due to the low energy tail of the RBS gold peak. No other method was employed to determine sample surface cleanliness, however, as shown in the next section, the ion fraction obtained in this study for H and He ions follows closely those of Buck et al<sup>119</sup> for his case of the clean gold surfaces. The present experiments have been done at normal incidence with a scattering angle,  $\theta_L$ , of  $150^\circ$  and primary ion energies between 125 - 130 keV.

#### 7.4 Results and Discussion

Figure 7.2 (a) shows the energy spectra of the total (charged + neutral) and neutral yields of 120 keV protons backscattered from the cleaned Au targets. The use of the ESA has indicated that both negative and multiply charged components of the backscattered beam are negligible in the present energy region for all ions except F. (The case of F will be discussed in more detail later.) Therefore the positive spectrum which is also shown is represented by the difference between the total and neutral yields. The charged fraction at any energy is then obtained by dividing the positive yield by the total yield at that energy. This is plotted in figure 7.3 for 120 keV protons. Figure 4.5(a) and (b) show results for 130 keV  $\text{He}^+$  in Chapter 4.

Figure 7.4 shows the charged fraction of H and D backscattered from Au plotted as a function of exit energy per nucleon. It is appropriate, at this time to comment on some interesting

Figure 7.4 The charged fractions of  $H^+$  and  $D^+$  backscattered from clean gold surfaces for  $E_0 = 130$  keV and  $\theta_L = 150^\circ$ . The theoretical curves and experimental points from other authors are included (see text).



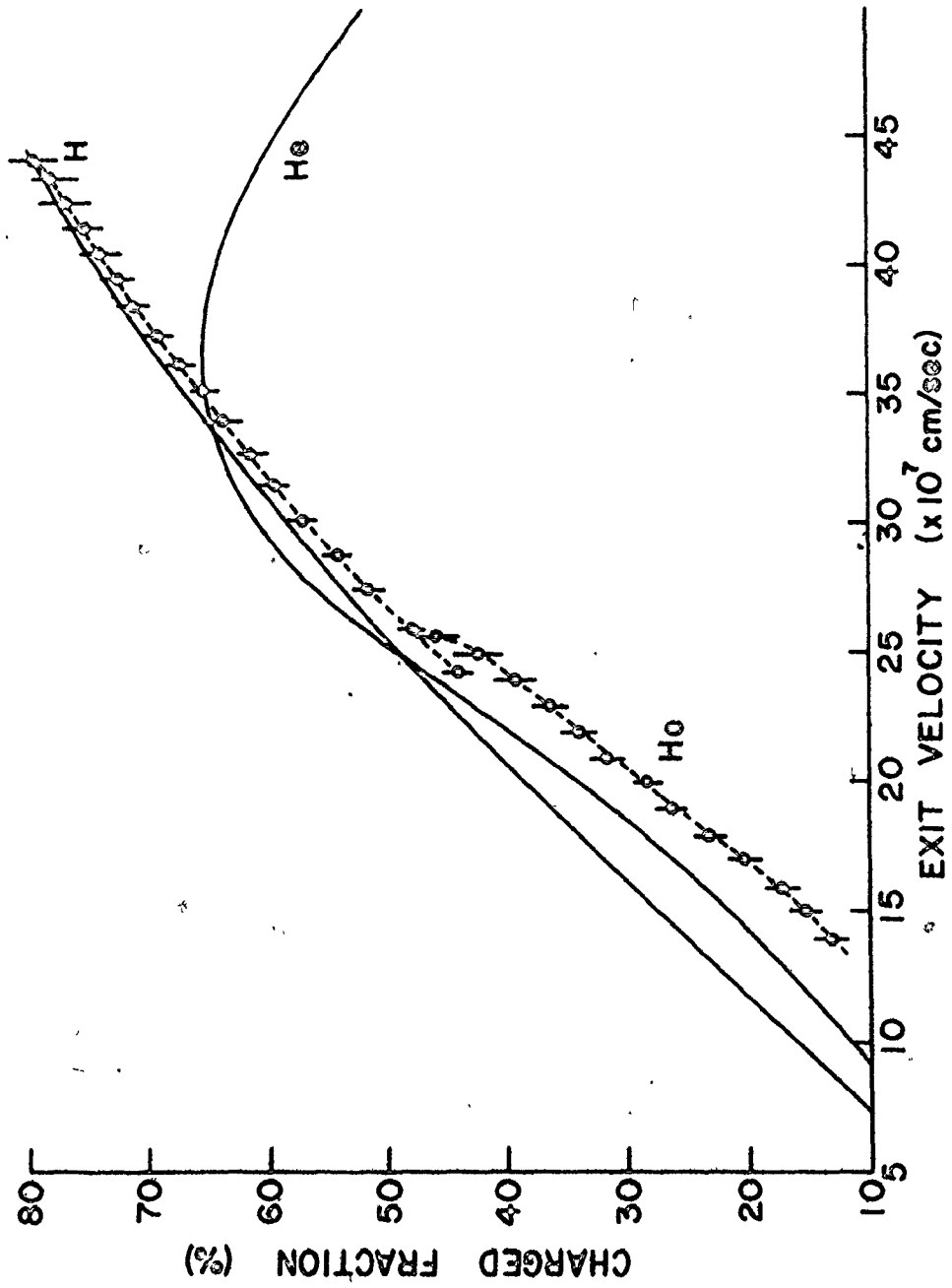
features of figure 7.4. The D data show a somewhat reduced charged fraction at higher exit energies compared to the H data. A similar behaviour for these ions, but in the lower energy region of 5 - 15 keV has recently been observed<sup>118</sup>. Whether this is a real isotope effect or perhaps a consequence of slightly different target surface conditions during the two experimental runs has not been determined. In fact, it is known that surface cleanliness has a large influence on charged fractions; in this energy regime the cleaner the surface, the lower the charged fraction<sup>119,120</sup>. Another noticeable effect is the upward turn for near surface scattering. The behaviour may be attributable to surface scattering before an equilibrium state is reached<sup>121</sup>. It should be noted that such an effect, although within the experimental uncertainty, only appears on a clean surface when equilibration of the charge of the particle backscattered from the Au surface cannot occur in exiting through the surface contamination layer.

The results for the charged fraction of He and H are plotted in figure 7.5 as a function of the exit velocity. It is interesting that on a velocity plot, they nearly fall on a common line indicating that the velocity rather than the identity of the particle may be a major factor which determines the neutralization. However, this is certainly not true for heavier ions as can be seen from figure 7.6, where the charged fraction of Li, B, C, N, F and Ne are also plotted as a function of exit velocity.

Recently Behrisch et al<sup>92</sup> have compared some of the theories of section 7.2.3 with their experimental results for H<sup>+</sup> backscattered from different materials. Although these theories predict qualitative trends, they all yield higher charged fractions when compared to the experimental results. This is found also to be true of the current data compared to theory in figure 7.4. For the capture and loss curve (using equation 7.5), the ratios  $\sigma_e/\sigma_C$  are taken from the experimental work of Hall<sup>122</sup> as a function of exit energy per nucleon. Here, reasonable agreement with experimental data is found. As for any other comparison, there can be none made since there are no other capture/loss cross sections available for these energies. A plot of the C/N ratio as derived from the Brandt and Sizmann<sup>95</sup> expression (equation 7.8) is also shown in figure 7.4. Note that above 40 keV exit energy, this model prediction coincides with the curve obtained from the capture and loss model. The final two theoretical determinations are those due to Yavlinskii et al<sup>97</sup> (equation 7.7 (b) with  $n_0 = 6 \times 10^{22} \text{ cm}^{-3}$  for gold) and Kitagawa and Ohtsuki<sup>99</sup>. Both are shown in figure 7.4 where the latter is the result of their numerical calculations for normal emergence of protons. The Kitagawa and Ohtsuki theory predicts a much stronger dependence of charged fraction on the emergence angle than is observed experimentally<sup>119,123</sup>. A part of the large discrepancy between this experimental result and their theoretical approach may therefore be attributed to the fact that the emergence angle used here is  $30^\circ$  with respect to the target surface normal and not zero on which their calculations are based.



Figure 7.5 The charged fractions for  $H^+$  and  $He^+$  ( $E_0 = 130$  keV,  $\theta_L = 150^\circ$ ) plotted against the exit velocity. The theoretical predictions from Marion and Young<sup>124</sup> for singly charged  $H^+$  and  $He^+$  are given by the solid lines.



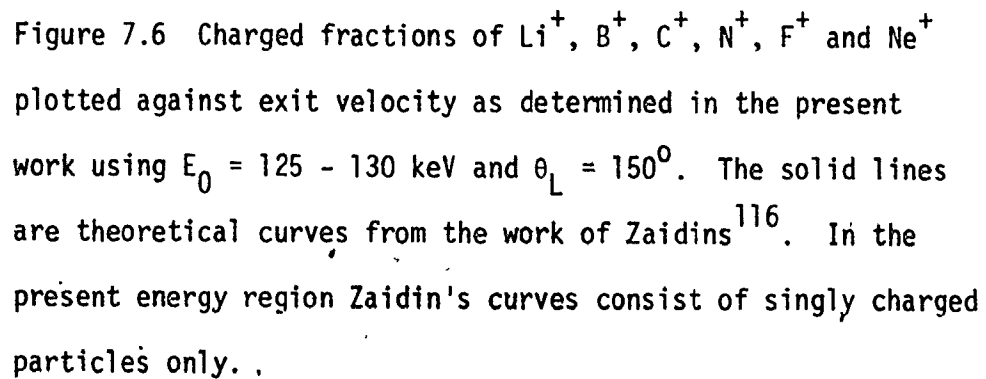


Figure 7.6 Charged fractions of  $\text{Li}^+$ ,  $\text{B}^+$ ,  $\text{C}^+$ ,  $\text{N}^+$ ,  $\text{F}^+$  and  $\text{Ne}^+$  plotted against exit velocity as determined in the present work using  $E_0 = 125 - 130$  keV and  $\theta_L = 150^\circ$ . The solid lines are theoretical curves from the work of Zaidins<sup>116</sup>. In the present energy region Zaidin's curves consist of singly charged particles only.

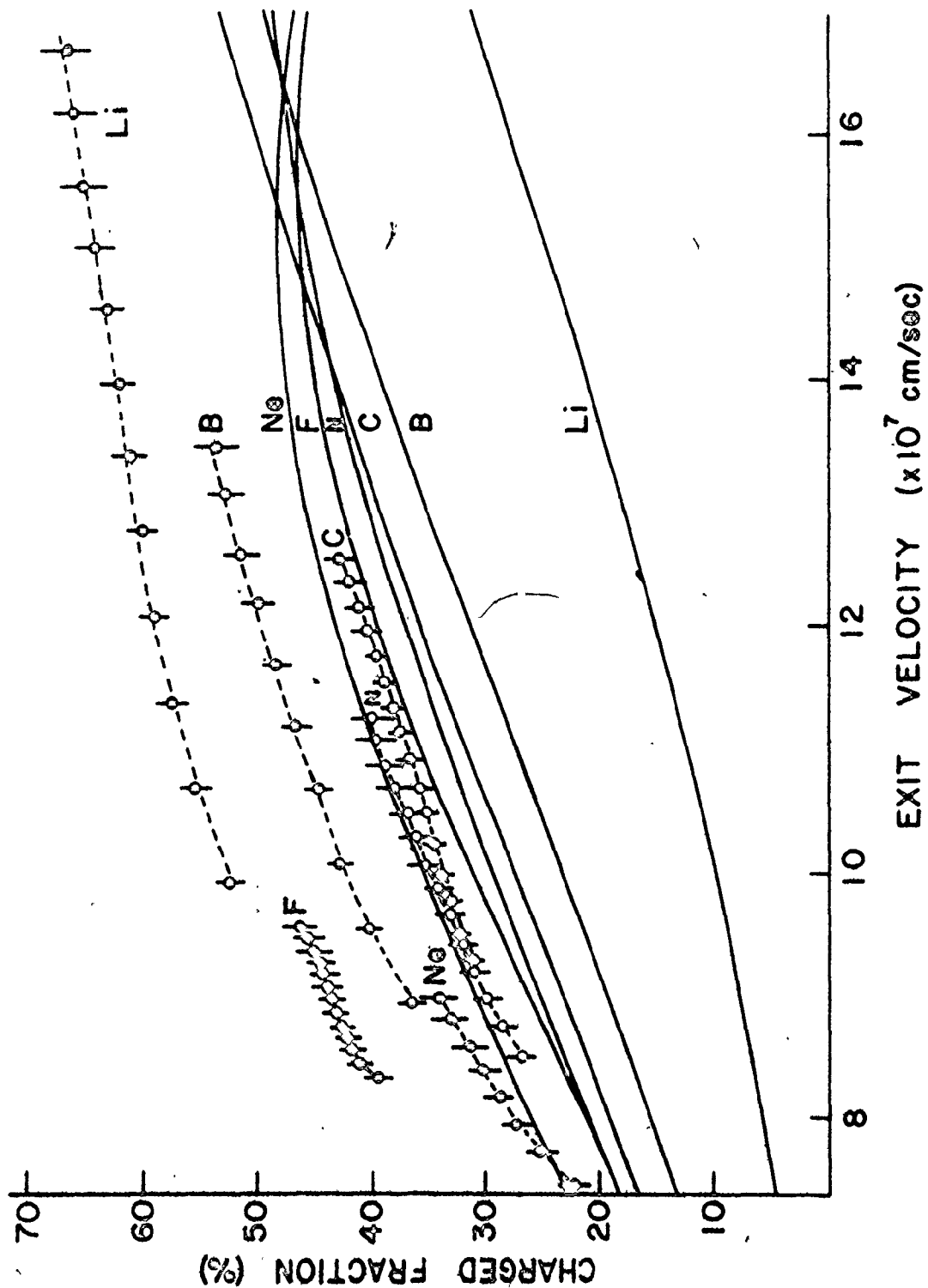


Figure 7.4 also compares the results determined here with those obtained earlier<sup>119,125</sup>.

The only calculation which attempts to deal explicitly with heavier ions is that due to Zaidins<sup>116</sup>. The results of his calculations are compared with the present experimental data in figures 7.5 and 7.6. It is readily seen that for  $H^+$ ,  $He^{++}$ , C, N, and Ne the calculated values agree reasonably well with the experimental values. However for Li, B, and F, the calculated curves are far too low compared to the experimental data. The reason for the discrepancies in the case of these latter ions is not clear. However, one observation can be made at this juncture. Due to insufficient experimental results for F, Zaidins has arbitrarily set some of the parameter values. Hence for F his prediction is somewhat suspect. Intuitively, it is expected that the probability for electron loss in a collision will increase with decreasing ionization potential. From equations 7.10 and 7.11 it can be seen that the reverse is predicted for the present region of interest, although, of course, there are complications due to the velocity dependence of all the probability terms. Notwithstanding the above arguments, since Li

---

† For the original reference by Zaidins<sup>116</sup> no negative component of charged fractions were considered and no results on H and He were presented.

‡ In the book by Marion et al<sup>124</sup>, the data of Armstrong et al<sup>107</sup> for He charged fractions and of Zaidins in a private communication for H charged fractions (including both positive and negative components) have been graphically reproduced. Therefore the H and He values have been directly transposed from the graphs since no fitting parameters have been published for these ions.

has the lowest ionization potential (5.39 eV) of all the ions in this study, it is not surprising that it shows the highest charged fraction. On the other hand, F, with an ionization potential of 17.4 eV shows a higher charged fraction than would be expected from the above reasoning. However, because of the large electronegativity of F, a significant component of the charged fraction could be negative. This has already been measured for 100 keV F in carbon films<sup>125</sup>. Here it is reported that the charged state ratios are  $F_{-1} : F_0 : F_{+1} : F_{+2} = 14 : 54 : 28 : 4\%$ .

In an attempt to find a unified description of the current experimental results with respect to ion fractions,  $f^+$ , similar to the relationship developed around equation 7.9, a plot of  $f^+$  against  $v/(v(Z_1)^{0.55})$  is given in figure 7.7. It has been found that 0.55 is the best choice and shows that such a representation is possible for H, He, Li, B, and N and to a lesser extent for C and D. Ne and F do not seem to follow such a scaling. As mentioned previously for F, a significant component of the charged fraction is expected to be negative and hence the  $F^+$  fractions will be considerably smaller than the experimental points in figure 7.7 (b) would indicate. There is, however, no reason offered to account for the observed behaviour of Ne under these considerations although any treatment such as this which ignores electron ionization effects could not be expected to scale satisfactorily from Li with low ionization to Ne with a very high ionization potential. It is therefore quite clear that the smooth behaviour of Li, B and N cannot be widely used for any reliable predictions. More experiments using some other ions are

Figure 7.7 The present work charged fractions plotted as a function of the reduced ion velocity (cf H. Betz<sup>115</sup>),

$V_R = (v/v_0)(Z)^{0.55}$  which is characteristic of capture and loss processes for light ions (a) and for heavy ions (b).

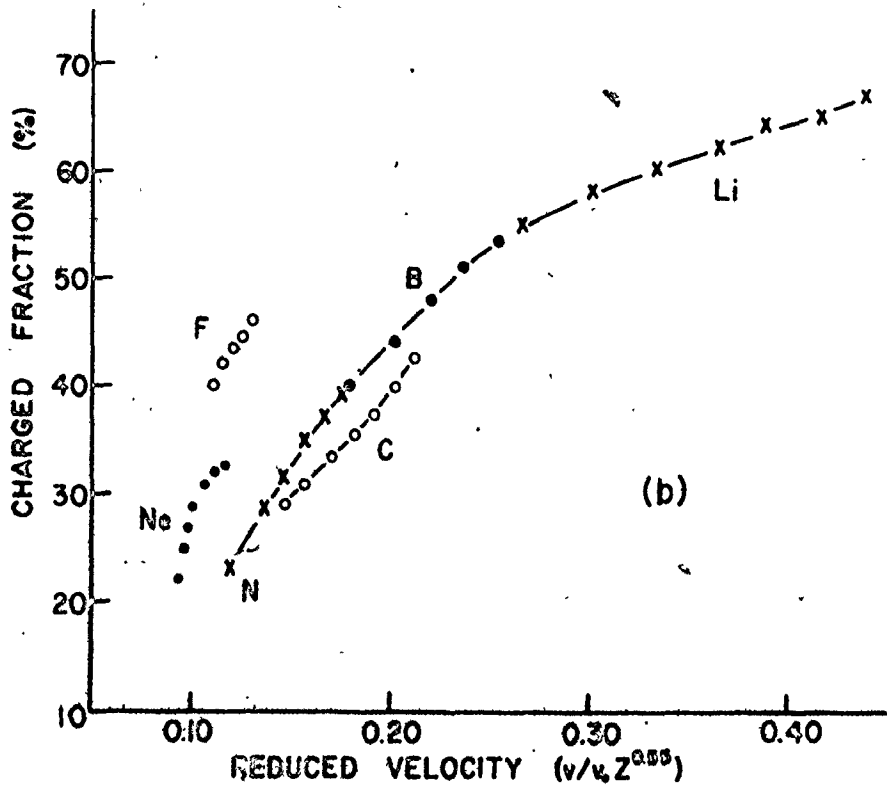
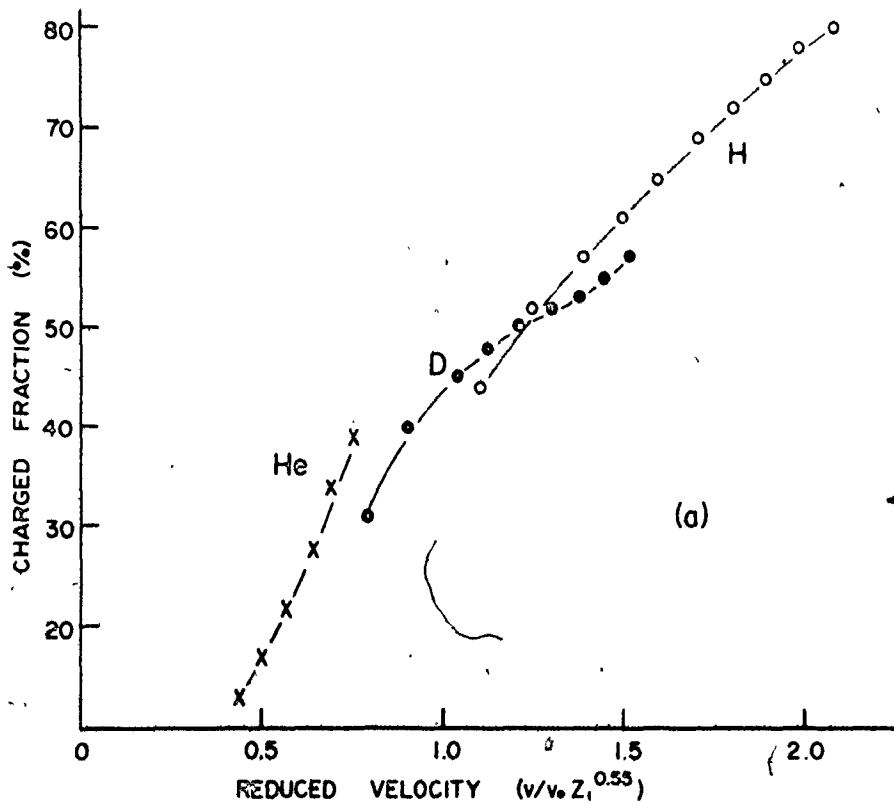
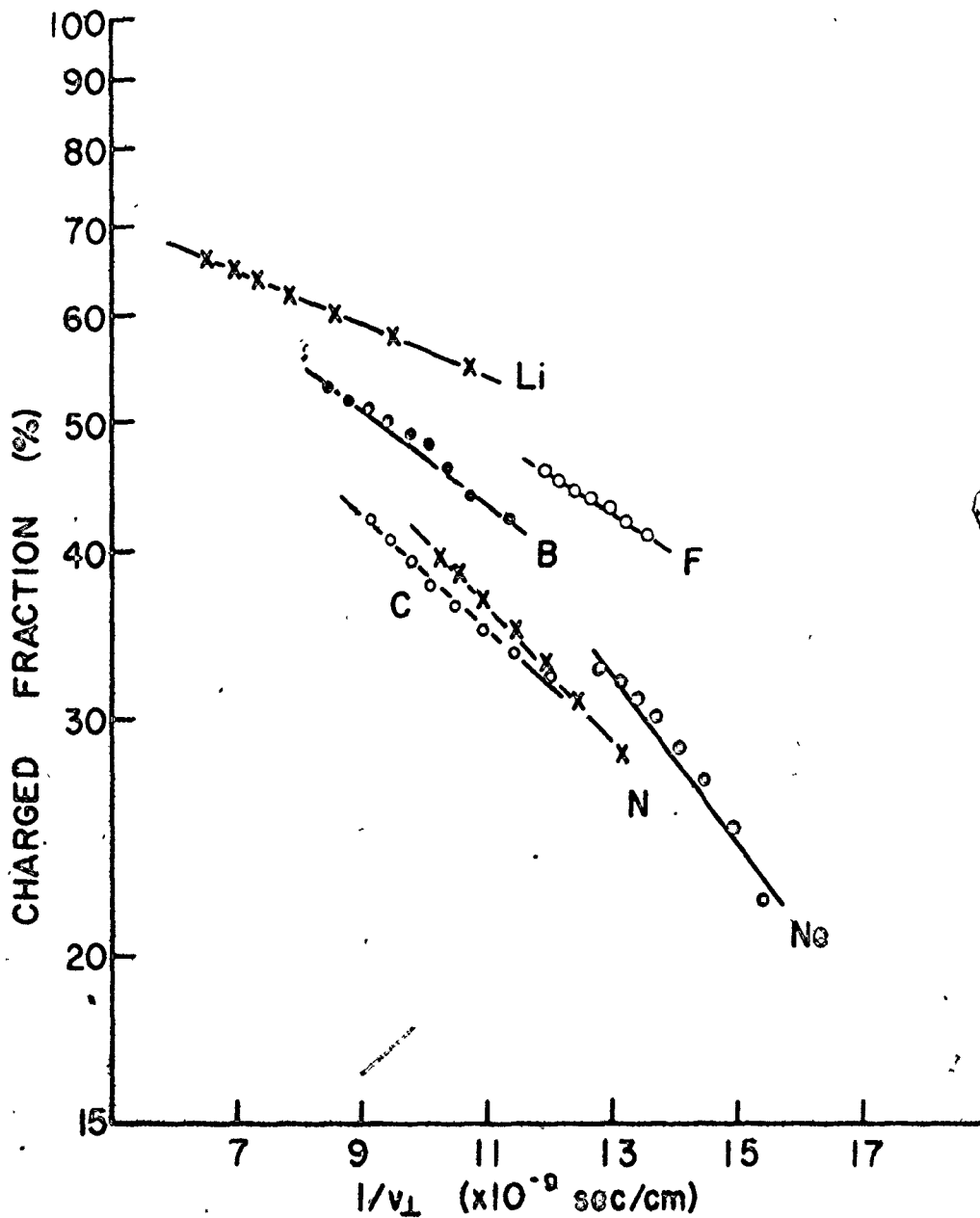




Figure 7.8 The present work charged fractions versus the reciprocal velocity component which is perpendicular to the target surface. Any tunnelling or Auger type processes would be expected to scale linearly on a semilogarithmic graph<sup>104,108</sup>.





necessary to clarify the situation.

Lastly, in the consideration of the charged fractions of heavy ions, it is pertinent to mention the near surface neutralization mechanism involving Auger type processes as explained in section 7.2.1. The results of a semilogarithmic plot, figure 7.8, of  $f^+$  vs the reciprocal of the surface normal component of the exit velocity,  $1/v_{\perp}$ , reveals that, except again for Ne, all the ions studied seem to follow the form of equation 7.3. One observation is that the transition constants of the process increase with  $Z$  except for F, which may be of some significance. These values are given in table 7.1 along with the Bohr velocities for each of the ions studied. Similar results have been found giving this order of magnitude as in the case of 80 keV Ar, although scattered at  $\theta_L = 90^\circ$  from copper rather than gold surfaces using optical emission studies<sup>126</sup>. Even for more energetic (MeV) heavy ions such as Iodine, it has been proposed that significant contributions from Auger type transitions occur<sup>127</sup> so that these near surface neutralizations may not be just confined to the usual lower (eV - keV) regions but occur at rather high energies as well.

It is thus clear that available theories on proton neutralization are not able to predict quantitatively the existing experimental data. In fact, all theoretical calculations yield higher charged fractions than actual results from experiments show. Obviously a much more complicated charge neutralization mechanism is in operation. Perhaps a mixing of prominent theoretical

TABLE 7.1

The Transition Parameters of Tunnelling Processes for Heavy Ions  
As Determined from the Present Work

Ion	$E_0$ (keV) (corresponding to $v_0$ )	Measured Exponents	
		survival parameter (cm/sec)	intercept (ideally 1.0)
H	25	----	----
D	50	----	----
He	100	----	----
Li	174	$4.50 \times 10^7$	0.95
B	271	$8.23 \times 10^7$	1.1
C	301	$9.69 \times 10^7$	1.0
N	351	$1.16 \times 10^8$	1.3
F	477	$6.89 \times 10^7$	1.0
Ne	506	$1.25 \times 10^8$	2.0

processes involving a capture/loss equilibrium in the bulk of the solid and recombination possibilities near the surface would lower predictions to current experimental values and be applicable to a broader range of incident particle species. For the heavier ions specifically however, a further clarification of the situation requires a much larger effort in both experimental and theoretical studies. Certainly the intermediate energy regime is at present an uncertain transition region with respect to electron pick up and release phenomena where high energy processes are ceasing to be important while low energy processes are becoming active.

## CHAPTER 8

### Stopping Cross Sections and Straggling Determinations

#### 8.1 Introduction

With the discovery of alpha particle emission from radioactive heavy isotopes, there was much curiosity in how these particles slowed down when traversing matter<sup>128</sup>. In the late 1930's Bohr developed a detailed analysis<sup>129</sup> for the energy loss process of energetic light mass charged particles in material. He proposed that the energy loss could be divided into two components: the nuclear stopping due to interactions with positive atomic nuclei, and electronic stopping due to interactions with atomic electrons. He also correctly deduced that the electronic stopping would be far greater than the nuclear stopping for energetic alpha particles. In the three decades that followed, considerable theoretical advances (mainly by LSS during the 1960's) were made.

Recently a renewed interest in refining the basic theory to better predict experiment has occurred. This is due to the need for reliable information on energy loss processes in several areas of application. Specific examples include fusion research and the use of ion beam scattering techniques as a surface layer microanalytical tool. As previously mentioned, there is a need to determine basic parameters of the ion-solid interaction if the application of MEIRS

to materials analysis is to become useful. In the energy region appropriate to MEIRS, very little reliable data are available on the energy dependence of the energy loss, and even those which are available are limited to two or three target materials<sup>130,131</sup>. Since the scattering processes which determine the energy loss are statistical (random) in nature, the penetrating particles at any depth in the target will not have unique energies but rather a distribution of energies called energy straggling<sup>156</sup>. This energy straggling will increase with depth of penetration and ultimately limit the depth and mass resolution of the technique. In order to estimate these limits, the magnitude of energy straggling must be determined<sup>132</sup>.

In the second section of this chapter, the theoretical outline given in chapter 6 is extended to include nuclear and electronic energy loss processes as well as current theories on energy straggling. Section 8.3 briefly describes the measurement procedure which requires use of both ESA and solid state detector systems, while section 8.4 provides a discussion of the results obtained. Use is also made of the methods of the previous chapter in order to obtain appropriate charge-to-neutral ratios which are then employed to correct the ESA spectra via methods given in chapter 4.

## 8.2 Collision Theory II

When an energetic ion strikes the target atoms, a chain of atomic collisions results in which several generations of recoiling

atoms are created. This collision sequence is referred to as the collision cascade and it is within this context that most theories begin their analytical descriptions. In these cases, the exact nature of the cascade is not required since the observed properties are the effects resulting from a very large number of incident particles. Accordingly a statistical description of the collision cascade is developed. Since the amount of electronic scattering depends on the impact parameter between the projectile and target atom as does the nuclear scattering, these processes are correlated<sup>133</sup>. However, it has been demonstrated that, to a good approximation, these energy loss processes can be considered independent, and, that the total stopping power is given by the sum of an elastic (nuclear) term and an inelastic (electronic) term<sup>2</sup>. Winterbon<sup>134</sup> has shown that correlated stopping has a negligible effect on the gross structure of the collision cascade.

### 8.2.1 The Stopping Powers

In the previous sections, the energy processes have been separated into elastic and inelastic components. In a similar approach, it is possible to define the total stopping power,  $dE/dR$ , which is the projectile energy loss per unit length of travel in the substrate, as

$$\frac{dE}{dR} = \left[ \frac{dE}{dR} \right]_n + \left[ \frac{dE}{dR} \right]_e \quad 8.1$$

Both stopping powers are proportional to their corresponding cross



sections,  $S(E)$ , via the target atom density,  $N$ , that is,

$$\left[ \frac{dE}{dR} \right]_n = -N S_n(E) \quad 8.2$$

$$\left[ \frac{dE}{dR} \right]_e = -N S_e(E) \quad 8.3$$

Nuclear stopping can be represented by a universal curve, that is, like the close encounter collision probability, the similarity property of the nuclear scattering cross section is obeyed for all ion-target combinations. The electronic cross section although similar in shape to the nuclear component, does not exhibit similarity scaling but rather gives rise to a family of curves based on various ion-target parameters as detailed by LSS theory.

This is shown in figure 5.1 where the stopping cross section curves are plotted as a function of energy for several ion-target systems.

### 8.2.2 Nuclear Stopping Cross Section

The nuclear stopping power is defined by using the differential scattering cross section of the previous section. Specifically,

$$\left[ \frac{dE}{dR} \right]_n = -N \int_0^{T_M} T d\sigma_n \quad 8.4$$

where  $T$  is the energy transfer during the collision and  $T_M$  is the maximum possible energy transfer. In terms of the dimensionless quantities,  $\epsilon$  and  $\rho$ , the stopping power can be written as

$$\left. \frac{d\epsilon}{d\rho} \right|_n = - S_n(\epsilon) \quad 8.5$$

$$= - \frac{1}{\epsilon} \int_0^\epsilon f(\tau^{1/2}) d(\tau^{1/2}) \quad 8.6$$

The universal nuclear stopping cross section curve as calculated from the Thomas-Fermi potential is given in figure 8.1. In the power law approximation, this becomes

$$S_n(\epsilon) = \frac{\lambda_m \tau^{1-2m}}{2(1-m)} \quad 8.7$$

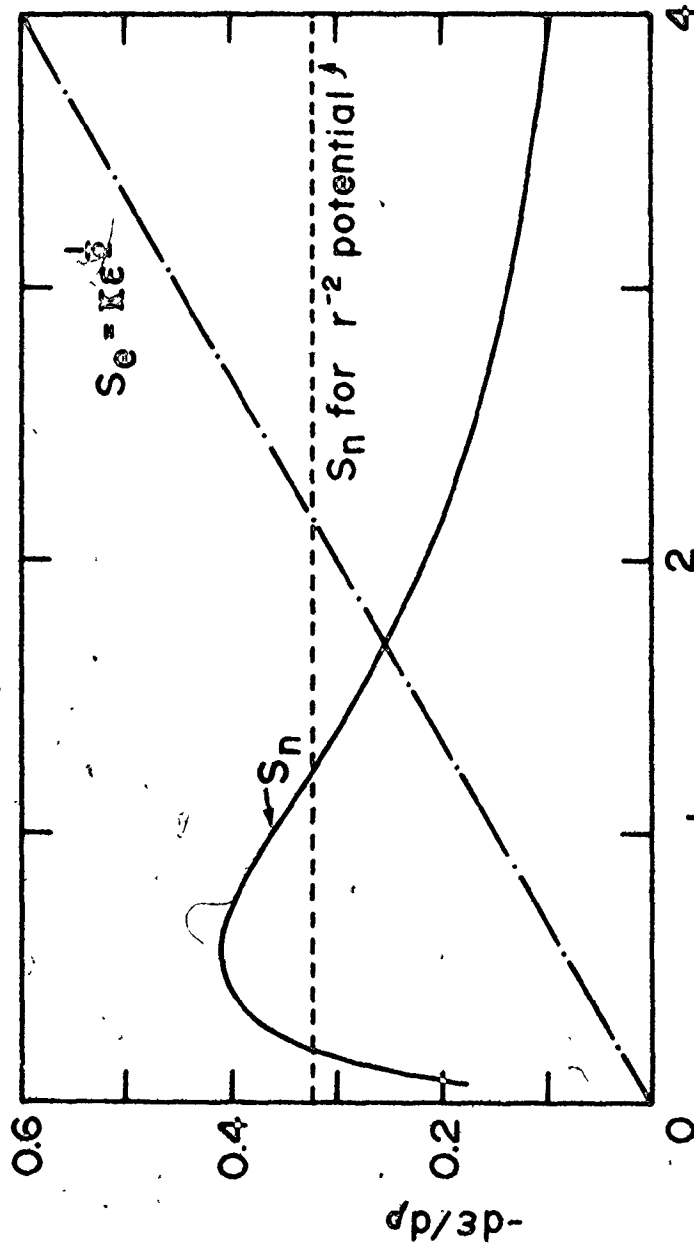
The regions of validity of  $m$  are given in chapter 6 and also apply here. Note that in the case of  $m = 1/2$ ,  $S_n(\epsilon) = 0.327$ , that is, a constant.

### 8.2.3 Electronic Stopping Cross Section

For electronic stopping three regions can be differentiated:  
 i) where the ion velocity  $v < v_0 Z_1^{2/3}$  with  $v_0$  as the velocity of the first Bohr orbital electron, the inelastic stopping process is predicted by LSS to be proportional to  $v$ ; ii) for  $v > v_0 Z_1^{2/3}$ , the stopping becomes inversely proportional to  $v$ ; and iii) for  $v \sim v_0 Z_1^{2/3}$  a natural maximum occurs yielding a smooth well-behaved stopping curve. (see in figure 5.1 the  $S_e$  curve). For light ions on heavy mass targets, the MEIRS operates in regions (i) and (iii) but for all other combinations involves only region (i). Region (ii) is relatively well-understood and the predictions of Bethe-Bloch



Figure 8.1 The nuclear and electronic stopping power in reduced units: nuclear stopping power (full solid line), electronic stopping power from LSS (dot-dashed line) and the power law approximation for nuclear stopping with the inverse square potential (dashed line).



THEORETICAL NUCLEAR STOPPING CROSS - SECTION IN  
 $\rho - \epsilon$  VARIABLES

theory<sup>135-137</sup> are reasonably accurate. It is in this region that RBS usually operates.

The theoretical approach of LSS, valid in region (i), predicts that the electronic stopping cross section,  $S_e(\epsilon)$  in terms of reduced units, can be expressed as

$$S_e(\epsilon) = - \left[ \frac{d\epsilon}{d\rho} \right]_e = \kappa \epsilon^{1/2} \quad 8.8$$

where  $\kappa = \kappa(M_1, M_2, Z_1, Z_2)$  so that a universal  $S_e(\epsilon)$  does not exist.

Since  $\epsilon$  is proportional to energy (see equation 6.5), the stopping cross section varies as velocity. A detailed derivation of the explicit form of  $\kappa$  has never appeared in the literature<sup>138</sup> but is given as

$$\kappa = Z_1^{1/6} \frac{0.0793 Z_1^{1/2} Z_2^{1/2} (M_1 + M_2)^{3/2}}{(Z_1^{2/3} + Z_2^{2/3})^{3/4} M_1^{3/2} M_2^{1/2}} \quad 8.9$$

Figure 5.1 illustrates various stopping cross sections for different values of  $\kappa$ . Some typical ion-target combinations used in this work are also shown with the calculated values of both  $\epsilon$  and  $\kappa$ .

This theory, however, has failed to predict the experimentally observed<sup>139-142</sup> oscillatory dependence of the stopping power on  $Z_1$ . This behaviour is attributed to the electronic shell structure of the atoms and theoretical models<sup>143,144</sup> based on a modified Firsov<sup>133</sup> method have successfully predicted the form of the oscillations as shown in figure 8.2. However, the magnitude

of the measured experimental values of stopping powers and both theories still show large deviations (up to  $\sim 70\%$  for LSS) so that slightly better than order of magnitude agreement can be expected between theory and experiment

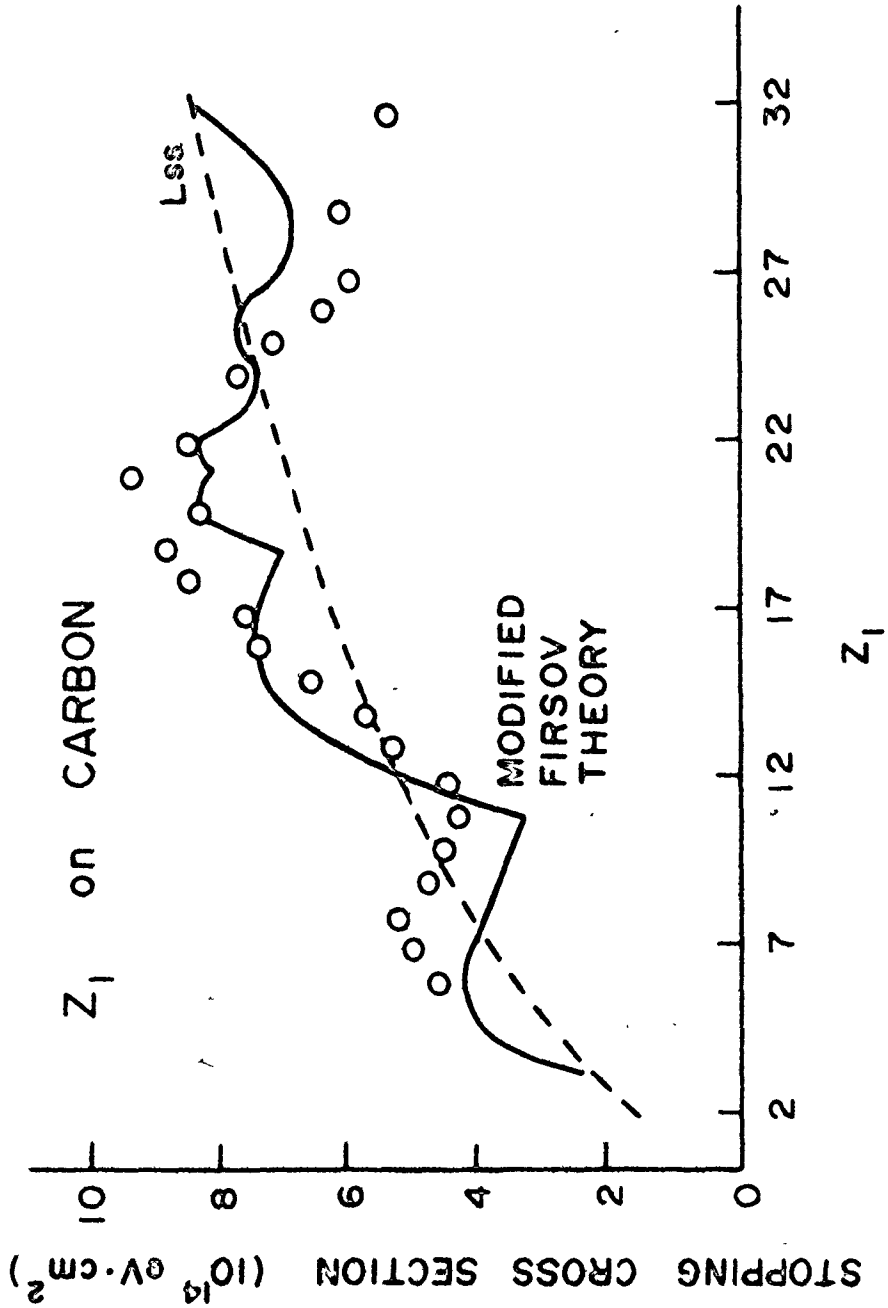
#### 8.2.4 Energy Straggling

Energy straggling has not received broad attention for several reasons: (i) it is a second order effect as shown below, (ii) it is difficult to measure accurately because of its intrinsic dependence on statistical variations, such as nonuniformities, continuity, etc., in the target material and (iii) it had small practical importance until the advent of backscattering spectrometry when used for materials analysis. It is essentially straggling effects which determine the depth resolution in backscattering experiments<sup>132</sup>.

As shown in the preceding section, the directional changes of a fast moving charged particle are determined by elastic nuclear collisions whereas its energy loss in the medium and high energy regime is mainly due to electronic processes. Thus, in the present study, the measured energy straggling is determined mainly by electronic collisions.

When an initially monoenergetic beam of particles passes through matter, the statistical nature of the collision process causes an energy spread in the beam. The mean square deviation,  $\Omega^2$ , of the energy distribution is called the energy straggling and is defined by Bohr<sup>1</sup> as

Figure 8.2 Electronic stopping power for incident ions with  $v = 0.63 v_0$  on carbon from Fastrup et al<sup>141</sup>. The solid curve represents the work of Land and Brennan<sup>144</sup> using the modified Firsov model. The dashed line represents the LSS prediction.





$$\Omega^2 = N\Delta z \int T^2 d\sigma \quad 8.10$$

where  $N\Delta z$  is the atom density of the matter traversed by the projectile and  $T$  is the energy transfer derived from both inelastic and elastic collisions. Assuming that the energy is a slowly varying function of distance and that the energy transfer is a function of the impact parameter alone, the straggling can be calculated as

$$\Omega^2 = N\Delta z \int_0^\infty T^2(p) 2\pi p dp \quad 8.11$$

Again, it is possible to invoke the "separation of inelastic and elastic component" approach of the energy transfer function. Using a semi-classical Thomas-Fermi treatment, Firsov<sup>133</sup> has calculated the inelastic energy transfer as a function of the impact parameter to be

$$T_e(p) = \frac{(Z_1+Z_2)^{5/3} 4.3 \times 10^{-8} v}{(1+3.1 \times 10^7 (Z_1+Z_2)^{1/3} p)^5} \text{ [eV]} \quad 8.12$$

Using equation 8.12 in 8.11, the energy straggling becomes

$$\Omega^2 = 80 N\Delta z (Z_1+Z_2)^{8/3} \frac{E}{E_0} \text{ [eV}^2 \text{ A]} \quad 8.13$$

where  $E_0$  is the energy of the projectile corresponding to the Bohr velocity,  $v_0$ . The quantity  $\Omega^2/N\Delta z$  is sometimes referred to as the normalized straggling since it removes the thickness dependence and

gives a ratio for any given ion-target combination which varies with ion energy.

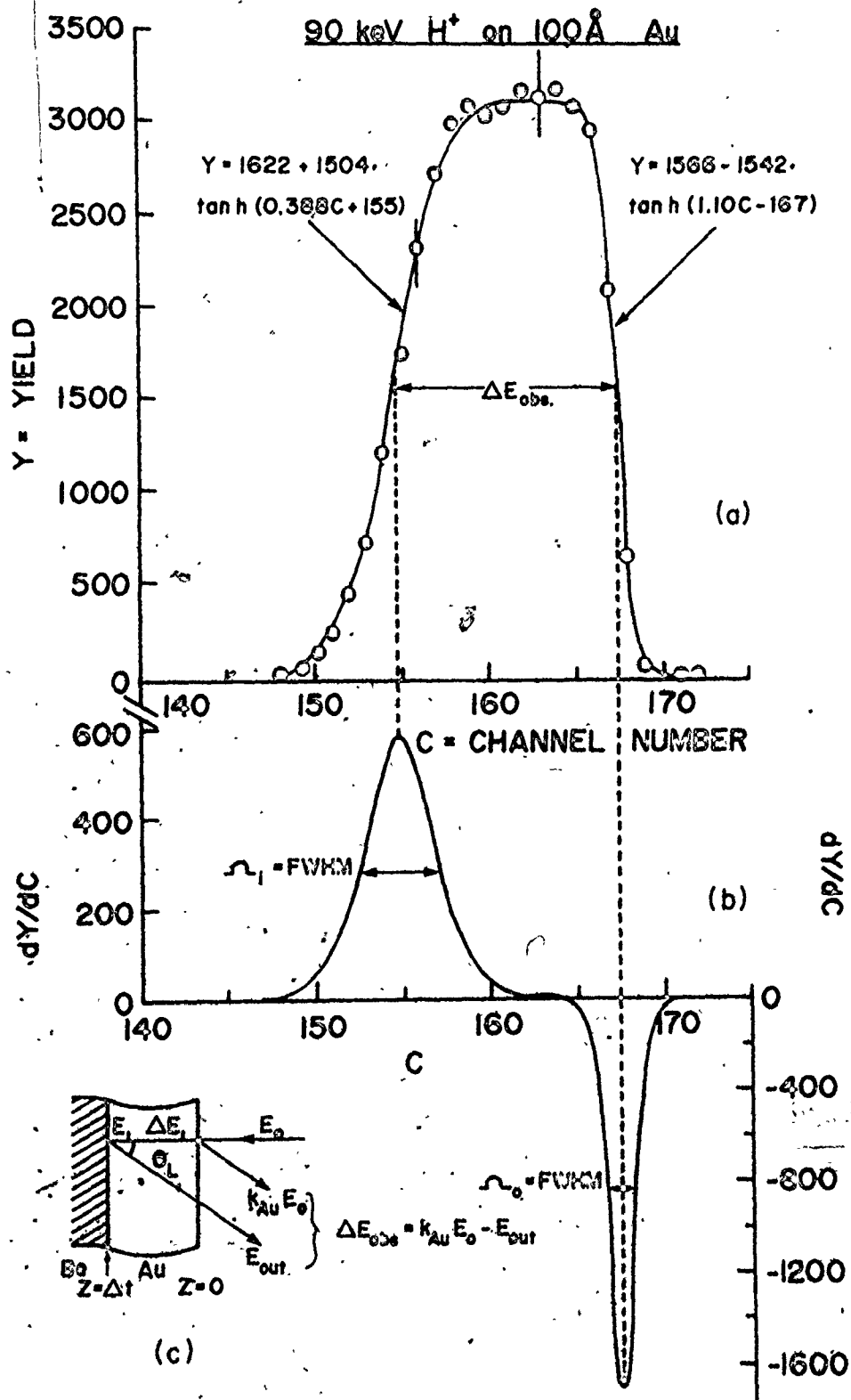
### 8.3 Experimental and Analysis Procedure

The samples used for this investigation are composed of thin gold layers on either Be or Si substrates. The element gold was selected for several reasons: (i) high purity continuous thin films of Au can be easily prepared by evaporation; (ii) many measurements have been reported<sup>130,131</sup> where the published data varies as much as  $\sim 50\%$  even though all authors estimate their data to be uncertain by typically  $\leq 5\%$  and (iii) accurate gold data is required in the proposed<sup>146</sup> use of thin gold overlays on reactive metal targets to eliminate oxidation. This will then allow stopping determinations by direct comparison with the gold stopping power while at the same time protecting the reactive metal surface.

#### 8.3.1 Stopping Cross Section Determination

Figure 8.3 provides a pictorial representation of the basic parameters needed and measured for the stopping power determinations. Section (a) gives a typical ESA spectrum including the measurement of the observed beam energy loss,  $\Delta E_{\text{obs}}$  while section (b) illustrates the differential results which are used in the energy straggling determinations as described later. The last section (c) shows the target-beam geometry and the associated energy parameters. The spectrum for the thickness,  $NAt$ , of the gold layer determination via 1 MeV  $\text{He}^+$  RBS analysis is not shown.

Figure 8.3 A typical ESA spectrum from 90 keV  $H^+$  on  $100 \text{ \AA}^0$  of gold showing (a) the fitting functions using the hyperbolic tangent, (b) and the analytically calculated differentiated result involving the hyperbolic secant squared which give the straggling measurements. The lower left inset (c) defines the geometry and basic energy variables ( $\theta_L = 150^\circ$ ).



Using the ESA, the energy loss,  $\Delta E_{\text{obs}}$ , of both H and He keV beams at various energies is measured. It is then related to an inbound energy loss,  $\Delta E_1$ . Thus the stopping cross section can be determined from

$$S(\bar{E}_{in}) = \frac{\Delta E_1}{N\Delta t} \quad 8.14$$

where  $\bar{E}_{in}$  is the average energy experienced by the projectile on its incoming path through the gold layer:

$$\bar{E}_{in} = \frac{\int E S N dz}{\int S N dz} \quad 8.15$$

Now, via RBS, the Au thickness,  $N\Delta t$ , can be directly measured. Using equation 6.27, the backscattered yield is

$$Y = \int_0^{N\Delta t} \Delta\Omega Q \frac{d\sigma(E_0)}{d\Omega} \left[ \frac{E_0}{E_z} \right]^2 Ndz \quad 8.16$$

where  $Q$  is the beam fluence,  $\Delta\Omega$  is the target-to-detector solid angle and

$$E_z \equiv E_0 - \int_0^z S(E_z) Ndz \quad 8.17$$

Here the dependence of the cross section upon energy, itself a function of  $Ndz$ , has been explicitly expressed. Assuming the stopping power to be slowly varying over the thin film thickness involved then

$$E_0 - E_z = dE_z = -NS(E_0)dz$$

so that

$$N\Delta t = \frac{Y}{\Delta\Omega Q \frac{d\sigma(E_0)}{d\Omega} \text{corr}} \left[ \frac{E_1}{E_0} \right]^2 \quad 8.18$$

where  $E_1 \equiv E_0 - NS\Delta t$

and  $\frac{d\sigma(E_0)}{d\Omega} \text{corr}$  is given by equation 6.23.

This equation is iterated to convergence and thereby takes into account the fact that at some average depth, depending on the stopping power of the material, the backscattering event takes place. The first estimate of  $N\Delta t$  is obtained by assuming  $E_0 = E_1$ . Next using the tabulated<sup>131</sup> stopping cross sections,  $S$ , for 1 MeV He,  $E_1$  is calculated which in turn yields another  $N\Delta t$ , and so on.

For the keV ions backscattered from a thin gold layer on a Be substrate, a typical spectrum, obtained via the ESA, is shown in figure 8.3 (a). As described in chapter 4, equation 4.1, the leading and trailing edges can be each fitted to a hyperbolic tangent, in this case leading to the solid lines drawn through the two edges. This is carried out after the two corrections to the ESA spectra involving resolution effects and charge-to-neutral ratios are applied. Both calculations have been explained in detail elsewhere (cf. Chapter 4). From these corrected spectra, the detected energy differences,  $\Delta E_{\text{obs}}$ , between the two inflection points of the front and rear backscattering

surfaces of the Au film is obtained. The energy difference,  $\Delta E_1$ , experienced by the projectile in traversing the gold layer front to back, a distance of  $\Delta t$ , is

$$\begin{aligned} \Delta E_1 &\equiv E_0 - E_1 \\ &= \int_0^{\Delta t} S(E) dx \\ &= S(\bar{E}_{in}) \Delta t \end{aligned} \quad 8.19$$

where  $\bar{E}_{in}$  is the average energy of the inbound beam in traversing the Au layer. In a similar manner, the outbound path energy loss is

$$\begin{aligned} \Delta E_2 &\equiv k E_1 - E_{out} \\ &= S(\bar{E}_{out}) \Delta t \sec \theta_L \end{aligned} \quad 8.20$$

where  $\bar{E}_{out}$  is the average energy of the outbound backscattered beam as it traverses the Au layer,  $\theta_L$  is the scattering angle ( $150^\circ$ ) in the laboratory frame (LABCS) and  $k$  is the kinematic scattering factor for  $H^+$  on Au (0.981) or  $He^+$  on Au (0.927). From equation 8.19 and 8.20,

$$\Delta E_2 = \Delta E_1 \frac{S(\bar{E}_{out})}{S(\bar{E}_{in})} \sec \theta_L \quad 8.21$$

$$\text{Since } \Delta E_{obs} = k E_0 - E_{out} \quad 8.22$$

$$\text{then } \Delta E_1 = \Delta E_{\text{obs}} \left[ k - \frac{S(\bar{E}_{\text{out}})}{S(\bar{E}_{\text{in}})} \sec \theta_L \right]^{-1} \quad 8.23$$

Note that  $\Delta E_1$  is calculated from the ratio of the cross sections at  $\bar{E}_{\text{in}}$  and  $\bar{E}_{\text{out}}$  so that the shape of the stopping curves and not their absolute value is the dependent parameter. An iterative procedure, based on the first estimated value of this ratio, is used to obtain the correct shape, and hence a final value of stopping power can be calculated.

From equation 8.23, the first estimate of  $\Delta E_1$  is obtained by using energies of  $\bar{E}_{\text{in}} = E_0$  and  $\bar{E}_{\text{out}} = E_{\text{out}}$ . The ratio  $S(E_{\text{out}})/S(E_0)$  is calculated using either LSS theoretical values or those given by Andersen and Ziegler<sup>130,131</sup>. (The final results based on either differ by < 1/2% when iterated to convergence).

Then applying equation 8.15,

$$S(\bar{E}_{\text{in}}) = \frac{\Delta E_1}{N\Delta t} \quad 8.24$$

$$\text{where } E_{\text{in}} = E_0 - \frac{\Delta E_1}{2}$$

Further iterations, to convergence, can now be performed employing the new energy values to determine  $S(E)$  terms in the ratio which yield a re-evaluated  $\Delta E_1$  and thus obtain a final stopping cross section as well as average energy values.

### 8.3.2 The Straggling Determinations

Straggling determinations can be obtained from the same measurements required for the stopping powers. An examination of



the front and back edges of the ESA spectra reveals information on the system resolution and the straggling<sup>148</sup>. Specifically the derivative of the front edge yields a Gaussian-like function whose full width at half maximum (FWHM) is characteristic of the detection system while the rear edge includes the above correlated with the energy straggling of that part of the beam which has traversed both full ingoing and outgoing paths through the gold layer. For analysis it is assumed that these responses are true Gaussians so that the energy straggling,  $\Omega^2$ , is obtained by calculating the difference in quadrature of the front edge FWHM,  $\Omega_i$ , and rear edge FWHM,  $\Omega_0$ :

$$\Omega^2 = \Omega_0^2 - \Omega_i^2 \quad 8.25$$

Now as shown in chapter 4, the spectral response of back-scattered particles from an interface which is an "edge" can be represented mathematically by the hyperbolic tangent of the form

$$Y(C) = A_1 + A_2 \text{TANH} (A_3(C + A_4)) \quad 8.26$$

where Y is the yield or number of counts in channel number C and the A's are the fitting parameters. Note that by suitable sign changes for the A parameters, either forward or backward edges may be represented. Since the energy, E, with a particular channel bears a linear relationship, the variable C can be replaced by E. In order to obtain FWHM data, the tangent term can be easily differentiated to give

$$\frac{dY(E)}{dE} = A_2 A_3 \text{sech}^2 [A_3(E + A_4)] \quad 8.26a$$

The value of E at half maximum is

$$E = \frac{\text{sech}^{-1}(1/\sqrt{2})}{A_3} - A_4 \quad 8.27$$

$$= \frac{\ln 3}{A_3} - A_4$$

where  $Y_{\text{max}} = A_2 A_3$  using the unity normalization property of the  $\text{sech}^2$ . Thus the FWHM becomes

$$\Omega = \frac{2 \ln 3}{A_3} \quad 8.28$$

The question of the determination of the average energy  $\langle E \rangle$ , at which the straggling is assumed to be evaluated is somewhat equivocal. Some authors<sup>147</sup> simply use  $E_0$ , the incident energy, while others<sup>148,149</sup> attempt to ascribe an average. According to Moorhead<sup>150</sup>:

$$\langle E \rangle = \frac{|\cos \theta_L| E_0 + E_{\text{out}}}{1 + k |\cos \theta_L|} \quad 8.29$$

where  $E_{\text{out}}$  is the backscattered energy measured at the inflection point of the rear edge of the Au, k is the kinematic scattering factor and  $\theta_L$  is the scattering angle ( $150^\circ$ ) in the laboratory frame of reference. It is this energy that is used in the following straggling determinations.

#### 8.4 Results and Discussion

Energy spectra for H and He in the energy range of 20 - 140 keV backscattered from various Au films (from 110 to 170 Å in

thickness) are obtained using the ESA. These films, produced via e-beam evaporation at a base pressure of  $\sim 5 \times 10^{-7}$  torr, were analyzed for continuity by Auger Electron Spectroscopy and further confirmed by observing that the backscattered yield at the peak was identical to that obtained from a thick (2000 Å) similarly evaporated Au film over the same channels. The stopping cross sections are determined to better than 5% accuracy.

#### 8.4.1 Stopping Cross Sections in Gold

The stopping cross section results are shown in figure 8.4 (a) and (b) for  $H^+$  and  $He^+$  respectively. They are plotted versus  $E^{1/2}$  since, especially for He, these results fall mainly within the velocity dependent stopping regime. Data from other researchers<sup>93, 151-154</sup> are also given and have been selected based on their close proximity to the best fit line representing the majority of available measurements (cf. references<sup>130</sup> and<sup>131</sup>).

For the  $H^+$  in Au data, good agreement is shown between this work and the earlier measurements<sup>93, 151, 152</sup>. Note the deviations from the velocity proportionality for  $v > v_0$  ( $E_0 \sim 30$  keV  $H^+$ ) which can be seen easily by the comparison of the current determinations with the LSS predictions. In the lower energy regime, where  $E_0 < 30$  keV, the measured values exceed the LSS values by 40%. The solid line drawn through the data points for this work is obtained via the usual least squares fitting procedure. However, since the form of the stopping curve predicted by LSS is not valid in the upper regions of the H data, the fitting

procedure uses an expression for the stopping cross section,  $S$ , as given by Andersen and Ziegler<sup>130</sup>

$$\frac{1}{S} = \frac{1}{S_{HI}} + \frac{1}{S_{LO}} \quad , 8.30$$

where  $S_{LO} = A(1)[E(\text{keV})]^{0.45}$

$$\text{and } S_{HI} = \frac{A(2)}{E(\text{keV})} \ln \left[ 1 + \frac{A(3)}{E(\text{keV})} + A(4) E(\text{keV}) \right]$$

The coefficients  $A(1)$  to  $A(4)$ , given by Andersen and Ziegler<sup>130</sup> for  $H^+$  on Au are shown in Table 8.1, as are the results obtained by the best fit calculated above (with statistical uncertainty < 5%).

TABLE 8.1

Comparison of Coefficients for Fitting H Stopping Power in Au.

Data Reference	Coefficients			
	A(1)	A(2)	A(3)	A(4)
Andersen-Ziegler <sup>130</sup>	5.46	$1.83 \times 10^4$	$4.38 \times 10^2$	$2.54 \times 10^{-3}$
Present Work	6.06	$2.17 \times 10^5$	0.682	$5.56 \times 10^{-4}$

The results for He stopping in Au are illustrated in figure 8.4 (b). Again, selected published data<sup>93, 153-155</sup> are shown for comparison together with the LSS predicted values and those of Ziegler<sup>131</sup>. Using the  $E^{1/2}$  dependence, the best fit curve calculated

- Figure 8.4 (a) Measured stopping cross sections for  $H^+$  in Au:  
o - current data;  $\Delta$  - after ref. 93; o - after ref. 151; x - after ref. 155. Also indicated are the theoretical productions of LSS and the best fit results of Andersen-Ziegler (ref. 130).
- (b) Measured stopping cross sections for  $He^+$  in Au:  
o - current data;  $\Delta$  after ref. 93; x - after ref. 154, 152;  $\square$  - after ref. 153; o - after ref. 154. Also indicated are the theoretical predictions from LSS and the best fit results of Ziegler (ref. 131). The solid line drawn through the current data points is the best fit following a  $E^{1/2}$  dependence.

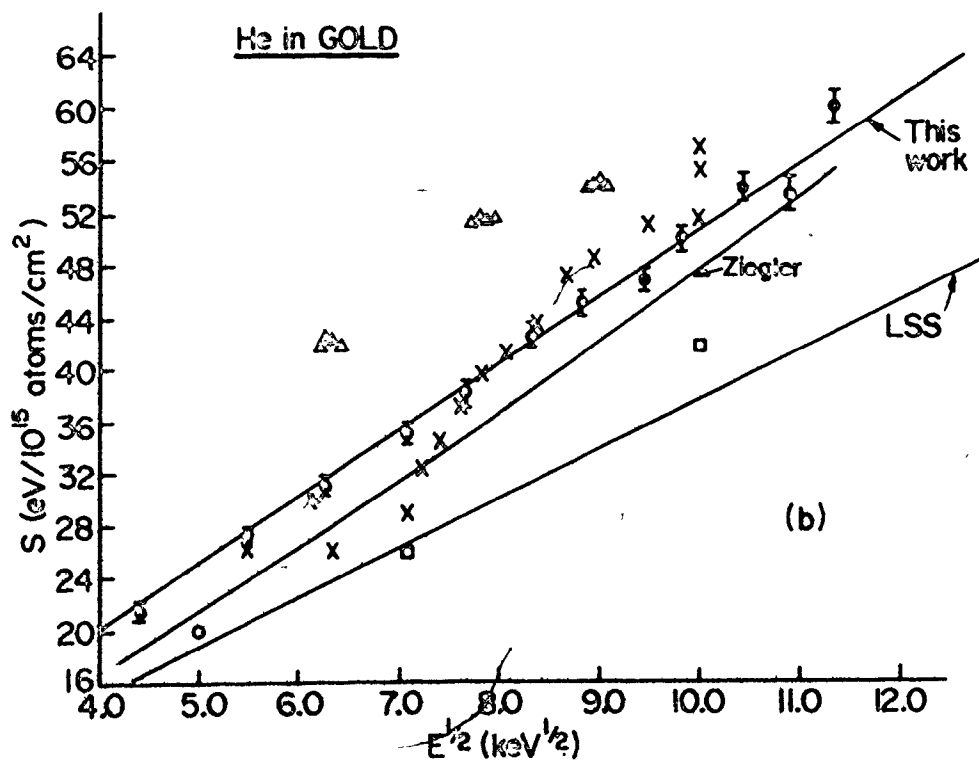
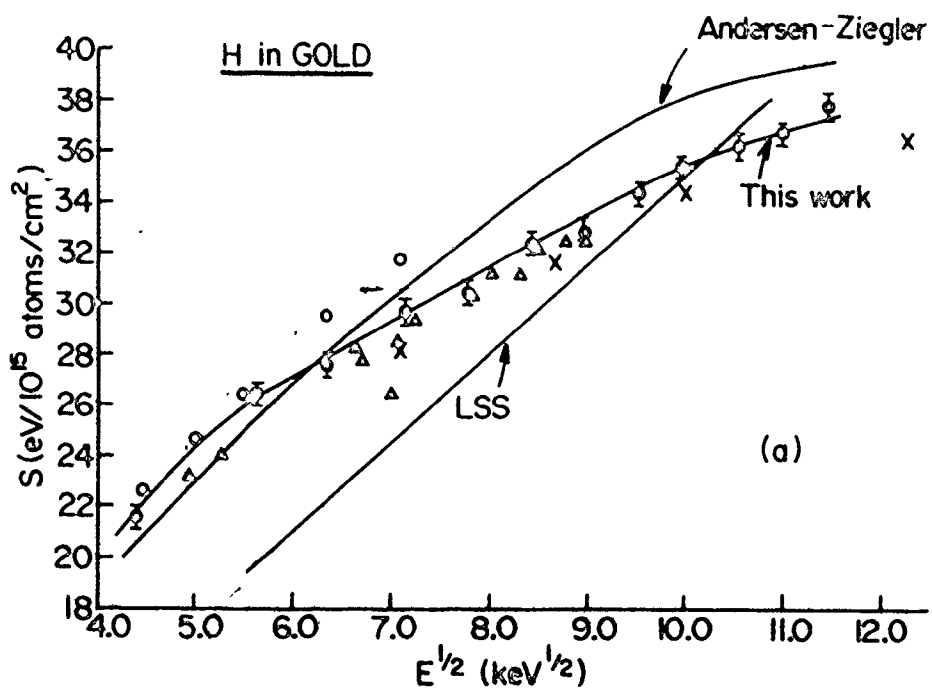
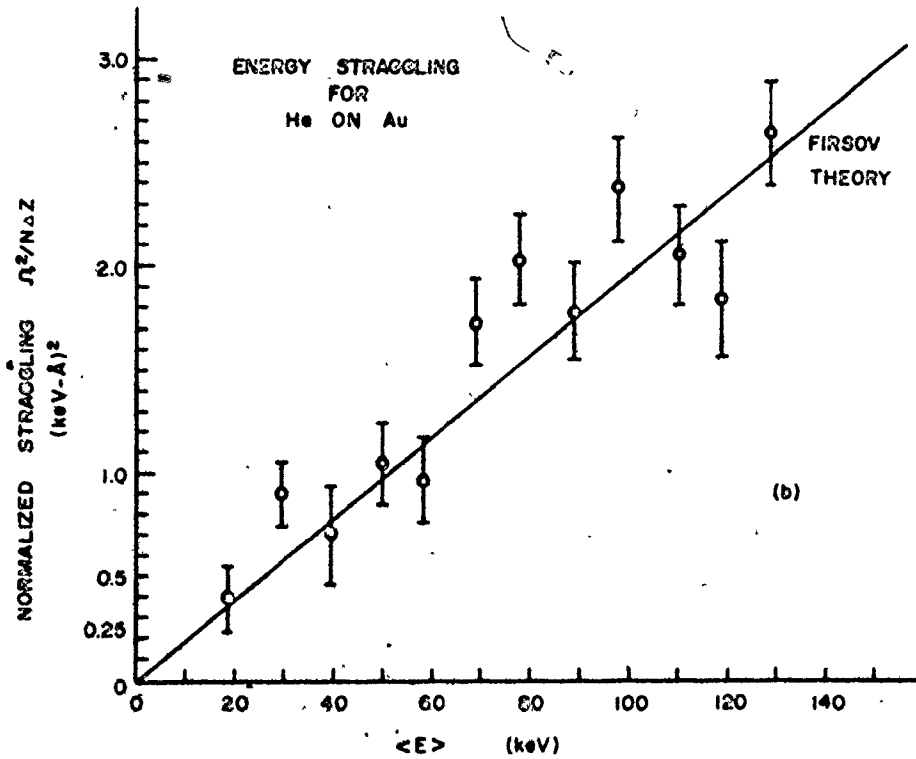
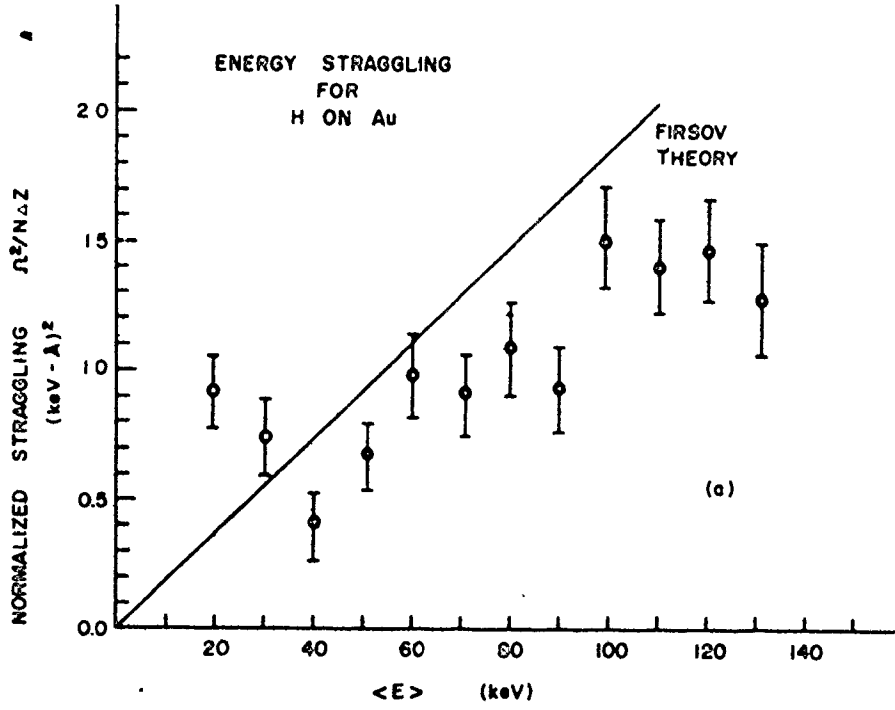


Figure 8.5 The normalized straggling measurements (cf. equations 8.13) versus the average energy (cf. equation 8.29) plotted to directly compare with Firsov theory<sup>133</sup> (solid line) for H on Au (a) and He on Au (b).







from the least squares procedure is given by

$$S = (5.08 \pm 0.09) \times 10^{-15} [E(\text{keV})]^{1/2} \text{ eV cm}^2/\text{atom} \quad 8.31$$

This curve is shown as the solid line drawn through the data point and is found to be  $\sim 34\%$  higher than LSS theory.

From the selected data, there is only one published report<sup>93</sup> which measures both H and He stopping in Au. In this determination, similar ESA measurements were carried out and approximate corrections were applied for theoretically estimated charged fractions<sup>154</sup>. The results, shown in figure 8.4 (a), indicate good agreement for the present measurements involving H in Au but for He in Au, figure 8.4 (b) the current data are approximately 40% lower than that given earlier<sup>93</sup>. No explanation can be offered for this discrepancy.

#### 8.4.2 Straggling in Gold

The straggling values have been extracted using equations 8.28 and 8.25. They are shown in figures 8.5 (a) and (b) for  $\text{H}^+$  and  $\text{He}^+$  respectively and are plotted as normalized straggling which removes the thickness dependence (see equation 8.13) versus the average energy as calculated from equation 8.29. Comparison with equation 8.13 due to Firsov<sup>133</sup> is illustrated by the solid line. The scaling of this approach for He seems valid, however, to the same degree this cannot be said of the H data. So far as is known, there exists no other data for the straggling of light ions in gold as determined via the backscattering techniques in this energy regime. The above comparison with Firsov must be

qualified since it is known that stragglings determinations are severely dependent on target continuity, uniformity (even on a microscopic scale) and texture<sup>157</sup>. Thus, in any measurement of this kind, a detailed analysis of the samples used must be included. The results, therefore present an upper limit to stragglings since these varying target conditions can only serve to increase the observed stragglings.

Leaf 212 omitted in page numbering

## CHAPTER 9

### Summary

This chapter summarizes the development of the Medium Energy Ion Reflection Spectrometer and the investigation of its capabilities when applied to the surface analysis of solids.

- 1) An electrostatic analyzer was designed and constructed. It performed in agreement with the design criteria, and provided good depth resolution for investigating solid surface layers. The necessary spectral corrections were developed and were discussed in relation to the analysis applications.
- 2) A solid state detector system was developed to perform a complementary role to the electrostatic analyzer. This detector allowed "in-situ" determination of the sample back-scattered charged fractions. These were applied to the electrostatic analyzer spectra in order to correct for the missing neutral component that was not analyzed electrostatically. The requirement that this correction be accomplished at equivalent exit energies was met by applying the results of solid state detector pulse height defect measurements. Both theoretical predictions and Monte Carlo simulation data were found to be lacking in sufficient accuracy to be used. The "in-situ" technique proved to be a distinct advantage since it was found that slight changes in solid surfaces radically altered the ion-to-

atom ratio of backscattered particles. Hence, when applied to the electrostatic analyzer data, these corrections improved the accuracy of quantitative electrostatic analysis results. Existing theoretical approaches in the area of charge neutralization however, are not advanced enough to provide reliable predictions of experimental results and therefore were not employed to correct the electrostatic analyzer spectra.

- 3) The scattering cross sections for large angle scattering of various ions in gold were measured in the screened Coulomb scattering region and were compared to the universal scattering screening function given by the LSS approach. The scaling properties of the cross section expected theoretically and those observed experimentally were comparable in the higher energy regions but differed somewhat in the lower energy regions. Hence the theoretical accuracy in reproducing experimental observations does not approach that of MeV regions.
- 4) The stopping powers of hydrogen and helium in gold were determined to a 2% uncertainty level and required the use of the full complement of analysis techniques available in the medium energy ion reflection spectrometer. The Rutherford backscattering facility allowed "in-situ" thickness measurements that were reliable and readily obtained. After the application of suitable corrections, the high resolution electrostatic analyzer provided spectra from which the observed energy loss was measured to relatively good precision. One such correction involved the ion-atom fractions obtained by the cooled solid state detector, again, "in-situ"

and with the appropriate pulse height defect considerations.

The use of medium energies to probe materials both in surface and bulk properties has the advantages of larger backscattering intensities, a greater sensitivity to changes in surface and near surface regions, and, with the inclusion of several particle detection systems, the ability to use existing ion implantation facilities as an "in-situ" analysis tool to determine both pre- and post- bombardment target conditions. While medium energy ion reflection spectrometry cannot, at present, approach the accuracy obtained by the higher energy regime, it can provide reliable results through the use of appropriate corrections. These should be determined from the characteristics of the spectrometer and, as much as possible, from the "in-situ" conditions of the sample under examination. Current theoretical estimates in the medium energy regime are not as well developed as those in the higher energy area. The lack of reliable quantitative theoretical information required by the spectrometer is due to various complications in the ion-solid interaction that cannot be accurately accounted for. In the medium energy region, the scattering cross sections are dominated by the screened nuclear collision. The stopping powers of a  $Z_1$  projectile in a material medium do not follow a simple velocity dependence but rather are disturbed by  $Z_1$  shell effects creating  $Z_1$  oscillations. Charge neutralization models, at energies accessible to the spectrometer are based on various mechanisms, neither one of which taken alone can reasonably predict the experimentally observed results. Thus, a great deal of experi-

mental information is required to investigate the many facets of the medium energy ion-solid interaction in order to provide a broader base on which more detailed theoretical studies can be constructed.



APPENDIX



Leaf 218 omitted in page numbering

A.1 MES11.MAC  
medium energy spectrometer control code  
for the PDP-11/05

.TITLE MES11.MAC USN 01-JUN-79  
PROGRAM CONTROL FOR THE MCMASTER UNIVERSITY  
MEDIUM ENERGY ION REFLECTING SPECTROMETER  
BY SWP JULY 1977

PS=177776  
SWR=177570  
TPB=177566  
TPS=177564  
TYB=177567  
TKS=177560  
LFS=177546  
MTRREG=164026  
AUXREG=164024  
SCLR=164022  
MRCR=164020  
ADC2=164014  
ADC1=164012  
ADCSR=164010  
MREG=164006  
YREG=164004  
XREG=164002  
DSPSR=164000  
KYBPRI=5  
PTRPRI=4  
CLKPRI=7  
ADCPRI=6  
SLRPRI=5  
GTRPRI=7  
INTPRI=7  
ERRWRD=52  
DATMSK=177740

MEMORY ALLOCATIONS

.MCALL ..V2...REGDEF,.GTIM,.INTEN,.DATE,.TTOUTR  
.MCALL .TTYIN,.TTINR,.TTYOUT,.PRINT,.EXIT  
.MCALL .CSIGEN,.WRITW,.READW,.CLOSE,.PROTECT  
..V2..  
.REGDEF  
K22=643 ; ADCSR ROB MASK  
BUFLN=40000 ; MAX. LENGTH OF THE DATA BUFFER  
K44=174000 ; MRCR ROB MASK  
BUFEND=BUFSA+BUFLN ; END ADDR FOR DATA BUFFER  
K4=170000 ; MREG ROB MASK

INTERRUPT VECTORS

.ASECT  
..=100 ; ELAPSED TIME CLOCK  
:K0: TMX ; LD VCTR ADDR FOR CLOCK  
:K2: 340 ; RUN AT LEVEL # 7  
..=130 ; ADC  
L0: ADCX ; LD VTR ADDR FOR ADC  
L2: 340 ; LEVEL 6  
..=150 ; SCALE AND INTEGRATERR  
:K0: SCALE ;LD VTR ADDR FOR SCALER  
:K2: 340 ; LEVEL 5  
:K4: INTEG ; LD VTR ADDR FOR INTEGRATER  
:K8: 340 ; LEVEL 7

.CSECT

START OF MAIN-LINE ROUTINE

START: BIC #40,CXRCR ; CLEAR RESET  
MOV #BUFSA,ADCSA ; INIT ADC S.A.

```

BIS #100,0#44      ; SET C SO DONT WAIT FOR TT INP
.PRINT #MSG1       ; PRINT THE TITLE
.DATE              ; DECOD&STOR DATE IN ASCII

TST R0             ; HAVE DATE?
BEG NOTSET         ; NO SO IGNOR DATE
CLR R1             ; INIT R1 AS FLAG
MOV R0,DATLOC     ; STOR DATE WORD
MOV R0,R4         ; GO AFTER YEAR
BIC #DATMSK,R4    ; 0 ALL BUT NEEDED
ADD #110,R4       ; DECODE THE YEAR
MOV R4,TEMP2      ; STORE THE YEAR
MOV DATLOC,R4     ; GO AFTER DAY
MOV #5,ROTCTR     ; RT ROTATE R4
JSR PC,ROTN       ; BY 5 BITS
BIC #DATMSK,R4    ; TAKE LAST 5 BITS
MOV #ASDAT,R5     ; SET UP STORAG PNTR
JSR PC,DECODE     ; STORE THE DAY
MOV8 #'-(R5)+     ; STORE -
MOV DATLOC,R4     ; GO AFTER MONTH
MOV #12,ROTCTR    ; RT ROTATE R4
JSR PC,ROTN       ; BY 10 BITS
CLR R1            ; R1 PTS TO ASCII MONTH
DLOUP1: DEC R4     ; USE MONTH # AS PTR
BEG OUT2         ; DUN? YES SO EXIT
ADD #3,R1        ; NO SO BUMP PTR
BR DLOUP1        ; GO AGAIN
OUT2:  ADD #MONTH,R1 ; GET PTR AS ADDR.
MOV8 (R1)+,(R5)+ ; MOV IN ASCII MONTH
MOV8 (R1)+,(R5)+
MOV8 (R1)+,(R5)+
MOV8 #'-(R5)+     ; ADD IN ASCII -
MOV TEMP2,R4     ; GET YEAR
CLR R1           ; INIT R1 FLAG
JSR PC,DECODE   ; AND STOR IT
CLR8 (R5)       ; STOR CR/LF
RSTRT: .DATE     ; DATE SET?
TST R0         ; NO SO BRANCH OVR
BEG NOTSET
.PRINT #ASDAT  ; PNT THE DATE
; ROUTINE TO INPUT GRP WIDTH AND SET UP GRPS
NOTSET: .PRINT #MSG2 ; PRINT GP WDNH
JSR PC,INPT1  ; INPUT GP WDNH
MOV R3,GPWDTH ; STORE IT
MOV R4,DSPLEN ; STOR # BYTES
CLR ESAERR    ; RESET SCAN ERR FLG
CLR WINM8     ; RESET SORTED WNDW FLG
CLR BCISSET   ; RESET DOSE FOR ESA MODE

;
;
;
INIT MARKER POSITIONS
CLR LTRKX     ; ZERO LEFT MARKER
MOV GPWDTH,RTKRX ; RIGHT MKR=GRP WIDTH
DEC RTKRX     ; -1
;
CALC #GPS     ;
MOV DSPLEN,R2 ; R2 = # BYTES
CLR R4        ; NO
CONTS: CMP #BUFLEN,R2 ; BEYOND BUF
BNI CONTS    ; SO R4 = GP # MAX
INC R4       ; CHECK MORE
ADD DSPLEN,R2 ; TILL BEYOND BUF
BR CONTS
CONTS: CMP R4,#36 ; GRP #>30?
BNI GOOD    ; NO SO O.K.
MOV #33,R4  ; YES SO SET TO 30
GOOD:  MOV R4,GRPNUM ; STOR GP #MAX
MOV #1,KRFLG ; INIT FLAG FOR PNT ONLY
.PRINT #XSB4 ; PNT: MAX GP #

```

```

JSR PC,PRNTDC          ; OUTPUT THE #
:
:
CLEAR SPECTRA,WINDOW AND TITLE BUFFER IF REQ'D
:
.PRINT #MSG5           ; ASK IF CLEAR WANTED
.TTYIN                 ; GET RESPONSE
CMPB #'Y,R0            ; IS RESPONSE "Y"?
BNE REDO                ; NO SO EXIT

JSR PC,WINCLR          ; CLR ALL WINDOWS
MOV #CLRALL,R1         ; POINT TO BUFFERS.A.
CLRSPC: CLR (R1)+       ; CLR BUFFER
CMP R1,#ALLEND        ; END OF BUFFER?
BNE CLRSPC             ; NO SO CLR MORE
.PRINT #MSG36          ; PNT:ADC2 GAIN=
JSR PC,NUMINI          ; GET CONV GN INPUT
MOV B,INX8,R1         ; STORE IT
MOV GPWDTH,R3         ; GET GRP WPTH
CLR R2                 ; ZERO CONV GN CTR
MLOOP2: ASR R1          ; GAIN/2
BEG CLRSPC             ; 0? YES SO ERROR
INC R2                 ; BUMP CTR
CMP R1,R3              ; SAME(DUN)?
BNE MLOOP2             ; NO SO CHK MOR
MOV R2,CONUX8 ; .YES SO HAV CNV#

:
:
COMMAND RE-ENTRY POINT
REDO: .PRINT #MSG0     ;PNT ">"
      CLR ERFLG        ;AND CLEAR ERROR FLG
:
:
GO TO BKGD TILL CHAR STRING INPUT
JPBKGD: JSR PC,BKGD I ;BKGD BRANCH
:
:
CMPB R1,#33            ;IS CHAR ESC?
BNE JPBKGD             ;NO SO CONTINU BKGD
:
:
ANALYZE INPUT COMND
RSTRT3: JSR PC,KBIN     ; INPUT COMND
MOV #TTBUF+1,TEMP1    ;POINT TO DIGITS
SUB #1,DCTR           ;DCTR HAS # DIGITS
CMP #0,DCTR            ;#DIGITS 0?
BNE CONT4              ; NO SO CONT.
CLR R4
DEC R4
MOV R4,GRCOM          ; YES SO GRCOM=-1
BR CONT3              ; JMP OUT OF ANALYSIS
CONT4:  CMPB #'M,TTBUF  ; IN MARKER COMMAND MODE?
BNE CONT44            ; NO SO BRANCH
MOV #1,DCTR           ; YES SO SET DIGIT CTR TO 1
CONT44: JSR PC,INBIN    ; CNVT TO BIN #
CMP #0,ERFLG         ; LEGAL #?
BEG CONT2             ; YES SO CONT
RSTRT4: .PRINT #MSG6    ; NO SO ?
BR REDO               ; RESTART
CONT2:  CMPB #'M,TTBUF  ; IN MARKER COMMAND?
BNE CONT22            ; NO SO NORMAL # CHECK
CMP #7,BINX3         ; COMPARE MARKER # TO 7
BMI RSTRT4           ; > SO ERROR
BR CONT23            ; JMP OVER NORMAL # CHECK
CONT22: MOV GRPNUM,R4   ; DEC # GRPS BY 1
DEC R4
CMP R4,BINX3         ; # TOO BIG?
BMI RSTRT4           ; YES SO RESTART
CONT23: MOV B,INX8,GRCOM ; STOR GP CMND
; SEARCH TABLE FOR WHERE TO BRANCH FOR COMMAND
CONT3:  MOV #JTBL,JPTR  ; SET JP TBL PTR
MOV #CTBLE,R4        ; R4 PTS TO VALID CMND
MOV #26,R5           ; SET UP CTR

```

```

LOOP10: CMPB  TTBUF,(R4)+      ; VALID CMND LETTER
        BNE  NOGD             ; NO SO GET NOTHR
        JMP  @JPTR           ; YES SO TO TBLE JMP
NOGD:   DEC  R5              ; DEC CTR
        BEB  RSTRT4         ; INVALID CHAR SO EXIT
        ADD  #4,JPTR        ; INC JPTR FOR JP TBL
        BR   LOOP10         ; NO SO CHECK MORE
;
; SUBROUTINE TO CLEAR ALL STARTING AND ENDING
; ADDRESSES OF BOTH WINDOW BUFFERS
;
WINCLR: MOV  #MRKBUF,R2      ; GET BUFR S.A.
        MOV  #WINBUF,R3
        MOV  #20,R1         ; CNTR(20WDS/BUFR)
WLOOP0: CLR  (R2)+          ; CLR ADDR
        CLR  (R3)+
        DEC  R1             ; DUN?
        BNE  WLOOP0        ; NO SO BRANCH
        RTS  PC            ; YES SO EXIT
;
ODT:    MOV  R1,REG1
        MOV  R2,REG2
        MOV  #20,R2
        MOV  NUMBER,R1
ODTLPO: ASL  R1
        BCC  NOT1
        .TTYOUT #'1
        BR  UPDAT
NOT1:   .TTYOUT #'0
UPDAT:  DEC  R2
        BCC  ODTLPO
        MOV  #40,R1
        .TTYOUT R1
        MOV  REG1,R1
        MOV  REG2,R2
        RTS  PC
;
REG1:   .WORD  0
REG2:   .WORD  0
NUMBER: .WORD  0
;
MONTH:  .ASCII /JANFEBMARAPRMYJUNJULAUGSEPOCTNOVDEC/
        .EVEN
CTBLE:  .ASCII /ASEPTKRGDXXXNLBICFOUXZ/
        .EVEN
JPTR:   .WORD  0              ; JMP TBLE PTR
JTBLE:  JMP  ADCST           ; ADC # 1 START ROUTINE
        JMP  STOP          ; ADC1 STOP ROUTINE
        JMP  ERASE         ; ERASE SPECTRUM
        JMP  PRNT         ; PRINT SPECTRUM
        JMP  TITLE        ; INPUT TITLE
        JMP  WRITE        ; WRITE ON DISK
        JMP  READ         ; READ FROM DISK 1
        JMP  GAIN         ; RESET GPMTH & REINITIATE
        JMP  DSPKXK       ; DISPLAY BETWEEN MARKERS ONLY
        JMP  MARKR        ; MARKER WINDOW SET ROUTINE
        JMP  PLOT         ; PLOT ROUTINE
        JMP  KLCLB        ; GROUP MANIPULATOR CALCULATOR
        JMP  LOGIT        ; ROUTINE TO DO NATURAL LOGS
        JMP  LISTH        ; WINDOW LIST CMND
        JMP  BEGIN        ; START THE SCAN LOOP
        JMP  INTSET       ; BCI PRESET SET
        JMP  CNDN         ; START C/N SCANNING MODE
        JMP  FREQ         ; INPUT HALF CYCLE TIME OF C/N SCAN
        JMP  OFF          ; TURN OFF SCANNING MODE(ESA OR C/N)
        JMP  CNTUE        ; RESUME SCANNING AFTER 0 CMND
        JMP  DUNP         ; PROGRAM EXIT
        JMP  ZERO         ; RECALIBRATE STEPPING MOTOR(ESA)
        JMP  RSTRT4       ; ILLEGAL CMND EXIT

```

```
.....
SUBROUTINE TO RIGHT ROTATE R4 BY ROTCTR BITS
(USES R3)
RROTN: MOV ROTCTR,R3      ; GET ROTN #
      BEQ RDUN            ; DUN?
RLOOP: ASR R4             ; NO SO LOOP
      DEC R3              ; DUN?
      BNE RLOOP          ; NO SO LOOP
RDUN:  RTS PC            ; NORMAL RETURN
.....
```

```
.....
SUBROUTINE TO CONVERT DAY & YEAR TO 2 DIGIT ASCII
AND 2 DIGIT MONTH TO 3 LETTER ASCII
(# IN R4 & R5 IS STORAGE POINTER)
DECODE: MOV #2,DCTR      ; 2 DIGIT STORE
      MOV VPTR,R3       ; SET UP TNPTR
      MOV R4,TEMP1     ; SAVE #
      CLR R0            ; USE R0 AS COEFF CTR
DLOUP2: MOV TEMP1,R4    ; GET #
      SUB (R3),R4      ; LEST 10 PWR FOUND
      BMI GOTIT        ; SUBTR 10 PWR
      MOV R4,TEMP1     ; SAVE THE RESULT
      INC R0            ; BUMP CNTR
      BR DLOUP2        ; REPEAT
GOTIT: ADD #60,R0       ; CONVERT TO ASCII
      MOV8 R0,(R5)+    ; STOR THE ASCII
      CMP8 (R3)+,(R3)+ ; UPDATE TN PTR
      DEC DCTR         ; BUMP CTR,DUN?
      BNE DLOUP2-2    ; NO SO MORE
      RTS PC           ; NORMAL RETURN
.....
```

```
VPTR:  .WORD TENPWR
TENPWR: .WORD 12,1,0 ; DECIMAL CONVERSION POWERS OF TEN
DATLOC: .WORD 0      ; DATE DATUM WORD
ROTCTR: .WORD 0      ; ROTATION COUNTER
ASDAT:  .BLKW 6      ; DECODED ASCII DATE
PLTW3:  .WORD 0      ; TIMED WAIT FLAG FOR PLOTTER
PLTFLG: .WORD 0      ; PLOT MODE FLAG
.....
```

```
.....
SUBROUTINE TO PLOT FROM DSPLSA FOR A LENGTH OF XEND
IN UNITS OF CHINK,BEGINNING AT CHNL XSTART.
PLOTIT: MOV XSTART,@XREG ; SET START AT CHNL X
      MOV DSPLSA,R3     ; R3 HAS DATA S.A.
LOOPLT: CLR PLTW3      ; CLR TIME OUT FLG
      MOV (R3)+,@YREG  ; LOAD Y WITH DATA
      MOV #1,@DPSR     ; PLOT IT
PTWATE: ADD #3,PLTW3   ; TIMED WAIT LOOP
      TST DSPFLG       ; IN SPECIAL MODE?
      BEQ .+10         ; NO SO NORMAL WAIT
      SUB #2,PLTW3     ; YES SO WAIT LONGER
      CMP PLTW3,#40000 ; DUN?
      BHI PTWATE       ; NO SO LOOP
      ADD CHNK,@XREG   ; YES SO UPDATE CHNL#
      CK? @XREG,XEND  ; DUN ALL DATA?
      BHI LOOPLT      ; NO SO MOR
      RTS PC           ; YES SO EXIT
.....
```

```
.....
SUBROUTINE TO CALCULATE EXPANSION ADDR. OFFSETS
(ADSET) AS A FN. OF CHANNEL INCREMENT(CHNK)
USES R1 & R3
ADSET: MOV GPWDTH,R1   ; SET UP DIVIDEND
      CLR R3           ; SET UP RESULT CNTR
ADLOOP: SUB CHNK,R1    ; DIV BY CHNK LOOP
      CNI AD2X        ; DUN?
.....
```

```

      INC R3          ; NO SO UPDATE RESULT
      BR ADLOOP      ; AND GO AGAIN
ADEX: BIC #1,R3      ; MAKE EVEN ADDR
      MOV GPWIDTH,R1 ; GET # CHNLS DSPLYD
      SUB R3,R1      ; CALCULATE OFFSET
      MOV ADFSET,DSPTMP ; GET MIDPT ADDR
      ADD R1,DSPTMP  ; STOR NEW ADDR OFFSET
      RTS PC         ; RETURN

```

```

ADFSET: .WORD 0      ; ADDR. OFFSET FOR MOTION MODE

```

```

      THIS IS THE END OF ASCII PAGE 1:KES11.MAC

```

```

GPWIDTH: .WORD 0    ; GP WIDTH (CHANNELS)
DSPLEN:  .WORD 0    ; DISPLAY LENGTH (BYTES)
GRPNUM:  .WORD 0    ; MAX # OF GRPS
EXCOM:   .WORD 0    ; COMMAND LETTER EXTRACTED
SISN:    .WORD 20   ; # BITS PER WORD
KMRN:    .WORD 0    ; KMR STORAGE SPACE
DSPLSA:  .WORD 0    ; DSPLY S.A.
XSTART:  .WORD 0    ; DISP. X-CHANNEL START
XEND:    .WORD 0    ; LAST CHANNEL DISPLAYED
ESASA:   .WORD 0    ; ESA SCANNING SPECTRUM S.A.

```

```

      SUBROUTINE TO CHECK TOGGLES FOR DSP GP

```

```

DSPLY: JSR PC,RSAVE ; POLL SWR'S
      JSR PC,POLL   ; UPDATE STATUS
      JSR PC,UPDATE ; EXT.SOFT.SW.#1 ON?
      BIT #1000,CCXCSR ; NO SO IGNORE
      BEQ NDLAP    ; DSPLY 1ST SECTION
      JSR PC,GPSEL ; GET MAX # GRPS
      MOV GRPNUM,R5 ; DIVIDE BY 2
      ASR R5       ; 0?
      BEQ NOLOG    ; YES SO DSPLY 1 GRP
      JSR PC,GPSEL ; DUN SO EXIT
      BR NOLOG     ; BIT 15 ON?
NDLAP: TST QFSKR   ; YES SO DSPLY 2 GRP
      BMI DOLOG    ; NO SO DSPLY 1 GRP
      JSR PC,GPSEL ; DUN SO EXIT
      BR NOLOG     ; GET MAX# GRPS.
DOLOG: MOV GRPNUM,R5 ; TAKE HALF
      ASR R5       ; 0 SO DSPLY 1 GRP
      BEQ NOLOG    ; UPDATE TO 2ND SEC.
DLOUP: ADD DSPLEN,DSPLSA ; UPDATE CNTR.
      DEC R5       ; DUN ALL? NO SO MOR
      BNE DLOUP    ; YES SO DSPLY 2ND SEC.
      JSR PC,GPSEL ; RESTOR REGS
NOLOG: JSR PC,RESTOR ; NORMAL RETURN
      RTS PC

```

```

      SUBROUTINE TO DSPLY GROUPS SELECTED BY TOGGLES ON THE
      SWITCH REGISTER OF THE PDP11/05 CONSOLE.

```

```

GPSEL: MOV GRPNUM,R5 ; R5 = MAXGRPS
      ASR R5         ; R5=MAX GRPS/2.0
      MOV CFSKR,R4  ; R4 HAS TOGGLE POSN
UP:    ROR R4        ; SET BIT ?
      BCC DOWN      ; NO SO GET ANTKER
      TST PLTFLG    ; IN PLOT CMD?
      BNE PLOTON    ; YES SO NO DSPLY
      JSR PC,DISP   ; YES SO DSP GP
DOWN:  ADD DSPLEN,DSPLSA ; MOV UP 1 GP
      DEC R5        ; DEC GRP CTR DONE?
      BNE UP        ; NO GET ANOTHER TOG
      RTS PC        ; NORMAL EXIT

```



```
PLOTON: JSR PC,PLOTIT      ; GO PLOT SPECTRUM
        BR  DOWN          ; DUN SO CHK TOGGLES
;
;
; SUBROUTINE TO CHECK STATUS OF OPERATION
; AND UPDATE PROGRAM RUN CONFIGURATION
;
UPDATE: TST  GOSIG          ; SCANNING?
        BEQ  UPEX1         ; NO SO DUN
        CMP  #2,GOSIG      ; C/N SCANNING?
        BEQ  CNOWN         ; YES SO UPDATE PPGSUM
        CMP  #7,GOSIG      ; ESA SCAN NEW POSN.?
        BEQ  NEWPOS        ; YES SO UPDATE HV.
        CMP  #5,GOSIG      ; ESA SCAN ON?
        BNE  CNDUN         ; NO SO CHK MORE
        JSR  PC,MOTO       ; YES SO MOTOR TO 0
        MOV  VSCSET,R4     ; GET SET CHNL #
        ASL  R4            ; CNVRT TO BYTE ADDR.
        ADD  ESASA,R4      ; ADD TO GRP ADDR.
        ADD  @VSCCLR,(R4)  ; UPDATE THIS CKNL
        BIS  #2,@MRCR     ; CLR THE SCALER
        BR  UPEX2         ; OUTPUT THE RESULTS
NEWPOS: MOV  #1,GOSIG      ; RESIGNAL ESA SCAN OK
        JSR  PC,ESASWP     ; UPDATE HV POSN.
        BIS  #40004,@MRCR ; INTEG&SCLR INTR ENABLE
        TST  ESAERR        ; ALL OK?
        BEQ  UPEX1         ; YES SO CONTU
        JMP  TSTESA        ; NO SO CHECK ERR TYPE
CNOWN:  MOV  CNSA,R1       ; PIK UP S.A. 4 PPG WNDW
        MOV  CNEA,R4      ; GET E.A. FOR CURRENT GRP
        CLR  R5           ; DO SUM IN R5
10$:    ADD  (R1)+,R5      ; SUM FOR PPGSUM
        CMP  R1,R4        ; DUN?
        BMT  10$          ; NO SO MORE
        MOV  R5,PPGSUM    ; YES SO STORTE IT
        BR  UPEX1         ; RETURN EXIT
CNDUN:  CMP  #6,GOSIG      ; CN MODE DUN?
        BNE  UPEX1         ; NO SO IGNOR
        CLR  @MTRREG      ; YES SO HV OFF
        MOV  #100,R1      ; GET CLK VCTR ADDR.
        MOV  MONCLK,(R1)+ ; RESTOR MONITR CLK ADDR
        MOV  MONPRI,(R1)  ; AND THE PRIORITY
        BIC  #200,@CLKS   ; CLR CLK INTRRPT
        BIS  #100,@CLKS   ; ENABLE THE CLOCK
        MOV  #INTEG,M4    ; NORMAL INTRGTR SRV RTNE
UPEX2:  CLR  GOSIG        ; FLAG DONE ALL
        .PRINT MSG27      ; PNT:ACC DOSE=
        MOV  INTLO,R4     ; OUTPUT ACC DOSE
        MOV  INTHI,R5
        JSR  PC,PRNTDP
        CLR  INTLO        ; 0 INTEGR RUNNG SUM
        CLR  INTHI
        .PRINT MSG32      ; PNT:DUN,CR/LF
        MOV  #12,R1       ; RING BELL 10X
        MOV  #7,R0        ; GET TTY BELL CMND
20$:    .TTYOUT R0        ; RING ITS CHIMES
        DEC  R1           ; DUN?
        BNE  20$          ; NO SO MORE(TEE,HEE)
UPEX1:  RTS  PC          ; NORMAL RETURN
;
; WILL CONTINUE FOR CHAR STRING INP TILL CR
;
BKGD1:  .TTINR
        MOV  R0,R1        ; MOVE CHAR TO R1
        BCC  OUTEXG       ; RETURN IF CR
        JSR  PC,DSPLY     ; DISPLAY ROUTINE
        BR  BKGD1        ; AND CHECK FOR CR
OUTEXG: RTS  PC          ; RETURN
;
;
```

```

: SUBROUTINE TO OUTPUT A CHAR DURING BKGD PGM
: # IN R1 AND USES R0
:
BKGD0: TST WRFLG ; IS IN WR MODE?
      BNE PRNT1 ; NO SO PRINT
      MOVB R1, @IOTMP ; PUT CHAR IN WR BUF
      INC IOTMP ; UPDAT PTR
      CMP IOTMP, #IOEND ; BUFFER FULL?
      BNE DOWN1 ; NO SO GET NOTHER
      .WRITW #AREA, #0, #IOBUF, #400, BLOCK ; WR BLK DATA ON DSK
      BCS WTERR ; BR IF WRITE ERROR OCCURED
      INC BLOCK ; INC BLK CTR
      MOV #IOBUF, IOTMP ; RESTOR BUF PTR
      MOV #IOBUF, R1 ; SET UP TO CLR BUFFER
CLRLP: CLR (R1)+ ; CLR BUFFER
      CMP R1, #IOEND ; DONE?
      BMI CLRLP ; NO SO CLR
      BR DOWN1 ; AND EXIT
PRNT1: MOV R1, R0 ; PRINT CHAR ROUTINE
      .TTOUTR
      BCC DOWN1 ; BUFF READY FOR CHAR?
      JSR PC, DSPLY ; NO SO DISPLAY
      BR PRNT1 ; AND RECHECK BUFF

DOWN1: RTS PC

SMCTR: .WORD 0 ; MOTR STEP CTR

: WRITE ERROR ROUTINE
WTERR: .PRINT #MSG7 ; PRINT ERROR MESSAGE
      JMP REDD ; GO TO BACKGROUND

:
: SUBROUTINE TO SAVE REGS R1 TO R5
RSAVE: MOV #STPTR, R0 ; R0 HAS STACK POINTER
      MOV R1, (R0)+
      MOV R2, (R0)+
      MOV R3, (R0)+
      MOV R4, (R0)+
      MOV R5, (R0)+
      RTS PC

:
: SUBROUTINE TO RESTORE CONTENTS OF REGS
RESTOR: MOV #STPTR, R0
      MOV (R0)+, R1
      MOV (R0)+, R2
      MOV (R0)+, R3
      MOV (R0)+, R4
      MOV (R0)+, R5
      RTS PC

STPTR: .WORD 0,0,0,0,0

:
: SUBR TO DISPLAY FROM DSPLSA FOR A LENGTH
: OF DSPLN IN DATA BUFFER (ADDR UNITS)
: AND DOUBLE DISPLAY OF ALL SET WINDOWS
DISP: MOV XSTART, @XREG ; SET XREG TO START
      MOV XEND, R2 ; SET X REG END #
      MOV DSPLSA, R3 ; R3 HAS DAT BUF S.A.
LOOP7: MOV (R3)+, @YREG ; LOAD YREG WITH DATA
      MOV #1, @DSPER ; INTENSITY LO DATA
      ADD @XREG, @XREG ; NEXT CHANNEL
      CMP @XREG, R2 ; LAST PT?
      ENI LOOP7 ; NO SO RECYCLE
      TST R0ET ; YES SO ANY KNDWS SET?
      BEQ DUN7 ; NO SO IGNOR
      MOV @XKXBUF, R3 ; YES SO DSP KNDWS
      MOV #11, KCTR ; SET UP KNDW CTR

```

```

LOOP77: DEC WCTR           ; DUN ALL WNDWS?
        BEQ DUN7         ; YFS SO DUN
        MOV (R3)+,R1     ; GET WNDW SA & EA.
        MOV (R3)+,ECTR   ; 0? YES SO IGNOR
        BEQ LOOP77      ; NO SO DSPLY
        MOV R1,R2       ; R1 HAS ADDR
        ADD DSPLSA,R2    ; GET CHNL CNTNTS
        MOV (R2)+,@#YREG ; TO DSPLY
        ASR R1          ; GET CHNL # IN R1
        MOV R1,@#XREG   ; DSPLY IT
        ASL R1         ; R1 HAS BYTE #
        MOV #1,@#DSPSR  ;
LOOP07: ADD CHINX,@#XREG ; NXT CHNL
        MOV (R2)+,@#YREG ; ; AND THE CONTENTS
        MOV #1,@#DSPSR  ; DSPLY IT
        ADD #2,R1       ; UPDATE CRRNT ADDR.
        CMP ECTR,R1     ; CRNT ADDR=E.A.?
        BMI LOOP77     ; YES SO DUN THIS SET
        BR LOOP07      ; NO SO DSP MOR
DUN7:   MOV @#MREG,R1   ; NEXT DSP MRKRS
        BIC #K4,R1     ; CLR BITS OF VOID ADDR
        BEQ NODOT      ; NO DISPLAY IF 0
        DEC R1         ; CHANNEL NUMBER
        MOV R1,@#XREG  ; LOAD XREG WITH CHAN#
        ASL R1         ; EVEN ADDR ONLY
        ADD DSPLSA,R1  ; CALC DATA ADDR
        MOV (R1),@#YREG ; LOAD Y REG
        MOV #3,@#DSPSR ; INTENSITY HI ON MRKRS
NODOT:  CMP #1,GOSIG   ; IF ESA ON
        BNE 52$       ; DISPLAY STATUS
        MOV VSCMIN,R1 ; DSPLYNLO SCAN LIMIT
        JSR PC,DSPHI
        MOV VSCMAX,R1 ; DSPLY HI SCAN LIMIT
        JSR PC,DSPHI
        MOV VSCSET,R1 ;DSPLY CRRNT H.V. POSN
        JSR PC,DSPHI
        MOV #3,@#XREG ; BCI DSPLY @ CHNL3
        MOV BCISSET,@#YREG ; GET PRESET DOSE
        MOV #3,@#DSPSR ; DSPLY IT
        MOV BCIACT,@#YREG ; GET CRNT DOSE
        MOV #3,@#DSPSR ; AND DSPLY IT
52$:   CMP #2,GOSIG   ; C/N SCANNING?
        BNE 55$       ; NO SO IGNORE
        MOV VSCMIN,R1 ; YES SO DISPLAY THE
        JSR PC,DSPHI ; PPG SET REGION
        MOV VSCMAX,R1 ; BOTH HI & LD LIMITS
        JSR PC,DSPHI ; AS INTEN POINTS
55$:   RTS PC        ; NORMAL EXIT

```

```

SUBROUTINE TO DISPLAY CHANNEL NUMBER IN R1
AT HI INTENSITY (USES R1 ONLY)

```

```

DSPHI: BIC #K4,R1     ; CLR UPPER BYTE
        MOV R1,@#XREG ; LOAD XREG
        ASL R1        ; GET BYTE #
        ADD DSPLSA,R1 ; GET ADDR
        MOV (R1),@#YREG ; CHNL CNTNTS TO YREG
        MOV #3,@#DSPSR ; INTENSIFY HI
        RTS PC       ; NORMAL RETURN

```

```

SUBROUTINE TO POLL THE DEVICES

```

```

POLL:  CMP #1,DSPFLO ; IN EXPAND DISP MODE?
        BEQ NOSA     ; YES SO S.A.'S ALREADY INIT
        MOV #3,DSPLSA ; INIT DISP S.A.
        CLR XSTART   ; READY X-CHANNEL START

```

```

MOV GPWIDTH,XEND ; INIT DISP END ADDR.
BIT #10000,@XREG ; IN MOTION MODE?
BEQ PLLSET ; NO SO CONTINUE
CMP #2,DSPFLG ; PREVIOUSLY IN M MODE?
BEQ DOSA ; YES SO SET UP S.A.'S
MOV #2,DSPFLG ; NO SO SET M MODE ON
MOV GPWIDTH,R1 ; GET GRP WIDTH
ASR R1 ; GET MID PT
MOV R1,MIDPT ; STOR THE VALUE
MOV #BUFSA,DSPTMP ; INIT TEMP DSPLY S.A.
POLEX2: MOV DSPTMP,DSPLSA ; INIT S.A.'S
JMP POLEX1 ; USE OLD S.A.'S
DOSA: BIT #30000,@XRCR ; P.B.'S ON?
BEQ POLEX2 ; NO SO EXIT
MOV @XREG,R3 ; YES SO GE MRKRS
BIC #10000,R3 ; STRIP OFF MODE BIT
BIT #10000,@XRCR ; P.B.#2 ON?
BEQ PB01 ; NO SO PB#1 ON
BIC #10000,@XRCR ; YES SO CLR IT
POLOOP: CMP MIDPT,R3 ; MRKR AT CNTR?
BEQ PBEXP ; YES SO EXP DSPLY
BMI INCADD ; MRKR TO RT OF CNTR
DEC MIDPT ; MRKR TO LEFT OF CENTER
SUB #2,DSPTMP ; UPDATE MID PNT
MOV DSPTMP,ADSET ; GET MID PNT S.A.
MOV #1,CHINK ; RESET CHNL INC=1
BR POLOOP ; LOOP TILL CENTERED
INCADD: INC MIDPT ; MOV SPECTRUM LEFT
ADD #2,DSPTMP ; UPDATE MID PNT
MOV DSPTMP,ADSET ; STOR MID PNT ADDR
MOV #1,CHINK ; RESET CHNL INC TO 1
BR POLOOP ; LOOP TILL CENTERED
PBEXP: JSR PC,ADSET ; CHECK FOR MAX EXP
CMP #20,R3 ; MAX? (16CHNLS)
BNE 3$ ; YES SO IGNOR P.B.'S
JMP POLEX1
3$: INC CHINK ; INC CHNL INCREMENT
JSR PC,ADSET ; UPDATE OFFSET ADDR
BR POLEX2 ; EXIT
PB01: BIC #20000,@XRCR ; CLR P.B.#1
CMP #1,CHINK ; CONTRCT TILL INC=1
BEQ POLEX1 ; INC=1 SO DUN
DEC CHINK ; UPDATE CHNL INC
JSR PC,ADSET ; UPDATE ADDR OFFSET
MOV #1,CHINK ; INIT CHANL INCREMNT
BR POLEX2 ; EXIT
NOSA: MOV DSPTMP,DSPLSA ; SET DISP S.A. FOR EXP MODE
MOV LTRKX,XSTART ; SET X START CHANNEL
MOV RTRKX,XEND ; SET X END CHANNEL
INC XEND ;
PLLSET: BIT #200,@DSPSR ; DIPLAY MODE ON?
BEQ PLOUT ; NO SO EXIT
MOV LTRKX,@XREG ; SET XREG TO LEFT MRK POS
CLR R5 ; CLR SWEEP CTR
SWP1: MOV #40,R1 ; READY DOT POS
MOV #3,R3 ; AND DOT INC
MOV #13,R4 ; AND DOT CTR
SWEEP: MOV R1,@YREG ; MOVE DOT POS TO YREG
MOV #3,@DSPSR ; AND INTENSITY HI
ASL R1 ; DOUBLE DOT POS
SUB R3,R1 ; AND SUB DOT INC
ADD #3,R3 ; INC DOT INC
DEC R4 ; FINISHED SWEEP?
BNE SWEEP ; NO SO CONT SWEEP
TST R5 ; LEFT AND RIGHT SWEEP DONE
BNE POLEX ; YES SO EXIT FROM SWEEP
INC R5 ; INC SWEEP CTR
MOV RTRKX,@XREG ; MOVE RIGHT MRK POS TO XREG

```

```

BR SWP1          ; AND SWEEP AGAIN
POLEX: DEC MRKCTR      ; UPDATE? (ONLY EVERY 10 SWEEPS)
      BNE POLEX1      ; NO SO EXIT
      CMP #1,DSPFLG   ; IN EXPAND MODE?
      BEQ DSPEXP      ; YES SO BRANCH
      JSR PC,MRKPOS   ; NO SO UPDATE MARKER POS.
      MOV #12,MRKCTR  ; RESET SWEEP CTR
      BR POLEX1      ; AND EXIT
DSPEXP: JSR PC,EXPAND  ; EXPAND DISPLAY
      MOV #12,MRKCTR  ; RESET SWEEP CTR
      BR POLEX1
PI OUT: CLR DSPFLG    ; NOT IN DISP MODE SO CLR FLG
      MOV #1,CHINK    ; RESET CHNL INC TO 1
      MOV @#KREG,R4   ; GET DOT
      BEQ POLEX1      ; 0? YES SO EXIT
      BIC #K4,R4      ; STRIP OFF HI BITS
      BIT #10000,@#MRCSR ; P.B.#1 SET?
      BEQ PB02        ; NO SO CHECK MORE
      .PRINT #MSG46   ; YES SO PNT DOT POSN
      JSR PC,PRNTDC   ; OUTPUT IT
PB02:  BIC #10000,@#MRCSR ; CLEAR PB#1
      BIT #20000,@#MRCSR ; PB2 SET?
      BEQ POLEX1      ; NO SO EXIT
      .PRINT #MSG45   ; YES SO PRINT DOT #
      DEC R4          ; CHNL#-1=ADDR
      ASL R4          ; GET EVEN ADDR
      ADD DSPLSA,R4   ; CASLC. DATA ADDR
      MOV GRPNUM,R5   ; GET MAX # GRPS
      ASR R5          ; MAX/2 FOR EACH PASS
      MOV @#SWR,R3    ; GET TOGGLE CONFIG
1$:    ROR R3          ; BIT SET?
      BCS 2$         ; YES SO HAVE ADDR
      ADD DSPLN,R4    ; NO SO NXT GRP
      DEC R5          ; DUN ALL TOGGLES?
      BMI POLEX1      ; YES SO EXIT
      BNE 1$         ; NO SO DO ANOTHER
2$:    MOV (R4),R4    ; GET CONTENTS OF ADDR
      JSR PC,PRNTDC   ; OUTPUT IT
      BIC #20000,@#MRCSR ; CLR PB#2
POLEX1: RTS PC        ; RETURN
;
LTRK:  .WORD 0        ; LEFT MARKER POSITION
RTRK:  .WORD 0        ; RIGHT MARKER POSITION
DSPFLG: .WORD 0      ; DISPLAY MODE FLAG
MRKCTR: .WORD 12     ; SWEEP CTR
CHINK:  .WORD 1      ; CHANNEL NUMBER DISPLAY INCREMENT
MIDPT:  .WORD 0      ; CHANNEL NUMBER AS SET BY MARKER
;
SUBR TO UPDATE MARKER POSITIONS
MRKPOS: BIT #40,@#DSPSR ; LEFT MOTION?
      BEQ TSTRT      ; NO SO TST FOR RIGHT MOTION
      BIT #100,@#DSPSR ; LT MOT-WHICH MARKER?
      BEQ LTMLT      ; LEFT
      DEC RTRK       ; RIGHT SO MOVE 1 LEFT
      CMP LTRK,RTRK  ; MARKER OVERLAP?
      BNE TSTRT      ; NO SO OK
      INC RTRK       ; YES SO RESTORE
      BR TSTRT
LTMLT:  TST LTRK      ; LEFT MRK AT ZERO?
      BEQ TSTRT      ; YES SO DON'T MOVE
      DEC LTRK       ; NO SO MOVE 1 LEFT
TSTRT:  BIT #10,@#DSPSR ; RIGHT MOTION?
      BEQ NOTOT      ; NO SO EXIT
      BIT #100,@#DSPSR ; YES SO WHICH MARKER
      BEQ LTRK       ; LEFT
      INC RTRK       ; RIGHT SO MOVE 1 RIGHT
      CMP @PWIDTH,RTRK ; BEYOND BUFFER?

```

```

        BNE NOXOT          ; NO SO OK
        DEC RTMRK         ; YES SO RESTORE
        BR NOXOT
LTMRT:  INC LTKRK         ; MOVE LEFT MKR 1 RIGHT
        CMP LTKRK,RTMRK  ; MARKER OVERLAP?
        BNE NOXOT        ; NO SO OK
        DEC LTKRK        ; YES SO RESTORE
NOXOT:  RTS PC           ; RETURN
:
:
ROUTINE TO DISPLAY ONLY BETWEEN MARKERS
EXPAND: BIT #10,#DPSR    ; MOVE DISPLAY LEFT?
        BEQ TSTRT1       ; NO SO TST RIGHT
        CMP DSPTMP,#BUFSA ; YES SO AT START OF BUFFER
        BEQ TSTRT1       ; YES SO DO NOTHING
        DEC DSPTMP       ; NO SO DEC S.A. BY 1
        DEC DSPTMP
TSTRT1: BIT #40,#DPSR    ; MOVE DISPLAY RIGHT?
        BEQ EXEND        ; NO SO EXIT
        MOV DSPTMP,R1     ; POINT TO DISP S.A.
        SUB #BUFSA,R1    ; SUBR BUF S.A.
        ASR R1           ; PUT IN #WRDS
        ADD RTMRK,R1     ; PNT TO END OF DISP
        SUB LTKRK,R1     ; R1 IS PTR
        INC R1
        CMP R1,GPWIDTH  ; BEYOND BUFFER?
        BEQ EXEND        ; YES SO EXIT
        INC DSPTMP       ; NO SO MOVE S.A. 1 WORD
        INC DSPTMP
EXEND:  RTS PC
:
:
SUBR TO INPUT GP WIDTH
INPT1:  JSR PC,KBIN      ; INPUT THE CHAR STRING
        MOV #TTBUF,TEMP1 ; TEMP1 HAS BUFF S.A.
        JSR PC,INBIN    ; CONV TO #
        CMP #0,ERFLG    ; LEGAL #
        BEQ CONT1       ; YES SO CNTUE
RSTRT1: .PRINT #MSGG    ; NO SO "?"
        BR INPT1        ; RESTART
CONT1:  CLR R1           ; IS # MULTPL OF 2
        MOV SISTN,R2    ; R2 HAS 16 BITS
        MOV BINY3,R4    ; R4 HAS #
        MOV R4,R3       ; SO DOES R3
RSTRT2: ASL R3           ; LEFT SFT #
        BCC HERE        ; CARRY?
        INC R1           ; YES SO CNT IT
HERE:   DEC R2           ; INC CTR & DONE?
        BNE RSTRT2      ; NO SO CHECK NOTHR
        CMP R1,#1       ; PWR OF 2?
        BNE RSTRT1      ; NO SO REINPT#
        MOV R4,R3       ; YES SO R3=#CHANLS
        ASL R4           ; R4 = # BYTES
        CMP #BUFLEN,R4  ; BEYOND BUFR
        BMI RSTRT1      ; YES SO REINPT #
        RTS PC          ; NORMAL RETURN
:
:
CMND STRING INPUT ROUTINE
KBIN:   CLR DCTR        ; CLR DIGIT CTR
        MOV #TTBUF,R1   ; SET PTR TO BUFFER
LOOP1:  .TTYIN (R1)+    ; INPT CHAR
        INC DCTR        ; BUMP CTR
        CMP3 #12,R0     ; LAST CHAR?
        BNE LOOP1      ; NO SO GET ANOTHER
        SUB #2,DCTR     ; SUB CR/LF #
        RTS PC         ; RETURN NORMALLY

```

```

SUBR TO CNVRT ASCII CHARS TO BIN NUMBER

INBIN:  MOV DCTR,R2          ; R2 = # DIGITS
        CLR ERFLG          ; RESET ERR FLAG
        CMP #5,R2          ; TOO BIG?
        BMI ERR1           ; YES SO "?"
        BR ENTR            ; JMP OVER DP E P
INBIN2: MOV DCTR,R2          ; GET # DIGITS
        CLR ERFLG          ; RESET ERR FLAG
        CMP #10,R2         ; 100 MIL-1 MAX
        BMI ERR1           ; MOR SO ERROR
ENTR:   MOV #BUFPTR,LOPTR   ; SET UP TN PWR PTR
        MOV #TNPLO,HIPTTR  ; HI & LO WORDS
        CMP #0,R2          ; TOO SMALL?
        BEQ ERR1           ; YES SO "?"
        MOV TEMP1,R1        ; R1 PTS TO BUFFR
        CLR R5              ; CLR HIGH BITS
LOOP2:  CLR R4
        MOVB (R1),R4        ; GET #
        SUB #60,R4          ; # FROM ASCII
        BMI ERR1
        CMP #11,R4
        BMI ERR1           ; VALID #? NO SO ERROR
        MOVB R4,(R1)+       ; RSTRE ASCII AS #
        SUB #2,LOPTR        ; DEC TN PWR PTR
        SUB #2,HIPTTR       ; 2X FOR ADDR
        DEC R2              ; FINI?
        BNE LOOP2          ; NO SO GET MORE
        CLR BINMB           ; PREP # LOC
        CLR BINHI          ; HI & LO ORDER WORDS
        MOV TEMP1,R1        ; YES SO CONVERT
LOOP5:  CLR R3
        MOVB (R1)+,R3       ; GET DIGIT
        INC R2              ; BUMP CTR
        CLR R4              ; READY COEFF CTR
        CLR R5              ; HI & LO WORDS
LOOP4:  DEC R3              ; DEC PWR CTR
        BMI LOOP6          ; FINI?
        ADD ELOPTR,R4       ; NO,ADD NTHR 10PWR
        ADC R5              ; IN D.P.
        ADD CHIPTR,R5
        BR LOOP4           ; AND GO AGAIN
LOOP6:  ADD #2,LOPTR        ; YES SO SCALE 10 PTR
        ADD #2,HIPTTR       ; 2X FOR ADDR
        ADD R4,BINMB        ; ADD TO PREV #
        ADC BINHI          ; IN D.P.
        ADD R5,BINHI
        CMP R2,DCTR         ; GOT ALL DIGITS?
        BEQ GUIT           ; YES SO EXIT
        BR LOOP5          ; CNVRT NEXT DIGIT
ERR1:   INC ERFLG          ; ERROR SO NOTE IT
GUIT:   RTS PC             ; EXIT

TEMP1:  .WORD 0             ; TEMP STOR
TEMP2:  .WORD 0             ; TEMP STOR TOO
TEMP3:  .WORD 0
LOPTR:  .WORD 0             ; PTR TO LO ORDER TN PWR'S
HIPTTR: .WORD 0             ; PTR TO HI ORDER TN PWR'S
TNPLO:  .WORD 230,17,1,0,0,0,0,0 ; HI ORDER 10 PWR'S
        .WORD 113200,41100,103240,23420,1750,144,12,1 ; SCALE FCTRS
BUFPTR: .WORD 0,0          ; BUFF PTR
TBUF:   .BLKW 50           ; TTY INPUT BUFFER
BINMB:  .WORD 0             ; CONVERTED HI ORDER #
BINMB:  .WORD 0             ; CONVERTED BIN NUMB
ADCSA:  .WORD 0             ; ADC S.A.
TNPTR:  .WORD 0             ; PTR TO TN PTR
DCTR:   .WORD 0             ; DIGIT CTR

```

```
ERFLG: .WORD 0 ; ERROR FLAG ON INPUT
:
: SUBROUTINE TO INPUT AN ASCII STRING
: AND CONVERT IT TO A BINARY NUMBER
: IN LOCATION BINX3
: S.P. ENTRY EXUMIN1, D.P. ENTRY EXUMIN2
:
NUMIN2: MOV #2,TEMP3 ; TAG ENTRY PT
BR NUMIN ; USUAL CONVERSION
NUMIN1: CLR TEMP3 ; TAG ENTRY PT
NUMIN: JSR PC,KBIN ; INPUT THE CHAR STRING
MOV #TTBUF,TEMP1 ; HAS CHAR BUF SA.
TST TEMP3 ; S.P. OR D.P.?
BEQ SPCALL ; S.P. SO BRANCH
JSR PC,INBIN2 ; D.P. SO GET #
BR CONTIN ; HAS BINARY SO CONT
SPCALL: JSR PC,INBIN ; GET S.P. #
CONTIN: TST ERFLG ; LEGAL #?
BEQ NUMDUN ; YES SO EXIT
.TTYOUT #'? ; NO SO PNT ?
CLR ERFLG ; CLR FLG OF ERROR
BR NUMIN ; RETRY #
NUMDUN: RTS PC ; NORMAL EXIT
:
: THIS IS THE END OF ASCII PAGE 2: MES11.MAC
:
: SUBR TO OUTPUT DOUBLE PREC. OR SINGLE PREC. # IN ASCII DEC.
: # TO BE OUTPUT IS IN R4-LO&R5-HI IF D.P.,OR IN R4 IF S.P.
:
:DOUBLE PREC. ENTRY-8 DIGIT OUTPUT
PRNTDP: MOV #10,DCTR ; SET DIGIT CTR TO 7
MOV #TNPL0,LOPTR ; PNT TO LO 10 PWR'S
MOV #TNPHI,HIPTR ; AND HI 10 PWR'S
BR DPENT ; AND BRANCH
: SINGLE PREC. ENTRY-5 DIGITS
PRNTDC: MOV #5,DCTR ; SET DIGIT CTR TO 5
MOV #TNPL0+S,LOPTR ; PNT TO SINGLE PREC. LO 10 PWR'S
MOV #TNPHI+S,HIPTR ; AND HI 10 PWR'S
CLR R5 ; CLEAR HI ORDER WORD
DPENT: CLR R1 ; READY UNIT CTR
LOOP3: SUB GLOPTR,R4 ; SUB LO ORDER
SBC R5 ; WATCH CARRY
SUB CHIPTR,R5 ; SUB HI ORDER
BNI FOUND ; BRANCH IF MINUS
INC R1 ; INC UNIT CTR
BR LOOP3 ; AND LOOP
FOUND: ADD #60,R1 ; CVT TO ASCII
JSR PC,BKGDD ; AND OUTPUT
ADD GLOPTR,R4 ; RESTORE LO ORDER
ADC R5 ; WATCH CARRY
ADD CHIPTR,R5 ; RESTORE HI ORDER
ADD #2,LOPTR ; PNT TO NEXT LO ORDER 10 PWR
ADD #2,HIPTR ; AND HI ORDER 10 PWR
DEC DCTR ; FINISHED?
BNE DPENT ; NO SO DO ANOTHER DIGIT
MOV #' ,R1 ; YES SO PRINT SPACE
JSR PC,BKGDD ; NOW
RTS PC ; YES SO EXIT
:
: SUBROUTINE TO OUTPUT A LINE OF SPECTRUM PRINT OUT
: ADDRESS IN R2,CHAN# IN INDEX, END ADDR IN STADDR
:
PRNTLN: TST KRFLG ; WRIT ON DSK?
BEQ OVER1 ; YES SO IGNOR KYBD
.TTIR ; CHAR ON KYBD?
ECC FINIS ; YES SO ABORT
OVER1: MOV INDEX,R4 ; R4 HAS CHAN #
JSR PC,PRNTDC ; PRNT IT OUT
```



```

MOV# #',R1          ; PRNT OUT SPACE
JSR PC,BKGDD        ; DO IT
MOV #12,CHKCNT      ; SET UP CTR(10CHAN/LN)
LOOP20: MOV (R2)+,R4 ; PICK CHANN CONTNTS
JSR PC,PRNTDC       ; PNT IT OUT
CMP R2,STADDR       ; FINISHED SPECTRUM?
BNE LOOP50          ; NO SO CONTINUE
FINIS: CLR STADDR   ; YES SO CLR FINISH FLAG
BR LOOP60           ; AND OUTPUT CR/LF AND EXIT
LOOP50: DEC CHCNT   ; FINISHED LINE?
BNE LOOP20          ; NO SO DO MOR
LOOP60: MOV# #15,R1 ; YES SO CR/LF
JSR PC,BKGDD
MOV# #12,R1
JSR PC,BKGDD
RTS PC              ; FLG FINISH
CHKCNT: .WORD 0

```

SUBROUTINE TO PRINT OUT R3 FRAMES OF PAP TAP.

```

LDR:  MOV #0,R1      ; PUT IN ASCII NULL
LOP15: JSR PC,BKGDD  ; PRINT IT
DEC R3                ; DONE?
BNE LOP15             ; NO SO MORE
RTS PC                ; YES SO EXIT

```

```

INDEX: .WORD 0      ; CHAN # FOR PNT CMND
STADDR: .WORD 0     ; END ADDR FOR PNT CMND

```

COMMAND SERVICE ROUTINES

SECTION TO MANUALLY SET ESA STEPPING MOTOR TO ZERO ONLY REQUIRED AFTER PREVIOUS MES11 ABORT

```

ZFRO:  CMP #0,GRCOM  ; CHK GRP CMND
BMI ERR3 ; NOT -1 SO ERROR
.PRINT #MSG39        ; PNT: INSTRUCTIONS
CLR R0                ; CLR TTY BFR RCVR
ZLOOP: BIT #1000,@MRCR ; EXT.SFT.SWCH.#1 ON?
BEQ ZMOR              ; NO SO CHK MOR
BIT #400,@MRCR        ; YES SO FWD STEP
BNE #-6               ; WHEN READY
ZMOR:  BIT #4000,@MRCR ; EXT.SFT.#2 ON?
BEQ ZCHK              ; NO SO CHK MOR
BIT #1,@MRCR          ; CHK IF MTR READY
BNE #-6               ; NO SO WAIT
ZCHK:  BIS #1,@MRCR   ; GO REV 1 STEP
.TTIN?                ; GET TTY KYBD INPUT
MOV R0,R1              ; STORE IN R1
BCS ZLOOP              ; HAV NO INPUT SO LOOP
CMP# R1,#15            ; HAVE LF?
BNE ZLOOP              ; NO SO MORE
CLR SNCTR              ; 0 STEP MTR COUNTER
JMP FINI              ; DUN SO EXIT

```

ADC1 START ROUTINE

```

ADCST: CMP GRCOM,#0  ; CHK GRP CMND
BMI ERR3 ; ERROR SO BRANCH
BIT #4,@ADCSR        ; ADC1 ON?
BNE ERR3             ; YES SO ERROR
CMP #2,GOSIG         ; CANNOT BE SCANNING OR
BEQ ERR3             ; HAVE ERROR
JSR PC,FETCH         ; GET ADCS.A.
MOV R4,ADCSA         ; AND STOR IT

```

```

      BIS #104,@#ADCSR      ; ADC #1 ON
      JMP FINI              ; END OF COMND
:
SECTION TO TURN OF THE ADC1 IF ON ONLY
STOP:  CMP #0,GRCOM        ; CHK GRP COMND
      BMI ERR3            ; NOT -1 SO EROR
      CMP #2,GOSIG        ; SCANNING C/N?
      BEQ ERR3            ; YES SO EROR
      BIT #104,@#ADCSR    ; ADC1 ON?
      BEQ ERR3            ; NO SO EROR
      BIC #104,@#ADCSR    ; YES SO TURN OFF
      JMP FINI            ; NORMAL E.O.C.
:
GRP ERASE ROUTINE
WILL ERASE CORRESPONDING TITLE BUFFER AS WELL
ERASE:  CMP  GRCOM,#0      ; PICK UP GP #
      BMI  ERR3           ; IS -1 SO EROR
      JSR  PC,FETCH       ; GET ERASE GROUP S.A
      MOV  DSPLN,R2       ; GET DSP LENGHT
      ADD  R4,R2          ; R2 HAS END ADDR
LOOP15: CLR  (R4)+         ; CLEAR CHANNEL
      CMP  R4,R2          ; DONE?
      BNE  LOOP15        ; NO SO LOOP
      JSR  PC,TITPTR      ; R2 HAS TITLE BUFF S.A.
      MOV  #100,R3        ; HAS 100 BYTES
      ADD  R2,R3          ; R3 PTS TO TITLE BUFF END
TITL0P: CLR  (R2)+         ; CLR BUFFER
      CMP  R3,R2          ; END OF BUFF?
      BNE  TITL0P        ; NO SO CONT CLR
      JMP  FINI           ; FINISHED SO
ERR3:   JMP  RSTR4        ; ADDR LINKS
:
PLOTTER CONTROL ROUTINE
PLOT:   CMP  #0,GRCOM     ; CHK GRP COMND
      BMI  ERR3           ; NOT -1 SO EROR
      .PRINT #MSG42      ; PNT:SET PLOT THEN <CR>
      CLR  @#XREG         ; 0 X&Y PLOT REGS
      CLR  @#YREG
      MOV  #1,@#DSPSR    ; SET DACS TO 0
TTCHK1: .TTYIN RO        ; GET CHAR FROM TTY
      CMPB #15,RO        ; HAVE LF?
      BNE  TTCHK1        ; NO SO WAIT
      MOV  #1,PLTFLG     ; YES SO SET PLT FLG
      JSR  PC,DSPLY      ; PLOT SPECTRUM
      .PRINT #MSG43      ; PNT:PLOT OFF THEN <CR>
      CLR  PLTFLG        ; RESET DUN FLAG
TTCHK2: .TTYIN RO        ; GET KYBD CHAR
      CMPB #15,RO        ; HAVE LF?
      BNE  TTCHK2        ; NO SO WAIT FOR IT
      JMP  FINI           ; YES SO DUN
:
GRP PRINT OR WRITE ON FLOPPY ROUTINE
WRFLG=0 IF WRITE ON FLOPPY
WRFLG=1 IF PRINT ENTIRE SPECTRUM
WRFLG=2 IF PRINT BETWEEN MARKERS
WRITE:  CMP  GRCOM,#0    ; LEGAL COMXAND?
      BMI  ERR3          ; NO SO EROR
      CLR  WRFLG
      CLR  BLOCK         ; CLR BLOCK CTR
      MOV  #IOBUF,IOTMP  ; SET BUFR PTR
      .PRINT #MSG3       ; PRINT FILENAM?
      JSR  PC,BXGDI      ; GET CHAR STRING
      MOV  @#B3+4,R2     ; INSERT IN CSIGEN CALL
      MOV  #7,R3         ; USE R3 AS CHAR CNT

```

```

BR GETC1
GETCHR: .TTYIN R1 ; CHAR PUT 1 IN R1
GETC1:  CMPB #15,R1 ; HAVE LF?
      BEQ CSI ; YES SO HAVE FILENAM
      DEC R3 ; NO SO GET NOTHR
      BNE GETC11 ; DONE?
      JMP ERR? ; NO SO ERROR
GETC11: MOV8 R1,(R2)+ ; STORE CHAR
      RR GETCHR ; AND GET ANOTHER
CSI:    MOV8 #'',(R2)+
      CLRB (R2)
      .CSIGEN #DEVSPC,#DEFEXT,#MSGS ; CREATE FILE
      BCC NO ; MOV OVER PNT FLG IF NO ERROR
      JMP CSIERR ; CSI ERROR SO BRANCH
PRNT:  MOV #1,WRFLG ; SET UP WRFLG FOR PNT
      BIT #200,@#DSPSR ; IN MARKER MODE?
      BEQ NO ; NO SO WRFLG=1
      MOV #2,WRFLG ; YES SO WRFLG=2
NO:    CMP GRCOM,#0 ; LEGAL GRP #?
      BMI ERR3 ; YES SO ERR EXIT
      .PRINT #ASDAT ; PRINT THE DATE
      JSR PC,TITPTR ; FETCH TITLE BUFF S.A. FOR GRP
      CMP #1,WRFLG ; IS WR CMND?
      BNE OVER ; YES SO NO LDR
      MOV #50,R3 ; DO LEADER
      JSR PC,LDR ; 50 X
OVER:  MOV8 (R2)+,R1 ; PICK UP CHAR IN R1
      JSR PC,BKGD0 ; PRINT OUT CHAR
      CMPB (R2),#0 ; ZERO? (LST CHAR)
      BNE OVER ; NO SO DO MOR
      JSR PC,FETCH ; YES SO TO SPECTRUM
      MOV R4,R2 ; R2 HAS S.A.
      CMP #2,WRFLG ; IN MARKER MODE?
      BEQ PNTEXP ; YES SO BRANCH
      ADD DSPLN,R4 ; SET UP LST PT
      MOV #1,INDEX ; SET UP CHNL CTR
      BR SETAD ; BRANCH
PNTEXP: CMP #1,DSPFLG ; WHICH MARKER MODE?
      BEQ PNTSOM ; EXPAND MODE SO BRANCH
      TST WINDS ; ANY WINDS SORTED?
      BNE PNTWIN ; YES SO PNT WINDS ONLY
      MOV LTKRK,R3 ; NORMAL MARKER MODE
      ASL R3 ; R3 HAS BYTE S.A.OFFSET
      ADD R3,R2 ; ADD TO S.A.
      MOV RTKRK,R3
      INC R3 ; INCL KRKR PT IN DSP
      ASL R3 ; R3 HAS BYTE END ADDR.
      ADD R3,R4 ; ADD TO S.A.
      MOV LTKRK,INDEX ; SET UP CHANNEL PTR
      INC INDEX
      BR SETAD ; DONE
PNTWIN: MOV #WINSUF,TEMP2 ; GET CHNL# IN PRS
      MOV #WINSUF+2,TEMP3 ; S.A. & E.A.
      MOV WINDS,TEMP1 ; USE AS WNDW CNTR
LOOP52: JSR PC,FETCH ; GET CURRENT OFFSET
      MOV @TEMP2,R3 ; GET CHNL #
      MOV R3,INDEX ; SET UP CHNL CNTR
      MOV R4,R2 ; STOR OFFSET
      ASL R3 ; CONV TO ADDR
      ADD R3,R2 ; GET ASS ADDR
      MOV @TEMP3,R3 ; GET E.A.
      INC R3 ; INCLD LAST CHNL
      ASL R3 ; CONV TO BYTE ADDR
      ADD R3,R4 ; GET ASS ADDR
      MOV R4,STADDR ; SET UP E.A.
      INC INDEX ; BUYP CHNL CNTR
LOOP54: JSR PC,PRINTLN ; OUTPUT 10 CHNLS
      CMP #0,STADDR ; DUV?

```

```

SEG THTALL                ;YES SO EXIT
MOV8 R1,BTEMP1
INC TEMP1                ;UPDTE TILE PTR
BR SET1                  ;AND CONT INPUT
THTALL: MOV TEMP1,R4      ;R4 HAS TITLE PTR
MOV8 #15,(R4)+          ;STORE CR
MOV8 #12,(R4)+          ;STORE LF
CLR8 GR4                 ;CLR LAST CHAR
JMP FINI                 ;RETURN
:
:
SECTION TO RESTART THE PROGRAM AND TO
RESET GROUP WIDTH AND STEPPING MOTOR
:
GAIN:  CMP #0,GRCOM       ;CHECK GRP COM
      BMI ERR2            ;NOT -1 SO ERROR
      TST GOSIG          ; NO SO SCANNING?
      BEQ GAIN1          ; NO SO EOK
      .PRINT #MSG38      ; PNT:ARE U SURE?
      CLR R0             ; CLR TTY INPT BFR
      .TTYIN             ; GET RESPONSE
      CMP8 #'Y,R0       ; IS IT YES?
      BNE ERR2          ; NO SO ERROR
GAIN1: BIT #104,@ADCSR   ; ADC1 ON?
      BNE ERR2          ; YES SO ERROR
      JSR PC,MOTO       ; NO SO ZERO MOTR
      JMP RSTRT         ; RESTART
ERR2:  JMP RSTRT4       ; ERROR SO RESTART
:
ROUTINE TO READ FILE FROM DX1 TO DISPLY BUFF
:
READ:  CLR EOFFLG        ; CLR EOF FLAG
      CMP GRCOM,#0      ; LEGAL GP #?
      BMI ERR2          ; YES S ERR
      .PRINT #MSG3      ; PRNT FILE NAM
      JSR PC,BXGDI      ; WAIT IN THE BKGD
      MOV #MSG9+5,R2    ; PT TO WHERE NAM GOS
      MOV #7,R3         ; 6 CHAR CTR
      BR READ2          ; 1ST CHAR THERE
RDCHR: .TTYIN R1        ; GET A CHAR
READ2: CMP8 #15,R1     ; CR?
      BEQ CSIRD         ; YES SO EXIT
      MOV8 R1,(R2)+    ; NO SO STOR CHAR
      DEC R3            ; MOR THAN 6 CAR?
      BNE RDCHR        ; NO SO GET NOTR
      JMP ERR2         ; YES SO ERROE
CSIRD: CLR8 (R2)+      ; CLEAR LAST BYTE OF COXMAND STRING
      .CSIEN #DEVSPC,#DEFEXT,MSG9 ; READY FOR RD
      BCC NRERR        ; BRANCH IF NO CSI ERROR
      JMP CSIERR       ; BRANCH IF ERROR
NRERR: CLR BLOCK       ; CLR BLK CTR
      JSR PC,RDXBLK    ; READ A BLOCK ON CHNL #3
      CLR CTR5         ; CLEAR TITLE CTR
RD10:  MOV #10,R2      ; SET UP MSSGE CTR
      MOV #XSGT,R3     ; PT TO ASCII CHECK
RD11:  INC CTR5        ; INC CHAR CTR
      DEC R2           ; DEC CTR, 0?
      BEQ RD12         ; YES SO BEYOND TITLE .EXIT
      CMP8 (R3)+,(R5)+ ; CHAR=?
      BEQ RD11        ; YES SO CHECK NEXT
      BR RD10         ; NO SO START ABAIN
RD12:  SUB #10,CTR5    ; SUB ERRON CTR
      MOV #IDBUF,R5    ; R5 POINTS TO DATA BUFFER
      JSR PC,TITPTR    ; R2 HAS TITLE BUFFER
RD13:  DEC CTR5        ; TITLE STORED?
      BMI RDOU         ; YES SO EXIT
      MOV8 (R5)+,(R2)+ ; NO SO STORE CHAR
      BR RD13         ; AND GET ANOTKER

```

```

      BEQ OUTS2                ; YES SO EXIT
      ADD #12,INDEX           ; NO SO BUMP CHNL CNTR
      BR LOOP54               ; DO 1 MOR LINE
OUTS2: DEC TEMP1              ; CKX IF DUN
      BEQ OUT1                ; YES SO EXIT
      ADD #4,TEMP2            ; BUMP S.A. PNTR
      ADD #4,TEMP3            ; BUMP E.A. PNTR
      BR LOOP52               ; LOOP AGAIN
PNTSOX: SUB #BUFSA,R2         ; SET UP FOR OFFSET
      ADD DSPTMP,R2           ; R2 HAS EXP MODE S.A.
      MOV RTKRX,R4            ; R4 HAS RT MKR
      SUB LTKRX,R4            ; R4 HAS LT-RT
      INC R4                  ; INCL MKR PT IN DSPLY
      ASL R4                   ; PUT IN BYTES
      ADD R2,R4               ; R4 HAS END ADDR.
      MOV DSPTMP,R1           ; SET UP CHANNEL INDEX
      SUB #BUFSA,R1           ; SUB BUFF S.A.
      ASR R1
      INC R1                   ; INCL MKR IN DSPLY
      MOV R1,INDEX
SETAD: MOV R4,STADDR          ; STORE END ADDR.
LOOP19: JSR PC,PRNTLN         ; PRINT 10 CHANNELS
      CMP #0,STADDR           ; CHECK IF DONE
      BEQ OUT1                ; DONE IF 0
      ADD #12,INDEX           ; INC CHNL INDEX
      BR LOOP19              ; DO MOR
OUT1:  TST WRFLG              ; HAVE WR CKND?
      BNE DONE1              ; YES SO NO LDR
      .WRITE #AREA,#0,#IOBUF,#400,BLOCK ; WRITE LAST BLOCK
      .CLOSE #0               ; CLOSE OUTPUT FILE
      BCS WTERR2             ; BR IF ERROR ON WRITE
      JMP FINI                ; EXIT
DONE1: CMP #1,WRFLG           ; TRAILER IF FULL PRINT MODE
      BEQ TRAIL
      JMP FINI                ; NO TRAILER SO EXIT
TRAIL: MOV #20,R3             ; DO TRAILER
      JSR PC,LDR              ; 20 X
      JMP FINI                ; FINISHED SO <
WTERR2: JMP WTERR

:
: ROUTINE TO SET FLAG IF IN DISP MODE
: WILL CAUSE DISPLAY ONLY BETWEEN MARKERS
:
DSPMKX: CMP #0,GRCON          ; LEGAL COMMAND?
      BNI ERR4                ; NO SO ERROR
      BIT #200,@DSPSR         ; IN DISPLAY MODE?
      BEQ ERR4                ; NO SO ERROR
      MOV #1,DSPFLG           ; YES SO SET DISP FLAG
      MOV #BUFSA,DSPTMP       ; SET DISP S.A.
      MOV LTKRX,R1            ; INDEX BY 2XLEFT MKR POS
      ASL R1
      ADD R1,DSPTMP
      JMP REDO                ; AND GO TO BACKGROUND
ERR4:  JMP RSTRT4             ; ERROR RETURN
DSPTMP: .WORD 0                ; TMP DISP S.A. FOR EXPAND MODE
:
:
: GRP TITLE STORAGE ROUTINE
:
TITLE: CMP GRCON,#0           ; GET GP # , OK?
      BNI ERR4                ; NO SO ERROR
      JSR PC,TITPTR           ; FETCH TITLE BUFF S.A. FOR GRP
      MOV R2,TEMP1            ; STORE TITLE BUFF PTR
      MOV #75,TEMP2           ; SET CHAR CTR
SET1:  JSR PC,EXGDI           ; CONT EXGD TILL CR
      CMP R1,#33              ; EOC?
      BEQ THTALL             ; YES SO EXIT
      DEC TEMP2               ; NO SO TOO MANY CHARS?

```

```

ONQUIT: CLPB (P?)          * CLEAR LAST BYTE
        ISR PC FETCH      * FETCH GRP S.A. IN P4
        MOV R4 TEMP2      * MOV S.A. TO TEMP2
        ADD DSPLN P4      * SET UP PTP TO END OF GRP
        MOV P4 TEMP3      * AND STORE AT TEMP3
        MOV #5 DCTR       * CHAP CTR
        MOV #TMPBLK TEMP1 * TEMP1 PTS TO TMP CHAR STORAGE
        MOV #12 CTR10     * SET UP DECODE CTRS
        MOV #7 CTR9
        MOV #5 CTR5

DECODE: CMP P5 IOTMP      * AT END OF I/O BUFFER
        BNE STOPE        * NO SO DECODE CHAP
        TST EOFFLG      * PAST END OF FILE?
        BNE RDCLSE      * YES SO CLOSE READ CHANNEL
        ISR PC BINBLK   * NO SO READ ANOTHER BLOCK
        DEC CTR9        * LEGAL #?
        BPI EYIT9       * NO SO IGNORE
        MOVB (P5)+ @TEMP1 * YES SO TEMP STORE
        INC TEMP1       * INC TEMP STORE PTP
        DEC CTR5        * END OF #?
        BNE DECOD      * NO SO GET NEXT CHAP
        JMP BINCON

PTN3IN: MOV #5 CTR5      * RESET CTR
        DEC CTR10       * END OF LINE?
        BNE EYIT8       * NO SO IGNORE SPACE
        MOV #12 CTR9    * RESET DECODE CTR
        MOV #12 CTR10   * RESET #/LINE CTR
        BP DECOD        * AND LOOP AGAIN
        EYIT6: MOV #1 CTR9 * SET TO IGNORE SPACE
        BP DECOD

EYIT9:  INC P5          * POINT TO NEXT CHAP
        BP DECOD        * AND LOOP

RDCLSE: .CLOSE #3      * CLOSE INPUT CHANNEL
        JMP RETD        * AND GO TO BKGD

EOFFLG: .WORD 0        * EOF FLAG
TEMP4:  .WORD 0        * TEMP STORAGE
CTR5:   .WORD 0        * DECODE CTR STORAGE
CTR9:   .WORD 0
CTR10:  .WORD 0
TMPBLK: .WORD 0,0,0   * TMP CHAR STRING STORAGE

        LOOP TO CONVERT ASCII STRING AT TMPBLK TO BIN#
        AND STORE IN PROPER GRP LOC

BINCON: MOV #TMPBLK TEMP1 * POINT TEMP1 TO START OF TEMP STORE
        MOV P5 TEMP4      * SAVE P5
        ISR PC IN3IN     * PERFORM CONV
        MOV TEMP4 P5     * RESTORE P5
        TST ERFLG       * HAS ILLEGAL CHAR READ?
        BNE NDR3        * NO SO STORE #
        .PRINT #MSG9    * YES SO PRINT ERROR MESSAGE
        JMP RDCLSE      * AND CLOSE INPUT CHANNEL
        AND STORE IN GRP

NDR3:   MOV BINY3 @TEMP2 * INC GRP PTR
        INC TEMP2
        INC TEMP2
        CMP TEMP3 TEMP2 * END OF GRP?
        BEQ RDCLSE     * YES SO CLOSE READ
        BR PTN3IN      * CONTINUE

ROUTINE TO READ BLOCK ON CHANNEL #3
WILL EXIT IF PREVIOUS READ REACHED EOF

PDR3K:  .READ #AREA #3 #IOBUF #100 BLOCK * DO READ
        BCC NDR3

NDR3:   MOV #1 EOFFLG   * IF READ ERROR SET EOFFLG
        ASL P0          * P0 HAS #BYTES READ
        ADD #IOBUF P0  * PNT TO END OF I/O BUFF
    
```

```

MOV RO,IOTMP          ; AND STORE AT IOTMP
MOV #IOBUF,R5         ; RESET R5 TO BUFF S.A.
INC BLOCK             ; INC BLOCK COUNT
RTS PC                ; EXIT

ROUTINE TO SET WINDOW BY MARKER SETTINGS
MUST BE IN NORMAL MARKER MODE

MARKR:  MOV #1,WRFLG      ; ENTER PRINT MODE
        TST GRCON        ; WAS A # INPUT?
        BMI NOXRK        ; NO SO PRINT MARKER CHANNELS ONLY
        MOV GRCON,R1     ; R1 HAS GRP #
        MOV #MRKBUF,R2   ; R2 POINTS TO MRK STOR BUFF
MRKCHK: DEC R1           ; DEC WINDOW CTR
        BMI MRKFND       ; AT WINDOW STORAGE YET?
        ADD #4,R2        ; NO SO INC R2 BY 4 LOC.
        BR MRKCHK        ; AND CHECK AGAIN
MRKFND: MOV# TTBUF+2,R1  ; R1 HAS MARKER CHAR COMMAND
        CMPB #15,R1     ; IS IT CR?
        BEQ MRKPNT       ; YES SO PRINT WINDOW CHANNELS
        CMPB #'S',R1    ; IS IT "S"?
        BEQ MRKSET       ; YES SO SET WINDOW
        CMPB #'E',R1    ; IS IT "E"?
        BEQ MRKERS       ; YES SO ERASE WINDOW
        CMPB #'M',R1    ; IS IT "M"?
        BEQ MRKMOV       ; YES SO MOV MARKERS TO WINDOW
        JMP RSTR4        ; NO SO ILLEGAL COMMAND

MRKPNT: MOV (R2)+,R4     ; R4 HAS LEFT MARKER
        MOV (R2),R3     ; R3 HAS RIGHT VALUE
        ASR R4           ; PUT IN BYTES
        ASR R3
        TST R3          ; WAS WINDOW SET?
        BNE MRK02       ; YES SO BRANCH
        .PRINT #MSG20   ; NO SO SAY SO
        JMP RSTR4        ; AND RETURN
MRK02:  .PRINT #MSG21   ; PRINT "WINDOW LOCATION:"
        INC R4           ; INC R4
        JSR PC,PRNTDC   ; PRINT IT
        INC R3
        MOV R3,R4
        JSR PC,PRNTDC   ; PRINT R3
        BR MEND         ; OUTPUT CRLF & EXIT
        BR FINI         ; AND RETURN
MRKSET: MOV (R2),R4     ; GET S CHNL OF WINDOW
        TST R4          ; 0?
        BNE ERR5        ; SET SO MUST ERS 1ST
        MOV LTRK,R4     ; R4 HAS LEFT MARKER
        BNE MNDTO       ; CHNL 0? NO SO OK
        INC R4          ; YES SO PUT=1
MNDTO:  MOV RTMRK,R3    ; R3 HAS RIGHT MARKER
        ASL R4           ; PUT IN BYTES
        ASL R3
        MOV R4,(R2)+    ; STORE THEM
        MOV R3,(R2)+
        INC MSET        ; WINDOW SET CTR + 1
        .PRINT #MSG18   ; PRINT "WINDOW SET:"
        CLR WINXS       ; SIGNAL WINDOW CHANGE
        BR NOXRK        ; AND PRINT CHANNELS
MRKERS: CLR (R2)+       ; ERASE WINDOW
        CLR (R2)
        DEC MSET        ; WINDOW CTR-1
        .PRINT #MSG11   ; AND SAY SO
        BR FINI         ; RETURN
MRKMOV: MOV (R2)+,R4     ; R4 HAS LEFT MARKER
        MOV (R2),R3     ; R3 HAS RIGHT MARKER
        ASR R4           ; PUT IN WORDS
        ASR R3
        TST R3          ; WAS A WINDOW SET?

```

```

BNE MKR01 ; YES SO BRANCH
.PRINT #MSG20 ; NO SO SAY SO
JMP RSTR4 ; AND RETURN
MKR01: MOV R4,LTKRK ; SET LEFT MARKER
MOV R3,RTMRK ; AND RIGHT MARKER
.PRINT #MSG19 ; AND SAY SO
MKR01: MOV LTKRK,R4 ; R4 HAS LEFT MARKER
INC R4 ; INC R4
JSR PC,PRNTDC ; PRINT IT
MOV RTMRK,R4 ; R4 HAS RIGHT MARKER
INC R4 ; INC R4
JSR PC,PRNTDC ; PRINT IT
MEND: MOV #15,R0 ; OUTPUT CR/LF
.TTOUTR
MOV #12,R0
.TTOUTR
BR FINI ; AND RETURN

FINI: JMP REDO ; NORMAL EXIT TO BKGD

ROUTINE TO POINT TO TITLE BUFFER S.A. FOR GIVEN GRP
R2 RETURNED AS PTR
R2,R3 USED

TITPTR: MOV GR0M,R3 ; R3 HAS GRP #
MOV #TITSA,R2 ; R2 HAS TITLE BUFF S.A.
ADDXOR: DEC R3 ; RIGHT GRP?
BMI SETUP ; YES SO RETURN
ADD #100,R2 ; NO SO PNT TO NEXT GRP BUFF
BR ADDXOR ; AND CHECK IT
SETUP: RTS PC ;NORMAL EXIT

ERR5: JMP RSTR4 ; ERROR RETURN ON CMND

ROUTINE TO PRINT OUT ALL WINDOWS:TAGS,POSITIONS AND CONTENTS
USES R1-R5

LISTW: CMP GR0M,#0 ; TEST FOR OK GRP #
BMI ERR5 ; NOT OK SO ERROR
TST MSET ; ANY WINDOWS SET?
BEQ ALLEX ; NO SO EXIT
.PRINT #MSG34 ; PNT THE HEADINGS
JSR PC,WNSRT ; ORDER IN ASENDNG WNDWS
JSR PC,FETCH ; GET GRP S.A.
MOV R4,SRTFLG ; AND STORE IT
MOV #WINBUF,R2 ; GET S.A. ON SRTD WNDWS
ALOOP0: MOV #XKXBUF,R1 ; GET S.A. ON INPUT WNDWS
MOV (R2),R4 ; GET WNDW S. CHNL
.TTYOUT #'# ; OUTPUT #
CLR R5 ; USE R5 AS CNTR
ALOOP1: MOV (R1),R3 ; GET WNDW S.A. AS INPT
ASR R3 ; CNVRT TO CHNL #
CMP R4,R3 ; FOUND TAG?
BEQ TAGOT ; YES SO CONTU
INC R5 ; NO SO INC CNTR
CMP (R1)+,(R1)+ ; UPDATE TO NXT S.A.
CMP R5,#7 ; DUN(AT MAX TAG)?
BNE ALOOP1 ; NO SO DO MOR
BR ERR13 ; YES SO ERROR
TAGOT: ADD #80,R5 ; CNVRT TAG TO ASCII
.TTYOUT R5 ; OUTPUT TAG
.TTYOUT #' ; OUTPUT :
INC R4 ; OUTPUT #
JSR PC,PRNTDC ; OUTPUT START CHNL
MOV (R2)+,R3 ; GET WNDW S. CHNL
ASL R3 ; GET CHNL ADDR.

```



```

ADD SRTFLG,R3      ; INCLD GRP # OFFSET
MOV (R2),R4       ; GET WNDW E. CHNL
INC R4            ; OUTPUT #
JSR PC,PRNTDC     ; OUTPUT END CHNL#
MOV (R2)+,R1      ; GET WNDW E. CHNL
ASL R1           ; CNVRT TO ADDR.
ADD SRTFLG,R1     ; ADD GRP # OFFSET
ADD #2,R1        ; INCLUDE LAST CHNL #
CLR R5           ; USE R5 AND R4 AS HI & LO
CLR R4           ; WORDS OF SUM IN D.P.
AI OOP2: ADD (R3)+,R4 ; DO SUM IN D.P.
ADC R5
CMP R3,R1        ; E. CHNL YET?
BNE ALOOP2      ; NO SO DO MOR
JSR PC,PRNTDP   ; YES SO OUTPUT SUM
.TTYOUT #15     ; OUTPUT CR/LF
.TTYOUT #12
DEC WINX3       ; DUN ALL WINDOWS YET?
BNE ALOOP0      ; NO SO DO MOR
MOV MSET,WINX3  ; YES SO RESET WNDW CNTR
ALI EX: JMP FINI ; NORMAL E. OF C.
ERR13: .PRINT #MSG35 ; PNT: OVERLAPPED GROUPS
MOV #17,R5      ; SIGNAL ERROR
BR TABOT       ; RETURN

```

ROUTINE TO PERFORM SPECTRAL GROUP MANIPULATIONS

```

KICLB: CMP GRCON,#0   ; CHK GRP CMND
BMI ERR44       ; NO GRP # SO ERR
TST KFLAG      ; 1ST TIME THRU?
BEQ KFIRST     ; YES SO BRANCH
CMP #1,KFLAG   ; NO SO 2ND TIME?
BEQ KSEC       ; YES SO BRANCH
MOV GRCON,GRP2SA ; STOR LAST GRP #
.PRINT #MSG44 ; PNT: GROUP #
MOV GRP3SA,GRCON ; GET GRP 3 S.A.
JSR PC,FETCH   ; PUT S.A. IN R4
MOV R4,GRP3SA  ; STOR IT
MOV GRCON,R4   ; PNT OUT GRP #
JSR PC,PRNTDC  ;
MOV8 #'-,R1    ; OUTPUT. =
JSR PC,BKGDO   ;
.PRINT #MSG44  ; PNT: GROUP #
MOV GRP1SA,GRCON ; GET 1ST GRP S.A.
JSR PC,FETCH   ;
MOV R4,GRP1SA  ; STOR IT
MOV GRCON,R4   ; GET GRP #
JSR PC,PRNTDC  ; PRINT IT
CLR R1         ; CLR FOR ASCII INPT
MOV8 #' ),R1   ; SET UP FOR OPERTN PNT
ADD KFLAG,R1   ; USING OFFSET FROM KFLG
JSR PC,BKGDO   ;
.PRINT #MSG44  ; PNT: GROUP #
MOV GRP2SA,GRCON ; GET 2ND GRP S.A.
JSR PC,FETCH   ;
MOV R4,GRP2SA  ; STOR IT
MOV GRCON,R4   ; PNT OUT GRP #
JSR PC,PRNTDC  ;
MOV #KFLAG,R4  ; GET INSTR. ADDR.
ADD KFLAG,R4   ; GOT + OR - INSTR.
MOV (R4),KLOOP1+2 ; DEPOSIT INSTR
MOV GPWIDTH,R5 ; USE R5 AS CNTR
MOV GRP1SA,R1  ; GET 1ST GRP ADDR
MOV GRP2SA,R2  ; GET 2ND GRP ADDR
MOV GRP3SA,R3  ; GET 3RD GRP ADDR
KLOOP1: MOV (R1)+,R4 ; GET GRP#1 DATA
.WORD 0        ; LOADED WITH #KFLAG+KFLG
MOV R4,(R3)+  ; STOR RESULT

```

```

DEC R5 ; DUN?
BNE KLOOP1 ; NO SO LOOP KOR
CLR KFLAG ; YES SO INIT FLAG
JMP FINI ; EXIT
KFIRST: INC KFLAG ; FLAG FOR SECND INPUT
MOV GRCOM,GRP3SA ; STOR RESULT GRP #
CLR ERFLG ; CLR RESET ERR ON INPT
JMP JPBKGD ; GET NXT CMND GRP
KSEC: INC KFLAG ; FLAG FOR THIRD INPT
MOV GRCOM,GRP1SA ; TOR 1ST GRP #
CLR ERFLG ; RESET INPT # ERR
JSR PC,KBIN ; GET TTY KYBD INPT
MOV #TTBUF,R1 ; GET CHAR BFR ADDR
CMPB #'',(R1) ; HAVE +?
BEQ KEX1 ; YES SO DUN
CMPB #'',(R1) ; NO SO HAV-?
BNE ERR44 ; NO SO ERROR
INC KFLAG ; YES SO FLAG IT
INC KFLAG ;
KEX1: JMP JPBKGD ; RETURN FOR FINAL GRP ADDR

ERR44: JMP RSTR4 ; ERROR CMND RETURN

GRP3SA: .WORD 0 ; GROUP S.A. FOR RESULT SPECTRUM
GRP2SA: .WORD 0 ; GROUP S.A. FOR 2ND SPECTRUM
GRP1SA: .WORD 0 ; GROUP S.A. FOR 1ST SPECTRUM
KFLAG: .WORD 0 ; MODE FLG(2ND TIME=1,3RD=2IF+OR4IF-)
ADD (R2)+,R4 ; INSTR TO BE LOADED DURING EXCTN
SUB (R2)+,R4

```

SECTION TO TAKE THE NATURAL LOGARITHM OF DATA

```

LOGIT: NOP
      JMP FINI ; NORMAL E. OF C.

```

THIS IS THE END OF ASCII PAGE 3:KES11.MAC

SUBROUTINE TO ZERO THE STEPPING MOTOR FOR  
FOR EXITS AND RESTARTS (USES R2)

```

MOTO: MOV SMCTR,R2 ; GET MOTOR STEP CTR
      BEQ MDUN ; 0?, YES SO EXIT
KLOOP: BIT #401,@MKRCSR ; NO SO INTR OK?
      BNE -8 ; NO SO WAIT FOR RESET
      BIS #1,@MKRCSR ; YES SO REV STEP
      DEC SMCTR ; DEC STEP CTR
      BNE KLOOP ; DUN? NO SO KOR
MDUN: RTS PC ; NORMAL RETURN

```

SUBROUTINE TO BUBBLE SORT WINDOW S.A. AND E.A.'S  
INTO ASCENDING ORDER TO FACILITATE SEQUENTIAL  
ESA SCANNING AND TO CONVERT (STORED IN WINBUF)  
BYTE ADDRESSES INTO CHANNEL NUMBERS(USES R1-R5)

```

KNSRT: MOV MSET,WIND3 ; INIT WINDOW PR CTR
      MOV EXRBUF,R1 ; GET STORAGE BUFR
      MOV WINBUF,R2 ; GET SORTED BUF ADDR
      MOV MSET,R3 ; GET # WINDOWS SET
      ASL R3 ; DBLE CNTR FOR ADDR.#
      CLR SRTFLG ; INIT EXCHNG FLG
KLOOP1: MOV (R1)+,R4 ; GET WINDOW ADDR
      ASL R4 ; CNVRT TO CHNL #
      MOV R4,(R2)+ ; STORE IT

```

```

DEC R3 ; DUN?
BNE WLOOP1 ; NO SO LOOP MOR
WOUT1: MOV WINX8,R5 ; R5 IS PR CTR
ASL R5 ; USE R5 AS ADDR CNTR
MOV #WINBUF,R1 ; PIK UP DATA IN PRS
MOV #WINBUF+2,R2 ; SET UP ADDRESSES
DEC R5 ; SORT # OF ADDR. - 1
WLOOP2: MOV (R1),R3 ; CHX IN PAIRS
MOV (R2),R4
CMP R4,R3 ; R4 < R3?
BMI EXCHG ; YES SO EXCHNG
WGX: CMP (R1)+,(R2)+ ; UPDATE ADDR PRS
DEC R5 ; DUN ALL WNDW ADPRS.?
BNE WLOOP2 ; NO SO CONTINUE
TST SRTFLG ; YES SO ANY PAST CHNGS?
BEQ WCNT1 ; NO SO DUN
CLR SRTFLG ; YES SO CLR FLG & RPT
BR WOUT1 ; DUN
EXCHG: MOV R4,(R1) ; DO EXCHNG
MOV R3,(R2) ; OF WINDOW EA & SA'S
INC SRTFLG ; NOTE EXCHANG
BR WGX ; CONTINUE
WCNT1: CLR CHANX8 ; INIT CKNL # SUM
MOV #WINBUF,R1 ; GET WINDOW BUFFER
MOV MSET,R4 ; USE R4 AS CNTR
WLOOP3: MOV (R1)+,R2 ; GET S.A.
MOV (R1)+,R3 ; GET E.A.
SUB R2,R3 ; NO SO GET # CHNLS
INC R3 ; INCLUDE E.A. CKNL
ADD R3,CHANX8 ; UPDATE THE SUM
DEC R4 ; DUN?
BNE WLOOP3 ; NO SO LOOP AGAIN
ASL CHANX8 ; #CHNLS/CMPLTE SCAN
WOUT2: RTS PC ; NORMAL RETURN

WINBUF: .BLKW 20 ; ASCENDING ORDER STORES OF WINDOW EA & SA'S
WINX8: .WORD 0 ; NUMBER OF SET WINDOW ADPRS.
SRTFLG: .WORD 0 ; NON ZERO IF FND REV PRS IN SORT LOOP
ESAERR: .WORD 0 ; ERROR FLG(=2 IF STEP MOT<0,=3 IF ADC2 OFF)

```

SUBROUTINE ESASWP TO UPDATE ESA HV POSITION TO THE SET POINT (USES R5)

```

ESASWP: BIS #12,@ADCSR ; STROBE ADC2
WATE: INC ADCN8 ; TIKED OUT?
BEQ NDADC ; YES SO NOTE IT
BIT #4000,@ADCSR ; CONV. DUN?
BNE WATE ; NO SO LOOP
MOV @ADC2,VSCACT ; YES SO GET CHNL#(4K)
MOV CONX8,R5 ; CNVRT TO GPWDTH CHNL#
WLOOP3: ASR VSCACT ; #/2
DEC R5 ; CONV # -1
BNE WLOOP3 ; DUN?NO SO MOR
BIC #10,@ADCSR ; CLR ADC2 AND LED
CLR ADCN8 ; CLR TIME OUT FLAG
CMP VSCACT,VSCSET ; YES SO CMP SET PT
BEQ EDUN ; ACT=SET SO DUN
BMI LOW ; VOLTAGE LO SO BR.
BIT #401,@XRCR ; MTR STEP READY?
BNE .-8 ; NO SO WAIT
BIS #1,@XRCR ; VOLTAGE HI SO REV MTR
DEC SXCTR ; MTR STEP CTR -1
BNE ESASWP ; 0?NO SO CHX MOR
MOV #2,ESAERR ; TAG ERROR FLAG
INC SXCTR ; RESTOR MTR CTR
BR EDUN ; EXIT & ASQRT
LOW: BIT #401,@XRCR ; MTR STEP READY?
BNE .-8 ; NO SO WAIT

```

```

      BIS #400, @#MRCR          : FWD ONE STEP
      INC 9MCTR                 : BUMP MTP STP CTR
      BR  ESASWP                : CHECK MORE
HOADC: MOV #3, ESAERR          : TAG THIS ERROR
      BIC #10, @#ADCSR         : CLR ADC2 & LED
      JSR PC, MOTO             : 0 STEPPING MTR
      EDUN: PTS PC              : NORMAL & ERROR RETURN

      EPR10: .PRINT #MSG25      : PNT: NO BCI SET
      JMP EPR5                 : ABORT BEGIN CMND
      ERR14: .PRINT #MSG33      : PNT: NOT LATEST WNDW DATA
      JMP PSTRT4               : ERROR RETURN
.
.
SECTION TO START ESA SCANNING ON BN COMMAND
WHERE N=GROUP NUMBER OF THE SPECTRUM
.
REGIN: CMP  GRCOM, #0          : CHK GP CMND
      BMI  EPR8                : -1 SO ERROR
      CMP  MSET, WIMX8         : CHK LATEST WNDWS USED
      RNE  ERR14               : NO SO NOTE IT & ERR EX
      JSR  PC, FETCH           : GET ESA S.A.
      MOV  P4, ESASA           : AND STORE IT
      CMP  #0, BCISSET         : BCI PRESET SET?
      BEQ  ERR10               : NO SO ERROR
      TST  @OSIG               : SCANNING?
      SNE  EPR8                : YES SO ERROR
      BIS  #2, @#MRCR         : ZERO SCALER
      MOV  #1, @OSIG           : SET SCAN FLAG
      MOV  WINSUF, VSCMIN      : SET UP START
      MOV  WINBUF+2, VSCMAX    : AND STOP CHNL #
      CLR  UPDXN               : SET FOR UP SCAN
      CLR  ADCNB               : INIT ADC TIM OUT FLAG
      CLR  BCIACT              : CLR INTEG RUNNING SUM
      MOV  WINSUF+2, CRNXPTR   : INIT CURNT WNDW PTR
      MOV  VSCMIN, VSCSET      : START AT LO LIMIT
      MOV  VSCMIN, P1          : DSPLY LO LIMIT
      JSR  PC, DSPHI           :
      MOV  VSCMAX, P1          : DSPLY HI LIMIT
      JSR  PC, DSPHI           :
      MOV  VSCSET, P1          : DSPLY SET POINT
      JSR  PC, DSPHI           :
      CLR  ESAERR              : INIT ERROR FLAG
      JSR  PC, ESASWP          : UPDAT HW TO SET PT
      MOV  VSCACT, @#YREG      : DSPLY CRNT HW POSN
      CLR  @#YREG              : KEEP Y HAL 0
      MOV  #3, @#DSPSR        : DSPLY HI
      TSTESA: TST  ESAERR       : HW ERROR?
      BEQ  MOV                 : NO SO OK
      CLR  @OSIG               : ABORT ESA SCAN
      BIC  #142104, @#MRCR    : STOP INTEG+SCLR
      CMP  #2, ESAERR          : ???
      BEQ  ESAERR              : YES SO STP MTP/0
      .PRINT #MSG24            : NO SO IS -3
      BR  EPR6                 : PNT: NO ADC SO ABORT
      ESAERR: .PRINT #MSG23     : PNT: MTP/0 SO ABORT
      BR  EPR6                 : EXIT UNDER ERROR
      MOV  #1, CRNTXN          : SET UP KNOW CTR FOR INTEG
      CLR  SCNX8               : INIT CMLTE SCM CNTR
      BIC  #142000, @#MRCR    : RESET INTRGTR
      MOV  #INTEG, M1          : GET INTEG ESA ROUTINE
      CLR  INTLO               : INIT INTRGTR RUNNING
      CLR  INTHI               : SUM
      BIS  #142104, @#MRCR    : SCLR & INTEG ENABLE
      JMP  FINI                : END OF BEGIN CMND
.
      EPR8:  JMP  PSTRT4        : RESTART AFTER ERROR
      EPR11: .PRINT #MSG22      : PNT: NO WINDOWS SET
      BR  ERR8                 : ABORT BEGIN CMND

```

```

UPDWN: .WORD 0 * SCANNING DIRECTION FLAG(0-UP 1-DWN)
BCISFT: .WORD 0 * BEAM CURNT DOSE PRESET DOSE(CLI)
BCIACH: .WORD 0 * ACTUAL BCI PUNNING SUM
ADCH8: .WORD 0 * ADC TIME OUT FLAG
USCHIN: .WORD 0 * LO LIMIT OF WINDOW UNDER SCAN(CHNL#)
USCHMX: .WORD 0 * HI LIMIT OF WNDW UNDER SCAN(CHNL #)
USCSET: .WORD 0 * SET POINT IN SCAN WINDOW (CHANNEL #)
USCACT: .WORD 0 * ADC DERIVED ACTUAL HV POSN IN CHNL #
TDOSHI: .WORD 0 * TOTAL DOSE-HI ORDER WORD
TDOSLO: .WORD 0 * TOTAL DOSE-LO ORDER WORD
SCHX8: .WORD 0 * NUMBER OF TOTAL SCANS COMPLETED
SCHMAY: .WORD 0 * NUMBER OF TOTAL SCANS REQUIRED

```

SECTION TO SET PRESET VALUE OF THE INTEGRATOR

```

INTSFT: CMP #0,GRCOM * CHECK GP CMND
        RMI ERR6 * NOT -1 SO ERROR
        BIT #42000,R#MRCR * INTEG ON?
        BNF ERR6 * YES SO ERROR
        TST GOSIG * SCANNING?
        RNF ERR6 * YES SO ERROR
        CMP #0,MSET * WINDOW(S) SET?
        BFP ERPI1 * NO SO ERROR
        .PRINT #MSG16 * PNT:TOTAL DOSE =
        JSR PC,NUMIN2 * GET DOSE IN D.P.
        MOV BINHI,TDOSHI * GET DOSE IN R1&R2
        MOV BINM8,TDOSLO
        .PRINT #MSG10 * PNT:# SCANS =
        JSR PC,NUMINI * GET S.P. # SCANS
        JSP PC,KNSRT * GET # CHNLS IN ALL WNDWS
        MOV BINX8,R3 * PUT #SCANS INTO R3
        MOV R3,SCNMAY * STORE IT
        MOV CHANM8,R4 * GET # CHNLS/SCAN
        CLP TEMP3 * INIT TOTAL # CHNLS CNTR
ILOOP0: ADD R4,TEMP3 * NO SO SUM # CHNLS
        DEC R3 * DUN?
        BEZ IOUTO * YES SO EXIT
        BR ILOOP0 * REPEAT LOOP
IOUTO: MOV TEMP3,R4 * GET # CHNLS/TOTAL DOSE
        MOV TDOSHI,R1 * GET TOTAL DOSE
        MOV TDOSLO,R2
        CLP R5 * USE R5 AS RESULT OF
ILOOP1: SUB R4,R2 * DIVIDING DOSE BY THE
        SBC R1 * TOTAL # OF CHANNELS
        SUB R3,R1 * DO IT D.P.
        BMT IOUT1 * DIV? YES SO BRANCH
        INC R5 * NO SO UPDATE RESULT
        BR ILOOP1 * REPEAT LOOP
IOUT1: MOV R5,BCISFT * STOP THE RESULT
        .PRINT #MSG76 * PNT:DOSE/CHNL =
        MOV R5,R4 * PNT OUT RESULT
        JSR PC,PRNTDC
        IMP FTNT * NORMAL RETURN

ERR6: CLP ESAERR * C/P ERROR FLAG
        IMP RSTPT4 * RESTART PGM WITH ?

```

SECTION TO TURN ON C/N COLLECTION OF DATA MODE  
ON CN COMMAND WHERE N IS AN EVEN NUMBERED  
SPECTRAL GROUP STORING NEUTRALS(KV ON) AND  
SPECTRUM N+1 CONTAINS CHARGE+NEUTRALS(KV OFF).

```

CNON: CMP GRCOM,#0 * CHECK GP CMND
        BMT ERPI5 * NO CMND N SO ERR
        TST GOSIG * SCANNING?
        RNF ERR15 * YES SO ERROR
        BIT #1,GRCOM * CHK IF N EVEN

```

```

BNE EPP15          * NO SO ERROR
TST PPGMAY         * HAS FREQ BEEN SET?
BEQ EPP15          * NO SO ERROR
BIT #104,@#ADCSR  * ADC1 ON?
BNE EPP15          * YES SO ERROR
BIC #177777,@#MTREG * TURN HV TO 0
CLR TMFLG          * CLR HV SWITCH FLG
CLR ONFLG          * CLR HV STATUS FLG
JSP PC.FETCH      * GET S.A. FROM N
MOV R4,ADCSA1     * STOR S.A.#1
MOV PPGSA,R3      * GET LTMK PPG GRP ADDR.
ADD R4,R3         * CONVERT TO BFR S.A.
MOV R3,CNSA1      * STORE IN HERE(HV OFF)
MOV PPGA,R3       * GET RTMK PPG GRP ADDR.
ADD R4,R3         * CONVERT TO BFR E.A.
MOV R3,CNEA1      * STORE HERE & USED IF HV OFF
ADD DSPLN,R4      * GET NEXT S.A.
MOV P4,ADCSA2     * STOR S.A.#2
MOV PPGSA,R3      * GET LTMK PPG GRP ADDR
ADD R4,R3         * CONVERT TO BFR S.A.
MOV R3,CNSA2      * STOR TO USE IF HV ON
MOV PPGA,R3       * GET PTMK PPG GRP ADDR
ADD R4,R3         * CONVERT TO BFR E.A.
MOV R3,CNEA2      * STOR TO USE IF HV ON
MOV P4,ADCSA     * HV OFF INITIALLY SO INIT ADCSA
MOV #2,GOSIG      * SET SCAN FLG ON
BIC #142000,@#MRCR * INTEG OFF
MOV #GRATE,M4     * GET INTEG C/N SERV RTNE
MOV #100,R1       * GET CLK VCTR ADDR
BIC #100,@#LKS   * CLK INTR OFF
MOV #TMX,(R1)+   * GET NEW INTR ADDR
MOV #340,(R1)    * RUN HERE AT L 7
CLR INTLO        * INTEG RUNNING SUM
CLP INTHI        * IN D.P. CLRED
BIC #200,@#LKS   * CLR CLOCK INTERRUPT
BIS #104,@#ADCSR * ADC1 ON
BIS #42000,@#MRCR * INTEG ON
BIS #100,@#LKS ; CLK ON *
JMP FINI         * NORMAL E. OF C.

```

```

EPP00: .PRINT #MSG31 * PNT:CLK UNAVAILABLE
EPP15: JMP RSTR4   * ERROR RETURN

```

```

ONTYM: .WORD 0 * 1/2 CYCLE TIME IN MSEC
CLKTIX: .WORD 0 * 1/2 CYCLE TIME IN TICKS
MONTIX: .WORD 0 * CLK RUN TIME AWAY FROM MONITOR
MONTOX: .WORD 0 * BOTH HI & LO ORDER WORDS
MONCLK: .WORD 0 * SAVED MONITR CLK VECTOR
MONPRI: .WORD 0 * SAVED MONITR CLK RUN LEVEL
TMFLG: .WORD 0 * OPS STATUS FLG(ACTIVE=0,SWITCHING=1)
ONFLG: .WORD 0 * HV STATUS (OFF=0,ON=1)
TIX: .WORD 0 * HI ORDER TICKS OF THE CLOCK
TOY: .WORD 0 * LO ORDER TICKS OF THE CLOCK
ADCSA2: .WORD 0 * ADC S.A. FOR DATA BUF OF C+N(HV OFF)
ADCSA1: .WORD 0 * ADC S.A. FOR DATA BUF OF N'S(HV ON)
CNSA1: .WORD 0 * PPG WNDW S.A. WHEN HV OFF
CNEA1: .WORD 0 * PPG WNDW E.A. WHEN HV OFF
CNSA2: .WORD 0 * PPG WNDW S.A. WHEN HV ON
CNEA2: .WORD 0 * PPG WNDW E.A. WHEN HV ON
CNSA: .WORD 0 * C/N PULSER WINDOW STARTING ADDR.
CNEA: .WORD 0 * C/N PULSER WINDOW END ADDRESS
PPGMAY: .WORD 0 * PPG PRESET FOR HV SWITCHING IN C/N
PPGSUM: .WORD 0 * PPG RUNNING SUM DURING ADC ON PERIOD
PPGSA: .WORD 0 * PPG WINDOW START ADDRESS
PPGEA: .WORD 0 * PPG WINDOW END ADDRESS

```

SECTION TO INPUT FREQUENCY OF OSCILLATION OF THE

```

: C/N DEFLECTING POTENTIALS AS WELL AS BCI PRESET DOSE
:
FPEC:  CMP  GPCOM,#0      : HAVE GRP # N?
      BMI  ERR15        : NO SO ERROR
      MOV  #100,R1     : GET CLK INTR VECTR
      .PROTECT #AREA,R1 : CLK VCTR IN USE?
      BCS  EPR00        : YES SO NOTE IT
      TST  GOSIG        : SCANNING?
      BNE  ERR15        : YES SO ERROR
      CLP  @#MTPG       : H/ TO OFF
      .PRINT #MSG29     : PNT:OPS TO ON
      ISP  PC FETCH     : GET ADC S.A.
      MOV  R4,ADCSA     : SET IT UP
      BIS  #104,@#ADCSR : START UP ADC#1
      .PRINT #MSG40     : PNT:MARKERS ABOUT PPG
      ISP  PC BYGDI     : DSPLY & WAIT FOR CP
      MOV  LTRPK,USCMIN : SET UP FOR DSPLY
      MOV  PTRPK,USCMAX : OF MKKED PPG REGION
      BIC  #104,@#ADCSR : STOP THE ADC#1
      .PRINT #MSG30     : PNT:INPUT ON TIME
      JSR  PC,NUMINI    : GET S.P. TIME
      MOV  BINM3,ONTYM  : STOR 1/2 CYCLE TIME
      CLP  TRFLG        : INIT H/ FLAG
      CLP  R1           : CNVRT CYCLE TIM TO TICS
FLOOPC: ADD  #3,R1      : 3TIV=50MSEC
      SUB  #62,BINX3    : DIV BY 50 LOOP
      BMI  FOUT0        : RESULT IN R1(-VE)
      BEQ  FCONTO       : DUN HERE IF 0
      BR   FLOOPC       : DO MOR IF +VE
FOUT0:  ADD  #10,BINX3  : GET NEAREST 17 MSEC
      BPL  FCONTO       : <8MSEC SO OK
      DEC  R1           : CORRECT TIX
      ADD  #21,BINX3    : ADD 17 MSEC
      BMI  FMORO        : STILL -VE SO MOR
      BR   FCONTO       : HAV IT SO OUT
FMORO:  DEC  R1         : CORRECT TIX
      ADD  #20,BINX3    : ADD 16 MSEC
      BPL  FCONTO       : HAV NEAREST 8 MSEC
      DEC  R1           : MUST CORRECT AGAIN
FCONTO: MOV  R1,CLKTIX  : STOR REQ'D TIX #
      .PRINT #MSG16     : PNT:TOTAL DOSE=
      JSR  PC,NUMIN2    : GET IT IN D.P.
      MOV  BINHI,TDOSHI : STOR IT IN D.P.
      MOV  BINX3,TDOSLO :
      CLR  TOY          :
      JSR  PC,FETCH     : RUN CLOCK TO GET PPG PRESET
      MOV  R4,ADCSA     : GET GRP TO RUN PPG IN
      MOV  LTRPK,R3     : SET UP ADC S.A. GRP
      ASL  R3           : SET UP PPG KNDW ADDR.
      MOV  R3,PPGSA     : GET ADDR IN GRP
      ADD  R4,R3        : STOR KNDW S.A.
      MOV  R3,CNSA      : GET ADDR. IN BFP
      ASL  R3           : STOR S.A. 4 PPG KNDW
      MOV  R3,PPGEA     : SET UP E.A. 4 SAME
      ADD  R4,R3        : HAVE BYTE #
      MOV  R3,CNEA      : STOR KNDW E.A.
      MOV  #100,R1      : HAVE ADDR.
      BIC  #100,@CLKS   : STOR PPG E. ADDR.
      MOV  #100,@CLKS   : GET CLK INTR ADDR
      MOV  #100,@CLKS   : TURN OFF CLK INTR
      MOV  #100,@CLKS   : SAV KNTR CLK VCTRS
      MOV  #100,@CLKS   : INSTALL NEW VCTR INTR
      MOV  #100,@CLKS   : SAV KNTR RUN LVL
      MOV  #100,@CLKS   : INSTALL LVL 7 PRIORITY
      BIS  #104,@#ADCSR : ADC#1 ON
      BIS  #100,@CLKS   : CLOCK ON
      JSR  PC,FETCH     : GET GROUP S.A.
      MOV  D9PLEN,R2    : SET UP TO EPASE
      ADD  R4,R2        : PULSER PEAK

```

IMP LOOP15 ; JUMP TO EPOSE CMND

SECTION TO TURN OFF C/N MODE OR ESA SCANNING MODES

```

OFF:  CMP #0 GPCOM      ; CHK GP NUMB.
      RMT EPR12        ; NOT -1 SO ERROR
      CMP #2 GOSIG     ; CN SCAN ON?
      BFP CNOFF        ; YES SO BRANCH
      CMP #1 GOSIG     ; ESA SCANNING?
      BNF EPR12        ; NO SO ERROR
      BIC #42104, @MPCSR ; YES SO SCLR&INTEG OFF
      MOV #3 GOSIG     ; SET OFF FLAG
      RP COUT          ; FYIT
CNOFF: CMP #2 GOSIG    ; C/N SCANNING?
      BNE EPR12        ; NO SO ERROR
      MOV #4 GOSIG     ; SET OFF FLAG
      BIC #100, @LKS   ; CLK OFF
      BIC #42000, @MPCSR ; INTEG
      BIC #104, @ADCSR  ; ADC1 OFF
      MOV #100, R1     ; GET CLK UCTR ADDR
      MOV MONCLK, (R1)+ ; RESTOR MNTR CLK
      MOV MONPRI, (R1) ; RESTOR CLK PRI LVL
      BIS #100, @LKS   ; CLK ON
COUT:  .PRINT #MSG27    ; PNT: ACC DOSE =
      MOV INTLO, R4    ; GET ACC DOSE
      MOV INTHI, R5    ; AND OUTPUT IT
      JSR PC, PRNTDP
      .PRINT #MSG28    ; PNT: PRESET DOSE
      MOV TDOSLO, R4   ; GET PRESET DOSE
      MOV TDOSHI, R5   ; AND OUTPUT IT
      JSR PC, PRNTDP
      .PRINT #MSG37    ; PNT: # SCANS=
      MOV SCNMB, R4    ; GET # SCANS DUN
      JSR PC, PRNTDC   ; OUTPUT IT
      JMP FINI         ; NORMAL EXIT

```

EPR12: JMP RSTPT4 ; ERROR RESTART CMND

SECTION TO RESUME SCANNING (ESA OR C/N) MODE FROM POSITION WHERE 0 CMND FIRST ISSUED

```

CONTUE: CMP #0 GPCOM      ; CHK GP CMND
      RMT EPR12        ; NOT -1 SO ERROR
      CMP #3 GOSIG     ; PREVIOUS ESA SCAN?
      BEQ ESAON        ; YES SO BRANCH
      CMP #4 GOSIG     ; PREVIOUS C/N SCAN?
      BNE EPR12        ; NO SO ERROR
      MOV #2 GOSIG     ; YES SO SCAN FLG ON
      BIC #100, @LKS   ; CLOCK OFF
      MOV #100, R1     ; GET CLK UCTR ADDR.
      MOV (R1), MONCLK ; SAVE MNTR CLK UCTR
      MOV #TMV, (R1)+  ; RSTR CLK TO PGM
      MOV (R1), MONPRI ; SAVE MNTR PRI LVL
      MOV #340, (R1)   ; PGM CLK AT LVL 7
      BIS #104, @ADCSR  ; ADC1 ON
      BIS #42000, @MPCSR ; INTEG ON
      BIS #100, @LKS   ; CLK ON
      BR COUT          ; NORMAL EXIT
FSAGN: MOV #1 GOSIG    ; SET SCAN FLAG
      BIC #100000, @MPCSR ; RESET INTEG
      BIS #42104, @MPCSR ; SCLR+INTEG ENBLE
COUT:  JMP FINI         ; NORMAL CMND EXIT

```

ROUTINE TO TURN OFF INTERRUPTS AND EXIT

IMP: CMP GPCOM, #0 ; ILLEGAL COMMAND?



```

SMT DUMP1          *NO SO BRANCH
IMP PSTRT4        * YES SO ERROR
DMP1: BIC #100 @#LKS      : CLK OFF
      BIC #42004 @#MRCR  : INTEG & SCLR
      BIS #2 @#MRCR      : SCLR RESET
      BIC #104 @#ADCSR    : ADC1 OFF
      CMP #2 GOSIG       : SCANNING C/N?
      BNE DMPEV          : NO SO EXIT
      MOV #100 R1        : GET CLK MCTR ADDR
      MOV MONCLK, (R1)+  : RESTOR MNTR CLF
      MOV MONPPI, (R1)   : RESTOR CLK PRI LVL
DMPEV: JSP PC, MOTO     : 0 MOTOR ON EXIT
      CLR R0             : RESET INTERRUPTS
      .EXIT             : AND EXIT

```

INTERRUPT HANDLERS

```

SCALE: .INTEN SLRPP1    : RUN AT LEVEL 5
      INC SCLR0         : STORE OFLO
      PTS PC           : NORMAL RETURN

```

ROUTINE TO SERVICE INTEGRATOR INTERRUPT  
IN THE C/N SCANNING MODE

```

GPATE: .INTEN GTPPPI    : RUN AT LEVEL 7
      ADD #1 INTLO      : INC INTEGRATOR BUFFER
      ADC INTHI         : WATCH CARRY
      BIT #4000 @#MRCR  : ABORT?(ESS#2 ON?)
      BEP TOUT4        : NO SO IGNORE
      MOV #6, GOSIG     : YES SO SIGNAL FINI
      BIC #100 @#LKS    : DISABLE CLOCK
      BIC #42000 @#MRCR : DISABLE INTEG
      BIC #104 @#ADCSR  : DISABLE ADC1
      RTS PC           : RETURN FROM DUN
TOUT4: BIC #100000 @#MRCR : RESET INTEG
      PTS PC           : RETURN

```

ROUTINE TO SERVICE INTEGRATER IN THE ESA  
SCANNING MODE

```

INTEG: .INTEN INTPPI    : RUN AT LEVEL 7
      ADD #1 INTLO      : INC DOSE SUM
      ADC INTHI         : WATCH CARRY
      BIT #4000 @#MRCR  : ESS#2 ON?(ABORT?)
      BNE TDUN         : YES SO DUN
      CMP TDOSSLO, INTLO : TOTL DOSE YET?
      BNE CHCKX        : NO SO CHK CKXL DOSE
      CMP TDOSHI, INTHI : TOTAL DOSE?
      BNE CHCKX        : NO SO CHK CKXL DOSE
      MOV #6, GOSIG     : YES SO STOP
      BIC #142104 @#MRCR : INTEG & SCLR OFF
      RTS PC           : NORMAL EXIT
CHCKX?: INC BCIACT      : UPDATE DOSE SUM
      CMP BCIACT, BCISCT : CMP BCI TO PRESET
      BNE NOTYET       : ENUF? NO SO EXIT
      BIC #4 @#MRCR    : YES SO STOP SCLR
      MOV %SCSET, R4   : GET SET CKXL
      ASL R4           : CKXL TO ADDR.
      ADD ESASA, R4    : ADD GP # TO GET ADDR
      ADD @%SCLR, (R4) : READ & STOR SCALR
      BIS #2 @#MRCR    : CLR SCLR
      TST UPCKX       : UP OR DXN SCANNING?
      BMT DXNCKX      : DXN SCAN SO BR
      UPCKX: CMP %SCSET, %SCMAX : UP SCAL SO END

```

```

BMT UPOX      * NO SO CONT
INC CPNTKN   * YES SO TO NXT WNDW
CMP MSET,CPNTKN * LAST WINDOW?
BMT PFUSCH  * YES SO REV SCAN
ADD #2,CRNWPT * NO SO SET NEW ADDR
MOV @CPNWPT,VSCMIN * PIK UP S.A.
ADD #2,CRNWPT * UPDATE PTP
MOV @CRNWPT,VSCMAX * PIK UP E.A.
MOV @VSCMIN,VSCSET * GET NXT SET PT
BR IOXOX     * LEAVE
DNXCHK: CMP @VSCMIN,VSCSET * DNX SCAN SO END
BMT DNOX     * NO SO CONT
DEC CRNTKN  * YES SO TO NXT WNDW
CMP CRNTKN,#1 * LAST WINDOW?
BMT FWDSCN  * YES SO REV SCAN
SUB #2,CRNWPT * NO SO SET UP NEW ADDR
MOV @CRNWPT,VSCMAX * STOR HI LIMIT
SUB #2,CRNWPT ; NEXT ADDR *
MOV @CRNWPT,VSCMIN * STOR LO LIMIT
MOV @VSCMAX,VSCSET * NEW SET PT FOR HV
BR IOXOX     * QUIT
FWDSCN: INC UPDWN * 0 FLG FOR FWD SCN
ADD #2,CRNWPT * RESET CRNT WNDW PTR
INC CRNTKN  * RESTOR CRNT WNDW CTR
INC SCNXB   * BUMP TOTAL SCAN #
CMP SCNXB,SCNXAX * DUN YET?
BEQ IDUN    * YES SO SIGNAL END
BR IOXOX     * LEAVE AT SAME CHNL
PFUSCH: DEC UPDWN * SET REV FLAG=-1
SUB #2,CRNWPT * RESET CRNT WNDW PTR
DEC CRNTKN  * RESTOR WNDW CTR
BR IOXOX     * QUIT AT SAME CHNL
DNOX: DEC VSCSET * DEC VOLT SET PT
BR IOXOX     * STOR IT
UPOX: INC VSCSET * INC VOLTAGE SET PT
IOXOX: CLR @CIACT * RESET BCI SUM=0
BIC #140000,@CXRCR * RESET INTEG BUT DSBLE INTR
MOV #7,@OBIG * FLAG HV NEW POSN REURD.
RTS PC      * RT-11 PTI
NOTYET: BIC #100000,@CXRCR * RESET INTEGRTR
RTS PC      * PT-11 RTI

```

```

CRNTKN: .WORD 0      * CURRENT WINDOW OF THE SCAN
CRNWPT: .WORD 0      * CURRENT WINDOW ADDRESS POINTER

```

```

* CLOCK HANDLER (C/N MODE ONLY)
* SERVICE ROUTINE TO COUNT TICKS AND OPERATE OPS TIMING CNTRL

```

```

TMV: .INTEN CLKPRI * RUN AT LEVEL 7
ADD #1,TOX * UPDATE CNTR
OBC TIY * IN D.P.
TST TKFLG * CHK OPS STATUS
BZ @ONCYCL * 0 SO ACTIV
CMP #144,TOX * HAS 1637 MSEC?
OBE @ONZE * NO SO MOR
CLR TKFLG * YES SO GO ACTIV
MOV @R3A,R4 * GET S.A. FOR PPG WNDW
509: CLR (R4)+ * ZERO CHNL CONTENTS
CMP R4,@R3A * DUN?
EMI 509 * NO SO 0 MOR
CLR @PDSUM * ZERO RUNNING SUM
BIS #100,@ADDCR * RESTOR ADC INTR
BIS #40000,@CXRCR * RESTOR INTEG INTR
OR @CLCEN * EXIT
ONCYCL: CMP @PDSUM,@PCMAX * DUN?
EMI @ONZE * NO SO EXIT
MOV #1,TKFLG * YES SO CHNG STATE
BIC #100,@ADDCR * DSABLE ADC1 INTR

```

```

BIC #40000,CCRCSR      : DISABLE INTEG INTR
TST OXFLG              : GET STATUS OF HV
BEE TURNON             : IS OFF SO BRNCH
BIC #177777,CONTREG   : IS ON SO TRN OFF
CMP TDOBLO,INTLO      : CHECK IF TOTAL DOSE
BNE NOTDUN            : HAS YET BEEN REACHED
CMP TDOSHI,INTHI      : IN DOUBLE PRECISION
BNE NOTDUN            : IF NOT SET UP ADDR.
MOV #8,GOISG          : SIGNAL FINISH
BIC #42000,CCRCSR     : TURN OFF INTRTER
BIC #104,CCRCSR       : TURN OFF ADC#1
BIC #100,CLKS         : DISABLE CLK INTR
BR TOUT1              : DUN SO QUIT
NOTDUN: MOV CNA2,CNA   : SET UP WNDW ADDR.
        MOV CNA2,CNA   : FOR PPG DTERCHTN
        MOV ADCSA2,ADCSA : INIT ADC S.A.
        CLR OXFLG      : UPDATE FLAG
        BR CLRCON      : EXIT
TURNON: BIC #177777,CONTREG : TURN ON HV
        MOV ADCSA1,ADCSA : INIT ADC S.A.
        MOV CNA1,CNA    : SET UP WNDW FOR
        MOV CNA1,CNA    : FOR PPG RUNNING SUM
        INC OXFLG       : SET FLAG
CLRCON: CLR TIX         : CLR CLK CNTRS
        CLR TOX
CODE:   BIC #200,CLKS   : CLR CLK INTR
TOUT1: RTS PC          : NORMAL RT11 RTI EXIT

```

SERVICE ROUTINE TO SET UP PPG AREA PRESET  
 WHEN APPROXIMATE SWITCHING TIME IS INPUT

```

TRY:   .INTEN CLKPRI      : LEVEL 7 INTERRUPT
        ADD #1,TOX        : UPDATE TICKS COUNTED
        CMP TOX,CLKTIX   : DUN?
        ENI YCON         : NO SO EXIT
        BIC #104,CCRCSR   : YES SO ADC#1 OFF
        MOV CNA,R3       : GET WNDW S.A.
        MOV CNA,R4       : AND E.A. FOR SWITCHING
        CLR PPRMAX       : ZERO DUN PRESET
Y1:    ADD (R3)+,PPRMAX   : GO SUM
        CMP R3,R4        : DUN?
        ENI Y1           : NO SO MORE
        BIC #100,CLKS    : CLOCK OFF
        RTS PC           : YES SO EXIT,CLK OFF
YCON:  BIC #200,CLKS    : CLR CLK INTR
        RTS PC           : NORMAL EXIT

```

ADC1 HANDLER (IN C/N MODE ONLY)

```

ADCS:  .INTEN ADCPRI     : RUI AT LEVEL 8
        MOV CCRDC1,R4    : R4 HAS CNVRTD DATA
        CMP CCRDTH,R4    : BEYOND BUFFER?
        ENI ADCX1        : YES SO IGNORE DATA
        ACL R4           : EVEN ADDR ONLY
        ADD ADCCA,R4     : CALC CHANNEL #
        INC (R4)         : +1 AT CHANNEL
ADCS1: INC CCRDCR       : CLEAR THE ADC
        RTS PC          : RETURN NORMALLY

```

ROUTINE TO POINT TO START OF BUFFER FOR CRP #  
 POINTER RETURNED IN R4  
 R3,R4 USED

```

PRTON: CLR R3           : SET UP CTR
        MOV CCRCA,R4    : WNDW BUFF S.A. TO R4
CRX1:  CMP CCRTH,R3     : TRIGHT CRP?
        CLR CCR2        : YES SO EXIT

```

```

ADD DSPLN,R4      :MOVE TO NEXT GRP S.A.
INC R3            :AND INC CTR
BZ BACK1         : LOOP AGAIN
BACK2: RTS PC     :NORMAL EXIT

```

DATA BUFFER FOR HDLRS

```

SCLPO: .WORD 0      : OFLO WORD FOR SCLR
INTHI: .WORD 0      : MSB FOR INTEGRTR SUM
INTLO: .WORD 0      : LSW FOR INTEGRATER SUM

```

CSI ERROR SERVICE ROUTINE  
CONTROL RETURNS TO USER ON ERROR

```

CSIERR: TSTB CERRWRD : IS ERROR BYTE=0?
        CBE CS11      : NO SO TEST MORE
        .PRINT MSG12  : YES SO PRINT MESSAGE
        BR CS1EX      : AND RETURN CONTROL

```

```

CS11:  CWPB #1,CERRWRD. : IS ERROR BYTE=1?
        CBE CS13      : NO SO TEST MORE
        .PRINT MSG13  : YES SO PRINT MESS
        BR CS1EX      : AND RETURN CONTROL

```

```

CS13:  CWPB #3,CERRWRD : IS ERROR BYTE =3?
        CBE CS14      : NO SO TES MOR
        .PRINT MSG14  : PRINT ERROR MESS
        BR CS1EX      : AND RETURN CNTRL

```

```

CS14:  CWPB #4,CERRWRD : IS ERRBYTE=4?
        CBE CS15      : YES SO PRINT ERR MESS
        .PRINT MSG15  : YES SO PRINT ERR MESS
        BR CS1EX      : RETURN CNTRL

```

MESSAGE CUFFER

```

.MLIST
MSG0:  .ASCII /?/
MSG1:  .ASCII /?/
MSG2:  .ASCII /MSG FOR MEN 01-JUN-79 OPERATIONAL /<200>
MSG3:  .ASCII /GROUP WIDTH:/<200>
MSG4:  .ASCII /INPUT FILENAME (MAX 8 CHAR'S)/
MSG5:  .ASCII /MAXIMUM NUMBER OF GROUPS IS /<200>
MSG6:  .ASCII /15*12/CLEAR SPECTRA CUFFER?(YES=Y):/<200>
MSG7:  .ASCII /DX1: /
MSG8:  .ASCII /WRITE ERROR HAS OCCURED -ABORT WRITE/
MSG9:  .ASCII /-DM1:/<200>
MSG10: .ASCII /ILLEGAL CHAR READ-ABORT READ/
MSG11: .ASCII /TOTAL NUMBER OF COMPLETE (10P-IDX) SCANS: /<200>
MSG12: .ASCII /WINDOW ERASED/
MSG13: .ASCII /ILLEGAL FILENAME/
MSG14: .ASCII /DISK #1 NOT READY/
MSG15: .ASCII /FILE NOT FOUND/
MSG16: .ASCII /INPUT TOTAL SAMPLE DOSE(CLIX) DURING THE SCAN:/<200>
MSG17: .ASCII /SET WINDOW CENTER WINDOW AND PRESS CR/
MSG18: .ASCII /WINDOW SET:/<200>
MSG19: .ASCII /WINDOW MOVED TO:/<200>
MSG20: .ASCII /NO WINDOW SET/<200>
MSG21: .ASCII /WINDOW LOCATION:/<200>
MSG22: .ASCII /NO WINDOW SET--START ABORTED/
MSG23: .ASCII /MOTOR FORCED TOO LOW--SCAN ABORTED/
MSG24: .ASCII /ADC2 NOT FUNCTIONAL--ABORTING SCAN/
MSG25: .ASCII /LX FREEST NOT FOUND--SCAN ABORT/
MSG26: .ASCII /DOSE(CLIX) PER CHANNEL = /<200>
MSG27: .ASCII /15*12/ACCUMULATED DOSE(CLIX) THIS FOR = /<200>
MSG28: .ASCII /15*12/ FREEST DOSE(CLIX) = /<200>
MSG29: .ASCII /NO CNTRL ZERGED SO PPG & GRS SUPPLIES TO ON/
MSG30: .ASCII /AND BRACKET NUMBERS ABOUT PPG PEAK THEN /<200>
MSG31: .ASCII /INPUT RATE /SCALE TIME IN MSEC(32K MAX): /<200>

```

```

MSG31: .ASCIIZ /CLOCK VECTORS UNAVAILABLE/
MSG32: .ASCII /15X12/DONE!/<76><200>
MSG33: .ASCIIZ /WINDOW CONFIGURATION CHNGD-USE I CMD BE4 B CMD/
MSG34: .ASCIIZ /15X12/TAG START END SUR/<15X12>
MSG35: .ASCIIZ /WARNING--WINDOW OVERLAP/
MSG36: .ASCII /INPUT ESA/ RESOLUTION(ADC2 CNV GN):/<200>
MSG37: .ASCII / COMPLETED SCANS = /<200>
MSG38: .ASCII /ARE YOU SURE(YES=Y)? /<200>
MSG39: .ASCIIZ /SET MTR CNTR TO 1000.05 THEN CR(SS#1=UP,SS#2=DXN)/
MSG42: .ASCII /ENABLE PLOTTER,<CR> WHEN READY/<200>
MSG43: .ASCII /DONE SO DISABLE PLOTTER,THEN<CR>/<200>
MSG44: .ASCII /GROUP #/<200>
MSG45: .ASCII / DOT =/<200>
MSG46: .ASCII / DOT AT /<200>
MSGT: .ASCIIZ /00001 /

```

```

.LIST
.EVEN
IOTMP: .WORD 0 : PTR TO I/O BUFFER FOR FLOPPY'S
AREA: .BLKW 10 : ENT ARG LIST FOR .KRITH
IOBUF: .=.+1000 : RESERVE 256 WORD BUFFER
IOEND: .BLKW 10 : END OF THE I/O BUFFER
DEFEXT: .RAD50 "DAT" : INPUT CHNL #3 DEFAULT EXTN
: .RAD50 "DAT" : OUTPUT CHNL #0 DEFAULT EXTN
: .WORD 0,0
BLOCK: .WORD 0 : WRITE BLOCK NUMBER COUNTER
KRFLG: .WORD 0 : WR FLG FOR FLOPPY WRITE

NCTR: .WORD 0 : WINDOW COUNTER
CNAK73: .WORD 0 : TOTAL # OF CHALS WITHIN THE WINDOW
CONK73: .WORD 0 : 4K ADC2 CONVERSION # TO GROUP WIDTH
KSET: .WORD 0 : # OF WINDOWS SET
KRELF: .BLKW 20 : WINDOW BUFFER OF E&S A'S
ECTR: .WORD 0 : WINDOW END ADDRESS
COSIG: .WORD 0 : SCAN FLAG (0=NO SCAN,1=ESA,2=C/N)
: (3=PREVIOUS ESA SCAN NOW SUSPENDED)
: (4=PREVIOUS C/N SCAN NOW SUSPENDED)
: (5=DUN ESA SCAN,6=DUN C/N SCAN)
: (7=ESA SCAN WITH IMPENDING CHAL ADVANCE)

DEVSPC: .WORD 0 : DEVICE HANDLER STARTING ADDRESS
: .=.+2000

```

THE FOLLOWING ARRAYS ARE LOCATED HERE IN HIGH CORE  
IN ORDER TO PRESERVE THEIR CONTENTS FROM  
DESTRUCTION THROUGH OVERRITES BY  
PIP,PIP15 EXECUTIONS BETWEEN MSG11 RESTARTS

```

.EVEN
CLRALL=
TITLE=+.10 : TITLE BUFFER
SUFEN=+.2500 : SPECTRAL DATA BUFFER
.EVEN
ALLEND=+.SUFLEN+2502

```

SPECTRAL CUFFER FOR THE COLLECTED DATA

END OF THE PROGRAM---TRACK CODE!!!!!!!!!!!!!!!!!!!!

.END START

A.2 MES11 operating instructions

A2.1 NOTE ON NOTATION IN THIS PAPER

1. ALL USER TYPED INSTRUCTIONS ARE ASSUMED TO BE INPUT ON THE TTY KEYBOARD AND THROUGHOUT THIS PAPER ARE INDENTED AND UNDERLINED.
2. ALL COMPUTER ORIGINATED OUTPUT IS ASSUMED TO BE OUTPUT ON THE TTY PRINTER AND IS INDENTED ONLY.
3. MOST USER COMMANDS ARE FOLLOWED BY TYPING THE TTY RETURN KEY WHICH IS DESIGNATED HEREAFTER AS <CR> AND IS USUALLY ECHOED ON THE TELEPRINTER AS CARRIAGE RETURN THEN LINE FEED (CR/LF).
4. SOME SPECIAL COMPUTER COMMANDS ARE COMPOSED OF SIMULTANEOUS DEPRESSION OF THE CONTROL KEY (CTRL) AND A LETTER. IN SUCH A CASE, THE COMMAND IS SO DENOTED BY A CIRCUMFLEX (^) AND THE LETTER. FOR INSTANCE, TO BRING THE MONITOR INTO CORE, PRESS ^C, THAT IS, STRIKE THE CTRL AND C KEYS TOGETHER. (MONITOR CONTROL IS EXPLAINED IN SECTION 3.4.)

A2.2 SYSTEM COMMUNICATION

THE MONITOR ALLOWS THE USER TO COMMUNICATE WITH THE RT-11 SYSTEM VIA SPECIAL FUNCTION KEYS AND TTY KEYBOARD COMMANDS IN ORDER TO, START PROGRAMS, MANIPULATE MEMORY IMAGES, GENERATE I/O RESETS, STORE CURRENT DATA, AND MANAGE TYPE-AHEAD TTY COMMANDS.

SPECIAL FUNCTION KEYS:

1. CTRL C -- INTERRUPTS PROGRAM EXECUTION AND RETURNS CONTROL TO THE KEYBOARD MONITOR AFTER ALL I/O OR TYPE-AHEAD COMMANDS COMPLETED. IMMEDIATE RETURN IS ACCOMPLISHED BY TWO CTRL C'S: ^C^C
2. CTRL U -- DELETES CURRENT INPUT LINE.
3. RUBOUT -- DELETES THE LAST CHARACTER FROM THE CURRENT LINE.

KEYBOARD COMMANDS:

1. R -- RUNS A PROGRAM FROM THE SYSTEM DISK, EG. R PIP
2. RU -- RUNS A PROGRAM FROM THE SPECIFIED DEVICE, EG. RU DX11:ES11

A2.3 MEIR SPECTROMETER CONTROL (MES11) -- ENABLES USE OF THE PDP11/05 AS A MULTICHANNEL ANALYZER AND/OR SCALER WITH AN 8192 CHANNEL BUFFER THAT MAY BE SUBDIVIDED IN INTO A MAXIMUM OF 30 GROUPS OF FROM 64 TO 4088 CHANNELS EACH. DURING THESE OPERATIONS, THE COMPUTER CONTROLS THE ELECTROSTATIC ANALYZER POTENTIALS (WHILE MULTICHANNEL SCALING) OR THE SOLID STATE DETECTOR ADC AND C/N CHARGE PARTICLE DEFLECTION PLATE POTENTIAL OSCILLATIONS (WHILE PULSE HEIGHT ANALYZING). THIS ALLOWS THE ACQUISITION OF SPECTRA UNDER CONTROLLED CONDITIONS FROM THE MEDIUM ENERGY SCATTERING (MES) PHENOMENA. THROUGHOUT THESE OPERATIONS THE DOSE TARGET CURRENT IS ACCUMULATED AND ALL APPROPRIATE DEAD TIME CORRECTIONS ARE MADE ON LINE AND IN REAL TIME. I/O AND M.E.T.R. INSTRUCTIONS ARE ACCOMPLISHED VIA THE TELETYPE KEYBOARD WITH ONE CHARACTER COMMANDS AND CAN BE CARRIED ON SIMULTANEOUSLY; THAT IS, THE COMPUTER CAN BE DIRECTED TO ACCUMULATE A SPECTRUM IN ONE GROUP WHILE THE TELEPRINTER IS OUTPUTTING ANOTHER SPECTRUM OR PORTION THEREOF WHICH IS CURRENTLY ON DISPLAY

-- S. W. POEHLMAN OCT 24, 1977.

A2.4 LOADING MES11 INTO CORE: . RU MES11 <CR>

IF THE LOAD IS SUCCESSFUL THE TELEPRINTER WILL RESPOND WITH  
MES11 PGM VEN (NUMBER) OPERATIONAL: (DATE)

GROUP WIDTH:

AT THIS JUNCTURE SET THE GROUP WIDTH, SAY 256 CHANNELS  
BY TYPING . . . 256 <CR>

AFTER WHICH IS PRINTED

MAXIMUM NUMBER OF GROUPS IS 00030

CLEAR SPECTRA BUFFER?(YES=Y):

IF ALL POSSIBLE GROUPS ARE TO BE ZEROED THEN TYPE

Y <CR>

ANY OTHER CHARACTER WILL BE ASSUMED AS A  
NEGATIVE RESPONSE. THIS LATTER CASE, WHEN SPECTRAL BUFFERS  
ARE NOT CLEARED, ALLOWS A RESTART OR RELOAD OF THE PROGRAM  
WHERE SPECTRA ARE TO BE RECLAIMED UNDISTURBED.

NOTE1: THIS IS TRUE ONLY WHEN NO INTERVENING PROGRAM  
HAS BEEN RUN BY THE MONITOR.

NEXT IS OUTPUT

INPUT ESAHV RESOLUTION(ADC2 CONV. GN): 4088

THE USER SHOULD TYPE IN, AS INDICATED HERE BY 4088,  
THE CONVERSION GAIN TO WHICH ADC2 (LOCATED IN THE PDP11  
NIM BIN) HAS BEEN SET OR SELECTED. THIS ADC IS USED  
AS THE FEEDBACK LOOP FOR THE ESA POTENTIALS AND IS  
NOT NEEDED FOR ADC1 MEASUREMENTS (INVOLVING ANY SOLID  
STATE DETECTORS).

AFTER THIS RESPONSE HAS BEEN SELECTED, THE  
PROGRAM RESPONDS WITH THE GREATER THAN SIGN, WHICH  
SIGNIFIES THAT ANY VALID COMMAND CHARACTERS  
WILL BE ACCEPTED. THESE ARE OUTLINED BELOW.



A2.5 OPERATING PROCEDURES:

ALL COMMANDS MUST BE PROCEEDED BY THE ESCAPE KEY WHICH IS ECHOED ON THE TELEPRINTER AS \$. ANY OTHER TELETYPE CHARACTERS FROM THE KEY BOARD ARE IGNORED BUT ECHOED SO AS TO ALLOW USER LOGGING OF COMMENTS ON THE TELEPRINTER. NOTE THAT THESE COMMENTS WILL BE ECHOED BY MES11 WITH BELL AFTER MORE THAN 80 CHARACTERS ARE INPUT ON THE TELETYPE KEYBOARD -- THIS IS EXCLUSIVE OF ANY COMPUTER GENERATED OUTPUT ON THE TELEPRINTER WHICH MAY INCLUDE CR/LF. WHEN THIS OCCURS ANY COMMANDS, EVEN IF PREFIXED WITH THE ESCAPE KEY (ESC) WILL BE IGNORED. THEREFORE, IF NO COMMANDS ARE BEING EXECUTED, USE THE CONTROL U OR "U TO DELETE THE LINE AND RETYPE WITH <CR> BEFORE 80 CHARACTERS.

THE CHARACTER TYPED AFTER THE ESC KEY IS A COMMAND LETTER WHOSE FUNCTION IS OUTLINED BELOW.

IN MOST CASES THE THIRD CHARACTER WILL BE A NUMBER WHICH INFORMS THE COMPUTER ON WHICH GROUP THE SPECIFIED ACTION IS TO TAKE PLACE.

EG. TO PRINT THE CONTENTS OF GROUP 0 ON THE TELEPRINTER TYPE: \$P0 <CR>

NOTE THAT THE 30 GROUPS, FOR DISPLAY PURPOSES, ARE LABELLED FROM 0 TO 14, BIT 15 DOWN, AND 0 TO 14 WITH BIT 15 UP (SEE LOG COMMAND). THEY CAN BE VIEWED SIMPLY BY LIFTING THE APPROPRIATE TOGGLE ON THE SIX OF THE PDP11-05 FRONT PANEL. OVERLAP DISPLAYS CAN BE SELECTED BY HAVING MORE THAN ONE TOGGLE IN THE UP POSITION AND BY USE OF THE EXTERNAL SOFTWARE SWITCH #1 (IF UP, ALL BIT 15 UP AND BIT 15 DOWN GROUPS ARE DISPLAYED).

1. RESTART PROCEDURE:

AFTER THE GREATER THAN SIGN IS PRESENT, THE PROGRAM CAN BE RESTARTED AT ANY TIME BY TYPING:

\$G <CR>

THE INITIAL DIALOGUE WILL BE REPEATED SO THAT EITHER BUFFER CLEAR OR DIFFERENT GROUP WIDTHS CAN BE SELECTED. THIS COMMAND IS IGNORED IF THE ? APPEARS AFTER THE <CR>. THIS ERROR CONDITION EXISTS IF THE ADC IS ON. TO REMEDY THE PROBLEM TURN OFF THE ADC AND REPEAT THE COMMAND. IF THE COMPUTER IS CURRENTLY SCANNING, THEN THE RESPONSE IS ARE YOU SURE (Y=YES)? Y <CR>

IF IT IS DESIRED TO RESET THE SCANNING MODE THEN TYPE Y. ANY OTHER RESPONSE WILL LEAVE THE SYSTEM UNCHANGED.

2. START AND STOP ACCUMULATION AS DESIRED BY THE ADC CONTROL COMMANDS.
3. OUTPUT THE SPECTRUM DISPLAYED WITH PRINT COMMAND. IF THE PUNCH IS TO BE USED, TURN OFF THE DISPLAY MODE AND ENABLE PUNCH IMMEDIATELY AFTER <CR>. IF THE HARDWARE DISPLAY MODE, AS SELECTED ON THE PDP11 POLL SWR'S MODULE, IS ON, THEN NO BLANK LEADER OR TRAILER WILL BE OUTPUT. NOTE THAT ANY BLANK LEADER PAPER TAPE CAN BE GENERATED DURING THE ABOVE PAUSE BY SETTING THE TELETYPE TO LOCAL MODE AND DEPRESSING THE HERE IS KEY THREE OR FOUR TIMES WITH THE PUNCH ON. RETURN THE TELETYPE TO LINE MODE AND RESUME NORMAL COMPUTER OPERATIONS. FOR PERMANENT STORAGE OF SPECTRA USE THE WRITE ON FLOPPY DISC COMMAND (W). AT A LATER TIME THE SPECTRA CAN BE TRANSFERRED TO THE PDP-15 FOR DATA ANALYSIS VIA THE PROGRAM PIP15 AND THE HIGH SPEED LINK.

4. PROGRAM ABORT PROCEDURE:

^C  
--  
^C  
--

AVOID USING THE ABOVE, ESPECIALLY IF SCANNING IN THE ESA MODE, AS THE STEPPING MOTOR POSITION IS LOST TO THE COMPUTER. AT ALL TIMES, WHEN RESTARTING MES11 AFTER SUCH A PREVIOUS ABORT ENSURE THAT THE STEPPING MOTOR IS ZEROED (THAT IS, THE COUNTER ON THE MOTOR FRONT PANEL READS 1000.05) USING THE \$Z COMMAND.

NORMAL EXIT COMMAND:

\$X <CR>

5. ERROR CONDITIONS:

THESE ARE NOTED WHEN ? APPEARS ON THE TTY OUTPUT AND INDICATE THAT THE PREVIOUS COMMAND WAS ILLEGAL OR THAT ILLEGAL CONDITIONS EXIST FOR IT TO TAKE PLACE. SPECIFICALLY IF THE LETTER AFTER THE \$ IS NOT AN ASSIGNED COMMAND THEN THE ? IS PRINTED. FOR ALL COMMANDS REQUIRING A GROUP NUMBER N, THE ? WILL BE OUTPUT IF N EXCEEDS THE MAXIMUM NUMBER OF GROUPS WHOSE VALUE IS OUTPUT DURING THE INITIAL DIALOGUE. OTHER ERROR CONDITIONS ARE A FUNCTION OF THE COMMAND GIVEN AND ARE EXPLAINED IN THE COMMAND SUMMARY BELOW.

6. COMMAND SUMMARY:

(A) SCANNING

(1) ESA -- THIS MODE OF OPERATION CONTROLS THE ELECTROSTATIC ANALYZER(ESA) PLATE POTENTIALS THROUGH A MULTICHANNEL SCALER WHOSE ADVANCE IS BASED ON DOSE PRESET INFORMATION.

> \$I <CR>

INPUT TOTAL SAMPLE DOSE(CLIX) DURING THE SCAN:80000<CR>

TOTAL NUMBER OF COMPLETE(IUP-1DXN) SCANS:4 <CR>

DOSE(CLIX PER CHANNEL) = 00022

-- THIS COMMAND INPUTS DOSE DATA, CALCULATES THE PRESET FOR EACH CHANNEL ADVANCE AND SORTS ALL SET WINDOW ADDRESSES IN ASCENDING ORDER. IT WILL NOT FUNCTION IF THE INTEGRATOR IS ON, THE COMPUTER IS ALREADY SCANNING OR THERE ARE OTHER PROBLEMS AS NOTED IN REAL TIME.

> \$BN <CR> -- THIS COMMAND STARTS THE ACTUAL ESA SCAN SCAN IN GROUP N, PROVIDED THAT THE I COMMAND WAS USED PREVIOUSLY AND OTHER CONDITIONS ARE MET (WHICH ARE NOTED AND SELF EXPLANATORY IF NOT MET).

(2) C/N -- THIS MODE CONTROLS THE CHARGED PARTICLE DEFLECTION PLATE POTENTIAL OSCILLATOR FREQUENCY AND ADC1 OF THE MULTICHANNEL ANALYZER.

> \$F <CR> KV CONTROL ZEROED SO POWER UP OPS SUPPLIES

INPUT HALF-CYCLE TIME IN MSEC(32K MAX):15000 <CR>

-- THIS COMMAND ALLOWS INPUT OF THE FREQUENCY USED FOR OSCILLATION OF THE CHARGED PARTICLE DEFLECTION PLATE POTENTIALS. IT WILL NOT FUNCTION IF THERE ARE ABNORMALITIES AS NOTED DURING THIS COMMAND EXECUTION.

> \$CN <CR> -- THIS COMMAND STARTS THE ACTUAL C/N MODE OF OPERATION BY TURNING ON ADC1 AND THEN STORING THE ACCUMULATED DATA. IN GROUP N IS LOCATED COUNTS DUE TO NEUTRALS(HV ON) AND IN N+1, CHARGE+NEUTRALS(HV OFF). COMMAND ABORTS OCCUR IF N IS NOT EVEN, THE COMPUTER IS ALREADY SCANNING, THE FREQUENCY HAS NOT BEEN SET OR ADC1 IS ALREADY ON.

(3) ADC

- > \$AN <CR> -- STARTS ADC1, ANALYZING IN GROUP N PROVIDING THE ADC IS NOT ALREADY ON, AND THE COMPUTER IS NOT SCANNING IN THE C/N MODE OF OPERATION.
- > \$S <CR> -- STOPS THE ADC

(4) MISCELLANEOUS

- > \$O <CR> -- THE OFF COMMAND SUSPENDS SCANNING IN EITHER C/N OR ESA MODE OF OPERATION AND OUTPUTS THE CURRENT ACCUMULATED DOSE. AT THIS POINT, RESUMPTION MAY BE REQUESTED VIA THE U COMMAND OR A COMPLETE RESTART VIA THE G COMMAND.
- > \$U <CR> -- THE CONTINUE COMMAND ALLOWS RESUMPTION FROM THE CURRENT SUSPENDED CONFIGURATION (WHEN THE O COMMAND WAS ISSUED): IN DOSE AND POTENTIAL POSITION OF THE ESA SCAN, AND ACCUMULATED DOSE OF THE C/N SCAN.

(8) DISPLAY

THE DISPLAY COMMANDS ARE IMPLEMENTED IN MES11 AT BOTH THE SOFTWARE AND HARDWARE LEVELS. THE HARDWARE OPTIONS ARE SELECTED BY THE LABELLED SWITCHES OF THE PDP11 POLL SIX'S SINGLE WIDTH NIM MODULE LOCATED ABOVE THE DISPLAY SCOPE. OPTING FOR THE DISPLAY MODE ON YIELDS TWO VERTICAL MARKER LINES VISIBLE AT THE ENDS OF THE SPECTRUM. THEIR POSITIONS MAY BE SET BY THE LOWER SWITCHES AS INDICATED BY THE FUNCTION LABELS. THE SOFTWARE COMMANDS ARE LISTED BELOW.

- < \$EN <CR> -- ZEROES GROUP N SPECTRUM AND ITS ASSOCIATED TITLE (SEE T COMMAND).
- < \$D <CR> -- THE PROGRAM NOW DISPLAYS ONLY THOSE CHANNELS BETWEEN THE MARKERS. TO EXPAND THE SCALE, DECREASE THE X RANGE SWITCH, BELOW THE DISPLAY, TO LESS THAN THE GROUP WIDTH. WHILE IN THE DISPLAY MODE, THE PRINT COMMAND OUTPUTS CHANNEL CONTENTS IN THIS RANGE ONLY, AND USE OF THE MARKERS MOTION SWITCHES WILL MOVE THE SPECTRUM THROUGH THIS WINDOW. THE MODE CAN BE TERMINATED BY TURNING OFF THE DISPLAY MARKER MODE SWITCH ON THE PDP11 POLL SIX'S MODULE.
- > \$M <CR> -- PRINTS OUT THE CURRENT CHANNEL NUMBERS OF THE MARKERS REGARDLESS OF THE DISPLAY MODE.

> \$H <CR>

ENABLE PLOTTER AND <CR> WHEN READY <CR>

-- ALLOWS A PLOT OF THE SPECTRUM THAT IS CURRENTLY ON DISPLAY. AFTER PLOTTER SCALES ARE SET UP VIA THE PLOTTER INPUT CONTROLLER SWITCH IT TO DISPLY AND PRESS THE RETURN KEY. WHEN THE PLOT IS DONE, RETURN CONTROLLER TO OFF AND PRESS <CR> TO RESUME NORMAL DISPLAY MODE.

(C) I/O

> \$TN<CR> -- MES11 NOW ENTERS THE TEXT MODE WHERE ALL FOLLOWING CHARACTERS (UP TO 80) ARE STORED INTO A TITLE BUFFER ASSOCIATED WITH GROUP N. ALL RUBOUT AND LINE DELETE COMMANDS ARE OPERATIONAL UNTIL TERMINATION OF THE TITLE MODE VIA ESC CR.

EG.

\$T0 <CR>

THIS IS A TEST <CR>

\$ <CR>

> \$PN<CR> -- NORMALLY PRINTS OUT THE FULL CONTENTS OF GROUP N IN THE FORMAT:  
TITLE (OF NO GREATER THAN 80 CHARACTERS)  
CHANNEL NUMBER AND 10 CHANNEL CONTENTS PER LINE  
IF THE DISPLAY MODE IS OPERATIONAL THEN ONLY THE CONTENTS OF THE CHANNELS BETWEEN THE MARKERS IS OUTPUT. IN A SIMILAR MANNER, IF AT ANY TIME THE L OR I COMMAND HAS BEEN USED AND THE SOFTWARE MARKERS ARE ON THE DISPLAY, THEN ONLY THE CHANNEL WINDOWS AND THEIR CONTENTS (WHICH WERE LISTED) WILL BE OUTPUT, OTHERWISE THE CONTENTS OF THE ENTIRE GROUP WILL BE PRINTED. TO ABORT THE PRINTOUT AT ANY TIME, PRESS <CR> WHEREUPON THE PROGRAM WILL COMPLETE ONLY THE CURRENT LINE IN THE OUTPUT BUFFER.

> \$LN <CR> -- PRINTS OUT ALL SET WINDOWS IN THE FORMAT OF TAG, POSITION (START AND END CHANNEL) AND INTEGRATED CONTENTS OF GROUP N. THIS COMMAND CHECKS AND NOTES ANY OVERLAPPED WINDOWS. IT ALSO SORTS THE WINDOW POSITIONS IN ASCENDING ORDER WHICH IS USED DURING ESA SCANNING.

> #KN <CR>

INPUT FILE NAME (MAX 6 CHAR'S)  
(EG:) RSW01<CR> -- WILL WRITE ON THE USER FLOPPY DISK (DX1)  
THE CONTENTS OF GROUP N WITH THE FILE NAME  
GIVEN; IN THIS CASE IT IS RSW01. IT IS  
STORED ON DX1 AS RSW01.DAT AND FOR 256  
CHANNEL SPECTRA REQUIRES 4 BLOCKS OF STORAGE.

> #RN <CR>

INPUT FILE NAME (MAX 6 CHAR'S)  
(EG:) SWP01<CR> -- READS INTO GROUP N OF THE ANALYZER THE  
SPECTRUM SWP01.DAT FROM DX1. IF THERE IS  
NO SUCH FILE, THE SYSTEM PRINTS THE  
APPROPRIATE MESSAGE.

(D) SPECIAL MODES OF OPERATION

(1) THE Z COMMAND:

-- THE USE OF THIS MODE ALLOWS THE STEPPING  
MOTOR, EMPLOYED IN ESA SCANNING, TO BE SET  
TO ZERO MANUALLY WITHOUT AFFECTING THE SOFT-  
WARE MAINTAINED STEPPING MOTOR COUNTER WHICH  
PREVENTS THE MOTOR FROM STEPPING BELOW ZERO  
POTENTIAL (THAT IS, FORCING THE POTENTIOMETERS  
BEYOND THEIR PHYSICAL STOPS). THIS IS DONE  
BY USING THE EXTERNAL SOFTWARE SWITCHES #1,  
& #2 (NORMALLY USED FOR DISPLAY OVERLAP AND  
DOSE STOP MODE) AND MANUALLY SETTING THE  
STEPPING MOTOR COUNTER TO 1000.05.

> #Z <CR> SET MTR CNTR TO 1000.05 THEN CR  
(ESS#1=UP, ESS#2=DOWN)  
<CR> -- TERMINATES SPECIAL "Z" MODE.

(2) MOTION DISPLAY:

-- THIS SPECIAL MODE OF DISPLAY HAS BEEN  
IMPLEMENTED THROUGH HARDWARE SWITCHES  
AND PUSH BUTTONS ONLY. TO ENGAGE THIS  
FUNCTION, PLACE THE MARKER TOGGLE BIT 12  
SWITCH TO "1". PRESSING P.B.#1 WILL MOVE  
THE HARDWARE MARKER POSITION TO MID SCREEN  
WHEREUPON THE SPECTRUM WILL EXPAND 2X FOR  
EVERY PUSH. PRESSING P.B.#2 WILL CONTRACT  
THE DATA DISPLAYED UNTIL NORMAL SIZE IS  
REACHED. THE ORIGINAL DISPLAY CAN BE RETURNED  
AT ANY TIME BY PLACING THE MARKER TOGGLE  
SWITCH TO "0".

(3) WINDOW:

> WM <CR> -- PRINTS OUT THE CURRENT LOCATIONS OF THE MARKERS REGARDLESS OF THE DISPLAY MODE.

-- UP TO 8 WINDOWS (0-7) MAY BE SET UP ON ANY SPECTRUM AND ANY WINDOWS SO OPERATIONAL WILL HAVE THEIR INTEGRATED COUNTS PRINTED WHENEVER THE L COMMAND IS USED. THESE REGIONS OF INTEREST, WHEN SET, ARE INTENSIFIED ON THE DISPLAY AND ARE USED MAINLY FOR SCANNING IN THE ESA MODE. WINDOWS ONLY WILL BE PRINTED OUT DURING THE P COMMAND IF THE DISPLAY MARKERS ARE "ON", OTHERWISE THE ENTIRE GROUP IS OUTPUT. OPERATIONS ON THESE REGIONS CAN BE ACCOMPLISHED THROUGH THE COMMANDS LISTED BELOW.

- > WM<CR> -- WILL PRINT THE CURRENT MARKER CHANNEL POSITIONS FOR WINDOW N IF IT IS OPERATIONAL. IF THE WINDOW IS NOT SET THEN THIS IS NOTED.
- > WNS<CR> -- WILL SET THE CURRENT MARKER LOCATIONS AS THE LIMITS FOR WINDOW N. THIS OCCURS REGARDLESS OF DISPLAY MODE.
- > WNE<CR> -- WILL ERASE THE LIMITS SELECTED FOR WINDOW N.
- > WNL<CR> -- MOVE THE MARKERS TO THE LIMITS FOR WINDOW N. IF NO WINDOW HAS BEEN SET THE APPROPRIATE MESSAGE IS OUTPUT.

(4) SPECTRAL GROUP MANIPULATIONS:

(A) ARITHMETIC OPERATIONS

> G3 <CR>

G2 <CR>

- <CR> (OR + INSTEAD OF -)

G1 <CR>

GROUP #3 = GROUP #2 - GROUP #1  
-- WILL RESULT IN GROUP 3 SHOWING THE SPECTRUM OBTAINED FROM SUBTRACTING (OR ADDING) GROUP 1 FROM (TO) GROUP 2; ANY GROUP NUMBERS MAY BE USED UP TO THE MAXIMUM NUMBER ALLOWED.

A.3.1 PIP15.MAC  
link control code for PDP-11/05



.TITLE PIP15.KAC VSN 28-OCT-70

PROGRAM TO TRANSFER ASCII FILES BETWEEN PDP11 AND PDP15

XCSR=175814  
XBUFF=175816  
RCR=175810  
RBUFF=175812  
ERRMOD=52

.MCALL ..V2....CSIGEN,.KRITH,.READX,.CLOSE,.REDEF  
.MCALL .TTYOUT,.PRINT  
..V2..  
.REDEF

PROGRAM MAINLINE

```

START1: CLR CXCSCR          ; CLEAR XCSR
        CLR CXCSCR        ; AND RCSR
START:  .TTYOUT #'H
LOOP1:  MOV C,FILE+5,R1    ; R1 PTRS TO READ FILENAME BUFFER
        BIT #200,CXCSCR   ; GET TRANSFER MODE
        BND LOOP1
        MOV3 C,RBUFF,MODFLG ; MOVE TO MODFLG
        CME R0FL         ; RECEIVE MODE?
        MOV C,FILE+4,R1   ; NO SO R1 PTRS TO WRITE FILENAME BUFF
RDFL:   .TTYOUT #'T
        JCR PC,FILEIN    ; INPUT FILENAME
        .PRINT NAME
        .CSIGEN CDEV3PC,CDEFEXT,NAME ; READY FILE
        CCR ERROUT      ; BRANCH IF ERROR
        MOV3 #5,CXBUFF   ; NO ERROR SO SEND #5 TO PDP15
LOOP2:  BIT #200,CXCSCR   ; AND WAIT FOR XMIT
        BND LOOP2
        CLR EOPFLG      ; CLR EOP FLAG
        CLR ELOCK       ; CLR ELOCK CTR
        TST0 MODFLG     ; WHICH MODE?
        CCR ACCEPT     ; RECEIVE SO BRANCH
DOWNE:  .TTYOUT #'S
        JCR PC,GETCLK    ; WAIT SO GET A CLOCK FROM DX1
RETRY:  JCR PC,TIMOUT    ; SEND THE CLOCK
LOOP3:  BIT #200,CXCSCR   ; WAIT FOR PDP15 TO FINISH
        BND LOOP3
        MOV3 C,RBUFF,STATUS ; STORE ERROR STATUS
        CME RETRY       ; ERROR SO RECEIVE CLOCK
        CME2 C0,EOPFLG  ; FINISHED SENDING?
        CCR DOWNE      ; NO SO GET NEW CLOCK
        .CLOSE #3      ; CLOSE READ CHANNEL
        ER START       ; YES SO RESTART
ACCEPT: .TTYOUT #'R
        MOV C3,CTR      ; READY ERROR PASS CTR
ADD1:   JCR PC,MOVE      ; RECEIVE A CLOCK
        TST EOPFLG     ; FINISHED?
        BND DOWNE      ; NO SO CONTINUE
        .CLOSE C0      ; YES SO CLOSE FILE
        ER START       ; AND RESTART
KORZ2:  DEC CTR         ; DEC ERROR PASS CTR
        CME KCC2       ; ER IF NOT ZERO
        CLR STATUS     ; ONLY RETRY RECEIVE 3 TIMES
ADD2:   MOV3 STATUS,CXBUFF ; SEND ERROR STATUS TO PDP15
LOOP4:  BIT #200,CXCSCR   ; WAIT FOR SEND
        BND LOOP4
        TST STATUS     ; RECEIVE ERROR?
        CME ADD1       ; YES SO RECEIVE AGAIN
        JCR PC,STORCK  ; WRITE CLOCK ON DX1
        ER ACCEPT      ; AND GET ANOTHER
ERROUT: NOP

```

```

WAIT2:  MOV B @ERRWRD,@XBUFF ; MOVE ERROR CEDE TO XMITER
        BIT #200,@XCSR      ; AND WAIT FOR XMIT
        BEG WAIT2
        RR RDFL             ; RETRY FILENAME

```

```

MODFLG: .WORD 0           ; TRANSFER MODE FLAG
STATUS: .WORD 0           ; ERROR STATUS
CTR:     .WORD 0           ; ERROR PASS CTR
EOFFLG: .WORD 0           ; EOF FLAG
DEFE XT: .RAD50 "DAT"      ; INPUT #3 DEFAULT EXT
        .RAD50 "DAT"      ; OUTPUT #0 DEFAULT EXT
        .WORD 0,0
BLOCK:  .WORD 0           ; BLOCK CTR
RFILE:  .ASCIZ /=DX1:
WFILE:  .ASCIZ /DX1:
        .EVEN

```

```

ROUTINE TO INPUT FILE NAME
R1 POINTS TO NAME BUFFER

```

```

FILEIN: MOV #12,R2        ; READY CHAR CTR
        MOV R1,R3        ; R3 POINTS TO NAME BUFFER
WAIT1:  BIT #200,@RCSR    ; WAIT FOR CHAR FROM PDP15
        BEG WAIT1
        MOV B @CRBUFF,R4 ; PUT CHAR IN R4
        CMPB #15,R4      ; CR?
        BEG FILEOX       ; YES SO NAME INPUT
        MOV B R4,(R3)+    ; NO SO STORE CHAR AT NAME BUFFER
        DEC R2            ; ONLY ACCEPT FIRST 10 CHARS
        BNE WAIT1        ; GET ANOTHER CHAR
FILEOX: MOV @RFILE,NAME   ; PNT TO READ CHAR STRING
        TSTB MODFLG      ; WHICH TRANSFER MODE?
        BNE FILEX        ; XMIT SO EXIT
        MOV @WFILE,NAME  ; RECEIVE SO PNT TO WRITE CHAR SRTING
        MOVB #'',(R3)+   ; END WRITE COMMAND WITH=
        CLRB (R3)        ; CLEAR LAST BYTE OF COMMAND
        RTS PC           ; RETURN
NAME :   .WORD 0         ; PTR TO COMMAND STRING

```

```

ROUTINE TO READ A BLOCK FROM DX1

```

```

GETBLK: JSR PC,CLRBK     ; CLEAR THE DATA BUFFER
        .READW @AREA,#3,#IOBUF,#400,BLOCK ; READ A BLOCK
        BCC NOERR       ; BRANCH IF NO ERROR
        TTYOUT #'Y
        INC EOFFLG      ; SET EOF FLAG
        INC BLOCK       ; INC BLOCK CTR
NOERR:  RTS PC           ; AND RETURN

```

```

ROUTINE TO SFND A BLOCK TO THE PDP15

```

```

TRANSM: MOV #IOBUF,R1    ; R1 PNTS TO DATA BUFFER
SNDXRE: MOV B (R1)+,@XBUFF ; MOVE CHAR TO XMITER
WAIT3:  BIT #200,@XCSR    ; AND WAIT TILL SENT
        BEG WAIT3
        CMP R1,#IOEND    ; END OF BLOCK?
        BNE SNDXRE       ; NO SO SEND MORE
        RTS PC           ; YES SO RETURN

```

```

ROUTINE TO RECEIVE BLOCK FROM PDP15

```

```

RCVE:   BIT #200,@RCSR    ; WAIT TILL PDP15 READY TO SEND
        BEG RCVE
        MOV B @CRBUFF,R2 ; NO SO CHECK AGAIN FOR READY
        JSR PC,CLRBK     ; READY SO CLEAR RCVE FLAG
        MOV #IOBUF,R1    ; CLR THE DATA BUFFER
        CLRB R2          ; R1 PNTS TO DATA BUFFER
        RTS PC           ; READY FOR TIME OUT CKECK

```

```
WAIT4: BIT #200,@#RCSR      ; WAIT TILL PDP11 GETS CHAR
      RNE TIME              ; CHAR SO STORE IT
      INC PC                ; CHECK FOR TIME OUT
      BNE WAIT4            ; NO SO CHECK AGAIN FOR CHAR
      INC EOFELG           ; TIME OUT SO SET EOF FLAG
      BR RCVEK             ; AND RETURN
TIME:  BIT #100000,@#RCSR   ; CHECK IF TRANSMIT ERROR
      BEQ ERRCHK           ; BR IF NO ERROR
      INC STATUS           ; INC STATUS FLAG IF ERROR
ERRCHK: MOVB @#RBUF,(R1)+   ; STORE CHAR IN BUFFER
      CMP R1,#IOEND        ; END OF BUFFER?
      BNE RETN             ; NO SO RECEIVE ANOTHER
RCVEK: RTS PC              ; YES SO RETURN

;
; ROUTINE TO WRITE A BLOCK ON DX1
;
STBLK: .WRITW #ARFA,#0,#IOBUF,#400,BLOCK ; WRITE A BLOCK
      INC BLOCK           ; INC BLOCK CTR
      RTS PC              ; AND RETURN
;
; ROUTINE TO CLR THE DATA BUFFER
;
CLRBLK: MOV #IOBUF,R1       ; R1 PNTS TO DATA BUFFER
CLR R1: CLR (R1)+          ; CLR THE WORD
      CMP R1,#IOEND       ; FINISHED?
      BNE CLR1            ; NO SO CLEAR MORE
      RTS PC              ; YES SO RETURN
;
IOBUF: .+1000              ; DATA BUFFER
IOEND: .WORD 0
AREA:  .WORD 10
DEVSPC: .WORD 0
;
.END START1
```

A.3.2 PIP11 SRC

link control code for PDP-15/20

C  
C  
C  
C  
C  
C  
C  
C  
C  
C  
C  
C  
C  
C  
C  
C  
C

FILE PIP11 (FTN) ON SMP 05  
PGM MAINLINE TO CONTROL TRANSFERS TO AND FROM THE PDP-11  
MUST BE RUN IN CONJUNCTION WITH THE PDP-11 PGM PIP15  
FOR CORRECT OPERATION.  
LINKAGES TO THE 11/15 XCVR ARE ACCOMPLISHED IN MACRO15  
WITH ALL IOFS DURING XCVR DEVICE OPERATION:  
XMIT(I) INTEGER BINARY SEND  
RCVE(I,IFLG) INTEGER BINARY RECEIVE--IFLG=0 IF CHAR OK  
  --IFLG=1 IF RCVR IN ERROR  
ASEND(A,MOD) ASCII ARRAY SEND--MOD=0 IF 5/7 ASCII  
  --MOD=1 IF 1/1 ASCII  
ASGET(A,IERR) ASCII ARRAY RECEIVE  
  -- IERR=0 IF XFER OK  
  IERR<0 IF TIMED OUT  
  IERR>0 IF ERROR

BY R.WALKER AND S.W.POEHLMAN OCT.1976.

DIMENSION A(256),B(16),FILNAM(2),FIL15(2),C(40)  
DATA EXTN /4M SRC/

C  
C  
C  
C  
C

ASCERTAIN DIRECTION OF XFER REQUIRED AND SEND MODE FLG TO 11  
FOR FILE 11 TO FILE 15, FLAG=1, USE ASGET MACRO  
FOR FILE 15 TO FILE 11, FLAG=0, USE ASEND MACRO

1

WRITE(2,1)  
FORMAT(" INPUT COMMUNICATION MODE: CONVERSATIONAL(1)  
1 OR EXPRESS(2)")

100

READ(1,KN)  
CALL LINKIT  
CONTINUE  
IF(KN.EQ.1) WRITE(2,2)  
FORMAT(" FLAG MODE: OBTAIN FILE FROM 11(1)"/,/,12X,  
1 "SEND FILE TO PDP-11(0)"/,/,")")  
IF(KN.EQ.2) WRITE(2,3)  
FORMAT(" FROM(1) OR TO(0) 11")  
READ(1,MODE)  
IF(MODE.EQ.1) GO TO 10  
IF(MODE.EQ.0) GO TO 10  
WRITE(2,4)

4

10

200

FORMAT(" ?")  
GO TO 100  
CALL XMIT(MODE)  
CONTINUE  
IF(KN.EQ.1) WRITE(2,6)  
FORMAT(" INPUT: 5 CHARACTER FILE NAME LEFT JUSTIFIED",  
1 /, " THEN DOT AND 3 CHARACTER PDP11 EXTENSION")  
IF(KN.EQ.2) WRITE(2,5)  
FORMAT(" FILNAM:")  
READ(1,8) FILNAM  
FORMAT(2A5)  
FIL15(1)=FILNAM(1)  
FIL15(2)=EXTN  
MODE = MODE + 1  
GO TO (11,12),MODE

C

C

C

ASCII FILE FROM PDP-11 TO PDP-15

12

CALL ENTER(5,FIL15)  
IF(KN.EQ.1) WRITE(2,27) FIL15  
FORMAT(" FILE ",2A5," CREATED ON PDP-15 DISK 1")  
IF(KN.EQ.2) WRITE(2,9)  
FORMAT(" OK")

9

MOD = 0  
CALL ASEND(FILNAM,MOD)  
CALL RCVE(IFLG,IERR)

C

GET FILNAM CHECK FROM PDP-11

C

```
C      IF(IEROR.EQ.0) GO TO 28
65     WRITE(2,29)
29     FORMAT(" RESTART BOTH PGMS: ERROR 02")
      PAUSE 2
      GO TO 100
28     IF(IFLG.EQ.5) GO TO 20
30     IFLG = IFLG + 1
      GO TO (21,22,23,24,25),IFLG
21     WRITE(2,31)
31     FORMAT(" ILLEGAL PDP-11 SYNTAX ")
      GO TO 200
22     GO TO 200
23     GO TO 200
24     WRITE(2,34)
34     FORMAT(" PDP-11 DIRECTORY FULL")
      GO TO 200
25     WRITE(2,35)
35     FORMAT(" FILE NOT FOUND ON PDP-11")
      GO TO 200

C
C      READY FOR INPUT FROM PDP-11,SET ERROR RETRY AT 3
C      PER 512 CHARACTER BLOCK
C
20     ITRY=3
      NBLK=1
      KDUN = 0
      KSTAT = 1
150    CALL ASGET(A,IER)
97     FORMAT(8I5)
      IF(IER) 62,61,63
      HAVE ERROR IN RCVR SO RETRY
63     ITRY = ITRY - 1
      WRITE(2,66) IER,NBLK
66     FORMAT(15," ERROR IN BLOCK",14," FROM PDP-11")
      IF(ITRY.EQ.0) GO TO 61
      IERR=1
      CALL XMIT(IERR)
      GO TO 150
C      HAVE EITHER HARD ERROR(ITRY=0) OR IS OK SO TO DISK
61     CALL UPK256(A,B,KSTAT,KDUN)
      IF(KSTAT.EQ.3) GO TO 81
      WRITE(5,52,ERR=75) (8(I),I=1,16)
52     FORMAT(1H ,16A5)
55     IF(KSTAT.EQ.4) GO TO 73
      GO TO 61
81     ITRY = 3
      IERR = 0
      NBLK=NBLK+1
      CALL XMIT(IERR)
      GO TO 150
C      TIMED OUT SO WRITE LAST BLOCK
62     KDUN = 4
      GO TO 61
75     WRITE(2,54) NBLK
54     FORMAT(" DISK15 WRITE ERROR IN BLOCK",15)
      GO TO 55
73     CALL CLOSE(5)
      IF(KN.EQ.1) WRITE(2,72) FIL15
72     FORMAT(" FILE ",2A5," CLOSED ON THE PDP-15")
      IF(KN.EQ.2) WRITE(2,9)
      GO TO 100

C
C      ASCII FILE TO PDP-11 FROM PDP-15
C
11     CALL FSTAT(5,FIL15,K)
      IFLG = 5
      MOD = 0
```

```
IFLAG = 5
IF(K.NE.0) GO TO 7
WRITE(2,32) FIL15
32 FORMAT(" FILE ",ZAS," DOES NOT EXIST ON DISK")
GO TO 200
44 FORMAT(" FILE ",ZAS," OPENED ON DX1,PDP15")
CALL ASEND(FILNAM,KOD)
CALL RCVE(IFLG,IERR)
IF(IERR.NE.0) GO TO 65
IF(IFLG.NE.5) GO TO 30
IF(NV.EQ.1) WRITE(2,14) FIL15
IF(NV.EQ.2) WRITE(2,9)
40 CALL SEEK(5,FIL15)
38 FORMAT(" FILE ",ZAS," NOW OPEN ON 15DX1")
LDUN = 0
NBLK = 1
KOD = 1
LSTAT = 1
NLINE = 0
88 READ(5,82,ERR=84,END=83) (B(I),I=1,16)
NLINE = NLINE + 1
82 FORMAT(16A5)
90 CALL SCAN(B,C)
92 CALL PAK258(A,C,LSTAT,LDUN)
IF(LSTAT.EQ.2) GO TO 88
94 CALL XMIT(KOD)
CALL ASEND(A,KOD)
CALL RCVE(IFLG,IERR)
NBLK = NBLK + 1
IF(IERR.NE.0) GO TO 65
IF(IFLG.NE.0) GO TO 94
88 IF(LSTAT.NE.4) GO TO 92
CALL CLOSE(5)
IF(NV.EQ.1) WRITE(2,77) FILNAM
77 FORMAT(" FILE ",ZAS," CLOSED ON THE PDP11,DX1")
IF(NV.EQ.2) WRITE(2,9)
IERR=0
CALL XMIT(IERR)
GO TO 100
84 IER = IERR(5)
WRITE(2,83) NLINE,IER
83 FORMAT(" READ ERROR IN LINE",I4," FROM FILE ON DISK15--OTS",I3)
GO TO 50
88 LDUN = 4
GOTO 80
STOP
END
```

```

/ FILE LINKIT ON SWP 05 OCT 1976
/ MACRO ROUTINE TO SET UP PDP-15 XCVR TO:
/ 4800BAUD,EVEN PARITY,2 STOP BITS,
/ AND INTERRUPT ON ERROR OFF.
/ CALLED FROM FORTRAN TO INIT XCVR
/ FIRST TIME VIA CALL LINKIT
/ PART OF THE FORTRAN PGM PIP11
/
/ .TITLE LINKIT
/ .GLOBL LINKIT
/
/ IOTS
/
RST=704104
LCR=704444
RRB=704112
CTF=704002
/
LINKIT XX
RST / INIT RCVR
LAC (000336) / SET UP STATUS REG
LCR / AS ABOVE
CTF / CLR XMTR FLG
RRB / CLR RCVR FLG
JMP* LINKIT / RETURN
/
/ .END
/
/
```



/ FILE XMIT ON SWP 05 OCT 1978  
/ MACRO ROUTINE TO XMIT TO PDP-11 THE  
/ BINARY VALUE OF I  
/ CALLED FROM FORTRAN VIA CALL XMIT(I)  
/ PART OF THE PROGRAM PIP11 FTN.  
/

.TITLE XMIT(I) I BIN TO PDP-11  
.GLOBL XMIT,.DA

/ IOTS  
/

STF=704001  
CTF=704002  
LTB=704004  
SRF=704101  
RRS=704112  
RST=704104  
SOE=704441  
RSR=704442  
LCR=704444  
TLS=700408  
TSF=700401  
TCF=700402  
KSF=700301  
KRS=700312  
CGLRS=CLG1LR8  
/

XMIT XX  
JMS\* .DA  
JMP .+1+1 / GET & JMP OVR ARG  
IPTR 0 / TAG OF I  
LAC\* IPTR / HAVE I  
CTF / CLR XMIT FLG  
LTB / LD XMIT BFR  
IOF  
STF / DUN?  
JMP .-1 / NO SO WAIT  
CTF / CLR FLG NO INTR)  
ION  
JMP\* XMIT / YES SO RETURN  
/

/ .END  
/

```
/ FILE RCVE ON SWP 05 OCT 1976
/ MACRO ROUTINE TO RCVE FROM PDP-11 THE
/ BINARY VALUE OF I
/ CALLED FROM FORTRAN VIA CALL RCVE(I,IFLG)
/ WHERE IFLG=0 IF OK
/ IFLG=1 IF ERROR
/ PART OF THE PROGRAM PIP11 FTN.
/
/ .TITLE RCVE(I,IFLG) GET I BIN FROM PDP-11
/ .GLOBL RCVE,.DA
```

```
/ IOTS
/
```

```
STF=704001
CTF=704002
LTB=704004
SRF=704101
RRB=704112
RST=704104
SOE=704441
RSR=704442
LCR=704444
TLS=700408
TSF=700401
TCF=700402
KSF=700301
KRB=700312
CBLRS=CLB!LRS
```

```
/
RCVE XX
JMS* .DA / GET 2 ARGS
JMP .+2+1 / JMP OVER THEM
IPTR 0 / TAG OF I
FLGPTR 0 / TAG OF IFLG
DZM* FLGPTR / NO ERROR YET
IOF
CLA / CLR ACC
SRF / GOT CHAR?
JMP .-1 / NO SO WAIT
RRB / TO ACC
D&C* IPTR / WORD INTO I
SOE / EXIT IF OK
JMP IONS / EXIT
ISZ* FLGPTR / HAVE ERROR
RST / RESET ERROR FLG
LAC (000335) / 4800,EP,258,IOF
LCR / TO STATUS REG
IONS ION
JMP* RCVE / SO FLG=1
/
/ .END
/
/
```

NOV 05 1976 11:21 AM

```
/ FILE SCAN ON SWP 05 OCT 1976
/ MACRO ROUTINE TO TAKE INPUT ARRAY B(16)
/ OF 80 CHARACTERS AND UNPACK 5/7 AS
/ 1/1 INTO ARRAY C(40)
/ CALLED FROM FORTRAN VIA CALL SCAN(B,C)
/ WHERE 8 SPACES = 1 TABULATION
/ AND WHERE EDL = CR / LF
/ PART OF THE PROGRAM PIP11 (PTN)
/
. TITLE SCAN(B,C) B(16) INTO C(40)
. GLOBAL SCAN,.DA
```

```
/
TTO=2
IOPS=2
OUT=1
ALFDC=3
/
STF=704001
CTF=704002
LTB=704004
SRF=704101
RRB=704112
RST=704104
SOE=704441
RSR=704442
LCR=704444
TLS=700408
TSF=700401
TCF=700402
KSF=700301
KR3=700312
CCLRS=CLQ!LRS
```

```
/
SCAN XX
JMS* .DA / GET 2 ARGS
JMP .+2+1 / JMP OVR THEM
B3 0 / PTR TO WD4 OF B(1)
CC 0 / PTR TO WD4 OF C(1)
/
```

```
/ SET UP POINTERS AND COUNTERS
LAX -116 / -78 DEC WDS
DAC CCCTR / STOR CHAR CNT
LAC* B8 / GET A(1) LOC
AND (77777) / STRIP OFF MODE
DAC B8 / STOR IT
DAC BBPTR / TO BE MODIFIED
LAC* CC / GET B(1) LOC
AND (77777) / STRIP OFF MODE
DAC CC / STORE IT
DAC CCPTR / TO BE MODIFIED
LAX -20 / -18 WD CNT
DAC B8CTR /
```

```
/
/ ROUTINE TO UNPACK 5/7 ASCII
CONT3 LAC B8PTR / GET PTR TO B
DAC T57PT / AND SAVE HERE
T57L1 -5 / START OF LOOP FOR
DAC T57C1 / GETTING WORD PAIRS
LAC* T57PT / TO UNPACK 5 CHARS
DAC T57BF / DEC PTR
ISZ T57PT /
LAC* T57PT / GET WORD
DAC T57BF+1 / STOR
ISZ T57PT / PT TO NXT WD
T57L2 -7 / SET TO ROTATE OFF
DAC T57C2 / 7 BITS OF PACKED
```

T57L3	CLL		/ WORD PAIR
	LAC	T57BF+1	/ GET 1ST WRD
	RAL		
	DAC	T57BF+1	/ STOR ROTATED
	LAC	T57BF	/ GET 2ND WRD
	RAL		/
	DAC	T57BF	/ STOR ROTATED
	CLA	RAL	
	TAD	T57BF+1	
	DAC	T57BF+1	
	ISZ	T57C2	/ ROT OUT 1 CHAR?
	JMP	T57L3	/ NO SO ROT AGAIN
	AND	(177)	/ MASK OFF 7 BITS
	SAD	(0)	/ NULL?
	JMP	T57I	/ YES SO IGNOR
STOR	DAC*	CCPTR	
	ISZ	CCPTR	/ UPDATE C PNTR
	ISZ	CCCTR	/ C FULL?
	SKP		/ NO SO CONT
	JMP	CFUL	/ YES SO BRANCH
T57I	ISZ	T57C1	/ DUN 1 WD PR?
	JMP	T57L2	/ NO SO DO MOR
	ISZ	BBCTR	/ YES SO FINI?
	JMP	T57L1	/ NO SO NXT PR
/			
CFUL	LAW	-1	/ BACK OFF 1
	TAD	CCPTR	/ ON C PTR
	DAC	CCPTR	/ AND GET CHAR
	LAC*	CCPTR	/
	SAD	(40)	/ HAVE SPACE?
	JMP	CFUL	/ YES SO CHECK MOR
	ISZ	CCPTR	/ NO SO ADD
	LAC	(15)	/ CR/LF
	DAC*	CCPTR	
	ISZ	CCPTR	/ BUMP PTR
	LAC	(12)	
	DAC*	CCPTR	
	LAW	-7	/ 7 SP=1 TAB
	DAC	NFLAG	
	LAC	CC	
	DAC	CCPTR	/ RESTOR PNTRS
	LAW	-120	
	DAC	CCCTR	
SPCE	LAC*	CCPTR	/ GET C(I)
	SAD	(40)	/ HAVE SPCE?
	JMP	INCF	/ YES SO CHK FLG
	SAD	(15)	/ HAVE CR?
	JMP*	SCAN	/ YES SO EXIT
NEXT	LAW	-7	/ RESTOR CONSECUTIVE
	DAC	NFLAG	/ SPACE COUNTER
	ISZ	CCPTR	/ BUMP CNTR
	ISZ	CCCTR	/ DONE?
	JMP	SPCE	/ NO SO MOR
	JMP*	SCAN	/ YES SO EXIT
INCF	ISZ	NFLAG	/ INC FLG,??
	SKP		/ NO SO MOR
	JMP	TABIT	/ YES SO TAB
	JMP	NEXT+2	/ CHK MOR CHRS
TABIT	LAW	-6	/ GET 1ST SP
	DAC	NFLAG	/ RESTOR CNTR
	TAD	CCPTR	
	DAC	CCPTR	/
	LAC	(11)	/ GET TAB & STOR
	DAC*	CCPTR	
	CLA		/ NULL ACC
LOOP25	ISZ	CCPTR	/ BUMP PTR
	DAC*	CCPTR	/ STOR NULLS
	ISZ	NFLAG	/ DUN 7 NULLS?

```
JMP LOOP25 / NO SO KOR  
JMP NEXT / YES SO NXT TAB
```

```
//  
//  
//  
//  
//  
//  
//  
//  
//  
//  
//  
//  
//  
//
```

BUFFER STORAGE FOR ROUTINES

```
KFLAB 0  
CCPTR 0  
CCCTR 0  
BSPTR 0  
B8CTR 0  
T57PT  
T57C1  
T57C2  
T57BF .BLOCK 5  
//  
//  
.END
```

```

/ FILE ASEND ON DECTAPE SWP 05 OCT. 1976
/   MACRO ROUTINE TO XMIT TO PDP-11 ANY
/   ONE DIMENSIONAL ARRAY ACCORDING TO
/   IF MOD=0 ARRAY IN 5/7 ASCII
/   IF MOD=1 ARRAY IN 1/1 ASCII
/   CALLED FROM FORTRAN VIA CALL ASEND(A,MOD)
/   WHERE MOD IS PACKING FLAG FOR ARRAY A
/   PART OF THE PGM PIP11 FTN
/

```

```

.TITLE ASEND(A,MOD) XMIT A TO 11
.GLOBL ASEND,.DA

```

```

/
TTO=2
IOPS=2
OUT=1
ALFNMC=3
/
STF=704001
CTF=704002
LTB=704004
SRF=704101
RRB=704112
PST=704104
SOE=704441
PSR=704442
LCR=704444
TLS=700406
TSF=700401
TCF=700402
KSF=700301
KRB=700312
CGLRS=CLB'LRS
/
/

```

```

ASEND   XX
        JMS*  .DA           / GET 2 ARGS
        JMP   .+2+1        / JMP OVER THEM
ARRAY   0                 / WD4 OF ARY. BLK
MODPTR  0                 / PTR TO MOD VAR
        LAC*  ARRAY        / HAVE A(1) LOC
        AND  (77777)      / STRIP OFF MODE
        DAC  ADRES        / STOR A TAG
        LAW  -3           / BACK 3 WDS
        TAD  ARRAY        / GET SIZE PTR
        DAC  SIZPTR       / STOR IT
        LAC* SIZPTR       / GET SIZE
        AND  (17777)     / STRIP OFF MODE
        DAC  WDCTR        / STOR IT
        LAC* MODPTR       / GET MODE
        SAD  (1)          / 5/7?
        JMP  ONE          / NO SO BRANCH
        LAC  ADRES        / GET A(1)
        DAC  .+3          / GIVE TO SUBR
        LAC  WDCTR        / GET # WDS
        JMS  TYP57        / SEND ARRAY
        0
        LAC  (15)        / SEND CR
        JMS  SEND         / AS LAST CHAR
        JMP* ASEND        / RETURN
ONE     LAC  WDCTR        / GET # WDS
        TCA          / HAVE -VE
        DAC  WDCTR       / STORE IT
LOOP1   LAC* ADRES        / GET A(I)
        JMS  SEND         / SEND A(I)
        ISZ  ADRES        / INC I
        ISZ  WDCTR        / DONE?
        JMP  LOOP1        / NO SO MOR
        JMP* ASEND        / YES SO RETURN

```

U

SIZEPTR 0  
ADRES 0

ROUTINE TO UNPACK 5/7 ASCII  
ENTER VIA JMS TYP57  
.DSA ADDRESS  
WHERE ADDRESS IS TAG OF BEGINING OF ARRAY TO BE UNPKD  
AND WHERE ACC = # OF WORDS TO BE SENT

```

TYP57  XX
      DAC WDCTR / STOR WD CNT
      LAC* TYP57 / GET PTR TO MSEG
      DAC T57PT / AND SAVE HERE
      ISZ TYP57 / INC RETRN ADRS PTR
T57L1 -5 / START OF LOOP FOR
      DAC T57C1 / GETTING WORD PAIRS
      LAC* T57PT / TO UNPACK 5 CHARS
      DAC T578F / DEC PTR
      ISZ T57PT /
      LAC* T57PT / GET WORD
      DAC T578F+1 / STOR
      ISZ T57PT / PT TO NXT WD
T57L2 -7 / SET TO ROTATE OFF
      DAC T57C2 / 7 BITS OF PACKED
T57L3 CLL / WORD PAIR
      LAC T578F+1 / GET 1ST WRD
      RAL
      DAC T578F+1 / STOR ROTATED
      LAC T578F / GET 2ND WRD
      RAL
      DAC T578F / STOR ROTATED
      CLA!RAL
      TAD T578F+1
      DAC T578F+1
      ISZ T57C2 / ROT OUT 1 CHAR?
      JMP T57L3 / NO SO ROT AGAIN
      AND (177) / MASK OFF 7 BITS
      SAD (15) / HAVE CR?
      JNZ TYCR / YES SO PRINT IT
      SAD (40) / SPACE?
      SXP / YES SO ICOND
      JMS SEND / SEND CHAR
T57I ISZ T57C1 / FINISHED 1 WD PR?
      JMP T57L2 / NO SO DO MOR
      LAM -2 / YES SO DUN?
      TAD WDCTR / DEC WD CTR
      DAC WDCTR / UPDATE WD CTR
      SZA / TO SEE
      JMP T57L1 / NO SO NXT
      JMP* TYP57 / YES SO RETURN
TYCR JNZ SEND / SEND CR
      LAC (12) / GET LF
      JMS SEND / SEND LF
      JMP T57I / CHECK FOR DUN

```

SUBROUTINE TO SEND ONE CHARACTER  
ENTER VIA JMS SEND  
WITH CHARACTER IN THE ACC

```

SEND  XX
      IOF
      CTF / CLR XMTR FLG
      LTB / LD XMTR BFR

```

```
STF           / DONE?  
JMP  .-1      / NO SO WAIT  
CTF           / CLR FLG(NO INTR)  
ION  
JMP* SEND    / YES SO RETURN
```

```
///  
///  
///  
///  
///  
///  
///  
///
```

BUFFER STORAGE FOR ROUTINES

```
T57PT  
WDCTR  
T57C1  
T57C2  
T57BF
```

.BLOCK 5

.END



/ FILE ASGET ON DECTAPE SMP 05 OCT 1976  
/ MACRO ROUTINE TO RECEIVE FROM PDP-11 512  
/ CHARACTERS TO BE STORED INTO A 256 ELEMENT ONE  
/ DIMENSIONAL ARRAY A ON A ONE/ONE BASIS  
/ CALLED FROM FORTRAN VIA CALL ASGET(A,IERR)  
/ WHERE ERROR RETURN STATUS IS OK IF IERR=0  
/ TIKED OUT IF IERR<0 OR  
/ ERROR RECEIVED IF IERR>0  
/ PART OF THE PIP11 FTN PGM  
/

.TITLE ASGET(A,IERR) RCVE A FROM 11  
.GLOBL ASGET,.DA

/ IOTS  
/

STF=704001  
CTF=704002  
LTB=704004  
SXF=704101  
RRS=704112  
RST=704104  
SOE=704441  
RRZ=704442  
LCR=704444  
CLRS=CLG!LRS  
/

ASGET XX  
JMS\* .DA / GET 2 ARGS  
JMP .+2+1 / JMP OVR THEM  
ARRAY 0 / WD4 PTR OF BLK  
ERPTR 0 / ERFLG PTR  
DZM\* ERPTR / ZERO IFLAG  
LAW -1000 / -512 OCTAL  
DAC WDCNT / STORE IT  
LAC\* ARRAY / GET A(1)  
AND (77777) / STRIP OFF KODE  
DAC ARRAY / STOR IT  
DAC WDPTR / STOR THEN MODIFY  
CLA / 0 ACC  
LOOP2 DAC\* WDPTR / NULL A(I)  
ISZ WDPTR / I=I+1  
ISZ WDCNT / DONE?  
JMP LOOP2 / NO SO MOR  
LAW -1000 / SET UP WD CNTR  
DAC WDCNT /  
LAC ARRAY / SET UP WD PTR  
DAC WDPTR /  
LOOP3 JMS GET / GET CHAR FROM 11  
LAC\* ERPTR / GET IFLAG  
TAD ERFLG / ADD # ERRORS  
DAC\* ERPTR / RESTOR UPDATE  
LAC TFLG / CHECK FOR TOUT  
SZA / TIKED OUT?  
JMP NOTOUT / NO SO BRANCH  
LAC (15) / YES SO CR  
DAC\* WDPTR / STOR IT  
ISZ WDPTR / BUMP PTR  
ISZ WDCNT / DONE?  
SXP / NO SO MOR  
JMP TIRO / YES SO OUT  
LAC (12) / GET LF  
DAC\* WDPTR / STOR IT  
ISZ WDPTR / BUMP PTR  
ISZ WDCNT / DONE?  
SXP / NO SO MOR  
JMP TIRO / YES SO OUT  
CLA / ACC = NULL

```

LOOP4  DAC*  WDPTR      / NULL REST
        ISZ  WDPTR      / INC I IN A(I)
        ISZ  WDCNT      / DONE?
        JMP  LOOP4      / NO SO MOR
TIMO    LAW  -1         / YES SO IERR<0
        DAC*  ERPTR     / TIMED OUT
        JMP* ASGET      / RETURN
NOTOUT  LAC  CHAR       / GET CHAR FRM STOR
        DAC*  WDPTR     / STOR IT IN A(I)
        ISZ  WDPTR     / INC I
        ISZ  WDCNT     / DONE?
        JMP  LOOP3     / NO SO MOR
        JMP* ASGET     / YES SO RETURN

```

```

/
WDCNT  0
WDPTR  0
ERFLG  0
TFLG   0
CHAR   0
/
/
/
/
/

```

```

SUBROUTINE TO RECEIVE A CHARACTER FROM THE PDP-11
ENTER VIA JMS GET AND EXIT WITH CHARACTER IN CHAR
UPDATES ERFLAG =0 IF XFER OK
                1 IF HAD ERROR
/
/
/

```

```

GFT    XX
        IOF
        LAC  (600000)   / SET UP FOR A
        DAC  TFLG      / 16 BIT TIME OUT
        DZM  ERFLG     / INIT ERFLG
        CLA                      / CLR ACC
RED     SRF            / GOT CHAR?
        JMP  TOUT      / NO SO CHECK TIM
        RRB                      / YES SO TO ACC
        DAC  CHAR      / STOR CHAR
        SOE            / HAVE ERROR?
        JMP  IOUT      / NO SO RETURN
        ISZ  ERFLG     / YES SO FLAG=1
        RST                      / RESET ERRORS
        LAC  (000336)  / SET UP STATUS
        LCR                      / OF THE XCVR
        JMP  IOUT      / RETURN
TOUT    ISZ  TFLG     / INC TIMER
        JMP  RED       / RECHECK FLG
        DZM  CHAR     / NULL CHAR
IOUT    IOB          / EXIT
        JMP* GET      / RETURN
        .END

```

```
/ FILE UPK258 ON SWP 05 OCT 1976
/ MACRO ROUTINE TO TAKE INPUT ARRAY A(258)
/ OF 512 CHARACTERS AND PACK AS 5/7 UNTIL CR
/ INTO ARRAY B(16).
/ CALLED FROM FORTRAN VIA CALL UPK258(A,B,KSTAT,KDUN)
/ WHERE KSTAT IS =1 FIRST TIME THRU
/                =2 IF B IS FULL
/                =3 IF A IS EXPTY
/                =4 IF DONE
/ AND KDUN IS   =4 IF TIMED OUT IN ASCET
/ PART OF THE PROGRAM PIP11 (FTN)
/
/ .TITLE UPK258(A,B,KSTAT,KDUN) A(258) INTO B(16)
/ .GLOBAL UPK258,.DA
/
/
STF=704001
CTF=704002
LTB=704004
SRF=704101
RRB=704112
RST=704104
SOE=704441
RSR=704442
LCR=704444
TLS=700406
TSF=700401
TCF=700402
KSF=700301
KR3=700312
RSA=700104
RBR=700112
RSF=700101
COLRS=CL0!LRS
/
UPK258 XX
      JMS* .DA      / GET 4 ARGS
      JMP  .+4+1    / JMP OVR THEM
ARRAYA 0          / PTR TO WD4 OF A(1)
ARRAYB 0          / PTR TO WD4 OF B(1)
KPTR 0           / PTR TO KSTAT
DPTR 0           / PTR TO DONE FLG
/ SET UP POINTERS AND COUNTERS
LAW -116         / -78 CHARS IN B
DAC BCNT         / STOR CHAR CNT
LAW -1000        / -512 DEC
DAC ACNT         / STOR CHAR CNT
LAC* ARRAYA     / GET A(1) LOC
AND (77777)     / STRIP OFF MODE
DAC ARRAYA      / STOR IT
DAC APTR        / TO BE MODIFIED
LAC* ARRAYB     / GET B(1) LOC
AND (77777)     / STRIP OFF MODE
DAC ARRAYB      / STORE IT
DAC BPTR        / TO BE MODIFIED
LAC* KPTR       / GET KSTAT
SAD (3)         / KSTAT=3?
JMP BCKX       / YES SO GET BPTR
/ FIRST TIME THRU SO NULL ALL OF B(I) OR B FULL PREVIOUSLY
NULLB  LAW -40   / -32 DEC WDS
      DAC BCNT   / IN B(20)
      CLA       / NULL ACC
LOOP9  DAC* BPTR / 0 B(I)
      ISZ BPTR  / INC I
      ISZ BCNT  / DONE?
      JMP LOOP9 / NO SO MOR
      LAW -143  / RESTORE
```

```
DAC BCNT / CHAR CNT
LAC ARRAYB / AND RESTOR
DAC BPTR / B LOC
LAC* KPTR / GET KSTAT
SAD (1) / KSTAT=2?
JMP CONT1 / NO SO 1ST TIM
JMP ACKX / YES SO GET APTR
/ BCHK GET POINTER TO THE FIRST NULL IN B
LAW -230 / -180 DEC 2X
DAC BCNT / INTO B CHAR CNT
LOOP8 LAC* BPTR / GET B(I)
SAD (0) / HAVE NULL?
JMP CONTO / YES SO OK
ISZ BPTR / NOSO INC I
LAC (5) / UPDATE CHAR CNTR
TAD BCNT / 2X NORMAL
DAC BCNT / STOR NEW VALU
JMP LOOP8 / CHECK MORE
CONTO LAC BCNT / GET 2X BCNT
RCR / NORMALIZE (/2)
DAC BCNT / RESTORE
SZL / IF LINK ON
ISZ BPTR / PARTIAL WD FILLD
JMP CONT1 / START UPAK
/ RCHK GET POINTER TO LAST NULL IN A
LAC* APTR / GET A(I)
SZA / HAVE NULL?
JMP CONT1 / NO SO DUN
ISZ ACNT / EXHAUST A?
SKP / NO SO MOR
JMP ENDA / YES SO DONE
ISZ APTR / INC I
JMP ACKX / CHECK MORE
/ CONT1 ALL POINTERS SET UP SO PACK 5/7 TO B(I)
LAC BPTR / SET UP FOR PAK
DAC +2
JMS P57I / INIT PK ROUTINE
0
LOOP10 LAC* APTR / GET A(I)
DAC CHAR / STOR IT
SAD (0) / HAVE NULL?
JMP +2 / YES SO IGNOR
JMS PAK57 / NO SO TO B(I)
CLA / ACC=NULL
DAC* APTR / NULL A(I)
LAC CHAR / GET CHAR
SAD (12) / HAVE LF?
JMP ENDB / YES SO B DONE
ISZ BCNT / B FULL?
SKP / NO SO CONT
JMP ENDB1 / YES SO EXIT
ISZ APTR / UPDAT APTR
ISZ ACNT / A EMPTY?
JMP LOOP10 / NO SO CONT
LAC* DPTR / GET DUN FLG
SAD (4) / =4?
JMP ENDA1 / YES SO BRANCH
JMS P57F / NO SO FINI B WD
ENDAZ LAC (3) / SET KSTAT=3
DAC* KPTR /
JMP* UPK256 / RETURN
END LAC* DPTR / GET DUN FLG
SAD (4) / =4?
SKP / YES SO FRCE B CR
JMP ENDA2 / NO SO EXIT
LAC (4) / SET KSTAT=4
DAC* KPTR /
LAC BPTR / FORCE CR ON B
```

```
DAC .+2 / SET UP FOR PK57
JMS P57I
0
ENDA1 LAC (15) / GET CR
      JMS PAK57 / PAK IT
      LAC (12) / GET LF
      JMS PAK57 / PAK IT
      JMS P57F / NULL FILL REST
      JMP* UPK258 / RETURN
END31 LAC (15) / FORCE CR ON B
      JMS PAK57 / STOR IT
      LAC (12) / GET LF
      JMS PAK57 / PAK IT
END3 JMS P57F / NULL FILL REST
      LAC (2) / KSTAT=2
      DAC* KPTR /
      JMP* UPK258 / RETURN
/
/ STORAGE BUFFERS FOR SUBROUTINES
/
TFLAG 0
ACNT 0
APTR 0
BCNT 0
BPTR 0
CHAR 0
P57P1
P57P2
P57CT
P57BF .BLOCK 5
/
/ SUBROUTINE TO PACK CHARS INTO 5/7 ASCII
/ INITIALIZE BY JMS PAK57I THEN .DEA ADRES
/ WHERE ADRES IS 1ST WD OF BUFR FOR PKED CHARS
/
/ ADD CHARS TO BUFFER VIA JMS PAK57
/
/ WHEN FINISHED CALL JMS P57F TO FILL NULLS
/
P57I XX
      LAC* P57I / GET PNTR TO BFR
      DAC P57P1 /
      ISZ P57I
      LAC (P57BF) / GET PNTR
      DAC P57P2
      -5
      DAC P57CT
      JMP* P57I / RETURN
/
PAK57 XX / ENTER WITH ASCII CHAR
      DAC* P57P2 / IN THE ACC
      ISZ P57P2 / STOR IN TEMP BFR
      ISZ P57CT / INC PNTR
      JMP* PAK57 / GOT MULTPL OF 5 CHAR
      -5 / NO SO RETURN NOW
      DAC P57CT / YES SO DO PAK
      LAC (P57BF) /
      DAC P57P2
      CLL / PAK 5 CHARS IN 2 WDS
      LAC P57BF
      ALS+7
      TAD P57BF+1
      ALS+4
      DAC* P57P1
      LAC P57BF+4
      CELR8+7
      LAC P57BF+3
```

LRS+7  
LAC P57BF+2  
LRS+3  
TAD\* P57P1  
DAC\* P57P1  
ISZ P57P1  
LACB  
DAC\* P57P1  
ISZ P57P1  
JMP\* PAK57

/  
P57F

XX  
LAC P57CT  
SAD (-5)  
JMP\* P57F  
CLA  
JMS PAK57  
JMP .-5

/  
.END

/ END OF SUBROUTINES

```
/ FILE PAX258 ON SWP 05 OCT 1978
/ MACRO ROUTINE TO TAKE INPUT ARRAY B(40)
/ OF 80 CHARACTERS AND PACK AS
/ 1/1 INTO ARRAY A(258)
/ CALLED FROM FORTRAN VIA CALL PAX258(A,B,LSTAT,LDUN)
/ WHERE LSTAT IS =1 FOR FIRST TIME THRU
/                =2 WHEN B IS EMPTY
/                =3 WHEN A IS FULL
/                =4 WHEN FINISHED
/ AND LDUN IS    =4 IF EOF DETECTED ON READ
/ PART OF THE PROGRAM PIP11 (FTN)
```

```
.TITLE PAX258(A,B,LSTAT,LDUN) B(40) INTO A(258)
.GLOBAL PAX258,.DA
```

```
/
TTO=2
IOPS=2
OUT=1
ALFXC=3
/
STF=704001
CTF=704002
LTB=704004
EXF=704101
RRB=704112
RST=704104
SOE=704441
RRF=704442
LCR=704444
TLS=700408
TEF=700401
TCF=700402
KSF=700301
KR3=700312
COLRS=CLQ!LRS
```

```
/
PAX258 XX
      JYS* .DA      / GET 4 ARGS
      JXP* .+4+1    / JMP OVR THEM
ARRAYA 0           / PTR TO WD4 OF A(1)
ARRAYB 0           / PTR TO WD4 OF B(1)
LPTR    0           / PTR TO LIN
DPNTR   0           / PTR TO DUN FLG
```

```
/
      SET UP POINTERS AND COUNTERS
      LAM -1000     / -512 ECC WDS
      DAC ACNTR    / STOR CHAR CNT
      LAC* ARAYA   / GET A(1) LOC
      AND (77777) / STRIP OFF MODE
      DAC ARAYA    / STOR IT
      DAC APNTR    / TO BE MODIFIED
      LAC* ARAYB   / GET B(1) LOC
      AND (77777) / STRIP OFF MODE
      DAC ARAYB    / STORE IT
      DAC BPNTR    / TO BE MODIFIED
      LAM -120     / -80 CHAR CNT
      DAC BCNTR    / STORE IT
/ CHECK INPUT STATUS AND BRANCH ACCORDINGLY
      LAC* LPTR    / LSTAT=2?
      BAZ (2)      / IF NO NULL A
      JXP AGET     / YES SO BRANCH
/ NULL ALL OF A(I)--- DONE IF A EMPTY OR 1ST TIME THRU
NULLA   CLA       / NULL ACC
LOOP19  DAC* APNTR / A(I)=0
        ISZ APNTR / INC I
        ISZ ACNTR / DONE?
        JXP LOOP19 / NO SO MORE
```

```
LAW -1000 / RESTORE A CNTR
DAC ACNTR /
LAC ARAYA / RESTORE A(1) LOC
DAC APNTR /
JMP CONT2 / GO PACK
/ GET POINTER TO THE FIRST NULL IN A
AGET LAC* APNTR / GET A(I)
SAD (0) / HAVE NULL?
JMP CONT2 / YES SO PACK
AGET1 ISZ ACNTR / NO SO A DONE?
SKP / NO SO MORE
JMP AEND / YES SO BRANCH
ISZ APNTR / UPDATE POINTER
JMP AGET / NO SO CONT
```

```
/
/
CONT2 LAC* BPNTR / GET CHAR
SAD (0) / HAVE NULL?
JMP GONUL / YES SO IGNORE
DAC* APNTR / STOR IN A(I)
DAC CHAR / TEMP STOR OF CHR
CLA / NULL ACC
DAC* BPNTR / NULL B(I)
ISZ APNTR / INC I
ISZ ACNTR / A FULL?
SKP / NO SO CONT
JMP AEND / YES SO EXIT
LAC CHAR / GET CHAR
SAD (12) / HAVE LF?
JMP BEND / YES SO EXIT
GONUL ISZ BPNTR / BUMP PTR
ISZ BCNTR / B EMPTY?
JMP CONT2 / NO SO KOR
BEND LAC* DPNTR / CHECK EOF FLG
SAD (4) / =4?
SKP / YES SO ACC=4
LAC (2) / NO SO ACC=2
DAC* LPTR / LSTAT=ACC
JMP* PAX258 / RETURN
AEND LAC (3) / LSTAT=3
DAC* LPTR /
JMP* PAX258 / RETURN
```

```
/
/
/ BUFFER STORAGE FOR THE ROUTINES
```

```
APNTR
BCNTR
BPNTR
ACNTR
CHAR
MOCTR
T57PT
T57C1
T57C2
T57BF
```

```
.BLOCK 5
```

```
.END
```



Leaf 290 omitted in page numbering

7

REFERENCES

Leaf 292 omitted in page numbering

## REFERENCES

1. N. Bohr, KGL. Dan Vid. Selsk. Mat. Fys. Medd. 18, No. 8 (1948).
2. J. Lindhard and M. Scharff, Phys. Rev., 124, 128 (1961).
3. J. Lindhard, M. Scharff and H.E. Schiott, KGL. Dan. Vid. Selsk. Mat. Fys. Medd., 33, No. 14 (1963).
4. J. Lindhard, V. Nielson and M. Scharff, KGL. Dan. Vid. Selsk. Mat. Fys. Medd., 36, No. 10 (1968).
5. J. Lindhard, V. Nielson, M. Scharff and P.V. Thompson, KGL. Dan. Vid. Selsk. Mat. Fys. Medd., 33, No. 10 (1963).
6. J. Bottiger and N. Rud, Inst. Phys. Conf. Ser. No. 28, Chapter 5, 224 (1976).
7. R. Behrisch, W. Eckstein, P. Meischner, B.M.U. Scherzer and H. Verbeek, Proc. 5th Int. Conf. on Atomic Collisions in Solids, Gatlinburg (September 1973).
8. J.E. Robinson, E.S. Marmor, D.A. Thompson and W.F.S. Poehlman, J. Nucl. Mater., 85 and 86, pp. 973-977 (1979).
9. G.M. McCracken and P.E. Stott, Nucl. Fusion, 19 889 (1979).
10. W.C. Turkenburg, H.H. Kersten, B.G. Colenbrander, A.P. de Jongh and F.W. Saris, Nucl. Instr. and Meth., 138, 271 (1976).
11. M. Hage-Ali and P. Siffert, Nucl. Instr. and Meth., 166, 411 (1979).
12. G. Dearnaley, J.H. Freeman, R.S. Nelson and J. Stephen, Ion Implantation, (North-Holland Publishing Co., Amsterdam, 1973), p. 343.

13. R.G. Wilson and G.R. Brewer, Ion Beams With Applications to Ion Implantation, (Wiley and Sons, NY, 1973).
14. S. Penner, Rev. Sci. Instr., 32, 150 (1961).
15. D.W. Jones, Vacuum, 13, 314 (1963).
16. A.H. Shapiro, Vacuum, 13, 83 (1963).
17. J.A. Davies and J.E. Baglin, private communication (1975).
18. J.P. Hobson and E.V. Kornelsen, Proc. 7th Int. Vac. Congress, Vienna, ed. R. Dobrezensky et al., 2663 (1977).
19. A.L. Hughes and U. Rojanski, Phys. Rev., 34, 284 (1929).
20. A.L. Hughes and J.H. McMillen, Phys. Rev., 34, 291 (1929).
21. E. Rudberg, Proc. Royal Soc. (London), A126, 628 (1930).
22. J. Adams and B.W. Manley, Philips Technical Review, 28, 156 (1967).
23. A. Egidi, R. Marconero, G. Pizzella and F. Sperli, Rev. Sci. Instr. 40, 88 (1969).
24. D.A.S. Walker, CRNL internal report (unpublished) #CI-234 (1970).
25. O. Klemperer, Electron Optics, (Cambridge at the University Press, Great Britain, 1953).
26. R.A. McNaught, Proc. of the 7th Canadian DECUS Symposium, Quebec, 45 (1974).
27. S. Tagesen, Proc. of DECUS Europe, Denmark, 5, 239 (1978).
28. J.B. Mitchell, S. Agamy and J.A. Davies, Rad. Effects, 28, 133 (1976).
29. P.R. Bevington, Data Reduction and Error Analysis for the Physical Sciences, McGraw Hill, Toronto, 1969).

30. D.W. Marquardt, J. Soc. Ind. Appl. Math., 11, pp. 431-441 (1963).
31. T.M. Buck, G.H. Wheatley and L.C. Feldman, Surf. Sci. 35, 345 (1973).
32. H. Grahmann and S. Kalbitzer, Atomic Collisions in Solids, ed. F.W. Saris and W.F. van der Weg (North Holland Publishing Co., Amsterdam, 1976), p. 119.
33. Y.S. Shen, G.L. Miller, D.A.H. Robinson, G.H. Wheatley and T.M. Buck, Surf. Sci., 62, 133 (1977).
34. W. Eckstein and H. Verbeek, J. of Vac. Sci. and Tech., 9, 612 (1972).
35. T.M. Buck and G.H. Wheatley, Surf. Sci. 33, 44 (1972).
36. D.A. Thompson and R.S. Walker, J. Nucl. Instr. and Meth., 132, 281 (1976).
37. W.K. Chu, M.A. Nicolet and J.W. Mayer, Backscattering Spectrometry, (Academic Press: New York, 1977).
38. J.A. Davies, private communication.
39. J.E. Robinson, D.A. Thompson, K.L. Wittan, and W.F.S. Poehlman, J. Nucl. Mater., 76, pp. 621-622 (1978).
40. R.L. Williams and P.P. Webb, IEEE Trans. on Nucl. Sci., NS-9, 160 (1962).
41. H.W. Schmidt and F. Pleasonton, Nucl. Instr. and Meth. 40, 204 (1966).
42. H.C. Britt and G.C. Benson, Rev. Sci. Instr., 35, 342 (1964).
43. K.B. Winterbon, Ion Implantation Range and Energy Deposition Distributions, 2, (Plenum Press, London, 1975).

44. R.S. Walker, Ph.D. Thesis (unpublished, 1977), McMaster University, Chapter III and Appendix A.1.
45. R.S. Walker and D.A. Thompson, Rad. Eff. 37, 113 (1978).
46. S.S. Johar, Ph.D. Thesis (unpublished, 1980), McMaster University.
47. D.A. Thompson, J.E. Robinson and R.S. Walker, Rad. Eff. 32, 169 (1977).
48. J.M. McKenzie, Nucl. Instr. and Meth., 162, 49 (1979).
49. H. Meyer, IEEE Trans. on Nucl. Sci., NS-13, 180 (1966).
50. E.C. Finch, M. Asghar and M. Forte, Nucl. Instr. and Meth., 163, 467 (1979).
51. J.B. Moulton, J.E. Stephenson, R.P. Schmitt and G.J. Wozniak, Nucl. Instr. and Meth., 157, 325 (1978).
52. R.H. Pehl, F.S. Goulding, D.A. Landis and M. Lenzlinger, Nucl. Instr. and Meth., 59, 45 (1968).
53. K.W. Kemper and J.D. Fox, Nucl. Instr. and Meth., 105, 333 (1972).
54. M. Martini, T.W. Raudorf, W.R. Stott and J.C. Waddington, IEEE Trans. on Nucl. Sci., NS-22, 145 (1975).
55. S.B. Kaufman, E.P. Steinberg, B.D. Wilkins, J. Unik, A.J. Gorski and M.J. Fluss, Nucl. Instr. and Meth., 115, 47 (1974).
56. E.C. Finch, M. Asghar, M. Forte, G. Siegert, J. Greif, R. Decker et al, Nucl. Instr. and Meth., 142, 539 (1977).
57. E.C. Finch, M. Asghar and M. Forte, Nucl. Instr. and Meth., 163, 467 (1979).

58. S. Rubin, Nucl. Instr. Meth., 5, 177 (1959).
59. D.A. Thompson, H.D. Barber and W.D. Mackintosh, Appl. Phys. Lett., 14, 102 (1969).
60. T.M. Buck, J.M. Poate, J. Vac. Sci. Tech., 11, 289 (1974).
61. W.K. Chu, J.W. Mayer, M.A. Nicolet, T.M. Buck, G. Amsel and F. Eisen, Thin Solid Films, 17, 1 (1973) Review).
62. H.H. Brongersma, L.C.M. Beirens, G.C.J. van der Ligt in Material Characterizations using Ion Beams, ed. J.P. Thomas and A. Cachard, p. 65 (New York: Plenum Press, 1978).
63. Ion Beam Handbook for Material Analysis, eds. J. W. Mayer and E. Rimini, (New York: Academic Press, 1977).
64. J.F. Chemin, I.V. Mitchell and F.W. Saris in Ion Implantation in Semiconductors and Other Materials, ed. W.L. Crowder, p. 295 (New York: Plenum Press, 1972).
65. R.G. Musket and W. Bauer, Thin Solid Films, 19, 69 (1973).
66. W. Beezhold, Thin Solid Films, 19, 387 (1973).
67. G. Amsel et al., Nucl. Instr. Meth., 92, 481 (1971).
68. E. Ligeon and A. Guivarch, Rad. Effects, 22, 101 (1974).
69. C.A. Evans, Anal. Chem., 47, 818A (1975).
70. C.A. Evans, Anal. Chem., 47, 855A (1975).
71. J.F. Ziegler, IBM Research Report, RC6463 (#27912), Yorktown Heights (1977).
72. N.F. Mott and H.S.W. Massey, Theory of Atomic Collisions Oxford University Press, London (1965) p. 110.
73. I. Iverhart, G. Stone and R.J. Carbone, Phys. Rev. 99, 1287 (1955).



74. E. Bonderup, lecture notes from the University of Aarhus, unpublished (1974).
75. R.S. Walker and D.A. Thompson, *Rad. Eff.*, 36, 205 (1978).
76. D.A. Thompson and R.S. Walker, *Rad. Eff.*, 36, 91 (1978).
77. H. Goldstein, Classical Mechanics, Addison-Wesley, Cambridge Mass. (1958).
78. M. Born and J.E. Mayer, *Z. Physik*, 75 (1), 96 (1932).
79. J. Lindhard, *KGL. Dan. Vid. Selsk. Mat. Fys. Medd.*, 34, No. 14 (1965).
80. O.B. Firsöv, *Sov. Phys. JETP*, 6 (33) 534 (1958).
81. P. Gombas, *Handbuch der Physik*, Ed. XXXVI (1956).
82. K.B. Winterbon, P. Sigmund and J.B. Sanders, *KGL. Dan. Vid. Selsk. Mat. Fys. Medd.*, 37, No. 14 (1970).
83. P. Sigmund, *Phys. Rev.* 184, 383 (1969).
84. J.L'Ecuyer, J.A. Davies and N. Matsunami, *Nucl. Instr. and Meth.* 160, 337 (1979).
85. M. Knudsen and P.M. Petersen, *Rad. Eff.*, 28, 147 (1976).
86. H.H. Andersen and H. Knudsen, *Phys. Rev.*, A10, 733 (1974).
87. H.H. Andersen, J. Bottiger and H. Knudsen, *Phys. Rev.*, A7, 154 (1973).
88. A. van Wijngaarden, E.J. Brimner and W.E. Baylis, *Can. J. Phys. Rev.* A7, 154 (1973).
89. H. Verbeek, W. Eckstein and R.S. Bhattacharya, *Nucl. Instr. and Meth.*, in press, 1980.
90. T.M. Buck, Inelastic Ion-surface Collisions, eds. N.H. Tolk, J.C. Tully, W. Heiland and C.W. White (Academic Press, NY, 1977) p. 47.

91. T.M. Buck, G.H. Wheatley and L.C. Feldman, *Surf. Sci.*, 35, 345 (1973).
92. R. Behrisch, W. Eckstein, P. Meischner, B.M.U. Scherzer and H. Verbeek, *Atomic Collisions in Solids*, Vol. 1, ed. S. Datz, B.R. Appleton and C.D. Moak, (Plenum Press, NY, 1975) p. 315.
93. A. van Wijngaarden, B. Miremadi and W.E. Baylis, *Can. J. Phys.* 49, 2440 (1971).
94. W. Brandt, *Atomic Collisions in Solids*, Vol. 1, ed. S. Datz, B.R. Appleton and C.D. Moak (Plenum Press, NY, 1975).
95. W. Brandt and R. Sizmann, *Phys. Lett.*, 37A, 115 (1971).
96. B.A. Trubnikov and Y.F. Yavlinskii, *Sov. Phys. JETP*, 25, 1089 (1967).
97. Y.N. Yavlinskii, B.A. Trubnikov and V.F. Elesin, *IZV. Akad. Nauk, SSSR, Ser. Fiz.* 30, 1917 (1966).
98. M. Kitagawa and Y.M. Ohtsuki, *Phys. Rev.*, 13B, 4682 (1976).
99. M.C. Cross, *Inelastic Ion-surface Collisions*, eds. N.H. Tolk, J.C. Tully, W. Heiland and C.W. White (Academic Press, NY, 1977) p. 253.
100. T.M. Buck, Y.S. Cheng, G.M. Wheatley and W.F. van der Weg, *Surf. Sci.*, 47, 244 (1975).
101. W.F. van der Weg, T.M. Buck and G.H. Wheatley, Abstract in *Atomic Collisions in Solids*, ed. F.W. Saris and W.F. van der Weg (North Holland Pub. Co., Amsterdam, 1976). Complete paper to be published in *Surface Science*.
102. F. Abel, M. Bruneaux, C. Cohen, J. Chaumont and J.L. Thom, *Solid State Comm.* 13, 113 (1973).

103. I.R.B. Alexander, P.T. Callaghan and J.M. Poate, Ion Implantation in Semiconductors and Other Materials, ed. W. Crowder (Plenum Press, NY, 1973) p. 477.
104. W. Heiland and E. Taglauer, Inelastic Ion-surface Collisions, eds. N.M. Tolk, J.C. Tully, W. Heiland and C.W. White (Academic Press, NY, 1977) p. 27.
105. M.C. Brinkman and H.A. Kramers, Proc. Akad. Amsterdam, 33, 973 (1930).
106. H.H. Heckman, E.L. Hubbard and W.G. Simon, Phys. Rev., 129, 1240 (1963).
107. J.C. Armstrong, J.V. Mullendore, W.R. Harris and J.B. Marion, Proc. Phys. Soc., 86, 1283 (1965).
108. H.D. Hagstrum, Inelastic Ion-surface Collisions, eds. N.M. Tolk, J.C. Tully, W. Heiland and C.W. White (Academic Press, NY, 1977) p. 1.
109. A. Cobas and W.E. Lamb, Phys. Rev. 65, 327 (1944).
110. H.D. Hagstrum, Phys. Rev., 96, 336 (1954).
111. W.F. van der Weg and P.K. Rol, Nucl. Instr. and Meth., 38, 274 (1966).
112. A. Chateau-Thierry, A. Gladioux and B. Delaunay, Nucl. Instr. and Meth., 132, 553 (1976).
113. D.R. Bates, Proc. R. Soc., A247, 294 (1958).
114. M.C. Cross, Phys. Rev., B15, 602 (1977):
115. H. Betz, Rev. Mod. Phys., 44, 465 (1972).
116. C. Zaidins, Ph.D. Thesis (1967), California Institute of Technology, Appendix I.

117. I.S. Dmitriev, Soviet Phys. JETP., 5, 473 (1957).
118. R.S. Bhattacharya, W. Eckstein and H. Verbeek, Surf. Sci. 94, in press, 1980.
119. T.M. Buck, L.C. Feldman and G.H. Wheatley, Atomic Collisions in Solids, Vol. 1, eds. S. Datz, B.R. Appleton and C.D. Moak (Plenum Press, NY, 1975), p. 331.
120. H. Verbeek and W. Eckstein, "Proceedings of the Seventh International Vacuum Congress and the Third International Conference on Solid Surfaces" (Vienna, 1977), p. 1309.
121. D.A. Thompson and W.F.S. Poehlman, "IV Int'l Conf. on Ion Beam Analysis, Aarhus, 1979", Nucl. Instr. and Meth. 168, 63 (1980).
122. T. Hall, Phys. Rev., 79, 504 (1950).
123. J.A. Phillips, Phys. Rev., 97, 404 (1955).
124. J.B. Marion and F.C. Young, Nuclear Reaction Analysis, (American Elsevier Pub. Co. NY, 1968) p. 34.
125. P. Hvelplund, E. Laegsgard, T.O. Olsen and E.H. Pedersen, Nucl. Instr. and Meth., 90, 315 (1970).
126. W.F. van der Weg and D.J. Bierman, Physica, 44, 206 (1969).
127. H.D. Betz and L. Grodzins, Phys. Rev. Lett. 25, 211 (1970).
128. Mme. Pierre Curie, Comptus Rendus, 130 76 (1900).
129. N. Bohr, Phil. Mag. 25, 10 (1913)
130. H.H. Andersen and J.F. Ziegler, Hydrogen Stopping Powers and Ranges in all Elements (Pergamon Press, NY, 1977).
131. J.F. Ziegler, Helium Stopping Powers and Ranges in All Elements (Pergamon Press, NY, 1977).

132. R.A. Langley and D.K. Brice, Nucl. Instr. & Meth., 149, 145 (1978).
133. O.B. Firsov, Sov. Phys. JETP, 36(9), 1076 (1959).
134. K. Winterbon, Rad. Eff., 30, 199 (1976).
135. H.A. Bethe, Ann. der Phys., 5, 325 (1930).
136. F. Bloch, Ann. der Phys. (Leipzig), 16, 285 (1933).
137. F. Bloch, Z. fur Phys., 81, 363 (1933).
138. E. Bonderup, private communication.
139. J.H. Ommrod and H.F. Duckworth, Can. J. Phys., 41, 1424 (1963).
140. J.R. MacDonald and H.E. Duckworth, Can. J. Phys. 43, 275 (1965).
141. B. Fastrup, A. Borup and P. Hvelplund, Can. J. Phys., 46, 489 (1968).
142. P. Apel, U. Muller-Jahreis, G. Rockstroh and S. Schwabe, Phys. Status Solidi, 3(a), K173 (1970).
143. I.M. Cheshire and J.M. Poate, Atomic Collision Phenomena in Solids, eds. D.W. Palmer, M.W. Thompson and P.D. Townsend (North Holland, Amsterdam, 1970), p. 351.
144. D.J. Land and J.G. Brennan, Nucl. Instr. & Meth. 132, 89 (1976).
145. P. Hvelplund, KGL. Dan, Uid. Selsk. Mat. Fys. Medd., 38, No. 4 (1971).
146. H.H. Andersen, H. Drudsen and V. Martini, Nucl. Instr. & Meth., 149, 137 (1978).
147. H. Matsumura and S. Furukawa, Rad. Eff., 27, 245 (1976).

148. J.M. Harris, W.K. Chu and M.A. Nicolet, *Thin Solid Films*, 19, 259 (1973).
149. F. Bernhard, J. Lippold, L. Meyer, S. Schwabe and R. Stolle, *Atomic Collision Phenomena in Solids*, eds. D.W. Palmer, M.W. Thompson and P.D. Townsend (North Holland, Amsterdam, 1970), p. 663.
150. R.D. Moorhead. *J. Appl. Phys.*, 36, 391 (1965).
151. H. Bätzner, *Ann. Phys.* 25, 233 (1936).
152. G. Thieme, *Vakuum-Technik*, 25, 5 (1976).
153. H.W. Wilcox, *Phys. Rev.*, 74, 1743 (1948).
154. C.J. Andreen and R.L. Hines, *Phys. Rev.*, 151, 341 (1966).
155. M. Badner, R.E. Pixley, F.J. Moser and W. Whaling, *Phys. Rev.*, 103, 32 (1956).
156. N. Bohr and J. Lindhard, *KGL. Dan. Vid. Selsk. Mat. Fys. Medd.*, 28, No. 7 (1954).
157. D.K. Brice and R.A. Langley, *Nucl. Instr. & Meth.*, 149, 195 (1978).
158. J.F. Gibbons, W.S. Johnson and S.W. Mylroie, *Projected Range Statistics for Semiconductors and Related Materials*, 2nd edition (Halsted Press, Stroudsburg, Pennsylvania, 1975).